Dipartimento di Scienze della Terra e dell'Ambiente

Direttore: Prof. Silvio Seno

Corso di Laurea in Geoscienze per lo Sviluppo Sostenibile – LM-74

Petrographic and Geochemical Characterization of MIL090206, MIL090405, NWA6077, NWA5363 and NWA11187 Ungrouped Meteorites: New Insights Towards a Potential Classification

Caratterizzazione petrografica e geochimica delle meteoriti "ungrouped" MIL090206, MIL090405, NWA6077, NWA5363 e NWA11187: verso una potenziale classificazione

Relatore:

Prof. Antonio Langone

Correlatori:

Prof. Mara Murri

Prof. Maria Chiara Domeneghetti

Mattia Giuseppe Raciti

Matricola 527587

A.A. 2023/2024

TABLE OF CONTENTS

0. RIASSUNTO

La tesi si focalizza sull'analisi petrografica e geochimica di cinque acondriti "ungrouped": MIL090206, MIL090405, NWA6077, NWA5363 e NWA11187. Il lavoro ha l'obiettivo di determinare la loro possibile affiliazione a gruppi di acondriti esistenti o di evidenziare nuove caratteristiche distintive.

Le meteoriti MIL090206, MIL090405, NWA6077 e NWA5363 sono state ufficialmente classificate come "*brachinite-like*" (Day et al. 2012; Goodrich et al. 2017), basandosi principalmente sui contenuti di calcio e cromo nell'olivina e sugli isotopi di ossigeno. NWA11187, invece, risulta avere valori isotopici paragonabili con quelli delle ureiliti (Li et al. 2018), ma presenta altre caratteristiche che sono rare perqueste acondriti, come la presenza di lamelle di essoluzione di clinopirosseno in ortopirosseno, un elevato contenuto di forsterite in olivina e la totale assenza di fasi carbonio.

Le metodologie impiegate per questo studio includono l'uso del microscopio elettronico a scansione (SEM), della microsonda elettronica (EPMA) e della spettrometria di massa con sorgente ad ablazione laser (LA-ICP-MS). Queste tecniche hanno permesso di identificare e caratterizzare le fasi mineralogiche presenti nei campioni studiati, tra cui olivina, ortopirosseno, clinopirosseno, plagioclasio e minerali accessori come apatite ricca di cloro, cromite e fasi di Fe-Ni.

I risultati delle analisi mostrano che le meteoriti condividono fasi mineralogiche simili e tessiture pecilitiche, ma differiscono nei dati chimici sugli elementi maggiori, minori e in tracce, in particolare NWA11187 si distingue dagli altri per concentrazioni elevate di forsterite in olivina e di diversi elementi. Ad esempio, NWA11187 presenta un contenuto medio di calcio nell'olivina molto più elevato rispetto agli altri campioni. Questa variazione nella composizione chimica suggerisce una diversa storia evolutiva e possibili differenti corpi genitori.

La tesi discute anche l'affinità tra MIL090206, MIL090405, NWA6077 e NWA5363 con le brachiniti, fornendo supporto a studi precedenti che ipotizzano una loro correlazione. Per quanto riguarda NWA11187, la possibilità che venga classificata come ureilite sarebbe significativa, dato che presenta caratteristiche uniche rispetto ad altre ureiliti conosciute, come l'alto contenuto di forsterite nell'olivina, l'assenza di fasi carbonio e la presenza di lamelle di essoluzione di clinopirosseno in ortopirosseno.

In conclusione, il lavoro offre nuove informazioni per la classificazione dei campioni dmeteoriti studiati, proponendo che MIL090206, MIL090405, NWA6077 e NWA5363 siano "*brachinite-like ungrouped achondrites*" e che NWA11187 possa essere una ureilite non convenzionale.

0. ABSTRACT

MIL090206, MIL090405, NWA6077, NWA5363 and NWA11187 are achondrite meteorites currently belonging to the ungrouped meteorites. In particular MIL090206, MIL090405, NWA6077, NWA5363 are classified as brachinite-like ungrouped meteorites. NWA11187 was classified as an ungrouped achondrite based on the exsolution lamellae of clinopyroxene in orthopyroxene and the forsteritic olivine composition. However, its oxygen isotopic values are similar to those of ureilites.

The aim of this thesis work is to characterize the petrography and the geochemistry of these five samples of meteorites by means of Scanning Electron Microscope (SEM), Laser Ablation Inductively Coupled Plasma Mass Spectrometer (LA-ICP-MS) and Electron Probe Micro- Analyzer (EPMA) to constrain their potential association to a specific achondrite group.

All these meteorites have similar mineralogical phases and petrographic textures. They are composed of olivine, orthopyroxene, clinopyroxene, plagioclase and accessory Cl-rich apatite, chromite, troilite and Fe-Ni phases. The samples also display a poikilitic texture. However, this study revealed the peculiarity of NWA11187 with respect to the other investigated samples. In particular, NWA11187 shows the presence of exsolution lamellae of clinopyroxene in orthopyroxene, in addition to their high magnesium content. Also, NWA11187 displays additional important differences in the minor and trace elements chemical data in olivine, orthopyroxene and clinopyroxene. Olivine in NWA11187 has a mean ^{44}Ca value of 1906.36 ppm (other meteorites 544.50-722.21 ppm) and a mean ^{51}V value of 96.22 ppm (other meteorites 15.06-18.34 ppm), orthopyroxene has a mean ^{27}Al value of 4612.69 ppm (other meteorites 1228.12-2985.50 ppm) and a mean ^{88}Sr value of 0.38 ppm (other meteorites 0.00-0.03 ppm), clinopyroxene has a mean ^{55}Mn of 2845.29 ppm (other meteorites 1667.42-2024.28 ppm) and a mean ^{66}Zn value of 172.17 ppm (other meteorites 64.39-84.86 ppm).

1. INTRODUCTION

The study of meteorites allowed scientists to obtain valuable insights into the early stages of our solar system's formation and evolution (McSween 1999). The meteorite classification system is rather complex, with many different groups and subgroups (usually called “clan(s)”; McSween 1999). In **Fig. 1.1** a simplified meteorite classification scheme is proposed.

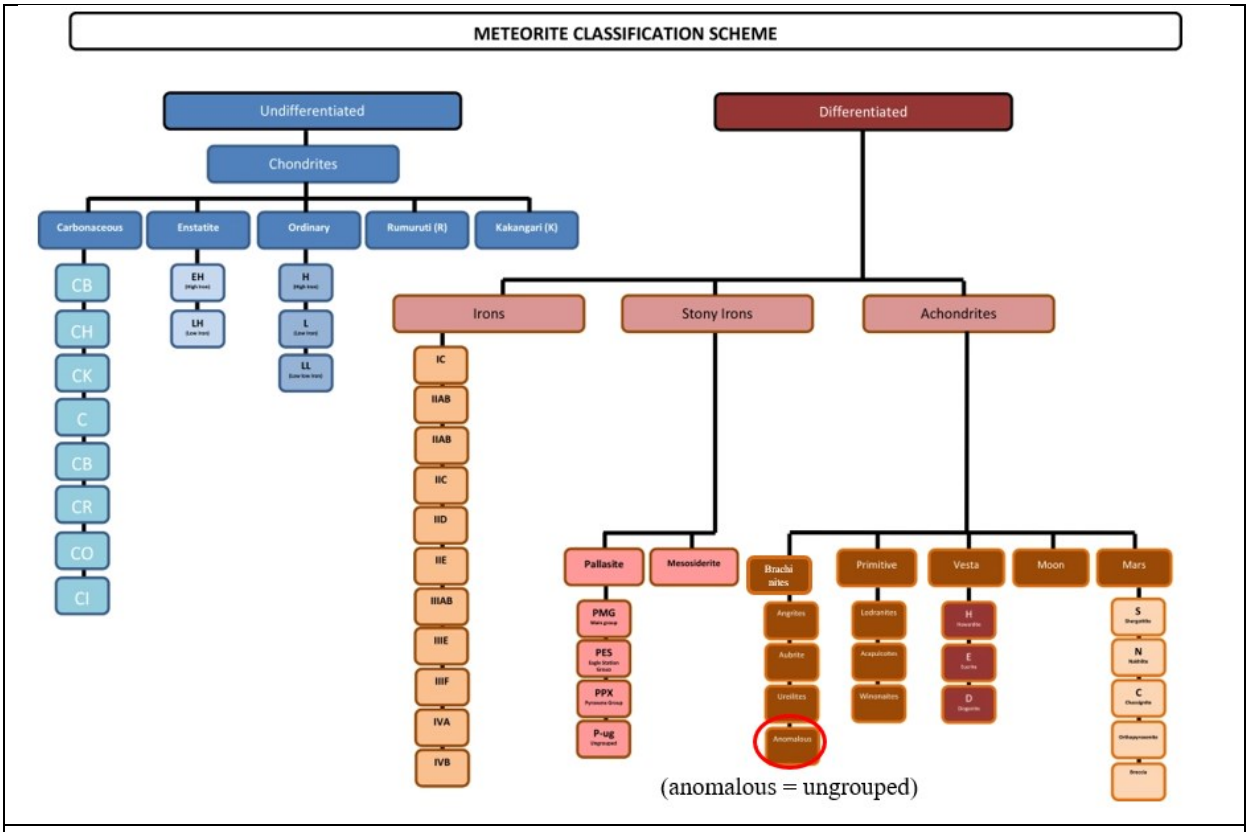

Fig. 1.1, meteorite classification scheme, image modified from NASA.

Meteorites can be subdivided in two different groups, the undifferentiated meteorites and the differentiated meteorites (McSween 1999). The undifferentiated meteorites (whose parent body did not have enough mass to undergo partial melting processes; **Fig. 1.2**) are the chondrites, which can be further subdivided in carbonaceous, enstatite, ordinary, rumuruti and kakangari (McSween 1999). The differentiated meteorites (whose parent body did have enough mass to undergo partial melting processes; **Fig. 1.2**) can instead be further subdivided in irons, stony irons and achondrites, which can be even further subdivided into many different subgroups, based on their petrography and geochemistry (McSween 1999).

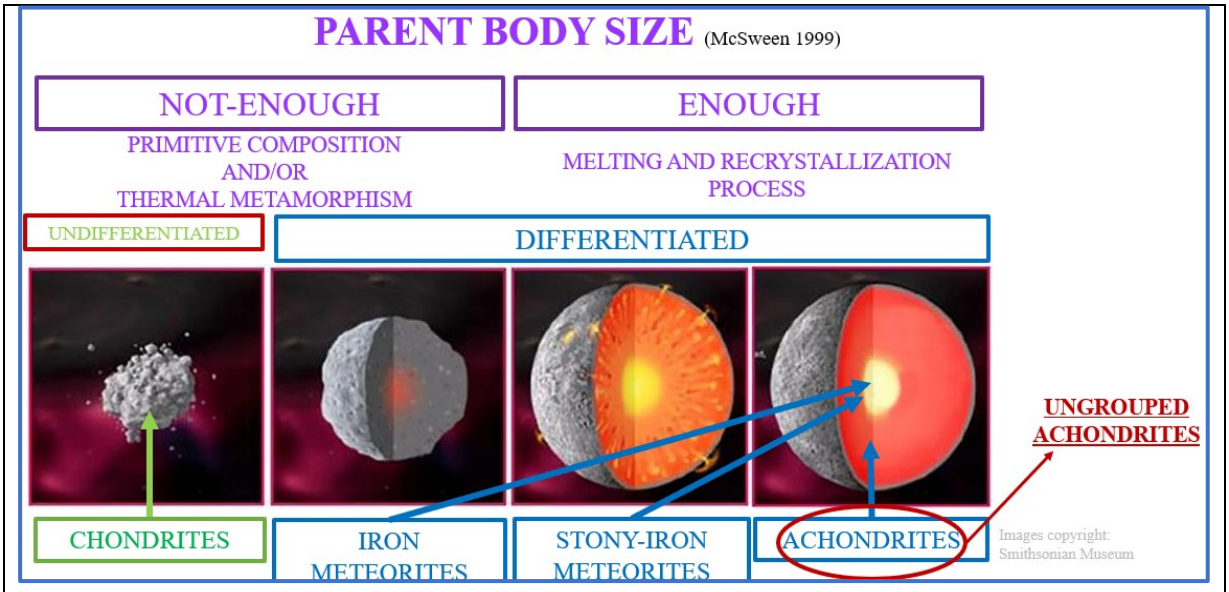

Fig. 1.2, formation process of undifferentiated and differentiated meteorites. Images from Smithsonian Museum.

Among the various types of meteorites, achondrites allow to understand differentiation processes, and, as a consequence, planetary processes (McSween 1999; Weisberg et al. 2006). While many achondrites are grouped based on similar mineralogical and petrological characteristics, there is a subset known as ungrouped achondrites, that defies easy classification (Weisberg et al. 2006). These meteorites present unique challenges and opportunities for researchers seeking to unravel the mysteries of our solar system's history.

Achondrites are meteorites that lack chondrules, the small, spherical grains found in chondritic meteorites (McSween 1999; Weisberg et al. 2006). They are believed to originate from differentiated planetary bodies such as asteroids, Mars, and possibly other planetary bodies within our solar system (McSween 1999; Weisberg et al. 2006). Achondrites are typically classified into several groups based on their mineralogical and petrological characteristics (e.g. HED and Martian meteorites)(McSween 1999; Weisberg et al. 2006). However, a subset of achondrites remains unclassified due to their unique composition and lack of clear association with known parent bodies (Weisberg et al. 2006; Jacquet 2022).

Ungrouped achondrites exhibit a wide range of petrological and mineralogical features, making their classification and origin challenging to ascertain (Mittlefehldt et al. 2022; Jacquet 2022). These meteorites often contain mineral assemblages not commonly found in other achondrite groups, such as unusual silicates, oxides, and sulphides (Mittlefehldt et al. 2022). As a consequence, it was not possible to classify these meteorites in any of the achondrite groups. Petrographic studies have revealed complex textures and structures within ungrouped achondrites, suggesting diverse formation histories and possibly multiple parent bodies (Jacquet 2022).

Geochemical analysis of ungrouped achondrites provides valuable insights into their origins and evolutionary histories (Weisberg et al. 2006). These meteorites exhibit a variety of elemental abundances and isotopic compositions, which can be compared with known achondrite groups and terrestrial samples to infer their parent body's nature and differentiation processes (McSween 1999; Weisberg et al. 2006). Isotopic studies, including radiogenic isotopes such as lead, neodymium, and oxygen isotopes, have been instrumental in tracing the origins of ungrouped achondrites and their relationship to other solar system materials (Weisberg et al. 2006).

The origin of ungrouped achondrites remains a subject of debate among researchers. Various hypotheses have been proposed, including their formation on unknown or extinct planetary bodies (Lauretta et al. 2006), impact mixing events (Yang et al. 2019), or from differentiated parent bodies that have undergone extensive alteration processes (Cloutis et al. 2018). Some ungrouped achondrites may represent fragments of larger parent bodies that were disrupted through collisions or other catastrophic events, leading to their unique compositions and characteristics (Lauretta et al. 2006).

Despite their enigmatic nature, ungrouped achondrites play a crucial role in advancing our understanding of planetary science and cosmochemistry (Weisberg et al. 2006). These meteorites provide valuable constraints on the processes involved in planetary differentiation, magma ocean crystallization, and thermal evolution within our solar system. By studying ungrouped achondrites alongside other meteorite groups and planetary samples, researchers can piece together the complex puzzle of solar system formation and evolution (Weisberg et al. 2006).

The five meteorites studied in this thesis work, MIL090206, MIL090405, NWA6077, NWA5363 and NWA11187, are currently classified as ungrouped achondrites (Ruzicka et al. 2014; Ruzicka et al. 2015; Garvie 2012; Gattacceca et al. 2019), but all of them share a complex story for their classification. MIL090206, MIL090405, NWA6077 and NWA5363 are in fact considered ungrouped achondrites related to brachinites, based on Ca and Cr content of the olivines, O isotopes, and grain boundary mineralogy (Warren and Rubin. 2012; Goodrich et al. 2012). In addition, MIL090206 and MIL090405 are considered as closely related to MIL090340, MIL090356, MIL090805 and MIL090963 (Warren and Rubin. 2012; Goodrich et al. 2012), while NWA6077 and NWA5363 are considered as closely related to NWA5400 (Weisberg et al. 2009). MIL090206 was originally classified as an ureilite (Satterwhite et al. 2011), and NWA11187 was considered to be related to ureilites, since the oxygen isotopes for this meteorite plot near the trend for ureilites, but was classified as an ungrouped achondrite based on the exsolution lamellae of clinopyroxene in orthopyroxene and the forsteritic olivine composition (Gattacceca et al. 2019).

Scanning Electron Microscopy (SEM) analyses were carried out on the samples in order to study their petrography and mineralogical assemblage, through acquisition of Back-Scattered Electron images (BSE) and elemental maps. Electron Microprobe (EPMA) analyses were carried on the samples in order to study the chemistry of the samples for major and minor elements, while Laser Ablation Inductively Coupled Plasma Mass Spectrometry (LA-ICP-MS) was used in order to study the chemistry of the samples for trace elements. In the following paragraphs the methods will be discussed in detail.

1.1 SAMPLES

The provenance and details about the following samples: MIL 090206, MIL 090405, NWA 5363 and NWA 6077 is reported below (for further details see Cuppone et al. in prep).

Miller Range 090206 and 090405 (brachinite like achondrites)

These meteorites were found in on the Miller Range icefield in Antarctica during the 2009 ANSMET season (Righter, 2011). They were first classified by C. Corrigan, L. Welzenbach,

A. Beck and N. Lunning as a ureilite and then reclassified as an ungrouped achondrite (Righter, 2012), possibly related to brachinites according to the petro-mineralogic and isotopic studies by Goodrich et al. (2012). The National Institute of Polar Research (NIPR) has loaned the sample that has been studied in this work and it consists of a small fragment.

Northwest Africa 5363 and 6077 (brachinite like achondrites)

NWA 5363: this ungrouped achondrite belongs to the pairing NWA 5400 group (Garvie, 2012), which also comprises NWA 6077 (Ruzicka et al., 2014). Both samples have been purchased by private dealers in the form of fragments.

Northwest Africa 11187

The meteorite has a total mass of 36.7 g, and was purchased by John Higgins in October 2016 from a dealer in Nouakchott, Mauritania (Gattacecca et al. 2019).

2. METHODS

The five meteorites MIL090206, MIL090405, NWA6077, NWA5363 and NWA11187 were embedded in epoxy resin, exposed and polished to be analysed.

2.1 Scanning Electron Microscopy (SEM)

SEM analyses were performed at Dipartimento di Geoscienze, Università degli studi di Padova through the use of a CamScan MX3000. In total, 32 BSE images were acquired (6 MIL090206, 8 MIL090405, 5 NWA6077, 7 NWA5363 and 6 NWA11187), in order to study the petrological fabric and mineralogical assemblages of the rocks and 7 elemental maps (2 for MIL090206 and MIL090405, 1 for every other meteorite), to study the distribution of Si, Ca and Na among certain areas of the samples. The BSE images are 16-bit gray scale and are 2560x2560 (same size as the elemental maps). The magnification used for their acquisition varies from 261x to 1620x, with an energy varying from 5 kev to 15 kev. Modal analyses were performed on the 32 BSE images, in order to study the distribution of minerals in the samples of the meteorites and their relationships. A 16-cell grid was applied to every image for this purpose (dimensions of the cells varying proportionally with magnification, for two images of MIL090206 an 8-cell and a 12-cell grid were applied).

2.2 Electron Microprobe

As reported by Cuppone et al. in prep EPMA analyses were carried out at the joined laboratory (LaMa, Laboratorio MicroAnalisi) of the Earth Sciences Department of the University of Firenze (DST) and the National Council of Research – Institute of Geosciences and Earth Resources (CNR-IGG) of Firenze using a JEOL JXA-8230 SuperProbe equipped with five Wavelength Dispersive Spectrometers (WDS). The acquisitions were obtained at operating conditions of 15 keV accelerating voltage, 20 nA beam current and a beam size of 1 μm. The following Astimex compositional standards have been used for the analyses: olivine, augite, enstatite, pigeonite, oligoclase, andesine, chromite, apatite. Augite (USNM 122142) and ilmenite (USNM 96189), provided by Smithsonian Institution, were also used as standards. All data were then processed with the iteratively corrective ZAF reduction model. Detection limits were 0.02 wt% 0.05wt% for major element oxide abundances.

2.3 LA-ICP-MS

LA-ICP-MS was carried out on the five meteorite samples at Instituto di Geoscienze e Georisorse (CNR) hosted by the Dipartimento di Scienze della Terra e dell'Ambiente, Università degli Studi di Pavia. The laser uses a pulsed Nd:YAG laser source Brilliant (Quantel, Les Ulis, France) whose

fundamental emission in the infrared (1064 nm) was converted into 266 nm by means of two harmonic generators. The particles produced by ablation were then analyzed by a triple quadrupole ICP mass spectrometer (QQQ) type 8900 from Agilent Technologies. The gas flow rates, torch parameters, ion-lenses and acceleration voltages on the QQQ were optimized by ablation of the National Institute of Standards and Technology (NIST) standard reference material SRM 610, representing a synthetic glass doped with trace elements. The NIST SRM 610 glass was ablated at a 10 Hz repetition rate, a 6 J/cm^2 fluence, a 50 μm beam size and with a pulse energy of about 0,1 mj. The operating conditions were set to obtain maximum sensitivity while maintaining equal sensitivity of Th and U, to ensure their complete ionization and minimize fractionation effects, and low ThO^+ production ($ThO^+/Th <$ 0.2%). Ablation signal integration intervals were selected by carefully inspecting the time-resolved analysis to ensure that no inclusions were present in the analyzed volume, and data reduction was performed by the software package GLITTER (4.4.4). NISTSRM 612 (Pearce et al., 1997) and BCR-2 USGS were used external standards, whereas as internal standard we used ^{44}Ca for clinopyroxene, ^{29}Si for olivine and orthopyroxene and ^{53}Cr for chromite. Before undertaking any measurements for a sample, two analyses of NIST SRM 612 and one of BCR-2 USGS were always performed, as they were also performed at the end of every run of measurements. Olivine, clinopyroxene, orthopyroxene and plagioclase minerals were analyzed in all the samples through the use of this technique. RSD values were consistently below 20%, with the exception of some REE elements with very low concentrations in some of the types of minerals previously mentioned. For every measurement, the analysis was composed of 30 s of background at the start, 60 s of ablation signal and another 30 s of background at the end, with a total time for every measurement of ~120 s.

3. RESULTS

3.1 Petrography

In **Table 3.0** the modal analyses for each meteorite studied in this work are reported.

Table 3.0, Modal analyses for the studied meteorites. a) Modal analysis of MIL090206; b) Modal analysis of MIL090405; c) Modal analysis of NWA6077; d) Modal analysis of NWA5363; e) Modal analysis of NWA11187.

a)

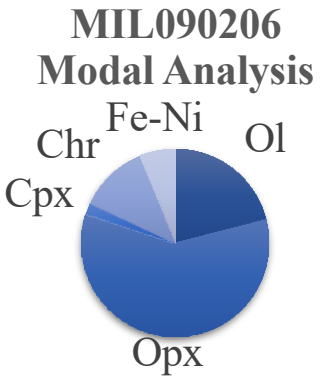

b)

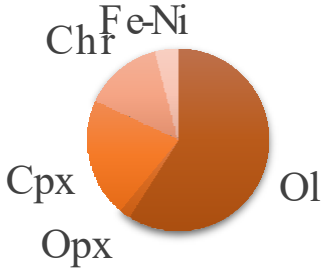

c)

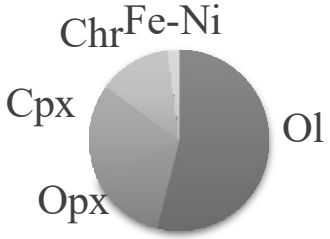

d)

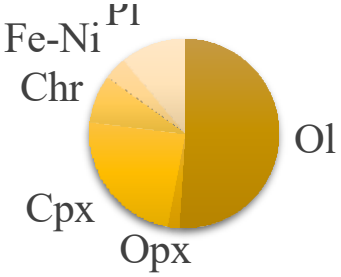

e)

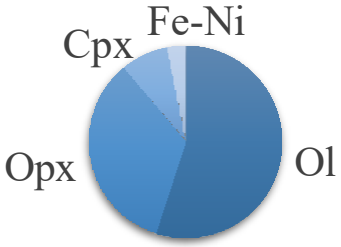

3.1.1. Miller Range 090206

By the modal analysis carried out on 6 BSE (**Table 3.0**) images of Miller Range 090206 (MIL090206) meteorite **(Fig. 3.1.1**) it results that its composition is made of orthopyroxene (59 vol%), olivine (21 vol%), chromite (12 vol%), Fe-Ni phases (6 vol%) and minor clinopyroxene (2 vol %). In the meteorite, it is possible to see triple junctions (**Fig. 3.1.2**), which suggests that the rock underwent some partial melting processes, which led to extensive recrystallization (Benedix et al. 1998). Fractures are often highlighted by the presence of chromite and Fe-Ni phases, the latter occur also as thin films at the grain boundaries (**Fig. 3.1.2**). Orthopyroxene is usually subhedral, equigranular and occur as poikiloblasts (**Fig. 3.1.3**), locally up to 1.0-1.2 mm in size. Olivine is equigranular and occurs usually as rounded inclusions within orthopyroxene, with an average size around 100-200 µm. Chromite and Fe- Ni phases are often subhedral, but some crystals can also be euhedral (**Fig. 3.1.4**), and their size tend to vary a lot (mainly Fe-Ni phases), in fact some Fe-Ni phases have size ranging from a few µm to 2.5 mm. Minor clinopyroxene is usually of small size (less than 100 µm), and can also appear as rounded crystals (**Fig. 3.1.3**). The meteorite is weathered, and the most weathered crystals are the olivine ones, as olivine is often replaced (both at the rim and in the core) by fine-grained intergrowths of orthopyroxene, Fe-Ni phases and locally spinel (chromite mainly, **Fig. 3.1.3, 3.1.5**). This, was one of the factors which led researchers to originally classify this meteorite as an ureilite (Carli et al. 2023).

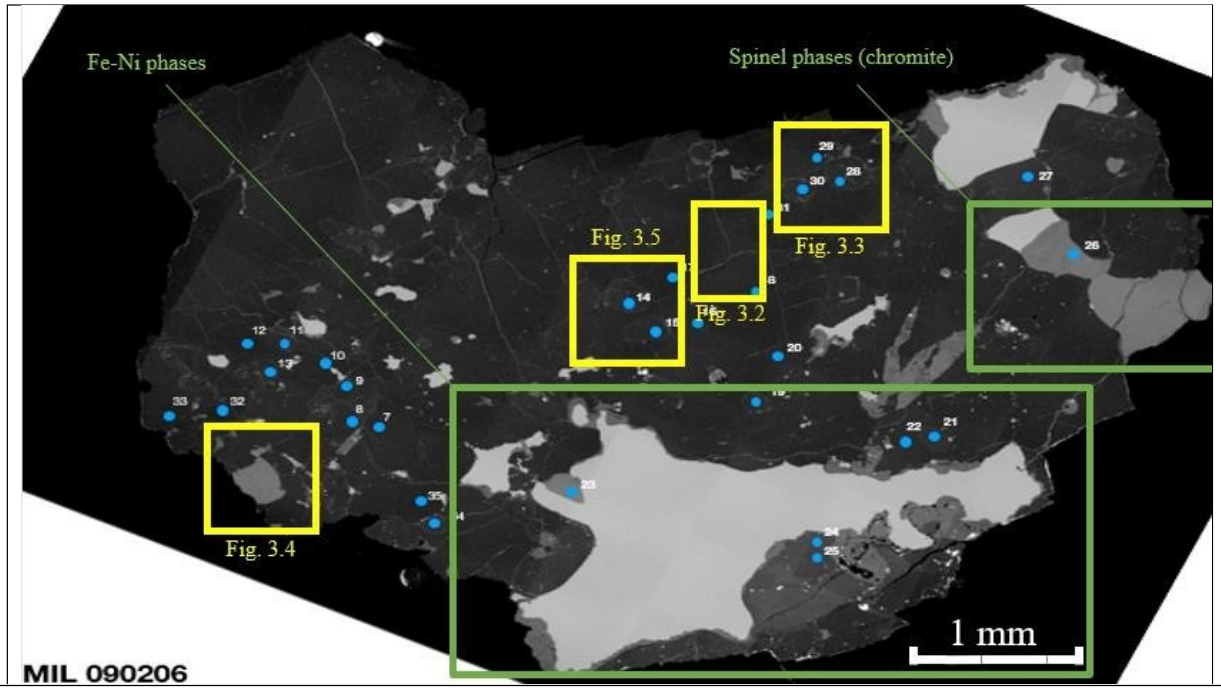

Fig. 3.1.1, a BSE image of the MIL090206 meteorite. The blue dots are the data points of the LA-ICP-MS Fe-Ni phases appear white in color with a size around 2.5 mm and chromite crystal in light-grey with a size around 0.9 mm (green rectangles). Yellow rectangles represent areas of the meteorite that will be further analyzed in the next images.

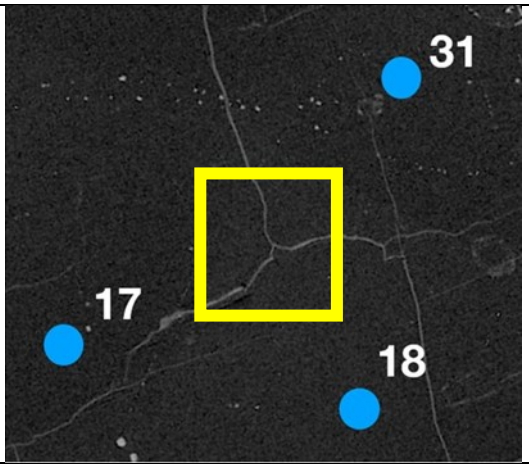

Fig. 3.1.2, BSE image of a triple junction between three orthopyroxene crystals (yellow rectangle). The triple junction, with fractures at 120°, is highlighted by the presence of Fe-Ni phases.

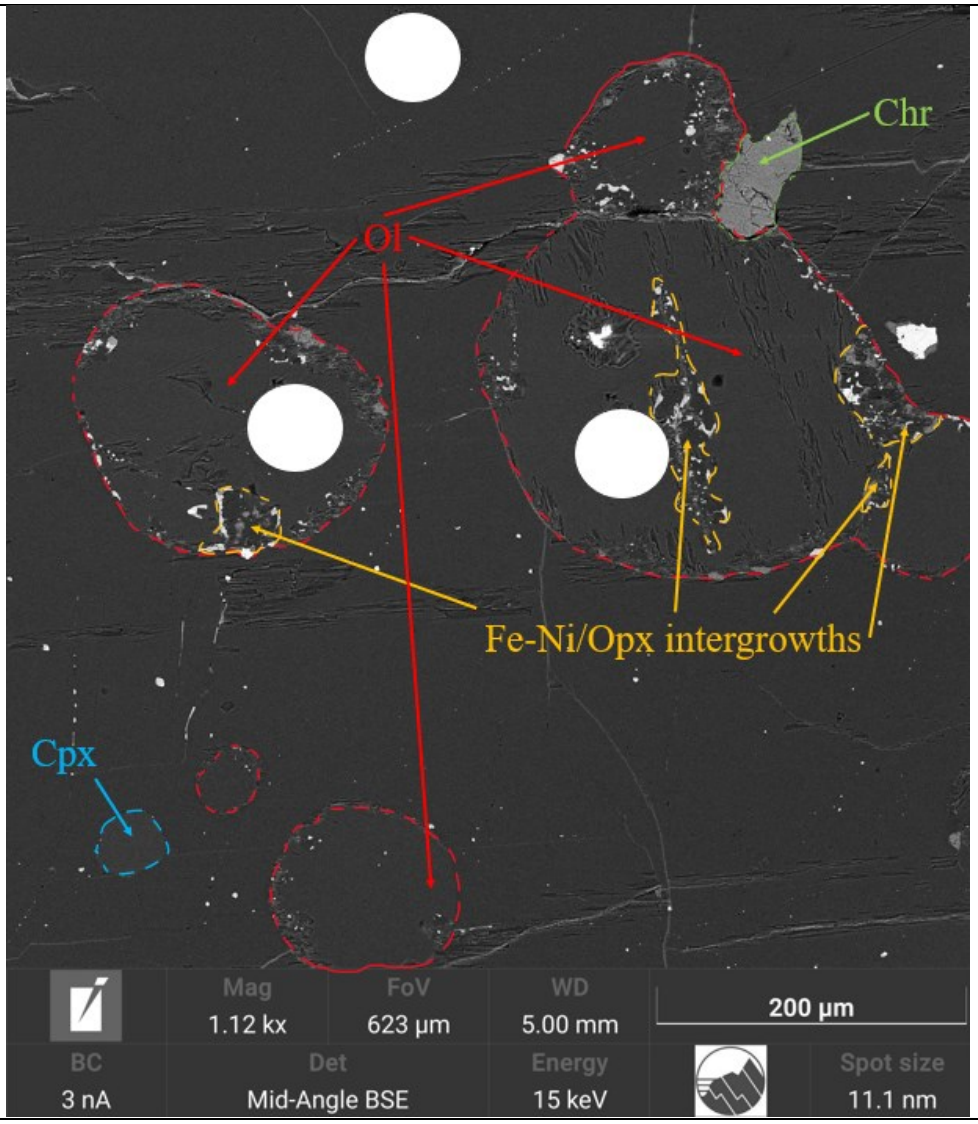

Fig. 3.1.3, a BSE image with orthopyroxene poikiloblasts. The red circled crystals are rounded olivines, with their weathered rims, the yellow circled areas are the main weathering zones (fine-grained intergrowths of orthopyroxene and Fe-Ni phases), the orange circled crystal is a clinopyroxene (clinopyroxene is easier to distinguish from olivine, as it is not weathered), while the white circled areas are the data points for LA-ICP-MS.

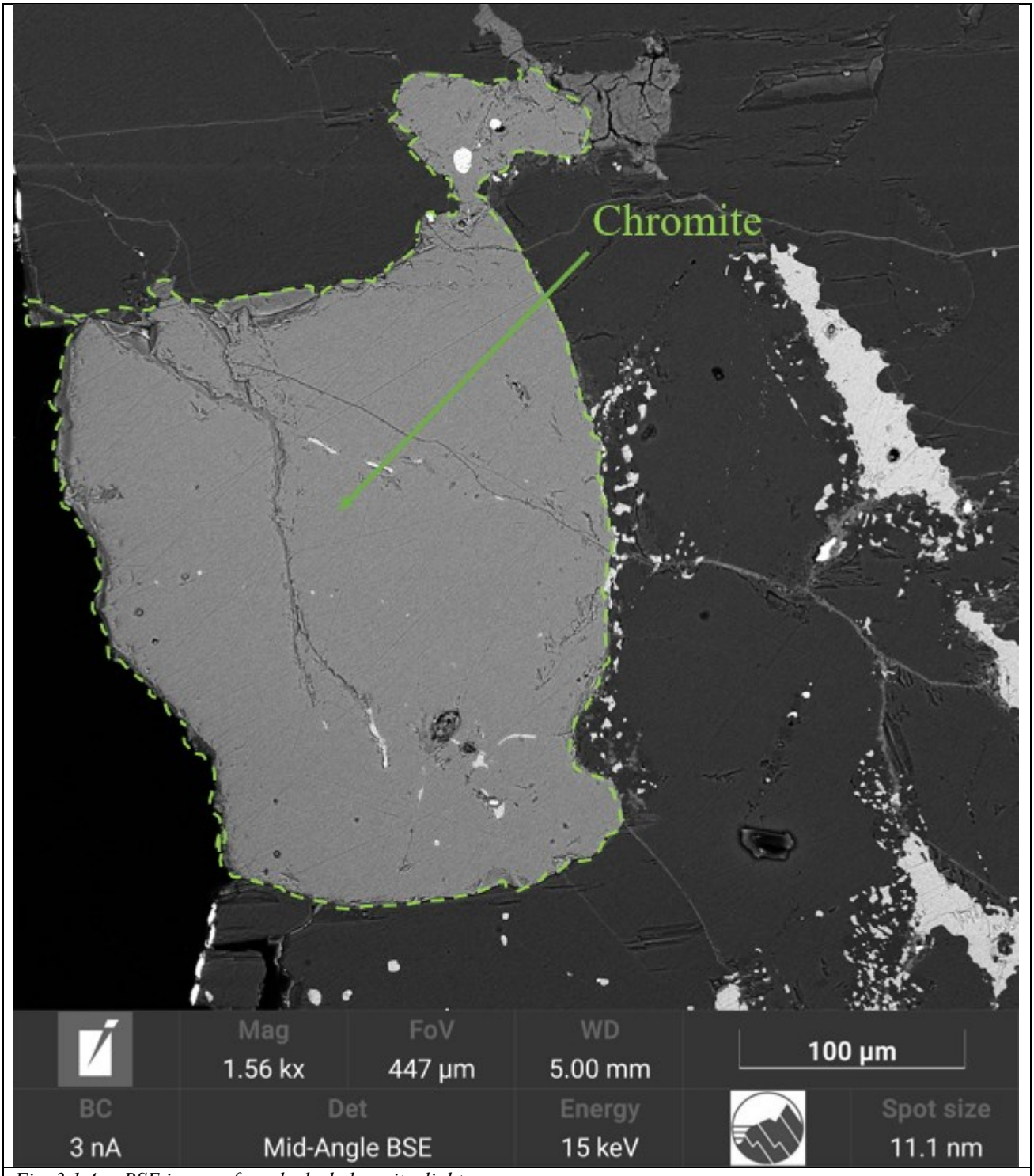

Fig. 3.1.4, a BSE image of a euhedral chromite, light-grey.

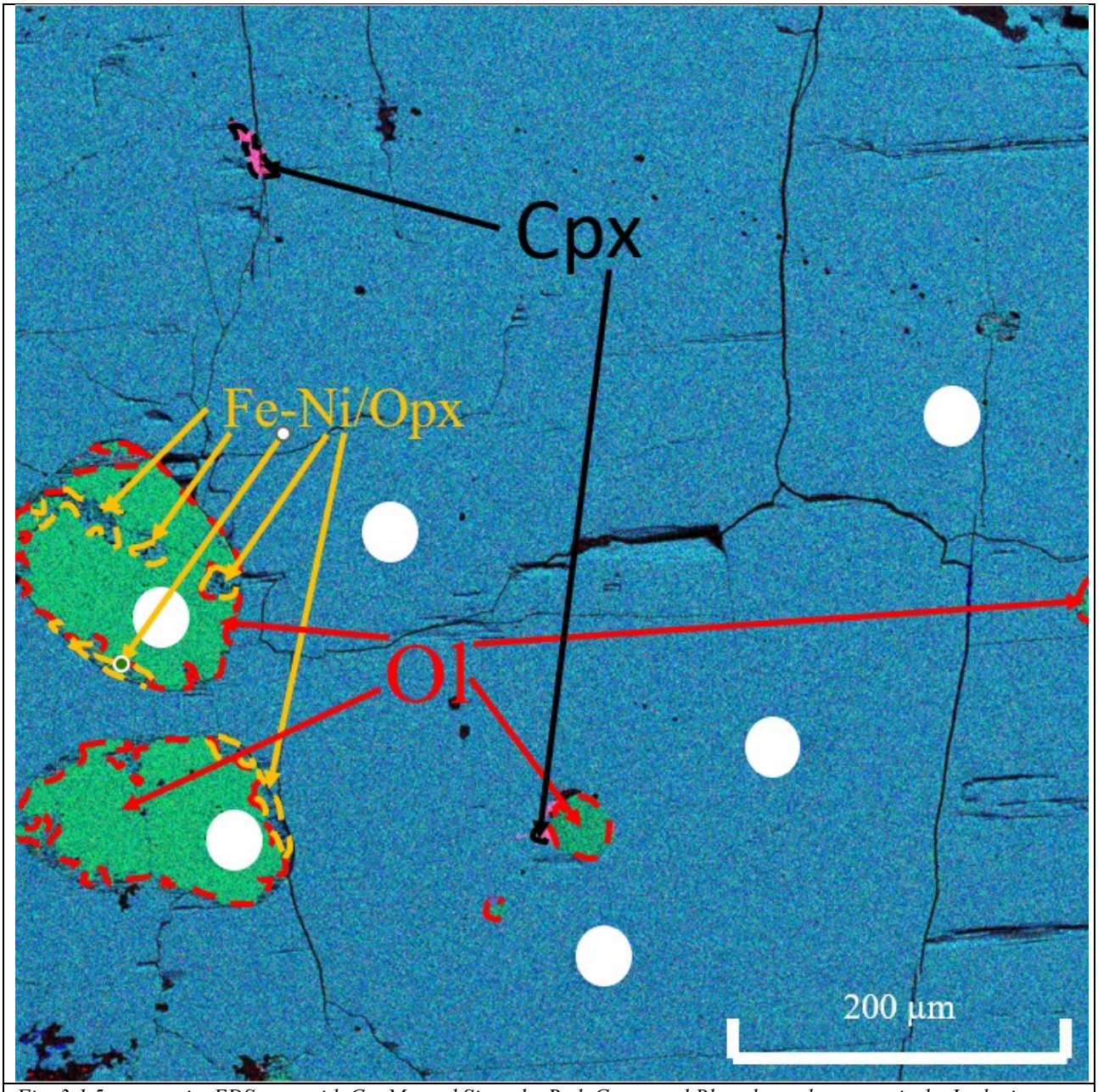

Fig. 3.1.5, composite EDS map with Ca, Mg and Si on the Red, Green and Blue channels, respectively. In the image, are shown four different minerals: orthopyroxene (light-blue), olivine (green) and clinopyroxene (pink-to-red). The white circled areas are the data points for LA-ICP-MS. In the weathered olivines it is possible to see the fine-grained assemblages of Fe-Ni phases and orthopyroxene.

3.1.2 Miller Range 090405

The modal analysis performed on 8 BSE images (**Table 3.0**) of Miller Range 090405 (MIL090405, **Fig. 3.1.6**) shows that this meteorite is composed of olivine (59 vol %), clinopyroxene (21 vol%), chromite (14 vol%), Fe-Ni phases (4 vol%) and Orthopyroxene (2%). Olivine is usually subhedral and equigranular, with an average size of about 200-300 µm. Clinopyroxene (**Fig. 3.1.7 a**) is usually equigranular with a crystal size up to 600 µm; some clinopyroxene are euhedral. Locally, clinopyroxene minerals poikilitically enclose small rounded olivine grains. The contact between these two primary phases is often at 120°. Fe-Ni phases and chromite are generally anhedral to subhedral, and often very fine-grained, occasionally chromite crystals can reach up to 300 µm in diameter (**Fig. 3.1.7 b**). Orthopyroxene is generally subhedral, with a size of a few µm. This meteorite has experienced more weathering than MIL090206; the most weathered crystals are the olivine ones (**Fig. 3.1.7 c**), as olivine is often replaced by fine-grained intergrowths of orthopyroxene, Fe-Ni phases and locally spinel (as for MIL 090206). MIL090405 is also more fractured than MIL090206 (**Fig. 3.1.7 d**). The fracture pattern is often characterized by the presence of chromite and Fe-Ni phases. Because of the high content in Fe-Ni phases triple junctions are more evident than in MIL090206 (**Fig. 3.1.8**).

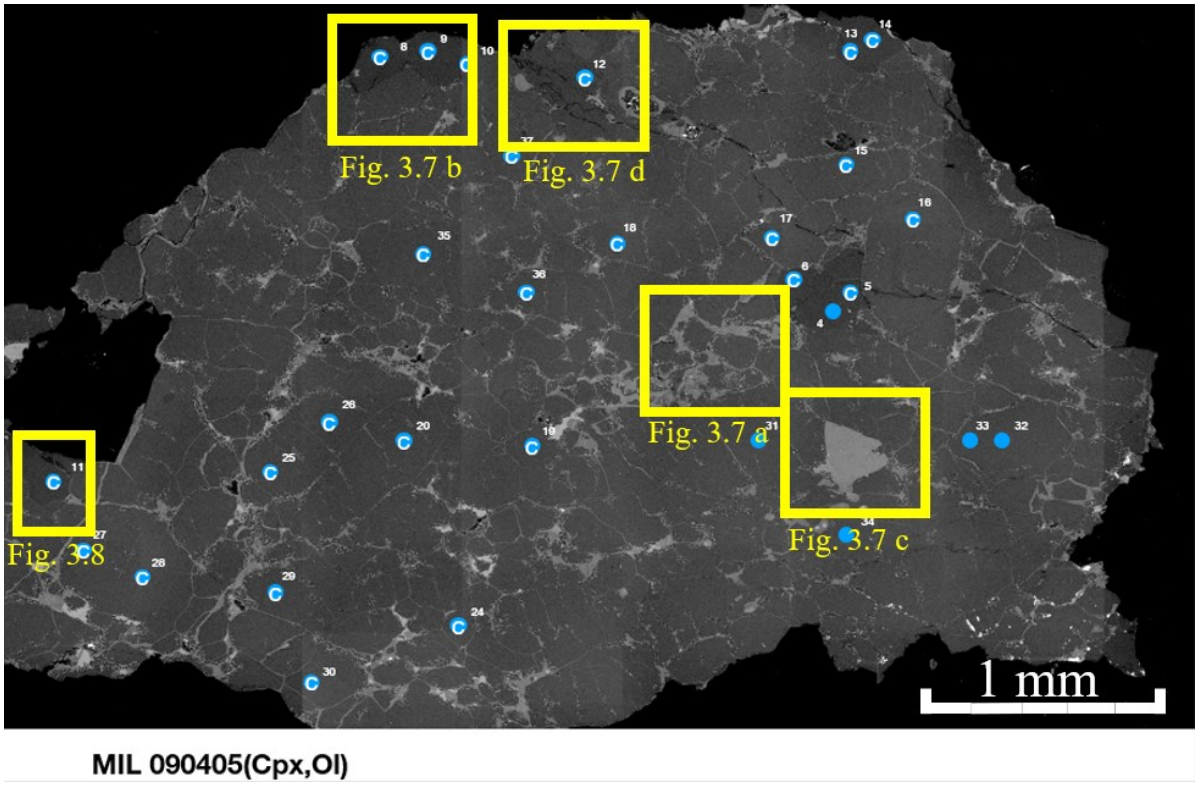

Fig. 3.1.6, a BSE image of MIL090405 meteorite. The blue dots are the data points of the LA-ICP-MS (the ones marked with a "C" were taken first, while the others were taken during a second session of analysis). Yellow rectangles represent areas of the meteorite that will be further analyzed in the next images.

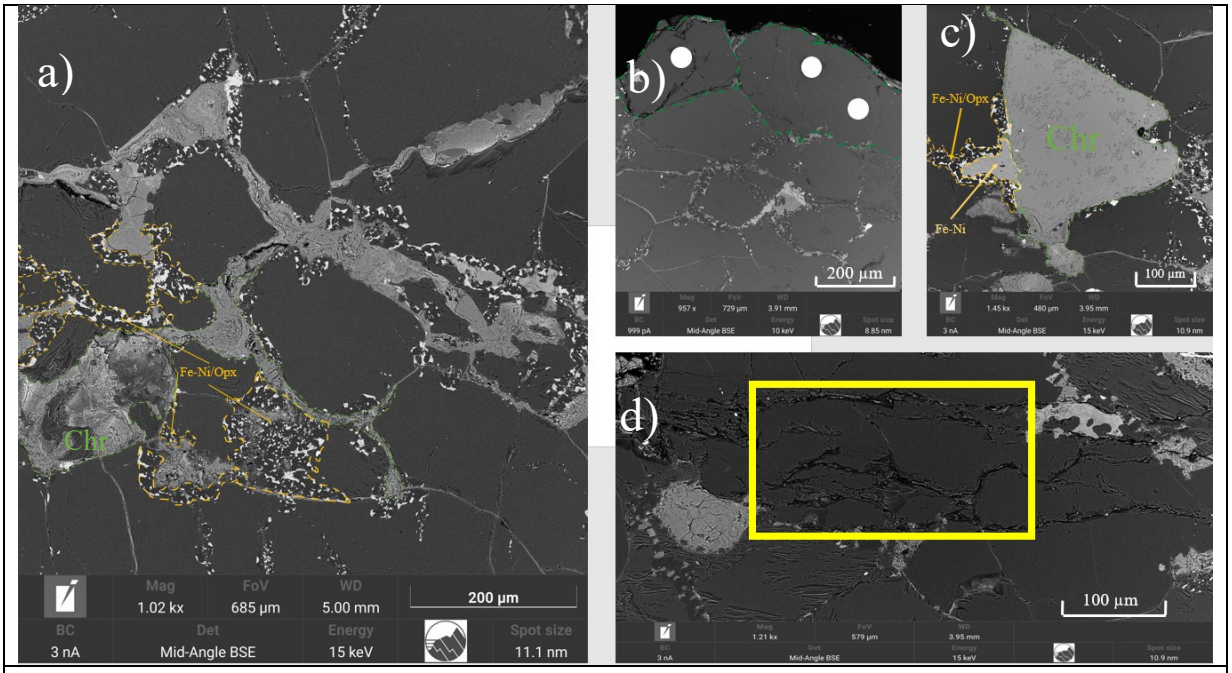

Fig. 3.1.7 BSE images of: a) weathered olivine and spinel veins (chromite). The orange contour encloses fine-grained intergrowths of orthopyroxene and Fe-Ni phases replacing olivine; b) subhedral-to-euhedral clinopyroxene, circled in green. The white circles are the LA-ICP-MS spots; c) chromite grain and Fe-Ni; d) intensely fractured area.

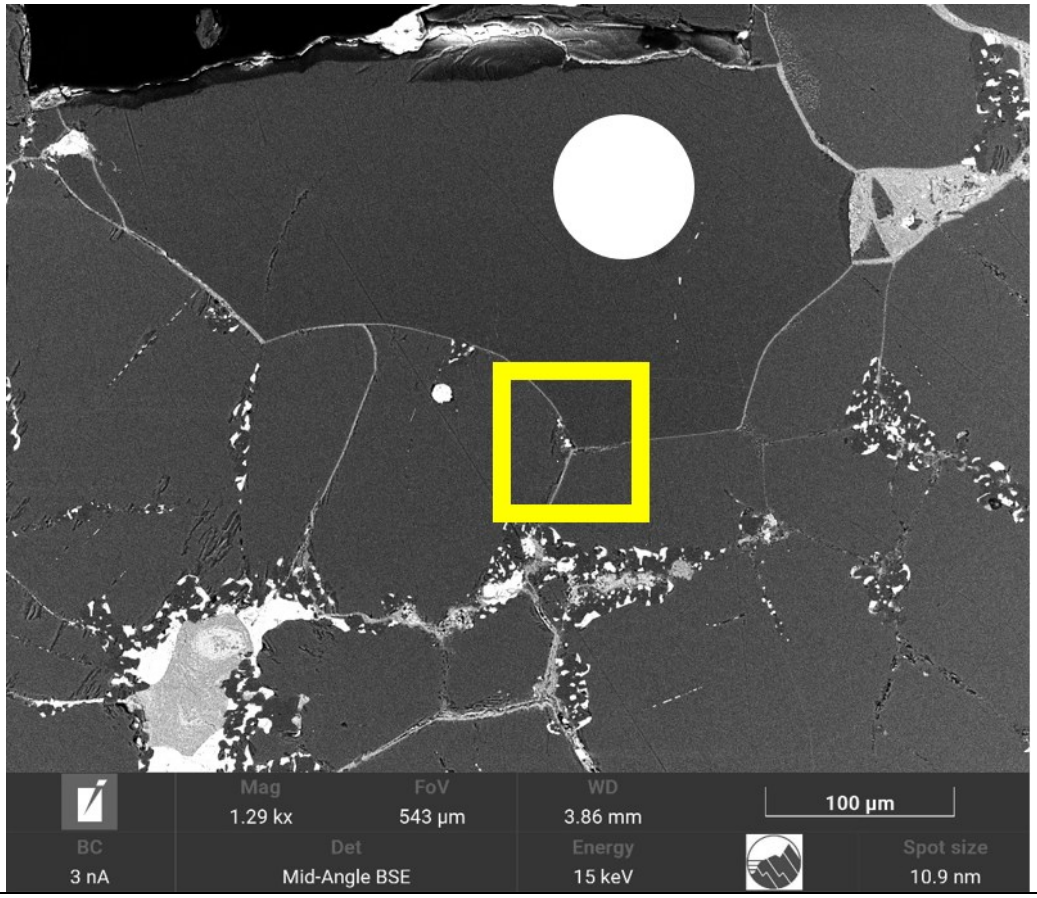

Fig. 3.1.8, a BSE image of a clinopyroxene. Some triple junctions between one clinopyroxene crystal and two olivine crystals (yellow rectangle). The blue circled areas are the data points for LA-ICP-MS.

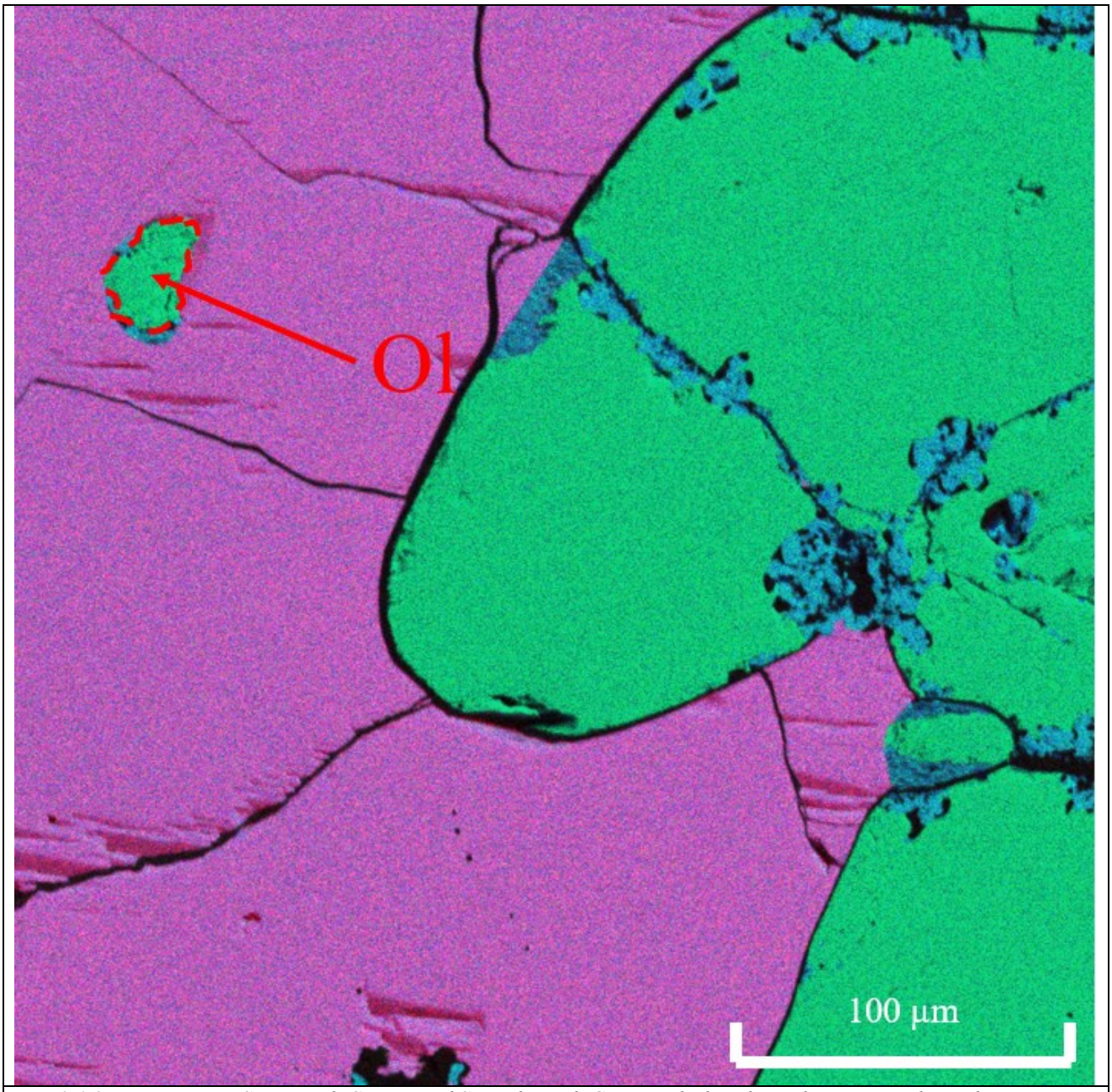

Fig. 3.1.9, composite EDS map with Ca, Mg and Si on the Red, Green and Blue channels, respectively. In the image, are shown four different minerals: orthopyroxene (light-blue), olivine (green), clinopyroxene (pink-to-red) and Fe-Ni phases (black with scattered red). In the weathered olivines it is possible to see the fine-grained intergrowths of Fe-Ni phases and orthopyroxene. A small rounded olivine is poikilitically enclosed in a clinopyroxene (red circle).

3.1.3 North West Africa 6077

By modal analysis made on 5 BSE images (**Table 3.0**) of the meteorite North West Africa 6077 (NWA6077, **Fig. 3.1.10**) it results that it is composed of olivine (54 vol%), clinopyroxene (17 vol%), orthopyroxene (14 vol%), chromite (13 vol%), Fe-Ni phases (2 vol%) and minor apatite (slightly above 0 vol%) as from the data collected. The meteorite shows a protogranular texture, with olivine subhedral to euhedral and equigranular, with an average size of about 400 micrometers. Some pyroxene crystals poikilitically enclose some olivine rounded crystals (**Fig. 3.1.11 a**). In this meteorite, there is a quite high amount of chromite and Fe-Ni phases, of various size. Apatite is usually subhedral, with an average crystal size of about 300-400 µm (**Fig. 3.1.11 b**). NWA6077 shows less weathering compared to MIL090206 and MIL090405 but a rather complex fracture network, probably due to a shock event (**Fig. 3.1.12** fine-grained intergrowths of Fe-Ni phases and orthopyroxene are still evident). Triple junctions in this meteorite are very clear, highlighted by the Fe-Ni content. Triple junctions suggest that the meteorite underwent pervasive partial melting processes, which led to extensive recrystallization.

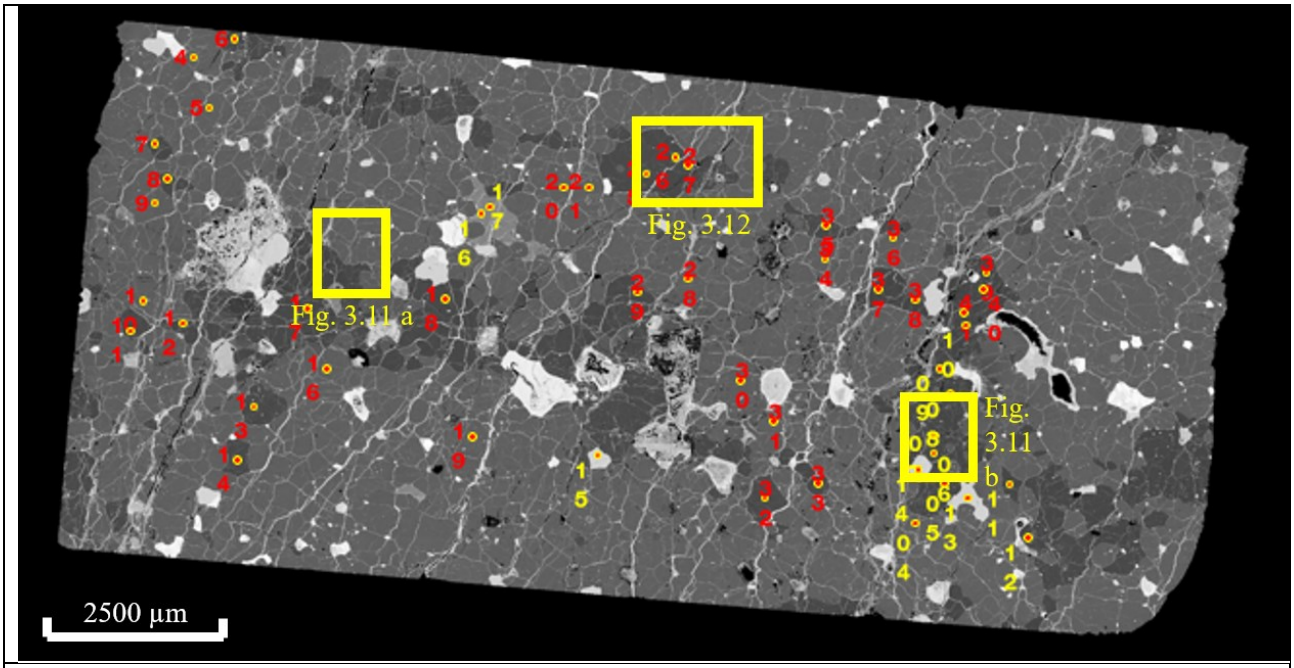

Fig. 3.1.10, a BSE image of NWA6077 meteorite. The red dots are the data points of the LA-ICP-MS (the ones marked with a red number were taken first, while the others were taken during a second session of analysis). Yellow rectangles represent areas of the meteorite that will be further analyzed in the next images. The network of fractures is highlighted by the white and grey light color related to Fe-Ni phases and oxides.

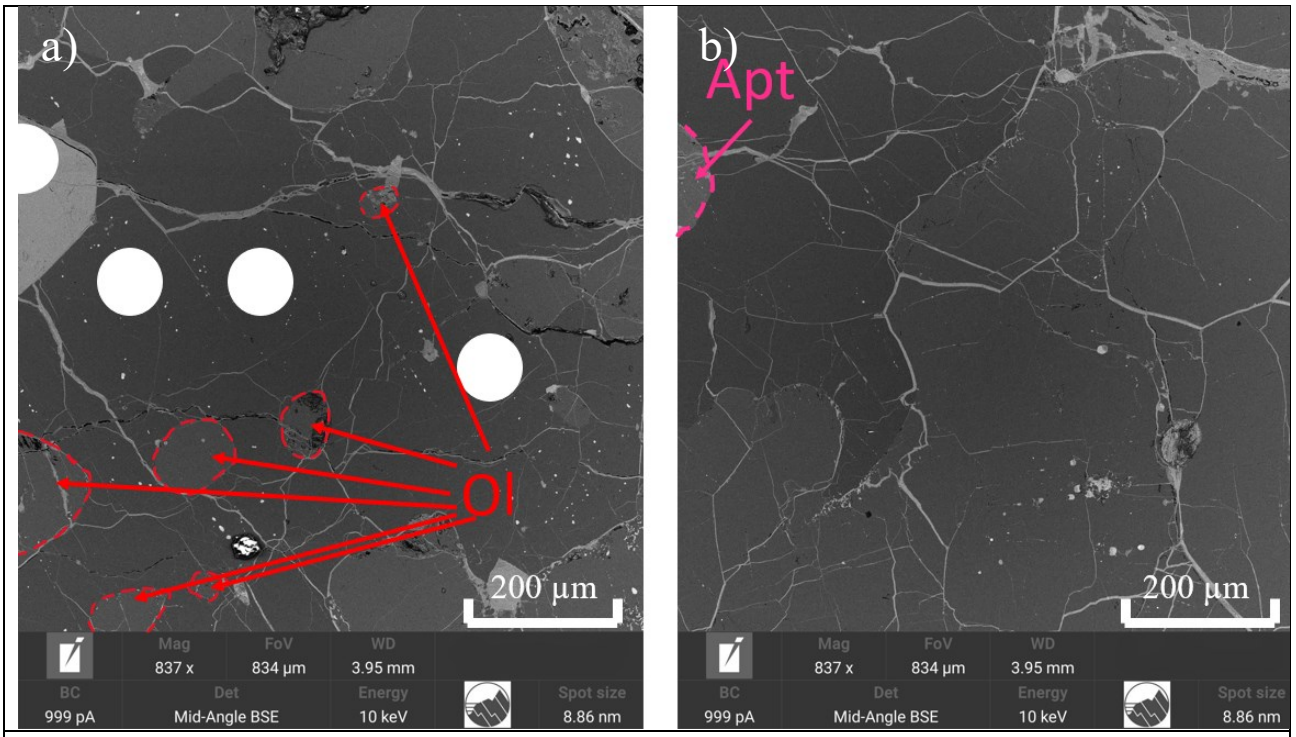

Fig. 3.1.11, BSE images of: a) orthopyroxene poikiloblasts enclosing some rounded olivines (red circles). The white circled areas are the data points for LA-ICP-MS; b) apatite crystal (purple circle).

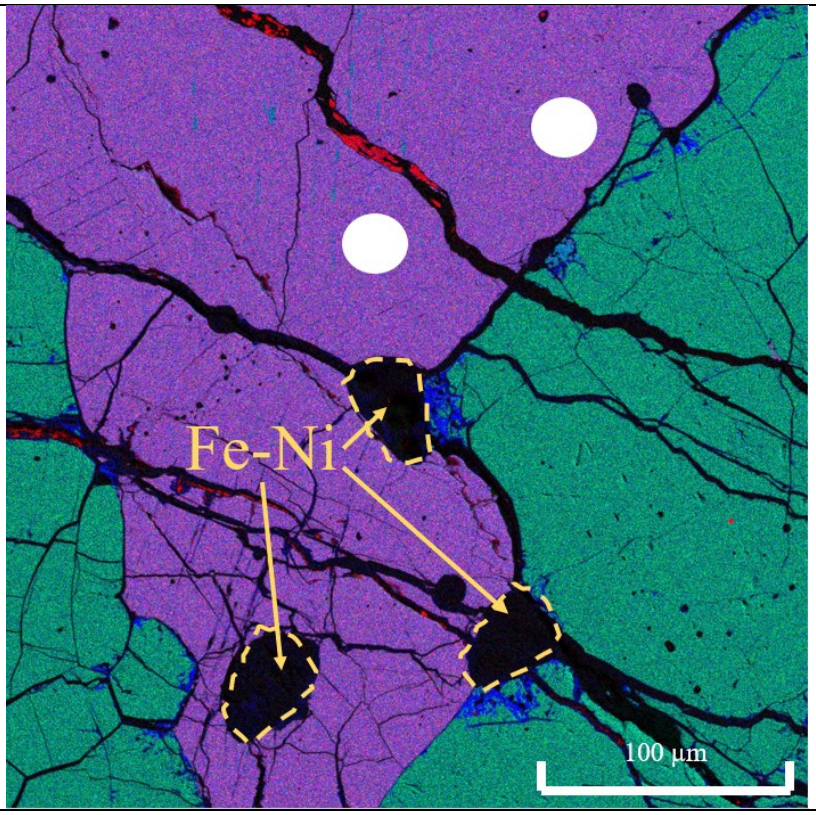

Fig. 3.1.12, composite EDS map with Ca, Mg and Si on the Red, Green and Blue channels, respectively. In the image, are shown four different minerals: orthopyroxene (light-blue), olivine (green), clinopyroxene (pink-to-red) and Fe-Ni phases (black with scattered red). The white circled areas are the data points for LA-ICP-MS. In the weathered olivines it is possible to see the fine-grained intergrowths of Fe-Ni phases and orthopyroxene.

3.1.4 North West Africa 5363

By modal analysis made on 7 BSE images (**Table 3.0**) of the meteorite North West Africa 5363 (NWA5363, **Fig. 3.13**) it results that it is composed of olivine (51 vol%), clinopyroxene (24 vol%), plagioclase (11 vol%), chromite (8 vol%), Fe-Ni phases (4 vol%) and minor orthopyroxene (2 vol%). Triple junctions (**Fig. 3.1.14**) are still evident (mostly between olivine crystals, with angles of 120°), as evidence of partial melting processes. Olivine crystals are subhedral and equigranular, and their average size is about 500-600 µm. olivine crystals can locally be poikilitically enclosed in plagioclase crystals (**Fig. 3.1.15**). Clinopyroxene and orthopyroxene crystals are subhedral, equigranular and slightly larger than olivine crystals, with an average size of 700-800 µm. Plagioclase is equigranular and subhedral to euhedral, with an average size of 800-900 µm. Fe-Ni phases and chromite crystals have instead different size and are subhedral. Olivine is locally replaced by fine-grained intergrowths of orthopyroxene, Fe-Ni phases and spinel. The meteorite has a complex fracture network, probably due to a shock event.

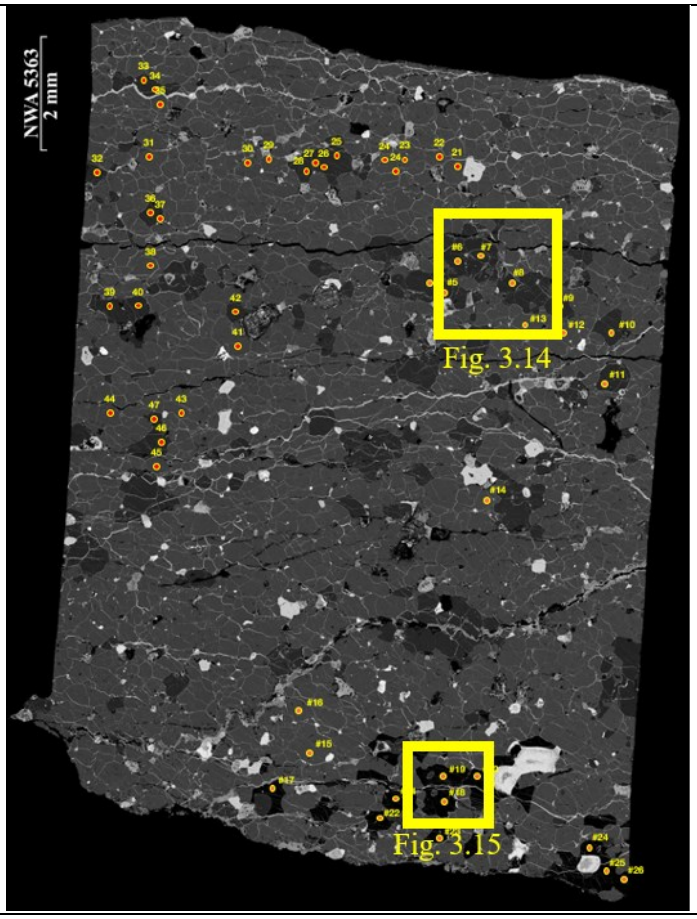

Fig. 3.1.13. a BSE image of NWA5363 meteorite. The red dots are the data points of LA-ICP-MS analysis (the ones marked with a "#" were taken first, while the others were taken during a second session of analysis). Yellow rectangles represent an area of the meteorite that will be further analyzed in the next images.

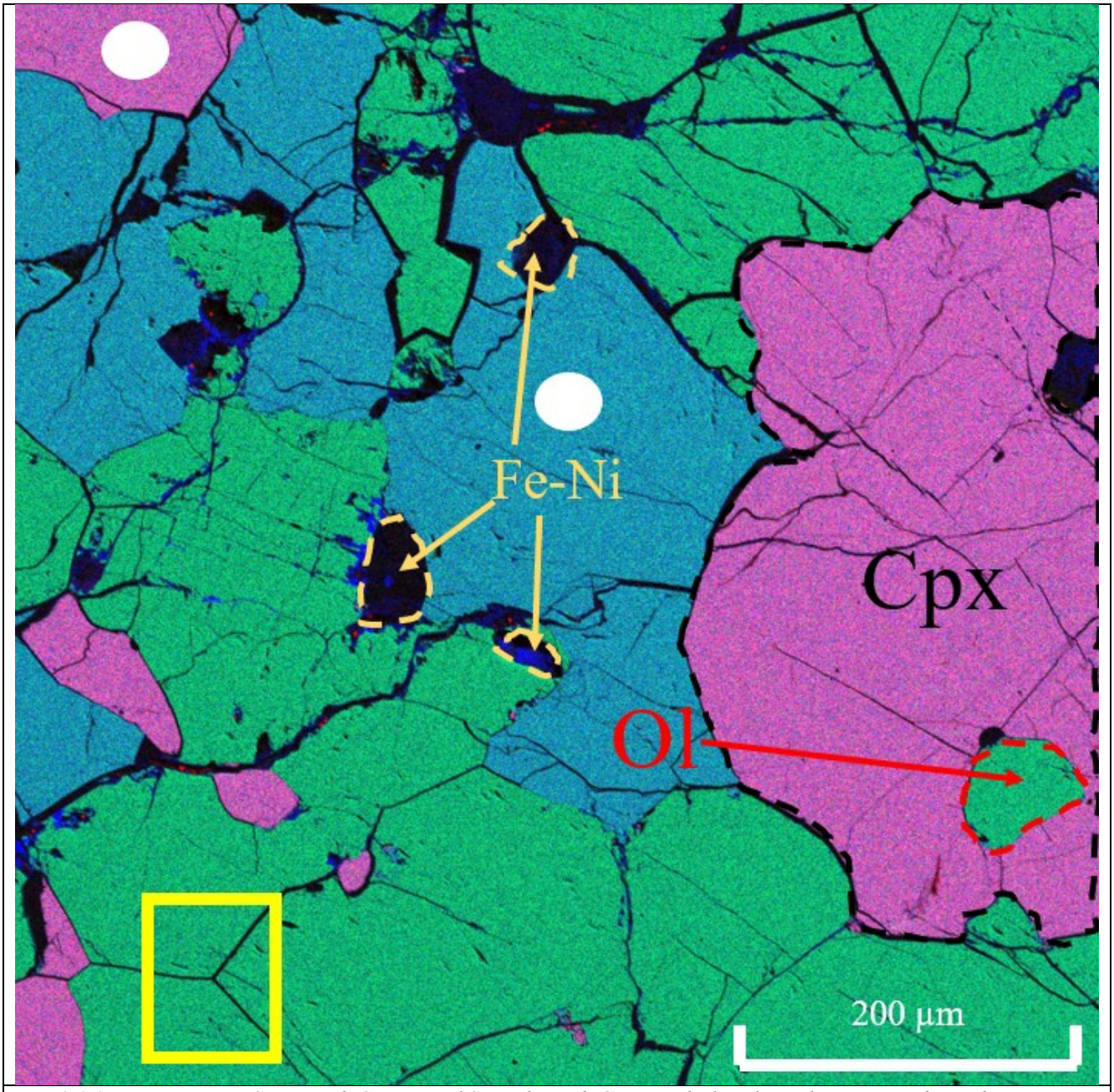

Fig. 3.1.14, composite EDS map with Ca, Mg and Si on the Red, Green and Blue channels, respectively. In the image, are shown four different minerals: orthopyroxene (light-blue), olivine (green), clinopyroxene (pink-to-red) and Fe-Ni phases (black with scattered red). In the weathered olivines it is possible to see the fine-grained intergrowths of Fe-Ni phases and orthopyroxene. A small rounded olivine is poikilitically enclosed in a clinopyroxene (red circle). In the yellow rectangle it is possible to see a triple junction between three olivine grains. The white circled areas are the data points for LA-ICP-MS.

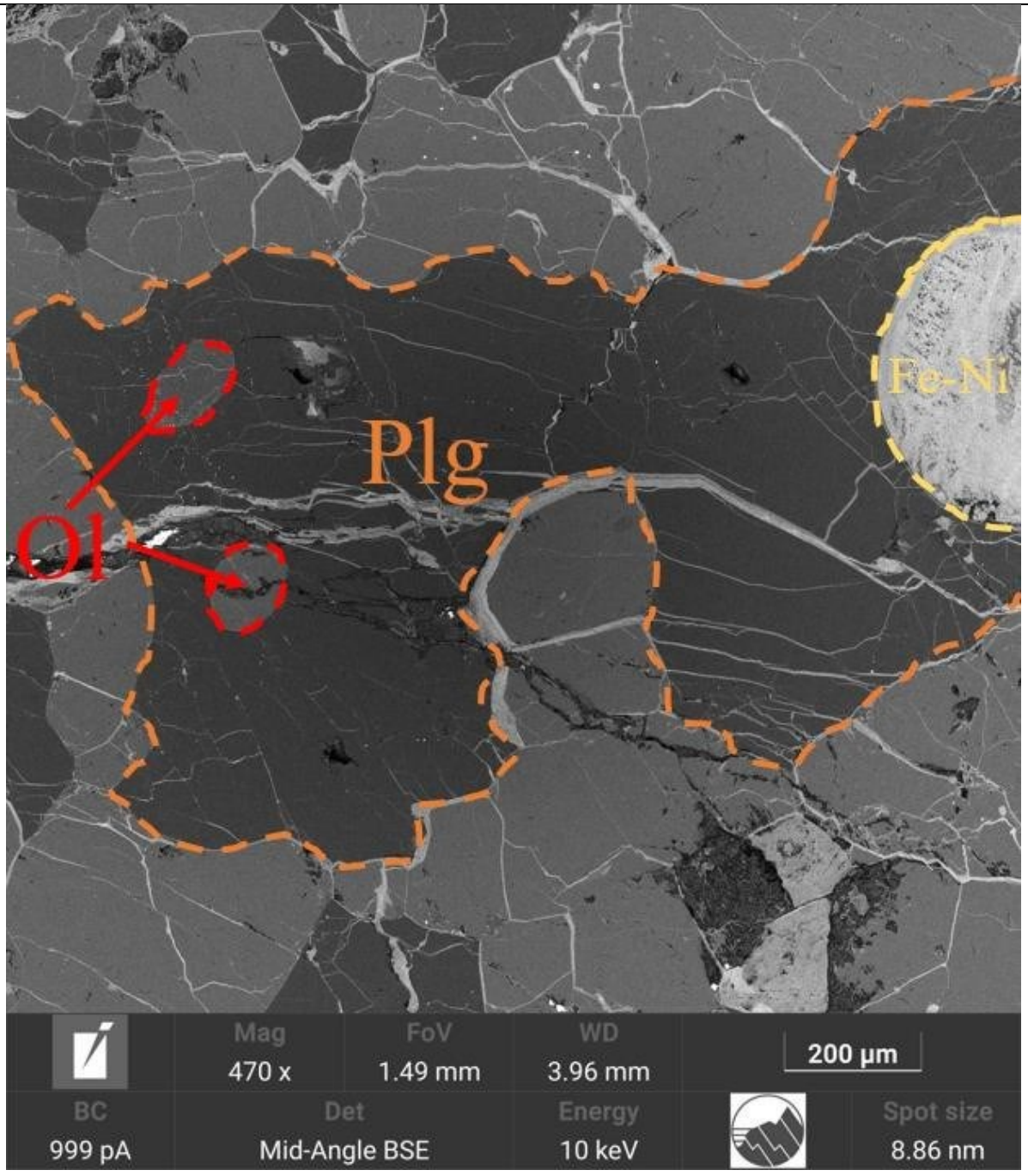

Fig. 3.1.15, a BSE image of olivine rounded crystals (red circles) poikilitically enclosed in plagioclase crystals (orange circles). Fine-grained assemblages of orthopyroxene and Fe-Ni phases are less frequent in this meteorite.

3.1.5 North West Africa 11187

By modal analysis made on 6 BSE images (**Table 3.0**) of the meteorite North West Africa 11187 (NWA11187, **Fig. 3.1.16**) it results that it is composed of olivine (55 vol%), orthopyroxene (34 vol%), clinopyroxene (8 vol%) and Fe-Ni phases (3 vol%). Triple junctions in this meteorite are evident (**Fig. 3.1.17**), and they are mainly between olivine crystal with a degree of 120°. As mentioned for the previous meteorites, they indicate that the meteorite underwent partial melting processes, which led to extensive recrystallization. Olivine crystals are equigranular, subhedral to euhedral and are of an average size of 500-600 µm, but locally they can reach 1 mm. Orthopyroxene crystals are subhedral and they are not equigranular, with their size varying between 500 and 1500-2000 µm. Clinopyroxene is often of various sizes and anhedral, but locally can be subhedral. Clinopyroxene is present mainly as exsolution lamellae in orthopyroxene (**Fig. 3.1.18, 3.1.19**), with an average size of 50-100 µm, but locally subhedral crystals can reach 300-400 µm. Fe-Ni phases are often anhedral. A slight preferral alignment of elongated grains (olivine mainly) can be noticed at the scale of the cut piece. This meteorite is less weathered compared to the ones previously described, therefore the fine-grained intergrowths of orthopyroxene and Fe-Ni phases here are less frequent. Fractures are often highlighted by Fe-Ni phases.

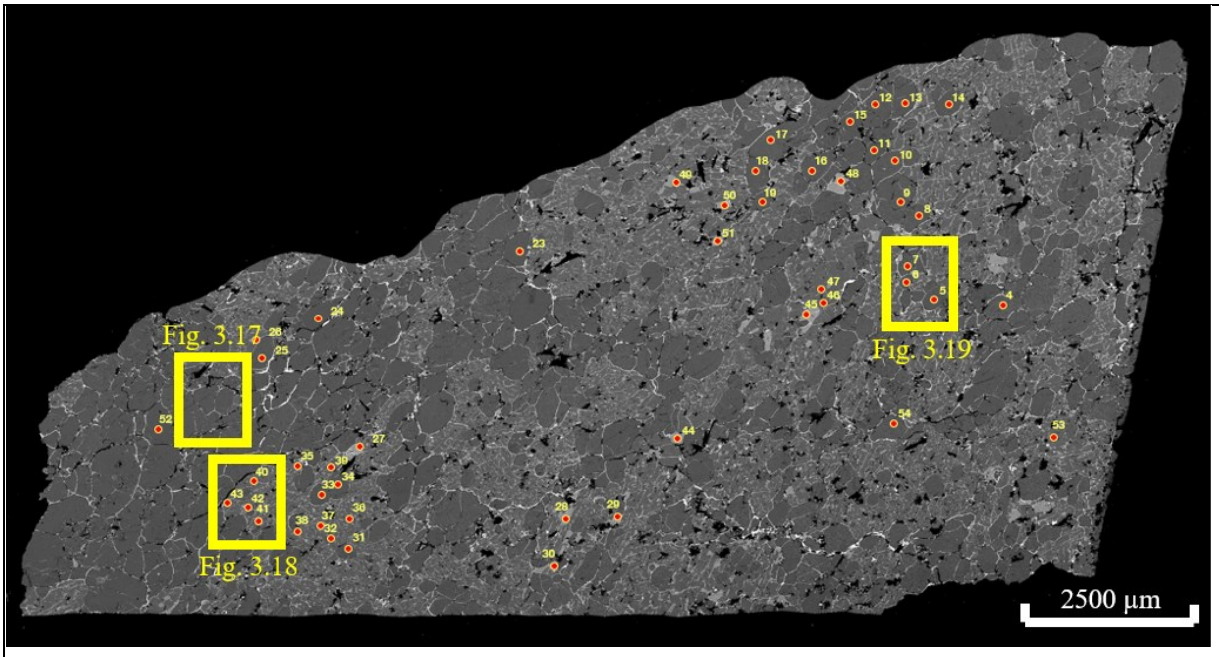

Fig. 3.1.16, a BSE image of NWA11187 meteorite. The red dots are the data points of the LA-ICP-MS analysis. Yellow rectangles represent areas of the meteorite that will be showed in the next images.

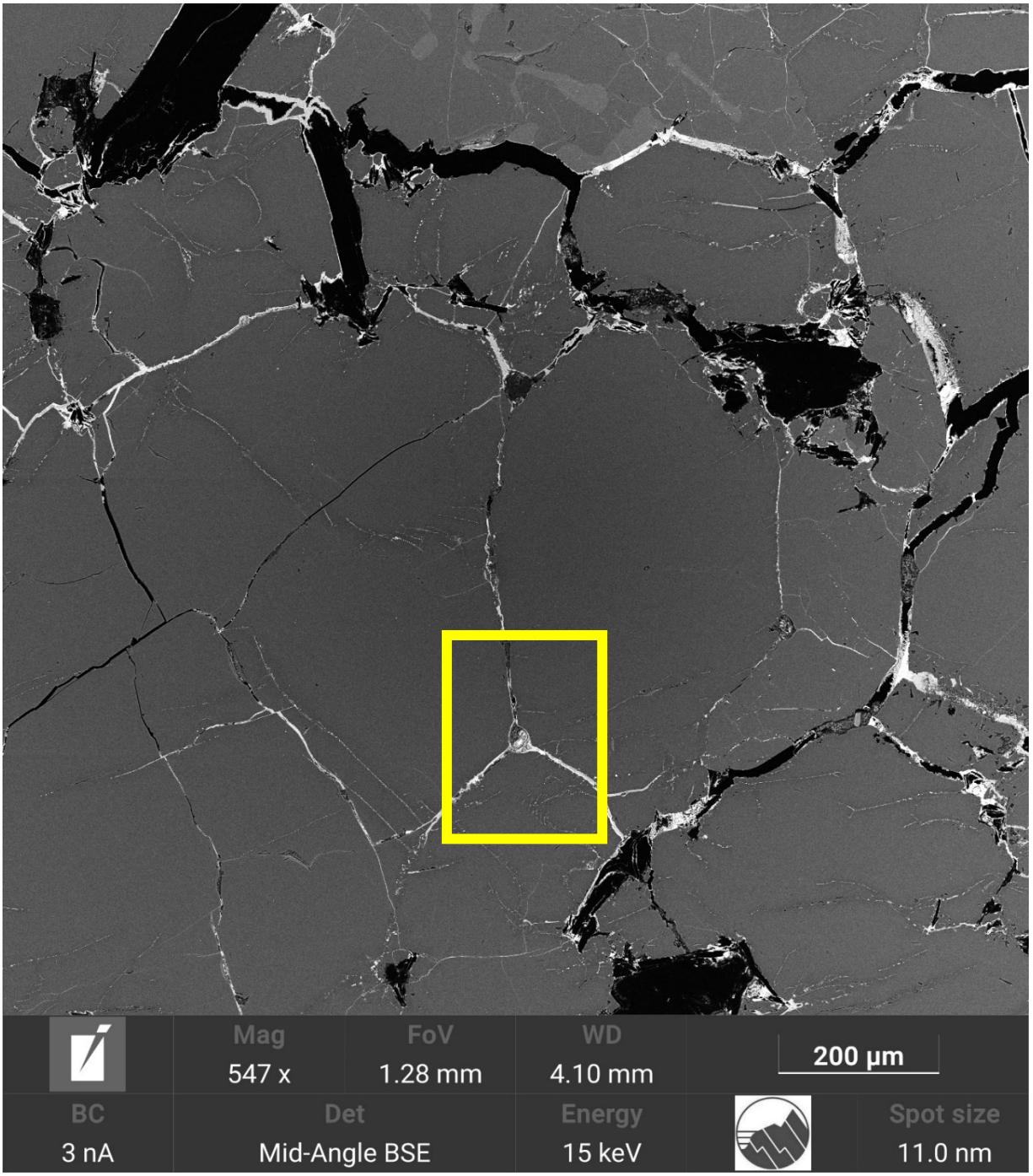

Fig. 3.1.17, a BSE image. Triple junction between olivine crystals, highlighted by Fe-Ni phases (yellow rectangle).

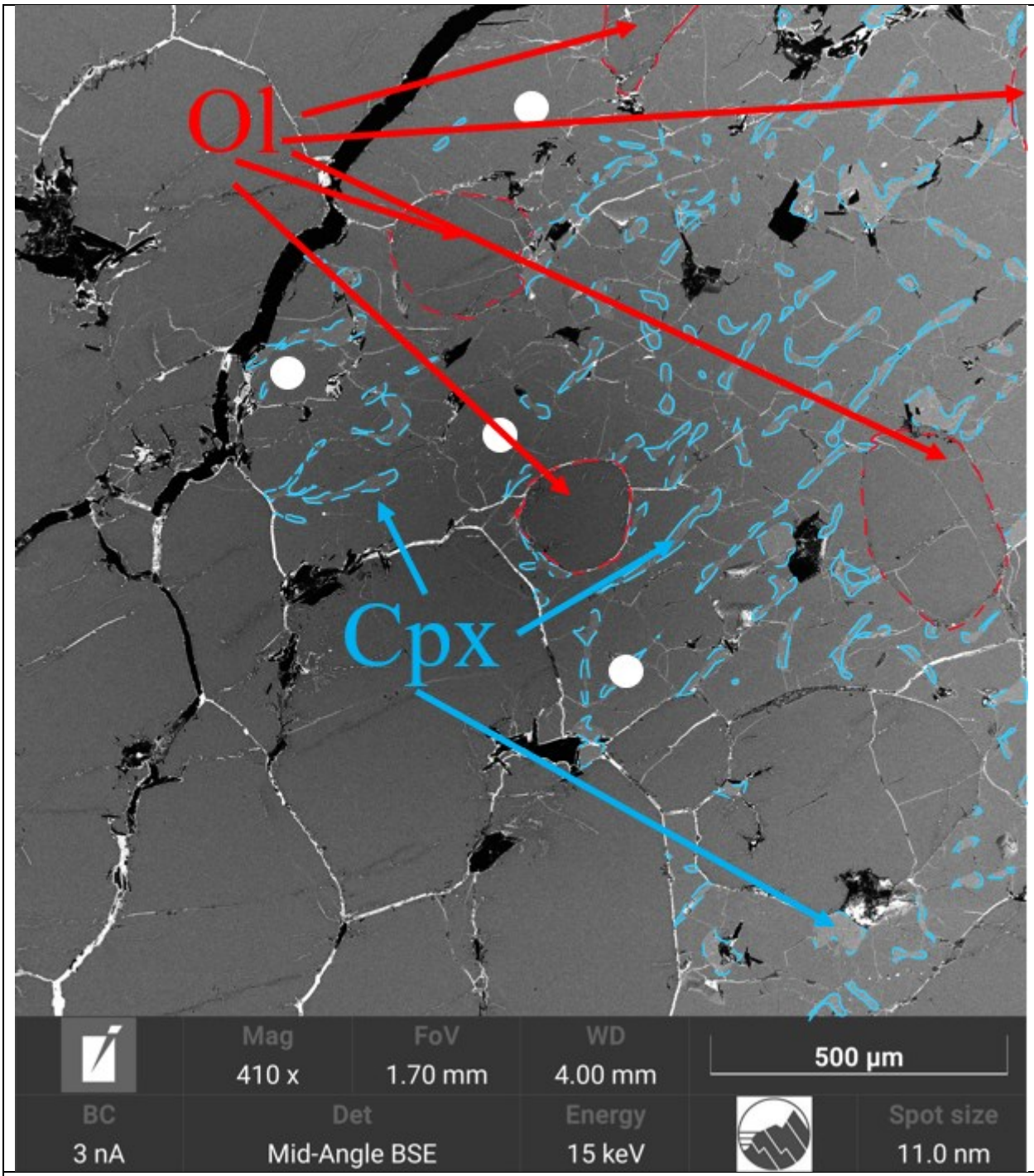

Fig. 3.1.18, a BSE image. Exsolution lamellae of clinopyroxene in orthopyroxene (light blue circled areas). Olivine rounded crystals enclosed in orthopyroxene (red circles). The datapoints of the LA-ICP-MS analysis (white circles).

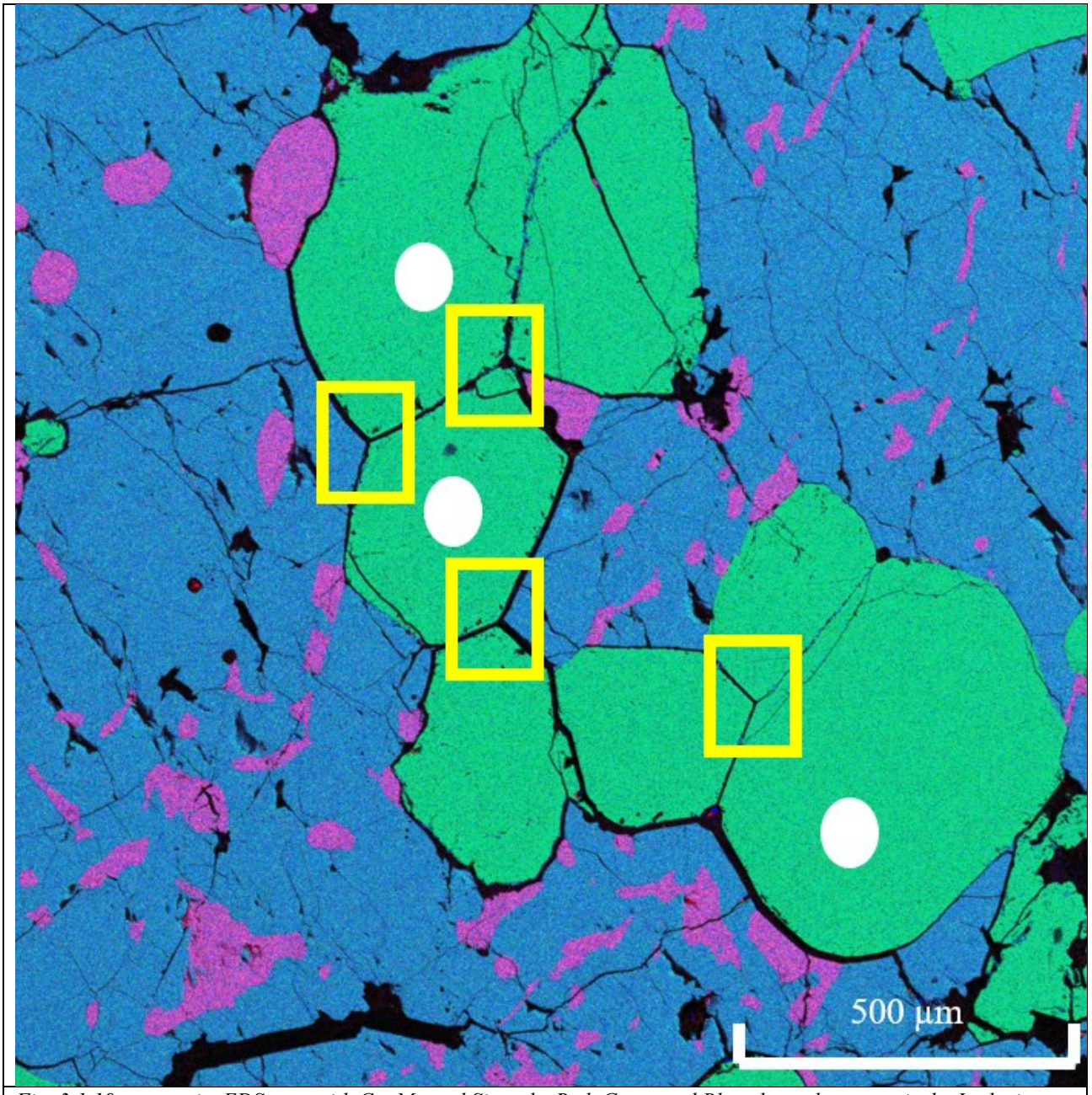

Fig. 3.1.19, composite EDS map with Ca, Mg and Si on the Red, Green and Blue channels, respectively. In the image, are shown four different minerals: orthopyroxene (light-blue), olivine (green), clinopyroxene (pink-to-red) and Fe-Ni phases (black with scattered red). In the yellow rectangles it is possible to see many triple junctions between both olivine and orthopyroxene grains. In addition, it is possible to see the exsolution lamellae of clinopyroxene in orthopyroxene. The white circled areas are the data points for LA-ICP-MS.

3.2 Mineral Chemistry

3.2.1 Major and Minor Elements (EPMA)

The raw chemical data of the four meteorite samples: MIL090206, MIL090405, NWA6077, NWA5363 have been acquired by Cuppone et al. in prep. The data was later re-organized. Standard Deviation (SD) and Relative Standard Deviation were calculated and then the data was displayed in tables, which have been reported here below for completeness for each major phase. In addition, also the raw data (still from Cuppone et al. in prep.) for the NWA11187 meteorite have been recently acquired, treated as for the other four meteorites of this study and reported here below.

3.2.1.1 Olivine

In **Table 3.1** the chemical data acquired on olivine grains of the five meteorites studied in this work are reported.

Table 3.1. Average olivine composition (EPMA) expressed as wt.% of oxides and atoms per formula unit (a.p.f.u.). The number of point analyses is reported close to the sample name. The standard deviations (SD) and relative standard deviations (RSD) are reported for each average. Content of Fo, Fa and Tp in mol% is also reported. The full dataset is available as supplementary Table S1.

Olivine

	MIL090206			MIL090405			NWA5363			NWA6077			NWA11187		
	(averaged 25 spots)			(averaged 38 spots)			(averaged 31 spots)			(averaged 33 spots)			(averaged 22 spots)		
wt%	mean	SD	RSD %	mean	SD	RSD %	mean	SD	RSD %	mean	SD	RSD %	mean	SD	RSD %
SiO_2	37.58	0.33	1	37.54	0.18	0	37.41	0.64	2	36.75	0.31	1	41.40	0.50	1
TiO_2	0.03	0.01	50	0.03	0.01	35	0.03	0.01	50	0.03	0.01	37	0.04	0.01	22
Al_2O_3	0.00	0.00	141	0.00	0.00	124	0.00	0.00	91	0.00	0.00	75	0.03	0.01	47
Cr_2O_3	0.05	0.07	136	0.05	0.04	90	0.17	0.22	129	0.20	0.27	138	0.57	0.03	6
FeOT	24.42	1.26	5	25.43	0.69	3	26.69	0.48	2	25.94	0.52	2	5.46	0.53	10
MnO	0.44	0.02	6	0.44	0.02	4	0.45	0.02	6	0.43	0.02	5	0.49	0.04	8
NiO	0.01	0.03	223	0.00	0.01	146	0.01	0.01	100	0.02	0.05	199	0.01	0.02	197
MgO	36.54	1.08	3	35.73	0.56	2	34.89	0.82	2	36.39	0.47	1	52.64	0.64	1
CaO	0.08	0.02	25	0.09	0.04	42	0.08	0.02	24	0.07	0.01	17	0.32	0.02	5
Total	99.15	0.32	0	99.31	0.51	1	99.72	1.27	1	99.84	0.47	0	100.95	0.77	1
a.p.f.u	normalization to 4 oxygens and <3 cations per f.u.														
Si	0.998	0.003	0	1.000	0.003	0	0.998	0.005	0	0.973	0.007	1	0.988	0.006	1
Ti	0.001	0.000	50	0.001	0.000	35	0.001	0.000	49	0.001	0.000	37	0.001	0.000	22
Al	0.000	0.000	141	0.000	0.000	124	0.000	0.000	91	0.000	0.000	75	0.001	0.000	48
Cr	0.001	0.002	135	0.001	0.001	90	0.004	0.004	128	0.004	0.006	138	0.011	0.001	6
Fe^{2+}	0.539	0.032	6	0.564	0.016	3	0.592	0.016	3	0.526	0.016	3	0.097	0.011	12
Fe^{3+}	0.004	0.005	131	0.002	0.003	151	0.004	0.007	162	0.049	0.013	27	0.012	0.011	90
Mn	0.010	0.001	6	0.010	0.000	4	0.010	0.001	6	0.010	0.000	5	0.010	0.001	9
Ni	0.000	0.001	224	0.000	0.000	146	0.000	0.000	100	0.001	0.001	200	0.000	0.000	198
Mg	1.445	0.032	2	1.418	0.017	1	1.387	0.013	1	1.436	0.013	1	1.872	0.011	1
Ca	0.002	0.001	25	0.003	0.001	43	0.002	0.001	25	0.002	0.000	17	0.008	0.000	6
cations	2.999	0.001	0	2.998	0.002	0	2.998	0.003	0	3.000	0.000	0	3.000	0.001	0
#mg	81.2	0.3	0	71.5	0.8	1	81.8	14.5	18	70.0	0.8	1	94.5	0.6	1
mol%															
Fo	72.4	1.6	2	71.1	0.8	1	71.1	12.6	18	69.6	0.8	1	93.6	0.6	1
Fa	27.1	1.6	6	28.4	0.8	3	28.4	5.1	18	29.9	0.8	3	5.5	0.5	10
Tp	0.5	0.0	6	0.5	0.0	4	0.5	0.3	52	0.5	1.6	202	0.5	0.0	9

The four meteorites MIL090206, MIL090405, NWA5363 and NWA6077, show quite similar olivine composition except for NWA11187 which shows significant chemical differences. SiO_2 values range from 36.75 wt% in NWA6077 to 41.40 wt% in NWA11187, (with R.S.D. values ranging from 0 to 2%). MgO value in NWA 11187 is around 52.64 wt%, whereas in the other samples ranges from 34.89 to 36.54 wt%. This indicates that the olivine in NWA 11187 is more forsteritic (average Fo = 93.6 mol%,) than in the other meteorites investigated in this study (Fig. 3.2.1.1).

MnO, TiO_2 and Al_2O_3 are instead almost identical in all the studied meteorites. with Cr_2O_3 and CaO values slightly higher in NWA11187 compared to the other meteorites. Furthermore, MIL090206 is characterized by a more pronounced internal variability of Fo content ranging from 69.7 to 75.7 mol% (see **Fig. 3.2.1.1**).

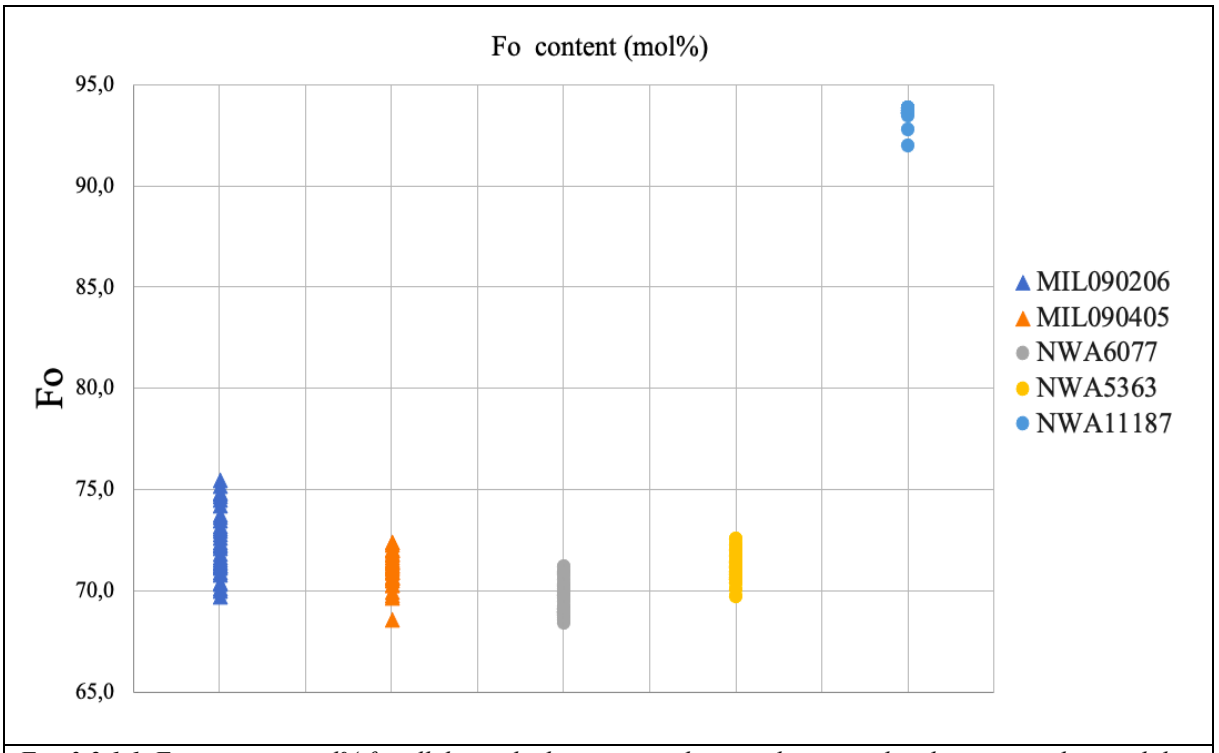

Fig. 3.2.1.1, Fo content in mol% for all the studied meteorites showing the internal and intra-sample variability.

3.2.1.2 Orthopyroxene

In **Table 3.2** the data acquired by EPMA on orthopyroxene grains of the five meteorites studied in this work are reported.

Table 3.2. Average orthopyroxene composition (EPMA) expressed as wt.% of oxides and atoms per formula unit (a.p.f.u.). The number of point analyses is reported close to the sample name. The standard deviations (SD) and relative standard deviations (RSD) are reported for each average. Content of Wo, En and Fs in mol% is also reported. The full dataset is available as supplementary Table S2.

Orthopyroxene

	MIL090206			MIL090405			NWA5363			NWA6077			NWA11187		
	(averaged 32 spots)			(averaged 3 spots)			(averaged 13 spots)			(averaged 19 spots)			(averaged 24 spots)		
wt%	mean	SD	RSD %	mean	SD	RSD %	mean	SD	RSD %	mean	SD	RSD %	mean	SD	RSD %
SiO_2	54.35	0.29	1	55.02	0.31	1	55.39	0.57	1	54.03	0.45	1	57.49	0.91	2
TiO_2	0.13	0.03	24	0.03	0.02	54	0.11	0.02	15	0.11	0.01	11	0.14	0.01	10
Al_2O_3	0.23	0.07	30	0.03	0.00	10	0.29	0.02	8	0.28	0.02	6	0.51	0.02	3
Cr_2O_3	0.18	0.04	24	0.07	0.01	17	0.20	0.02	7	0.19	0.02	8	0.85	0.02	2
FeOT	16.66	0.52	3	15.23	0.13	1	15.71	0.17	1	15.64	0.23	1	3.47	0.11	3
MnO	0.40	0.02	6	0.41	0.02	5	0.27	0.04	15	0.26	0.01	2	0.48	0.02	5
MgO	26.34	0.94	4	28.14	0.28	1	27.18	0.34	1	27.79	0.15	1	34.67	0.55	2
CaO	1.07	0.23	21	0.51	0.05	9	1.08	0.02	2	1.09	0.03	2	2.86	0.60	21
Na_2O	0.03	0.02	66	0.01	0.01	90	0.03	0.01	40	0.03	0.01	41	0.04	0.01	33
K2O	0.01	0.01	110	0.00	0.01	154	0.00	0.00	115	0.01	0.01	104	0.00	0.00	128
Total	99.39	0.29	0	99.45	0.46	0	100.27	0.80	1	99.42	0.57	1	100.51	0.94	1
a.p.f.u	normalization to 6 oxygens and <4 cations per f.u.														
Si	1.983	0.015	1	1.987	0.001	0	1.992	0.005	0	1.955	0.009	0	1.965	0.016	1
Ti	0.004	0.001	24	0.001	0.000	54	0.003	0.000	14	0.003	0.000	11	0.004	0.000	10
Al	0.010	0.003	30	0.001	0.000	10	0.012	0.001	8	0.012	0.001	6	0.021	0.001	3
Cr	0.005	0.001	24	0.002	0.000	17	0.006	0.000	8	0.006	0.000	8	0.023	0.001	3
Fe^{2+}	0.492	0.048	10	0.439	0.003	1	0.470	0.006	1	0.404	0.014	4	0.077	0.029	38
Fe^{3+}	0.016	0.033	205	0.021	0.003	13	0.002	0.006	260	0.069	0.019	27	0.023	0.029	130
Mn	0.012	0.001	6	0.012	0.001	5	0.008	0.001	16	0.008	0.000	2	0.014	0.001	5
Mg	1.433	0.044	3	1.515	0.008	1	1.457	0.007	0	1.499	0.005	0	1.767	0.030	2
Ca	0.042	0.009	22	0.020	0.002	10	0.042	0.001	2	0.042	0.001	2	0.105	0.022	21
Na	0.002	0.001	66	0.001	0.001	90	0.002	0.001	40	0.002	0.001	41	0.003	0.001	33
K	0.000	0.000	110	0.000	0.000	154	0.000	0.000	115	0.000	0.000	104	0.000	0.000	128
cations	3.999	0.003	0	4.000	0.000	0	3.995	0.003	0	4.000	0.000	0	4.000	0.002	0
#mg	73.8	0.012	2	76.7	0.003	0	75.5	0.003	0	76.0	0.003	0	94.7	0.002	0
mol%															
Wo	2.1	0.5	22	1.0	0.1	10	2.1	0.0	2	2.1	0.1	2	5.3	1.1	21
En	71.8	1.5	2	75.5	0.4	1	73.6	0.4	1	74.1	0.2	0	89.0	1.2	1
Fs	26.1	1.0	4	23.5	0.3	1	24.3	0.4	2	23.8	0.3	1	5.7	0.2	3

The composition of the orthopyroxene reported in **Table 3.2** is quite similar for the four meteorites MIL090206, MIL090405, NWA5363 and NWA6077; while NWA11187 shows some differences. CaO values are subjected to variations between NWA11187 and the other meteorites, with a value for NWA11187 being 2.86 wt% with a higher RSD value of 21% compared to the other samples. In addition, also Cr_2O_3 values show some differences between NWA11187 and the other samples, with the value of NWA11187 being 0.85 wt% (with an RSD value of 2%) and the other meteorites having values in the range between 0.07 and 0.20 wt% (with RSD values from 7 to 24%). The average composition of the orthopyroxene in the different meteorites is reported below (**Fig. 3.2.1.2**):

- **MIL090206** En71.8Fs26.1Wo2.1
- **MIL090405** En75.5Fs23.5Wo1.0
- **NWA6077** En74.1Fs23.8Wo2.1
- **NWA5363** En73.6Fs24.3Wo2.1
- **NWA11187** En89.0Fs5.7Wo5.3

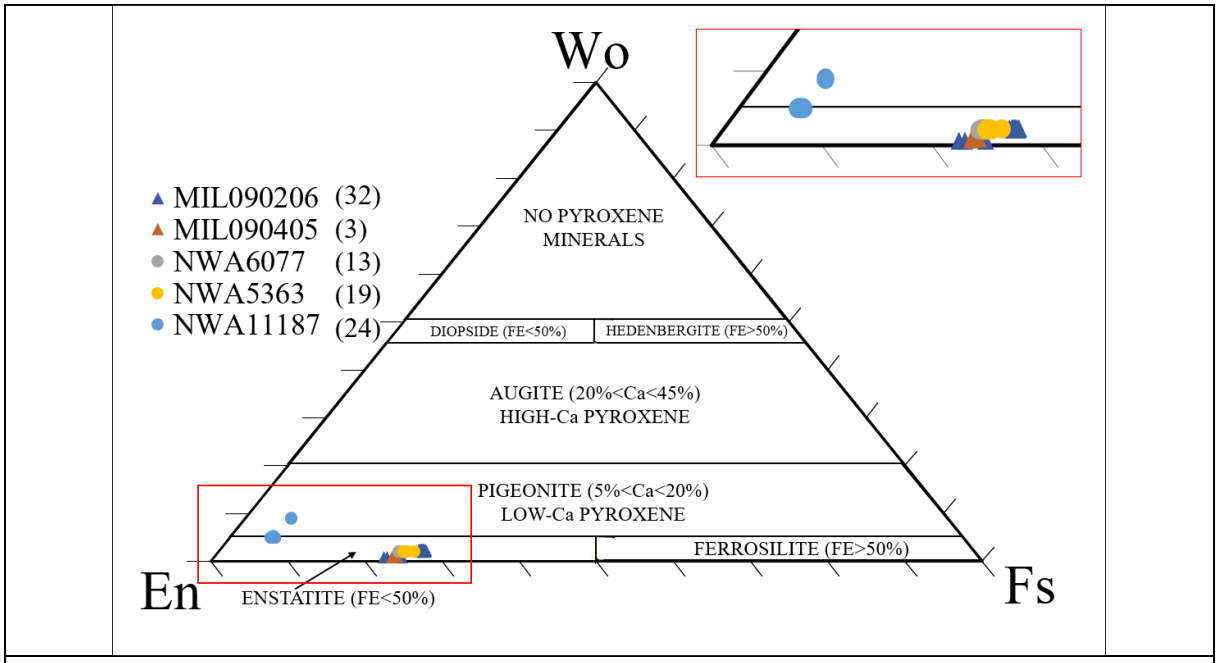

Fig. 3.2.1.2, En vs Fs vs Wo (orthopyroxene) for all the studied meteorites. All the orthopyroxene grains in NWA11187 are pigeonitic, while orthopyroxene grains from the other four meteorites are enstatitic. The number of point analyses is indicated next to the meteorite name.

3.2.1.3 Clinopyroxene

In Table 3.3 the data acquired by EPMA on clinopyroxene grains of the five meteorites studied in this work are reported.

Table 3.3. Average clinopyroxene composition (EPMA) expressed as wt.% of oxides and atoms per formula unit (a.p.f.u.). The number of point analyses is reported close to the sample name. The standard deviations (SD) and relative standard deviations (RSD) are reported for each average. Content of Wo, En and Fs in mol% is also reported. The full dataset is available as supplementary Table S3.

Clinopyroxene

	MIL090206			MIL090405			NWA5363			NWA6077			NWA11187		
	(averaged 2 spots)			(averaged 19 spots)			(averaged 22 spots)			(averaged 23 spots)			(averaged 32 spots)		
wt%	mean	SD	RSD %	mean	SD	RSD %	mean	SD	RSD %	mean	SD	RSD %	mean	SD	RSD %
SiO_2	53.51	0.07	0	53.59	0.22	0	54.02	0.61	1	53.41	0.34	1	55.11	1.07	2
TiO_2	0.31	0.01	2	0.30	0.02	6	0.22	0.02	7	0.21	0.02	8	0.25	0.01	6
Al_2O_3	0.63	0.01	1	0.65	0.04	7	0.74	0.06	7	0.68	0.07	10	0.84	0.03	3
Cr_2O_3	0.73	0.02	2	0.78	0.07	9	0.80	0.05	7	0.73	0.05	6	0.83	0.02	2
FeOT	6.61	0.14	2	6.57	0.18	3	6.18	0.21	3	6.00	0.20	3	2.08	0.18	9
MnO	0.21	0.01	6	0.20	0.02	9	0.21	0.04	18	0.13	0.01	7	0.36	0.02	4
MgO	15.80	0.00	0	15.87	0.10	1	15.89	0.24	1	16.73	0.12	1	21.97	0.48	2
CaO	21.21	0.17	1	21.13	0.25	1	21.08	0.34	2	21.45	0.19	1	18.71	0.23	1
Na2O	0.49	0.01	2	0.51	0.04	8	0.46	0.03	5	0.46	0.04	9	0.17	0.02	10
K2O	0.00	0.00	94	0.00	0.00	123	0.00	0.00	106	0.00	0.00	96	0.00	0.00	139
Total	99.50	0.21	0	99.59	0.33	0	99.60	0.78	1	99.80	0.44	0	100.32	0.80	1
a.p.f.u	normalization to 6 oxygens and <4 cations per f.u.														
Si	1.981	0.006	0	1.982	0.004	0	1.992	0.009	0	1.962	0.008	0	1.964	0.025	1
Ti	0.009	0.000	2	0.008	0.001	6	0.006	0.000	7	0.006	0.000	8	0.007	0.000	6
Al	0.028	0.000	1	0.028	0.002	7	0.032	0.003	8	0.029	0.003	10	0.035	0.001	3
Cr	0.021	0.001	2	0.023	0.002	9	0.023	0.002	7	0.021	0.001	6	0.023	0.001	2
Fe^{2+}	0.196	0.008	4	0.196	0.009	5	0.189	0.008	4	0.137	0.016	12	0.044	0.019	43
Fe^{3+}	0.008	0.012	141	0.007	0.007	96	0.001	0.005	360	0.048	0.017	35	0.018	0.020	113
Mn	0.007	0.000	6	0.006	0.001	9	0.007	0.001	18	0.004	0.000	7	0.011	0.000	4
Mg	0.872	0.002	0	0.875	0.006	1	0.874	0.013	1	0.916	0.007	1	1.168	0.029	2
Ca	0.842	0.005	1	0.837	0.009	1	0.833	0.010	1	0.844	0.008	1	0.715	0.012	2
Na	0.035	0.001	2	0.036	0.003	8	0.033	0.002	6	0.033	0.003	9	0.012	0.001	10
K	0.000	0.000	94	0.000	0.000	123	0.000	0.000	107	0.000	0.000	96	0.000	0.000	138
cations	3.999	0.001	0	3.999	0.002	0	3.990	0.007	0	4.000	0.000	0	3.997	0.019	0
#mg	81.0	0.331	0	81.2	0.461	1	82.2	0.554	1	83.3	0.476	1	95,0	0.415	0
mol%															
Wo	43.7	0.1	0	43.6	0.3	1	43.7	0.5	1	43.3	0.3	1	36.6	0.3	1
En	45.3	0.3	1	45.5	0.2	1	45.9	0.3	1	47.0	0.3	1	59.7	0.4	1
Fs	11.0	0.1	1	10.9	0.3	3	10.4	0.4	4	9.7	0.3	3	3.7	0.3	7

The data in **Table 3.3** are similar among the four meteorites MIL090206, MIL090405, NWA5363 and NWA6077, while NWA11187 shows some differences. MgO values display a significant variability between NWA11187 and the other meteorites, with the value of MgO for NWA11187 being 21.97 wt% (with an RSD value of 2%), while the value for the other meteorites range between 15.80 and 16.73 wt% (with RSD values from 0 to 1%). CaO is also similar in all the samples, but the value in NWA11187 is slightly lower than the values from the other samples, being 18.71 wt% (with an RSD value of 1%), and the values of the other samples being in the range between 21.08 and 21.45 wt% (with RSD values ranging between 1 and 2%). MnO values, instead, are slightly higher in NWA11187 compared to the values of the other samples, with the value in NWA11187 being 0.36 wt% (with an RSD value of 4%). The average composition of the clinopyroxene in the different meteorites are reported below and in **Fig. 3.2.1.3**:

- **MIL090206** En45.3Fs11.0Wo43.7
- **MIL090405** En45.5Fs10.9Wo43.6
- **NWA6077** En47.0Fs9.7Wo43.3
- **NWA5363** En45.9Fs10.4Wo43.7
- **NWA11187** En59.7Fs3.7Wo36.6

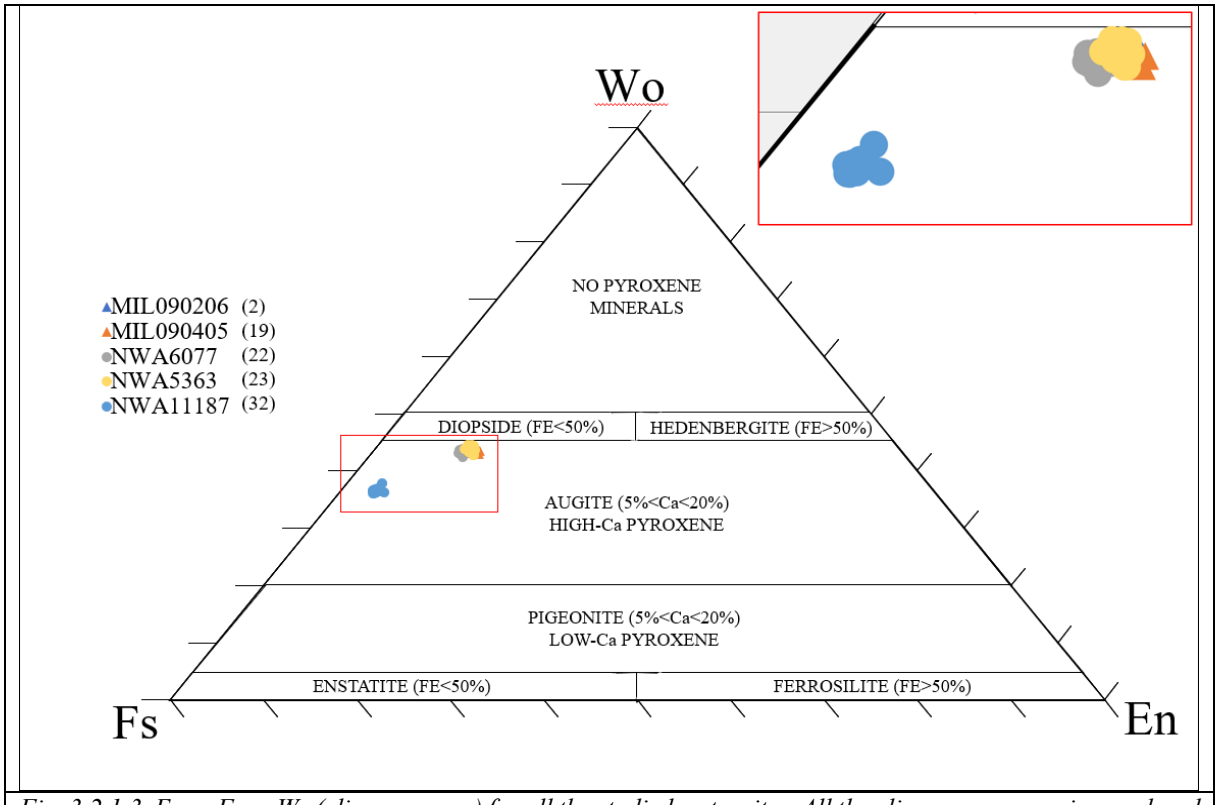

Fig. 3.2.1.3, En vs Fs vs Wo (clinopyroxene) for all the studied meteorites. All the clinopyroxene grains analysed are augitic. The number of point analyses is indicated next to the meteorite name.

3.2.1.4 Plagioclase

In the following table the chemical data acquired on plagioclase grains are reported. In particular, plagioclase grains have been found only in the sample NWA 5353.

Table 3.4. Average plagioclase composition (EPMA) expressed as wt.% of oxides and atoms per formula unit (a.p.f.u.). The number of point analyses is reported close to the sample name. The standard deviations (SD) and relative standard deviations (RSD) are reported for each average. Content of An, Ab and Or in mol% is also reported. The full dataset is available as supplementary Table S4.

Plagioclase			
wt%	NWA5363		
	(averaged 10 spots)		
	mean	**SD**	**RSD%**
SiO_2	63.06	0.30	0
TiO_2	0.04	0.01	28
Al_2O_3	23.62	0.16	1
FeO	0.16	0.04	27
MnO	0.01	0.01	86
MgO	0.02	0.01	37
CaO	5.38	0.36	7
Na_2O	7.87	0.37	5
K_2O	0.29	0.04	15
BaO(Mass%)	0.05	0.01	21
SrO(Mass%)	0.046	0.022	48
Total	100.55	0.29	0
a.p.f.u	cations calculated per f.u. assuming FeT=Fe2+		
Si	2,099	0,010	0%
Ti	0.001	0.000	27
Al	1.226	0.010	1
Cr	0.000	0.000	//
FeT	0.006	0.002	27
Mn	0.001	0.000	86
Ni	0.000	0.000	//
Mg	0.001	0.001	37
Ca	0.254	0.017	7
Na	0.672	0.031	5
K	0.016	0.002	15
mol%			
An	26.950	2.279	8
Ab	71.320	2.270	3
Or	1.730	0.267	15

From the data reported in **Table 3.4**, plagioclase in NWA5363 is enriched in Na (**Fig. 3.2.1.4**). Eight plagioclase grains over the ten analysed in NWA 5363 are close to oligoclase composition, one to andesine and the other one shows an intermediate composition between oligoclase and andesine.

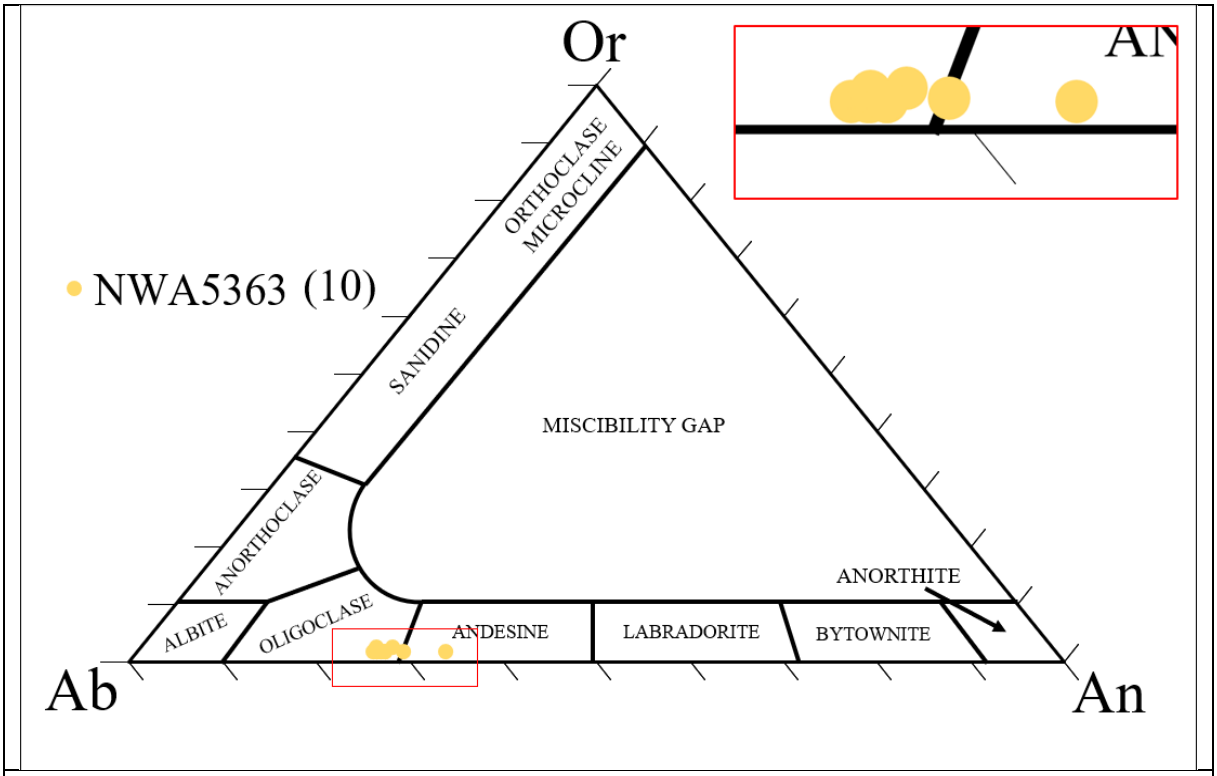

Fig. 3.2.1.4, Or vs Ab vs An for NWA5363. The number of point analyses is indicated next to the meteorite name.

3.2.1.5 Phosphates

In the following table are reported the chemical data acquired on phosphate grains. Phosphates have been found only in NWA5363 and NWA6077.

Table 3.5. Average phosphate composition (EPMA) expressed as wt.% of oxides. The number of point analyses is reported close to the sample name. The standard deviations (SD) and relative standard deviations (RSD) are reported for each average. The full dataset is available as supplementary Table S5.

Phosphates						
wt%	**NWA5363**			**NWA6077**		
	(averaged 6 spots)			(averaged 15 spots)		
	mean	**SD**	**RSD%**	**mean**	**SD**	**RSD%**
P_2O_5	34.38	8.22	24	39.81	6.23	16
F	0.32	0.18	55	0.25	0.21	83
SiO_2	1.73	2.32	134	0.39	0.61	155
SrO	0.02	0.01	84	0.02	0.03	148
Cl	3.03	3.24	107	2.73	3.01	110
SO_3	0.51	0.46	91	0.62	1.50	242
FeO	//	//	//	11.86	19.98	168
CaO	26.47	28.11	106	38.49	20.18	52
Na2O	0.17	0.12	73	0.48	0.39	83
MgO	0.12	0.08	71	1.28	1.63	127
Total	66.75	37.52	56	95.93	7.98	8

From the data reported in **Table 3.5**, there is a significant difference between the values for NWA5363 and NWA6077. It is also important to consider that three types of phosphates have been identified for NWA6077: Cl-apatite, Fe-phosphates and merrillite. This difference in the minerals identified probably also caused the considerable difference in values between NWA5363 and NWA6077. P_2O_5 is quite similar in both the samples, but the value of NWA6077 is slightly lower than the one of NWA5363, 34.58 wt% compared to 39.81 wt%, respectively (RSD values range from 16 and 24%). F and SrO values are very similar between NWA5363 and NWA6077.

3.2.1.6 Spinels

In **Table 3.6** all the chemical data related to spinel are reported here below. In the following table are reported the data acquired by EPMA on spinel grains from the four samples where spinel grains were found, MIL090206, MIL090405, NWA5363 and NWA6077.

Table 3.6. Average spinel composition (EPMA) expressed as wt.% of oxides and atoms per formula unit (a.p.f.u.). The number of point analyses is reported close to the sample name. The standard deviations (SD) and relative standard deviations (RSD) are reported for each average. The full dataset is available as supplementary Table S6.

	Spinels											
wt%	**MIL090206**			**MIL090405**			**NWA5363**			**NWA6077**		
	(averaged 10 spots)			(averaged 9 spots)			(averaged 16 spots)			(averaged 23 spots)		
	mean	**SD**	**RSD %**	**mean**	**SD**	**RSD %**	**mean**	**SD**	**RSD %**	**mean**	**SD**	**RSD %**
TiO_2	2.16	0.56	26	1.94	0.63	33	1.46	0.02	2	1.43	0.03	2
Al_2O_3	5.87	2.04	35	4.90	2.69	55	7.80	0.08	1	7.59	0.11	1
V_2O_3	0.66	0.07	11	55.07	4.32	8	0.66	0.03	5	0.67	0.03	4
Cr_2O_3	52.46	4.01	8	0.67	0.09	13	56.06	0.44	1	55.85	0.59	1
FeO	27.95	0.92	3	29.68	0.62	2	27.66	0.46	2	27.60	0.67	2
MnO	0.28	0.04	13	0.29	0.02	8	0.18	0.02	11	0.19	0.02	10
NiO	0.02	0.03	133	0.02	0.03	166	0.01	0.02	115	0.02	0.02	111
MgO	3.98	0.68	17	3.33	0.67	20	4.02	0.24	6	4.34	0.34	8
CaO	0.01	0.01	132	0.01	0.01	92	0.01	0.01	98	0.01	0.01	95
ZnO	0.03	0.03	130	0.03	0.03	106	0.11	0.07	58	0.11	0.04	35
CoO	0.05	0.02	44	0.03	0.03	97	0.03	0.03	85	0.00	0.00	//
CuO	0.08	0.07	89	0.03	0.05	153	0.02	0.03	184	0.00	0.00	//
TOT	93.54	0.99	1	96.19	0.92	1	98.02	0.49	1	97.80	0.63	1
a.p.f.u												
Ti	0.488	0.124	25	0.430	0.137	32	0.311	0.005	2	0.307	0.006	2
Al	2.080	0.722	35	1.695	0.929	55	2.610	0.026	1	2.544	0.032	1
V	0.159	0.017	11	12.889	1.218	9	0.149	0.007	5	0.153	0.006	4
Cr	12.485	1.021	8	0.159	0.023	15	12.588	0.055	0	12.563	0.062	0
Fe	7.036	0.301	4	7.338	0.120	2	6.569	0.115	2	6.567	0.177	3
Mn	0.071	0.010	14	0.073	0.006	8	0.044	0.005	11	0.047	0.005	11
Ni	0.011	0.014	133	0.009	0.014	165	0.006	0.007	115	0.007	0.008	111
Mg	1.783	0.284	16	1.464	0.277	19	1.700	0.100	6	1.841	0.140	8
Ca	0.002	0.003	133	0.002	0.002	91	0.003	0.003	98	0.004	0.004	94

As from the data reported in Table 3.6, the spinel analysed in the meteorites MIL090206, NWA5363 and NWA11187 is chromite, while for MIL090405 the spinel is not chromite. In fact, Cr_2O_3 values are completely different in MIL090405 from the other three meteorites. Cr_2O_3in MIL090405 is 0.67 wt% with an RSD value of 13%, while the values for the other samples range between 52.46 and 56.06 wt% (with RSD values ranging from 1 to 8%). Also V_2O_3 values in MIL090405 are very different from the other three samples, with the value for MIL090405 being 55.07 wt% (with an RSD value of 8%), while the values for the other three meteorites range between 0.66 and 0.67 wt% (with RSD values from 4 to 11%). FeO, Al_2O_3, MgO, TiO_2, MnO, are instead very similar among all the four meteorites.

3.2.2 Trace Elements

In the following paragraphs the trace element contents of the four major mineralogical phases (olivine, orthopyroxene, clinopyroxene and plagioclase) encountered in the five meteorites (MIL090206, MIL090405, NWA6077, NWA5363 and NWA11187) are reported. All the trace elements are organized based on their average content in all the studied meteorites, and are subdivided in five broad categories, based on their abundances in ppm:

- Category A (>1000 ppm);
- Category B (100<average ppm content<1000);
- Category C (10< average ppm content<100);
- Category D (1< average ppm content<10);
- Category E (<1 ppm).

For each mineral, only the trace elements showing the most significant variations among the studied samples have been reported. All the remaining data are shown in the supplementary material **Tables S7-S9**.

3.2.2.1 Olivine

LA-ICP-MS was performed on 72 olivine grains (8 for MIL090206, 16 for MIL090405, 16 for NWA5363, 10 for NWA6077 and 22 for NWA11187) and the following elements have been measured and subdivided in the following categories according to their abundance:

- Category A (^{55}Mn);
- Category B (^{44}Ca, ^{53}Cr);
- Category C (^{49}Ti, ^{60}Ni, ^{23}Na, ^{59}Co, ^{51}V, ^{66}Zn, ^{27}Al);
- Category D (^{45}Sc, ^{7}Li)
- Category E (^{95}Mo, ^{63}Cu, ^{89}Y and REE).

The average for each element, with relative standard deviation and R.S.D., is reported in **Table 3.7**. Trace elements representative of the different categories are shown in **Fig. 3.2.2.1** whereas the remaining diagrams are reported as appendix (**Table S7**).

Table 3.7, the olivine trace element content, subdivided and sorted based on their average abundance in the meteorites.

Olivine																
		MIL090206			**MIL090405**			**NWA6077**			**NWA5363**			**NWA11187**		
		averaged 8 spots			averaged 16 spots			averaged 10 spots			averaged 16 spots			averaged 22 spots		
Category	ppm	**Mean**	**St. Dev.**	**RSD%**	**Mean**	**St. Dev.**	**RSD%**	**Mean**	**St. Dev.**	**RSD%**	**Mean**	**St. Dev.**	**RSD%**	**Mean**	**St. Dev.**	**RSD%**
A	^{55}Mn	3735.95	173.51	5	3184.03	99.67	3	3131.02	194.52	6	3283.94	63.71	2	3761.96	85.50	2
B	^{44}Ca	551.42	57.54	10	722.71	421.38	58	701.83	579.37	83	544.50	53.85	10	1906.36	75.26	4
	^{53}Cr	330.17	62.93	19	232.52	45.74	20	310.27	167.17	54	242.51	38.74	16	4229.40	194.55	5
C	^{23}Na	47.12	9.77	21	28.93	4.23	15	22.47	4.41	20	23.01	2.73	12	73.81	8.27	11
	^{27}Al	44.05	22.75	52	25.32	12.36	49	273.28	421.03	154	151.70	90.67	60	19.39	5.65	29
	^{49}Ti	33.25	13.68	41	33.26	12.15	37	26.75	8.98	34	24.57	9.31	38	41.44	2.07	5
	^{51}V	25.03	3.94	16	15.01	5.44	36	48.62	16.38	34	50.15	8.25	16	9.92	0.80	8
	^{59}Co	18.34	1.21	7	15.06	1.29	9	17.11	3.87	23	16.04	1.21	8	96.22	3.01	3
	^{60}Ni	14.80	4.17	28	14.81	5.34	36	42.47	8.16	19	48.91	19.90	41	613.32	17.24	3
	^{66}Zn	13.46	12.71	94	8.40	8.13	97	14.64	11.69	80	37.67	65.70	174	205.00	8.90	4
D	^{7}Li	3.89	0.57	15	3.33	0.34	10	3.10	0.25	8	3.43	0.38	11	4.66	0.57	12
	^{45}Sc	2.06	0.58	28	1.67	0.49	29	1.94	0.52	27	2.15	0.75	35	2.60	0.65	25
E	^{63}Cu	0.30	0.16	54	0.60	0.22	36	0.24	0.12	50	0.43	0.28	64	0.57	0.32	55
	^{95}Mo	0.16	0.15	99	0.07	0.02	30	0.64	1.24	196	0.26	0.26	102	0.13	0.03	25

Olivine

Fig. 3.2.2.1, Trace Elements content for olivine in the meteorites MIL090206, MIL090405, NWA6077, NWA5363 and NWA11187. All values are in ppm. a)^{44}Ca values; b)^{53}Cr values (log scale); c)^{60}Ni values (log scale); d)^{59}Co values (log scale); e)^{51}V values; f)^{66}Zn values (log scale); g)^{27}Al values (log scale). Modal analyses for the same meteorites are reported in h).

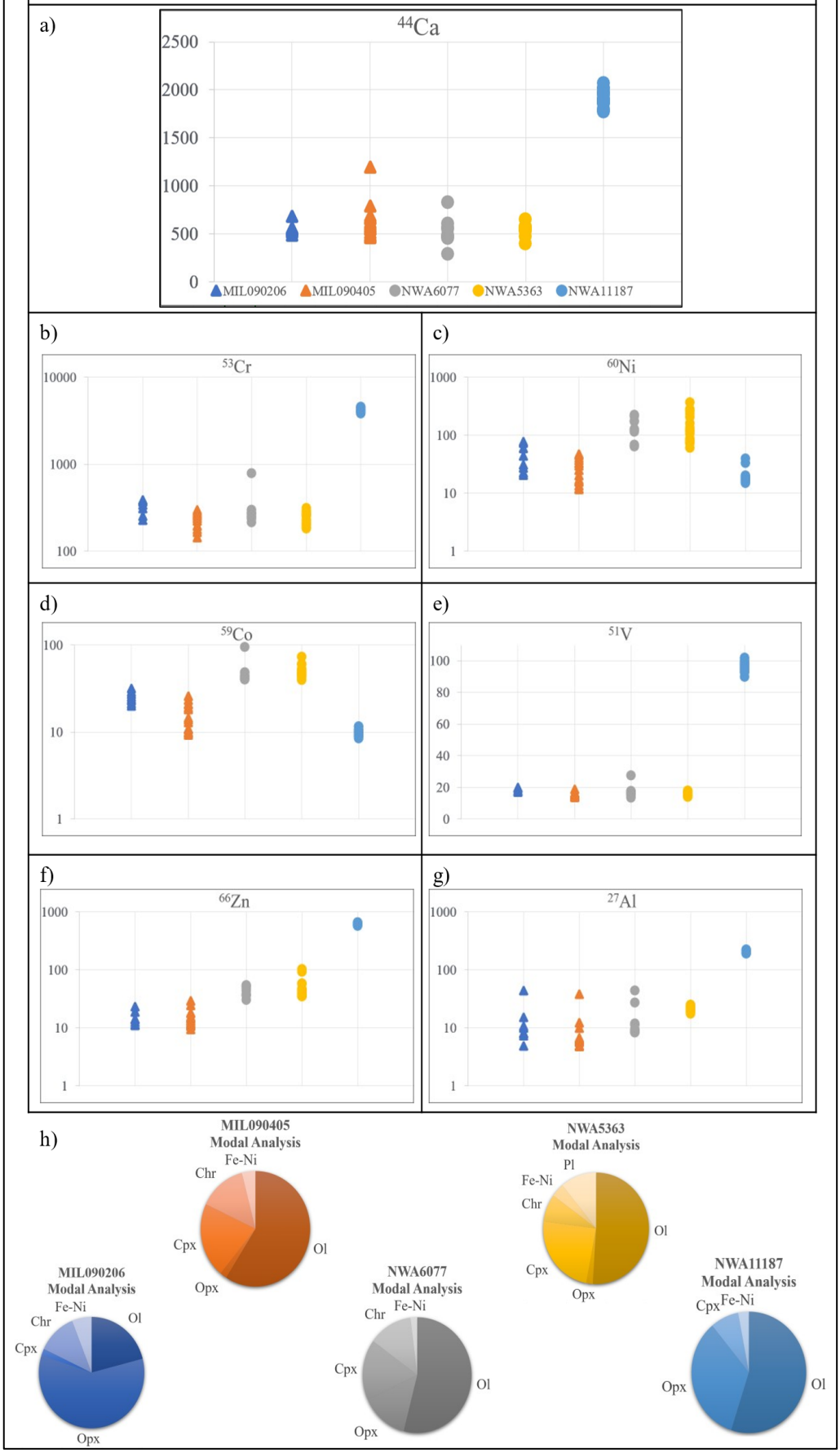

Category A:

^{55}Mn values range from a minimum average value of 3131.02 ppm in NWA6077 to a maximum average value of 3761.96 ppm in NWA 11187, in every meteorite the R.S.D. is always less than 7%.

Category B:

^{44}Ca values range from a minimum average value of 544.50 ppm in NWA5363 to 1906.36 ppm in NWA11187 (**Fig. 3.2.2.1.a**). R.S.D. values for ^{44}Ca in all the studied meteorites show different values: in only 3 of the studied meteorites R.S.D. is 10% or less (MIL090206, NWA5363 and NWA11187), while in MIL090405 and NWA6077 they are considerably higher, 58% and 83% respectively. ^{53}Cr values range from a minimum average value of 232.52 ppm in MIL090405 to a maximum average value of 4229.40 ppm in NWA11187. NWA11187 is showing considerably different values from the other 4 meteorites studied (**Fig. 3.2.2.1.b**), and the R.S.D. values are always below 20%, with the exception of NWA6077, with an R.S.D. value of 54%.

Category C:

^{23}Na values range from a minimum average value of 22.47 ppm to a maximum average value of 73.81 ppm in NWA11187. R.S.D. values are always equal or less than 20%, with the exception of MIL090206, which shows a slightly higher value, 21%. ^{27}Al values range from a minimum average value of 19.39 ppm in NWA11187 to a maximum average value of 273.28 in NWA6077, showing therefore a sharp difference in ^{27}Al content among the meteorites **(Fig. 3.2.2.1.c**). R.S.D. values are always higher than 20%, with a maximum R.S.D. value of 154% in NWA6077 and a minimum value of 29% in NWA11187. ^{49}Ti values range from a minimum average value of 24.57 in ppm in NWA5363 to a maximum average value of 41.44 ppm in NWA11187. R.S.D. values are usually higher than 20%, with the only exception of NWA11187, which has a value of 5%. ^{51}V values range from a minimum average value of 9.92 ppm in NWA11187 to a maximum average value of 50.15 ppm in NWA5363 (**Fig. 3.2.2.1.d**). R.S.D. values are usually slightly higher than 20%, with the exception of NWA11187 and NWA5363, with values of 8% and 16%, respectively. ^{59}Co values vary from a minimum average value of 15.06 ppm in MIL090405 to a maximum average value of 96.22 ppm in NWA11187. The values are all similar for all the meteorites studied, with the noticeable exception of NWA 11187, which have way higher values compared to the other meteorites (**Fig. 3.2.2.1.e**). R.S.D. values are always below 10%, and NWA11187 has the lowest, 3%. ^{60}Ni values range from a minimum average value of 14.80 ppm in MIL090206 to a maximum average value of 613.32 ppm in NWA11187 (**Fig. 3.2.2.1.f**). NWA11187 ^{60}Ni values are way higher than the values of the other meteorites (average values ranging from 14.80 to 48.91 ppm). R.S.D. values are usually higher than 20%, except for NWA11187, which has an R.S.D. value of 3%. ^{66}Zn values range from a minimum average value of 8.40 ppm in MIL090405 to a maximum average value of 205.00 ppm in NWA11187 (**Fig. 3.2.2.1.g**).

^{66}Zn values are usually less than 50 ppm, with the exception of NWA11187. R.S.D. are very high, but R.S.D. value of NWA11187 is small, only 4%.

Category D:

^{7}Li values vary from a minimum average value of 3.10 ppm in NWA6077 to a maximum average value of 4.66 ppm in NWA11187, therefore showing very low dispersion among the meteorites. R.S.D. values are always lower than 20%, averaging around 10%. ^{45}Sc values vary from a minimum average value of 1.67 ppm in MIL090405 to a maximum average value of 2.60 ppm in NWA11187, therefore showing very low dispersion among the meteorites. R.S.D. values are always slightly higher than 20%.

Category E:

^{63}Cu values range from a minimum average value of 0.24 ppm in NWA6077 to a maximum average value of 0.60 ppm in MIL090405. The dispersion of ^{63}Cu values is therefore low Among the studied meteorites. R.S.D. values of Mo are usually high, always above 20%, with the maximum R.S.D. values being 64% in NWA5363. ^{95}Mo values vary from a minimum average value of 0.07 ppm in MIL090405 to a maximum average value of 0.64 ppm in NWA6077. R.S.D. values tend to vary to the lower values of 25 and 30% in NWA11187 and MIL090405, respectively, to the higher values of 102 and 196% in NWA5363 and NWA6077, respectively.

^{89}Y and REE are displayed in the REE (Rare Earth Elements) patterns (**Fig. 3.2.2.2**), normalized to average CI carbonaceous chondrite composition (McDonough and Sun, 1995).

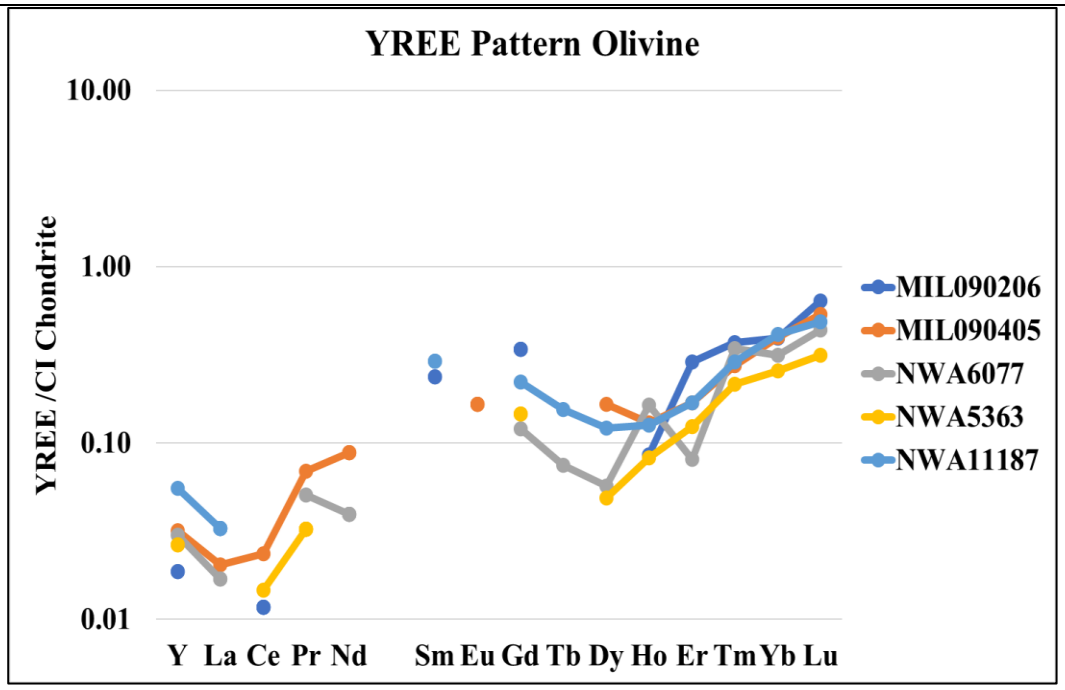

Fig. 3.2.2.2 Y-REE pattern for olivine (logarithmic scale), normalized to average CI carbonaceous chondrite composition (McDonough and Sun, 1995).

3.2.2.2 Orthopyroxene

Orthopyroxene occurs within all the studied meteorites but within the MIL090405 it is rare and small (smaller than the LA-ICP-MS spot size; 5-50 µm) and the obtained geochemical data are contaminated by the surrounding mineral phases and thus they were discarded. LA-ICP-MS was performed on 27 mineral grains (9 MIL090206, 2 NWA5363, 8 NWA6077, 8 NWA11187) and the following elements were detected and subdivided in categories as a function of their abundance:

- Category A (^{44}Ca, ^{55}Mn, ^{53}Cr, ^{27}Al);
- Category B (^{49}Ti, ^{66}Zn, ^{23}Na);
- Category C (^{51}V, ^{60}Ni, ^{59}Co, ^{45}Sc);
- Category D (^{89}Y);
- Category E (^{90}Zr, ^{95}Mo, ^{93}Nb, ^{88}Sr and REE).

The average for each element, with relative standard deviation and R.S.D., is reported in **Table 3.8** Trace elements representative of the different categories are shown in **Fig. 3.2.2.3** whereas the remaining diagrams are reported in the appendix (**Table S8**).

Table 3.8, the orthopyroxene trace element content, subdivided and sorted based on their average abundance in the meteorites.

Orthopyroxene													
		MIL090206			**NWA6077**			**NWA5363**			**NWA11187**		
		averaged 9 spots			averaged 8 spots			averaged 2 spots			averaged 8 spots		
Category	ppm	**Mean**	**St. Dev.**	**RSD%**	**Mean**	**St. Dev.**	**RSD%**	**Mean**	**St. Dev.**	**RSD%**	**Mean**	**St. Dev.**	**RSD%**
A	^{44}Ca	8701.17	787.86	9	7182.79	573.91	8	7652.21	277.09	4	16228.37	1629.24	10
	^{55}Mn	3221.24	200.08	6	3116.25	106.21	3	3365.05	148.14	4	3474.67	121.43	3
	^{53}Cr	1489.48	90.64	6	1457.38	72.55	5	1721.38	31.19	2	5805.77	238.21	4
	^{27}Al	1228.18	57.88	5	1912.18	596.58	31	2986.50	186.66	6	4612.69	292.45	6
B	^{49}Ti	902.69	55.15	6	563.31	31.31	6	646.54	64.07	10	778.51	43.54	6
	^{66}Zn	291.34	25.95	9	291.19	16.21	6	337.10	24.50	7	378.84	20.51	5
	^{23}Na	247.15	32.43	13	193.13	6.95	4	214.80	0.45	0	237.64	13.19	6
C	^{51}V	72.92	4.13	6	68.84	3.08	4	76.98	5.14	7	111.49	3.79	3
	^{60}Ni	53.74	57.87	108	195.71	145.49	74	20.68	0.79	4	33.73	47.78	142
	^{59}Co	28.19	5.42	19	32.11	8.18	25	23.14	1.56	7	5.45	2.34	43
	^{45}Sc	15.34	1.38	9	11.95	1.15	10	14.22	0.60	4	15.47	1.06	7
D	^{89}Y	1.06	0.13	12	0.44	0.14	33	0.40	0.06	15	0.80	0.14	18
E	^{90}Zr	0.94	0.18	19	0.08	0.07	87	0.08	0.01	7	0.16	0.12	72
	^{95}Mo	0.22	0.08	37	0.27	0.16	59	0.22	0.31	141	0.56	0.26	47
	^{93}Nb	0.04	0.02	56	0.01	0.03	210	0.00	0.00	//	0.05	0.03	64
	^{88}Sr	0.03	0.02	68	0.02	0.02	105	0.00	0.01	141	0.38	0.41	110

Orthopyroxene

Fig. 3.2.2.3, Trace Elements content for orthopyroxene in the meteorites MIL090206, NWA6077, NWA5363 and NWA11187. All values are in ppm. a) ^{27}Al values; b) ^{49}Ti values (log scale); c) ^{51}V values; d) ^{60}Ni values (log scale); e) ^{59}Co values; f) ^{90}Zr values; g) ^{95}Mo values; h) ^{88}Sr values (log scale)Modal analyses for the same meteorites are reported in i).

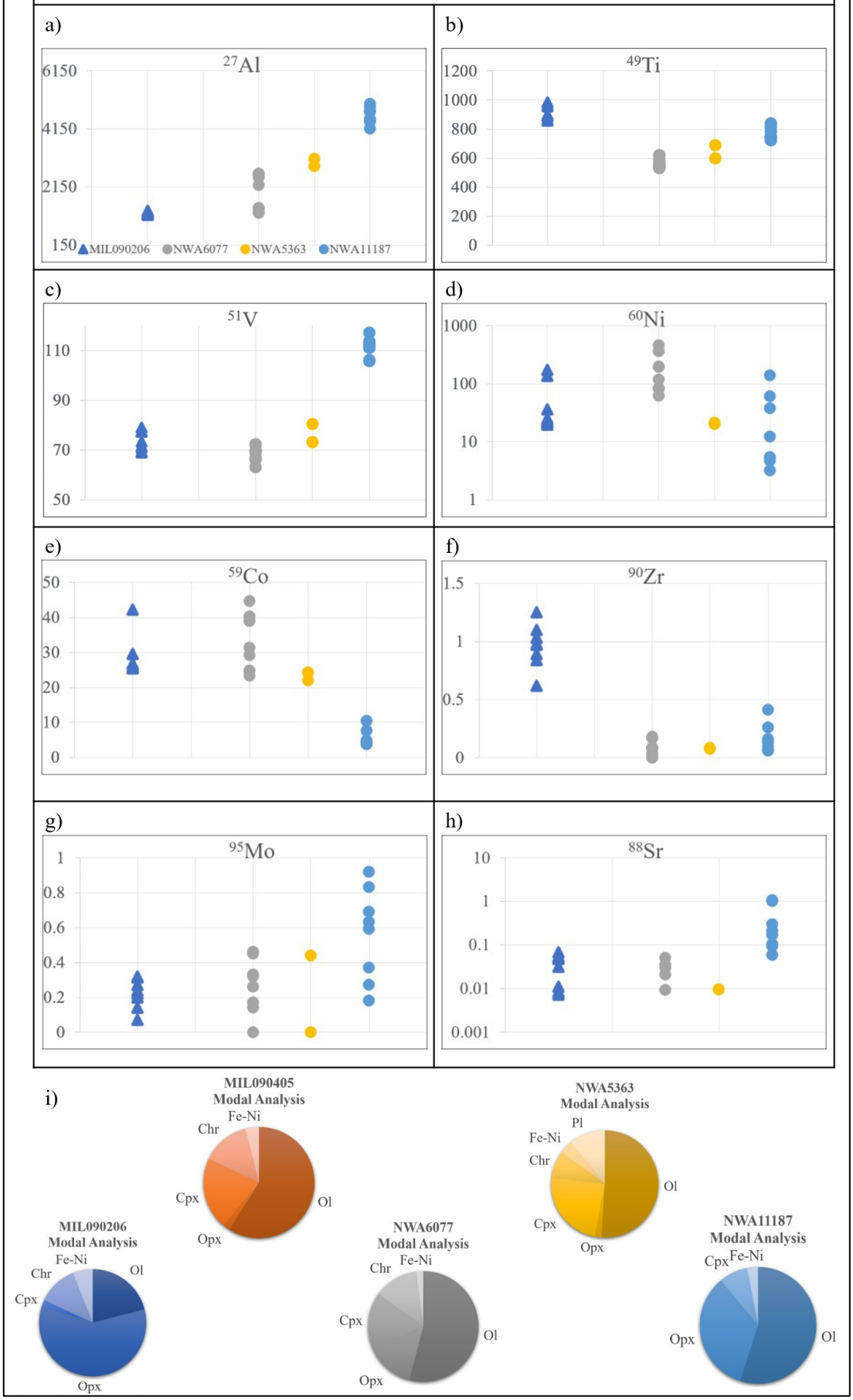

Category A:

^{44}Ca values vary from a minimum average value of 6971.46 ppm in NWA6077 to a maximum average value of 16228.37 ppm in NWA11187, showing therefore a noticeable difference among the studied meteorites. R.S.D. values are usually very low, less than 10% (NWA5363 has the smallest value, 4%). ^{55}Mn values vary from a minimum average value of 3116.25 ppm in MIL090206 to a maximum average value of 3474.67 ppm in NWA11187. R.S.D. values are low, usually around 4%. ^{53}Cr values vary from a minimum average value of 1392.70 ppm in MIL090206 to a maximum average value of 5805.77 ppm in NWA11187, confirming the variation already observed in EMPA data reported in Table 3.2. ^{27}Al values vary from a minimum average value of 1228.18 ppm in MIL090206 to a maximum average value of 4612.69 ppm in NWA11187 (**Fig. 3.2.2.3.a**). R.S.D. values are always below 20%.

Category B:

^{49}Ti values vary from a minimum average value of 540.57 ppm in NWA6077 to a maximum average value of 902.69 ppm in MIL090206 (**Fig. 3.2.2.3.b**). R.S.D. values are always below 20%. ^{66}Zn values vary from a minimum average value of 291.34 ppm in MIL090206 to a maximum average value of 378.84 ppm in NWA11187. R.S.D. values are always lower than 20%. ^{23}Na values vary from a minimum average value of 197.17 ppm in NWA6077 to a maximum average value of 247.15 in MIL090206. R.S.D. values are always below 20%.

Category C:

^{51}V values range from a minimum average value of 68.84 ppm in NWA6077 to a maximum average value of 111.49 in NWA11187, (**Fig. 3.2.2.3.c**). R.S.D. values are always below 20%. ^{60}Ni values vary from a minimum average value of 20.68 ppm in NWA5363 to a maximum average value of 243.55 ppm in NWA6077, showing therefore a remarkable difference between ^{60}Ni values in the studied meteorites (**Fig. 3.2.2.3.d**). R.S.D. values are usually very high, with a maximum value of 142% in NWA11187 and a minimum value of 4% in NWA5363.

^{59}Co values vary from a minimum average value of 5.45 ppm in NWA11187 to a maximum average value of 34.69 in NWA6077, showing a considerable difference between the meteorites (**Fig. 3.2.2.3.e**). R.S.D. values are usually slightly higher than 20%, with a maximum value of 43% in NWA11187 and a minimum value of NWA5363. ^{45}Sc values vary from a minimum average value of 12.27 ppm in NWA6077 to a maximum average value of 15.47 ppm in NWA11187, with the values of ^{45}Sc in orthopyroxene being therefore similar between the studied meteorites. R.S.D. are usually low, always below 20%.

Category D:

^{89}Y values range from a minimum average value of 0.35 ppm in NWA6077 to a maximum average value of 1.06 ppm in MIL090206. R.S.D. values are usually low, less than 20%, with the exception of NWA6077, with a value of 43%.

Category E:

^{90}Zr values vary from a minimum average value of 0.08 ppm in NWA5363 to a maximum average value of 0.94 ppm in MIL090206, showing therefore a considerable difference between the studied meteorites (**Fig. 3.2.2.3.f**). R.S.D. values are usually high, almost always more than 20%, with a maximum value of 85% in NWA6077 and a minimum value of 7% in NWA5363. ^{95}Mo values range from a minimum average value of 0.22 ppm in MIL090206 ppm to a maximum average value of 0.56 ppm in NWA11187 (**Fig. 3.2.2.3.g**). R.S.D. values are high (141% in NWA5363 is the highest), while the lowest is in NWA6077, 26%. ^{93}Nb was not detected in NWA5363 and was detected only once in NWA6077, while its maximum average value was detected in NWA11187 (0.05 ppm). When detected, ^{93}Nb values provide very high R.S.D. values. ^{88}Sr was detected in all the studied meteorites, but it wasn't detected in all the sampling points. ^{88}Sr values vary from a minimum average value of less than 0.001 ppm in NWA5363 to a maximum average value of 0.038 ppm in NWA11187, showing therefore a considerable difference between the studied meteorites (**Fig. 3.2.2.3.h**). The R.S.D. value for NWA11187 is 110%. REE patterns are displayed in **Fig. 3.2.2.4**, normalized to average CI carbonaceous chondrite composition (McDonough and Sun, 1995).

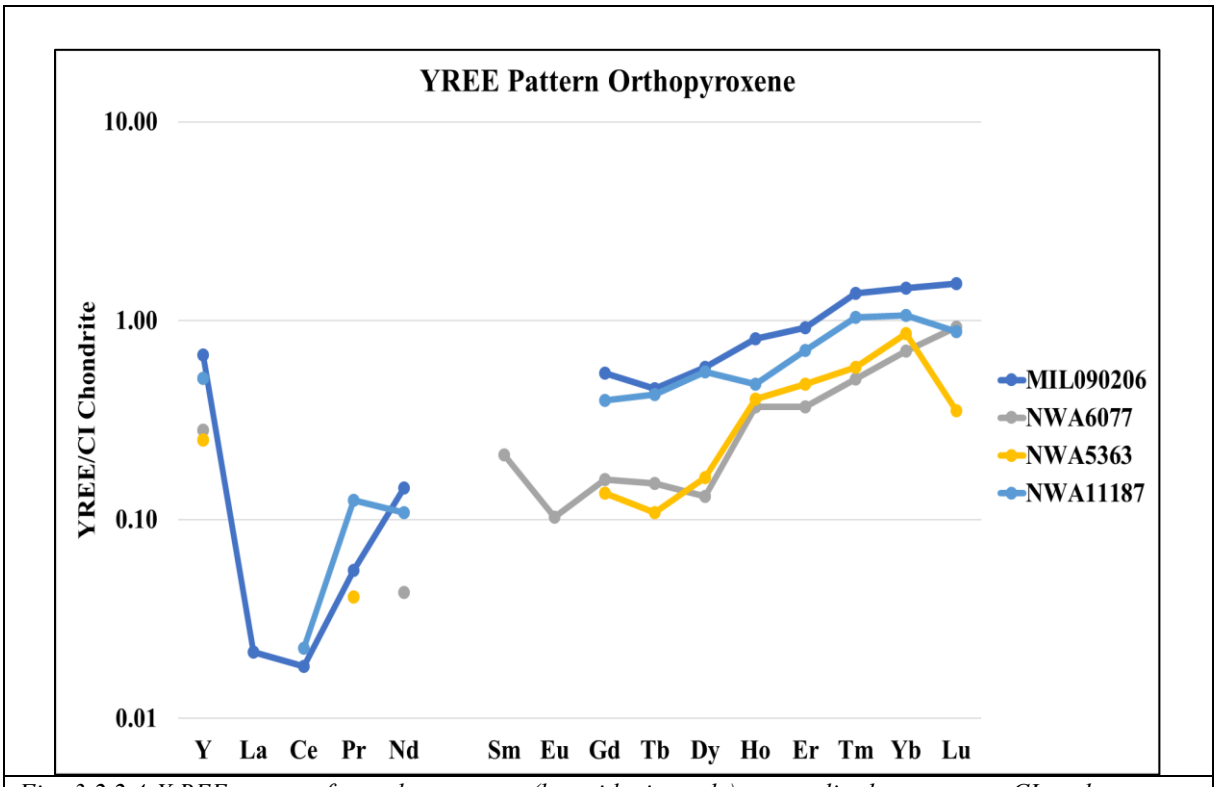

Fig. 3.2.2.4 Y-REE pattern for orthopyroxene (logarithmic scale), normalized to average CI carbonaceous chondrite composition (McDonough and Sun, 1995).

3.2.2.3 Clinopyroxene

Clinopyroxene occurs in all the studied samples but within the MIL090206 it is always smaller than 100 μm is of small size and the available data were discarded due to the contamination from the surrounding mineral phases. LA-ICP-MS was performed on 41 mineral grains (8 MIL090405, 15 NWA5363, 10 NWA6077, 8 NWA11187) and the detected elements are organized according to their abundance as following:

- Category A (^{53}Cr, ^{23}Na, ^{27}Al, ^{49}Ti, ^{55}Mn);
- Category B (^{51}V);
- Category C (^{45}Sc, ^{66}Zn, ^{90}Zr, ^{60}Ni, ^{89}Y, ^{59}Co);
- Category D (^{88}Sr, ^{163}Dy, ^{146}Nd, ^{167}Er, ^{157}Gd, ^{140}Ce);
- Category E (^{173}Yb, ^{149}Sm, ^{177}Hf, ^{165}Ho, ^{63}Cu, ^{95}Mo, ^{93}Nb, ^{141}Pr, ^{159}Tb, ^{139}La, ^{169}Tm, ^{175}Lu, ^{151}Eu).

The average for each element, with relative standard deviation and R.S.D., is reported in **Table 3.9**. Four measurements from NWA6077 differ significantly from the others resulting in very high RSD values. Trace elements representative of the different categories are shown in **Fig. 3.2.2.5** whereas the remaining diagrams are reported in appendix (**Table S9**). The REE patterns are reported in **Fig. 3.2.2.6**, normalized to average CI carbonaceous chondrite composition (McDonough and Sun, 1995).

Table 3.9, the clinopyroxene trace element content, subdivided and sorted based on their average abundance in the meteorites.

Clinopyroxene													
		MIL090405			**NWA6077**			**NWA5363**			**NWA11187**		
		averaged 8 spots			averaged 10 spots			averaged 15 spots			averaged 8 spots		
Category	ppm	**Mean**	**St. Dev.**	**RSD%**	**Mean**	**St. Dev.**	**RSD%**	**Mean**	**St. Dev.**	**RSD%**	**Mean**	**St. Dev.**	**RSD%**
A	^{53}Cr	5943.04	281.53	5	6379.17	398.45	6	6026.47	1684.04	28	6054.31	198.16	3
	^{23}Na	3703.43	144.27	4	3550.58	231.90	7	3536.93	978.17	28	1295.41	17.02	1
	^{27}Al	2973.97	101.72	3	3712.83	251.70	7	7118.68	2074.09	29	8360.07	223.40	3
	^{49}Ti	1738.01	63.39	4	1370.56	62.14	5	1256.32	346.20	28	1612.84	53.05	3
	^{55}Mn	1667.42	57.92	3	1780.72	93.90	5	2024.28	720.38	36	2845.29	68.77	2
B	^{51}V	395.56	13.84	3	382.21	9.20	2	366.05	95.38	26	237.07	6.65	3
C	^{66}Zn	64.39	2.40	4	84.86	6.23	7	84.44	9.42	11	172.17	5.91	3
	^{45}Sc	88.32	5.01	6	81.56	4.19	5	79.95	21.36	27	40.87	0.99	2
	^{90}Zr	35.10	1.25	4	2.28	0.27	12	1.55	0.46	30	0.31	0.17	54
	^{60}Ni	16.81	4.96	29	62.64	69.45	111	152.88	257.00	168	33.31	45.50	137
	^{89}Y	11.61	0.51	4	5.80	0.42	7	4.91	1.41	29	4.41	0.39	9
	^{59}Co	11.31	0.65	6	12.34	3.42	28	22.51	21.32	95	3.57	1.98	6
D	^{88}Sr	3.64	0.18	5	6.43	0.37	6	5.54	1.60	29	4.73	0.48	10
	^{163}Dy	1.82	0.18	10	0.98	0.21	21	0.88	0.30	34	0.84	0.07	9
	^{146}Nd	1.62	0.26	16	0.68	0.20	30	0.61	0.23	38	0.37	0.13	36
	^{167}Er	1.35	0.23	17	0.71	0.12	17	0.58	0.20	35	0.47	0.10	22
	^{157}Gd	1.15	0.10	9	0.70	0.17	24	0.58	0.23	39	0.50	0.21	42
	^{140}Ce	1.06	0.10	10	0.33	0.06	18	0.30	0.10	32	0.14	0.05	34
E	^{173}Yb	0.96	0.19	20	0.76	0.19	26	0.59	0.24	40	0.51	0.11	21
	^{149}Sm	0.86	0.22	25	0.34	0.11	32	0.33	0.17	51	0.27	0.12	44
	^{177}Hf	0.77	0.18	23	0.09	0.06	71	0.07	0.05	80	0.01	0.01	186
	^{165}Ho	0.45	0.09	20	0.23	0.04	16	0.19	0.06	31	0.17	0.02	13
	^{63}Cu	0.44	0.13	28	0.43	0.34	79	2.25	4.04	179	0.26	0.16	60
	^{95}Mo	0.34	0.08	24	0.28	0.21	74	0.28	0.23	80	0.42	0.21	50
	^{93}Nb	0.32	0.04	14	0.03	0.02	60	0.04	0.02	58	0.05	0.02	42
	^{141}Pr	0.27	0.06	24	0.09	0.02	20	0.07	0.02	33	0.04	0.02	41
	^{159}Tb	0.24	0.02	10	0.13	0.04	29	0.12	0.04	35	0.09	0.02	18
	^{139}La	0.21	0.02	12	0.06	0.03	42	0.05	0.02	39	0.02	0.01	56
	^{169}Tm	0.17	0.03	15	0.11	0.01	13	0.10	0.04	36	0.07	0.01	21
	^{175}Lu	0.14	0.03	18	0.11	0.02	22	0.10	0.04	38	0.07	0.03	43
	^{151}Eu	0.05	0.02	52	0.05	0.02	39	0.06	0.02	43	0.03	0.02	63

Clinopyroxene

Fig. 3.2.2.5, Trace Elements content for olivine in the meteorites MIL090206, MIL090405, NWA6077, NWA5363 and NWA11187. All values are in ppm. a)^{53}Cr values; b)^{51}V values; c)^{66}Zn values; d)^{45}Sc values; e) ^{90}Zr values (log scale); f)^{60}Ni values (log scale); g) ^{59}Co values (log scale); h)^{146}Nd. Modal analyses for the same meteorites are reported in i).

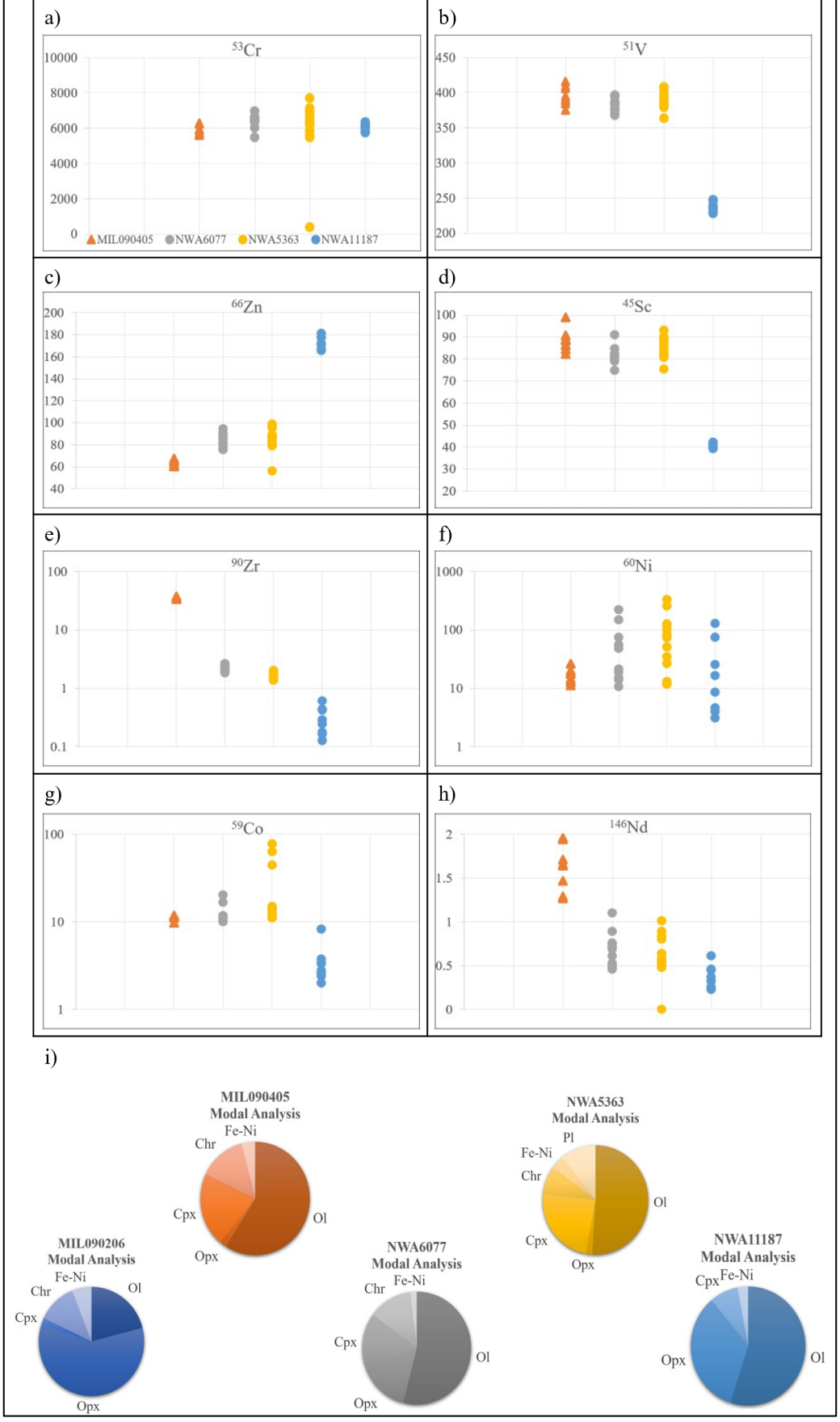

Category A:

^{53}Cr values vary from a minimum average value of 5943.04 ppm in MIL090405 to a maximum average value of 6379.17 ppm in NWA6077 (**Fig. 3.2.2.5.a**). ^{23}Na values vary from a minimum average value of 1295.41 ppm in NWA11187 to a maximum average value of 3703.43 ppm in MIL090405, showing therefore a noticeable difference among the studied meteorites. ^{27}Al values range from a minimum average value of 2973.97 ppm in MIL090405 to a maximum average value of 8360.07 ppm in NWA11187, showing therefore a noticeable difference among the studied meteorites. ^{49}Ti values range from a minimum average value of 1256.32 ppm in NWA5363 to a maximum average value of 1738.01 ppm in MIL090405, having therefore similar values in all the studied meteorites. ^{55}Mn values range from a minimum average value of 1667.42 in MIL090405 to a maximum average value of 2845.29 in NWA11187. In fact, the values in the three meteorites are similar within the standard deviation, with the exception of NWA11187.

Category B:

^{51}V values range from a minimum average value of 237.07 ppm in NWA11187 to a maximum average value of 395.56 ppm in MIL090405 (**Fig. 3.2.2.5.b**).

Category C:

^{66}Zn values vary from a minimum average value of 64.39 ppm in MIL090405 to a maximum average value of 172.17 ppm in NWA11187 (**Fig. 3.2.2.5.c**). ^{45}Sc values range from a minimum average value of 40.87 ppm in NWA11187 to a maximum average value of 88.32 ppm in MIL090405 (**Fig. 3.2.2.5.d**). values show little dispersion in all of the studied meteorites (always lower than 10%), with the exception of NWA5363, which has a R.S.D. value of 27%. ^{90}Zr values vary from a minimum average value of 0.31 ppm in NWA11187 to a maximum average value of 35.10 ppm in MIL090405, showing therefore a noticeable difference in the values among the studied meteorites (**Fig. 3.2.2.5.e**). The R.S.D. values vary from 4% to 54% (MIL090405 and NWA11187, respectively). ^{60}Ni values vary from a minimum average value of 16.81 ppm in MIL090405 to a maximum average value of 152.88 ppm in NWA5363, showing therefore a noticeable difference among the studied meteorites (**Fig. 3.2.2.5.f**). R.S.D. values show a very high dispersion in the studied meteorites, since they are always higher than 20% and sometimes can be even higher than 100% (111%, 137% and 168% in NWA6077, NWA11187 and NWA5363, respectively). The large dispersion could have been caused by the "contamination" from Fe-Ni inclusions in Clinopyroxene minerals, or Fe-Ni grains between small clinopyroxene minerals. ^{89}Y values vary from a minimum average value of 4.41 ppm in NWA11187 to a maximum average value of 11.61 ppm in MIL090405 (**Fig. 3.2.2.6**). R.S.D. values range between 4% and 29%, showing therefore low dispersion in the values of the studied meteorites. ^{59}Co values vary from a minimum average value of 3.57 ppm in NWA11187 to a maximum average value of 22.51 ppm in NWA5363, showing therefore a noticeable difference among the studied

meteorites (**Fig. 3.2.2.5.g**). three out of four meteorites show high dispersion in the R.S.D. values, since they are greater than 20% (from 28% in NWA6077 to 95% in NWA5363), with the only exception of MIL090405, which has a value of 6%.

Category D:

^{88}Sr values vary from a minimum average value of 3.64 ppm in MIL090405 to a maximum average value of 6.43 ppm in NWA6077. The dispersion in the values is usually quite low, with R.S.D. values always below than 10%, with the only exception of NWA5363, which has a value of 29%. ^{163}Dy values vary from a minimum average value of 0.84 ppm in NWA11187 to a maximum average value of 1.82 ppm in MIL090405 (**Fig. 3.2.2.6**). R.S.D. values are usually low, around 20%, with the only exception of NWA5363, which has a value of 34%. ^{146}Nd values vary from a minimum average value of 0.37 ppm in NWA11187 to a maximum average value of 1.62 ppm in MIL090405, showing therefore a noticeable difference among the studied meteorites (**Fig. 3.2.2.5.h**). R.S.D. values are high, being usually over 20%, with the only exception of MIL090405, which has a value of 16%. ^{167}Er values vary from a minimum average value of 0.47 ppm in NWA11187 to a maximum average value of 1.35 ppm in MIL090405 (**Fig. 3.2.2.6**). R.S.D. values are usually not high, below 20%, with some exceptions: NWA11187 and NWA5363 with values of 22% and 35%, respectively. ^{157}Gd values range from a minimum average value of 0.50 ppm in NWA11187 to a maximum average value of 1.15 ppm in MIL090405 (**Fig. 3.2.2.6**). R.S.D. values are usually higher than 20%, with the only exception of MIL090405, with a value of 9%. ^{140}Ce values vary from a minimum average value of 0.14 ppm in NWA11187 to a maximum average value of 1.06 ppm in MIL090405, showing therefore a noticeable difference among the studied meteorites (**Fig. 3.2.2.6**). R.S.D. values are high, showing dispersion in the data, since NWA11187 and NWA5363 have values of 34% and 32%, respectively.

Category E:

^{89}Yb values vary from a minimum average value of 0.51 ppm in NWA11187 to a maximum average value of 0.96 ppm in MIL090405 (**Fig. 3.2.2.6**). R.S.D. values are always equal or higher than 20%, with the highest value being 40% in NWA5363. ^{149}Sm values vary from a minimum average value of 0.27 ppm in NWA11187 to a maximum average value of 0.86 ppm in MIL090405 (**Fig. 3.2.2.6**). R.S.D. values are always higher than 20%, with the highest being 51% in NWA5363. ^{177}Hf values vary from a minimum average value of 0.01 ppm in NWA11187 to a maximum average value of 0.77 ppm in MIL090405, showing therefore noticeable difference among the studied meteorites (**Fig. 3.2.2.6**). R.S.D. values are very high, with the lowest being 23% in MIL090405 and the highest 186% in NWA11187. ^{165}Ho values vary from a minimum average value of 0.17 in NWA11187 ppm to a maximum average value of 0.45 ppm in NWA5363 (**Fig. 3.2.2.6**). R.S.D. values are usually lower than 20%, with the only exception of NWA5363, which has a value of 31%. ^{63}Cu values vary from a minimum average value of 0.26 ppm in NWA11187 to a maximum average value of 2.25 in

NWA5363, showing therefore a noticeable difference among the studied meteorites. R.S.D. values are high, with a minimum value of 28% in MIL090405 and a maximum value of 179% in NWA5363, showing therefore dispersion in the data of the meteorites. ^{95}Mo values vary from a minimum average value of 0.28 ppm in NWA5363 and NWA6077 to a maximum average value of 0.42 ppm in NWA11187. R.S.D. values are high, always higher than 20%, with the highest being 80% in NWA5363. ^{93}Nb values vary from a minimum average value of 0.03 ppm in NWA6077 to a maximum average value of 0.32 ppm in MIL090405, showing therefore a noticeable difference among the studied meteorites (**Fig. 3.2.2.6**). R.S.D. values are high, from 42% to 60%, with the exception of MIL090405, which has a value of 14%. ^{141}Pr values vary from a minimum average value of 0.04 ppm in NWA11187 to a maximum average value of 0.27 ppm in MIL090405 (**Fig. 3.2.2.6**). R.S.D. values are always equal or higher than 20%, with the highest being 41% in NWA11187. ^{159}Tb values vary from a minimum average value of 0.09 ppm in NWA11187 to a maximum average value of 0.24 ppm in MIL090405 (**Fig. 3.2.2.6**). R.S.D. values range from a minimum value of 10% in MIL090405 to a maximum value 35% in NWA5363. ^{139}La values vary from a minimum average value of 0.02 ppm in NWA11187 to a maximum average value of 0.21 ppm in MIL090405, showing therefore a noticeable difference among the studied meteorites (**Fig. 3.2.2.6**). R.S.D. values are always higher than 20%, with the highest being 56% in NWA11187, with the exception of MIL090405, which has a value of 12%. ^{169}Tm values vary from a minimum average value of 0.07 in NWA11187 to a maximum average value of 0.17 ppm in MIL090405 (**Fig. 3.2.2.6**). R.S.D. values can vary, for MIL090405 and NWA6077 the values are, in fact, lower than 20%, while NWA11187 and NWA5363 have value of 36% and 21%, respectively. ^{175}Lu values vary from a minimum average value of 0.07 ppm in NWA11187 to a maximum average value of 0.14 ppm (**Fig. 3.2.2.6**). R.S.D. values can vary, for MIL090405 the value is, in fact, 18%, while the other three meteorites have values always higher than 20%, with the highest one being 43% in NWA11187. ^{151}Eu values vary from a minimum average value of 0.03 ppm in NWA11187 to a maximum average value of 0.06 ppm in NWA5363 (**Fig. 3.2.2.6**). R.S.D. values are always higher than 20%, with the values ranging from 39% in NWA6077 to 63% in NWA11187.

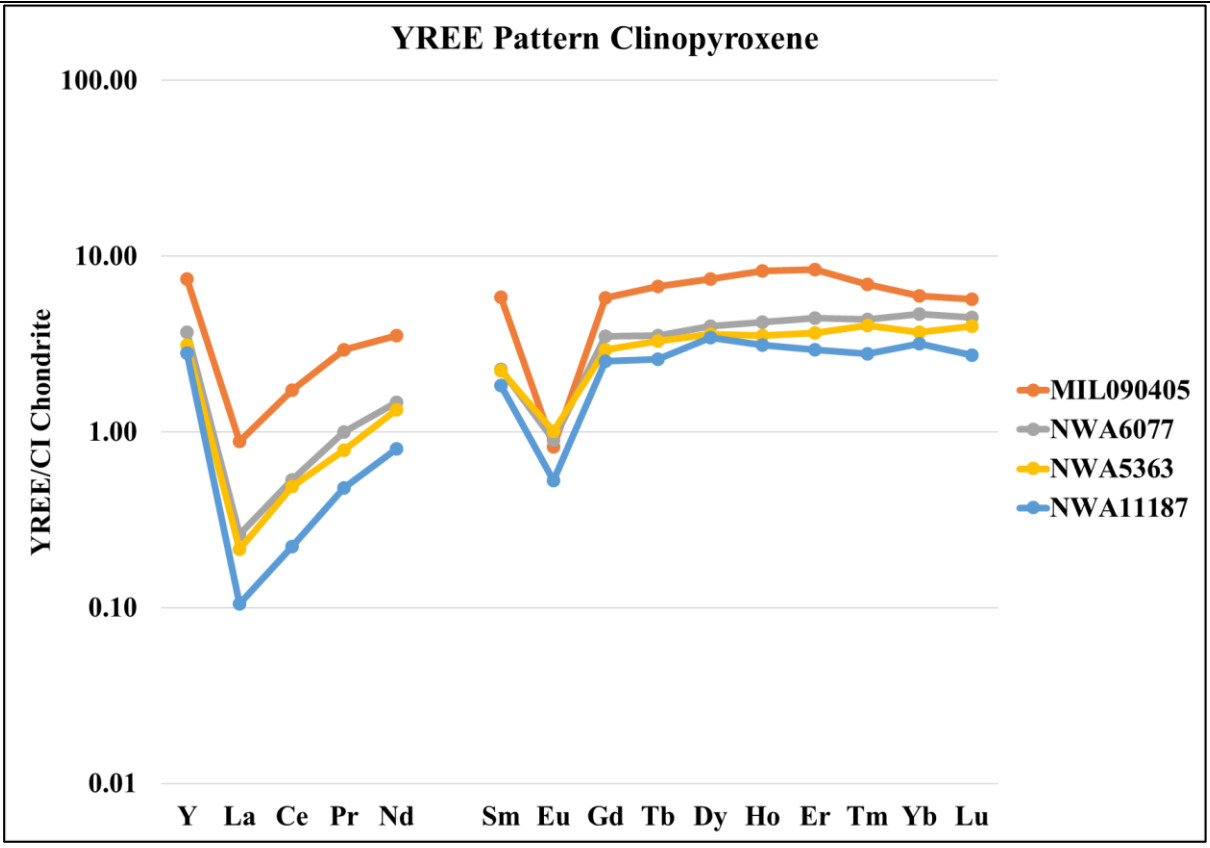

Fig. 3.2.2.6 Y-REE pattern for clinopyroxene (logarithmic scale), normalized to average CI carbonaceous chondrite composition (McDonough and Sun, 1995).

3.2.4 Plagioclase

Plagioclase was found in only one of the five meteorites studied in this work, in NWA5363. In order to study plagioclase, LA-ICP-MS was performed on 5 mineral grains contained in the meteorite. These elements were detected and subdivided in categories based on their abundance:

- Category A (^{57}Fe, ^{60}Ni);
- Category B (^{25}Mg, ^{88}Sr, ^{49}Ti, ^{59}Co);
- Category C (^{55}Mn, ^{63}Cr, ^{138}Ba, ^{63}Cu);
- Category E (^{45}Sc, ^{51}V and REE).

The average for each element, with relative standard deviation and R.S.D., is reported in **Table 3.10**. The REE patterns are reported in **Fig. 3.2.2.7**, normalized to average CI carbonaceous chondrite composition (McDonough and Sun, 1995).

Table 3.10, the orthopyroxene trace element content, subdivided and sorted based on their average abundance in the meteorites.

Plagioclase				
		NWA5363		
		Averaged 6 spots		
Category	ppm	**Mean**	**St. Dev.**	**RSD%**
A	^{57}Fe	11525.23	13608.10	118
	^{60}Ni	1382.86	1379.33	100
B	^{25}Mg	653.97	532.57	81
	^{88}Sr	148.62	8.76	6
	^{49}Ti	132.08	10.87	8
	^{59}Co	100.21	100.19	100
C	^{55}Mn	75.99	33.54	44
	^{53}Cr	19.12	16.55	87
	^{138}Ba	19.07	1.11	6
	^{63}Cu	14.41	15.78	110
E	^{45}Sc	0.84	0.37	44
	^{151}Eu	0.67	0.17	26
	^{51}V	0.55	0.27	49
	^{140}Ce	0.06	0.03	48
	^{139}La	0.03	0.03	84

Only few of the elements provided a Relative Standard Deviation (RSD) lower than 20% (^{138}Ba, ^{88}Sr and ^{49}Ti), while only one of the elements has values of RSD ranging between 20% and 40% (^{151}Eu, 26%) but most of the elements have values of RSD way higher than 40% (^{45}Sc, ^{55}Mn, ^{140}Ce, ^{51}V, ^{25}Mg, ^{139}La, ^{53}Cr, ^{59}Co, ^{60}Ni, ^{63}Cu and ^{57}Fe), with ^{57}Fe having the highest value, 118%. The high RSD values for ^{57}Fe, ^{60}Ni and ^{53}Cr are probably due to the presence of many ^{57}Fe-^{60}Ni and chromite veins in the plagioclase grains, combined with a low number of performed measurements. Also, the other high values of RSD are probably due to a low number of measurements. Y-REE pattern for plagioclase (NWA5363) is shown in **Fig. 3.2.2.7**.

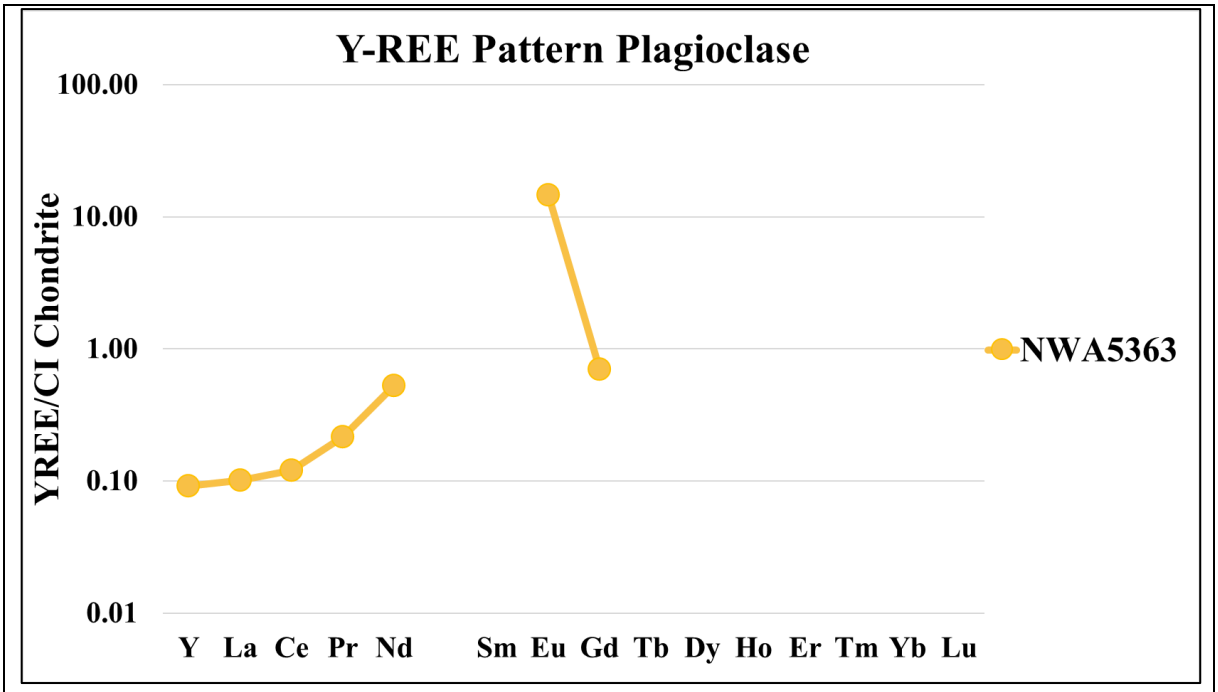

Fig. 3.2.2.7 Y-REE pattern plagioclase (logarithmic scale), normalized to average CI carbonaceous chondrite composition (McDonough and Sun, 1995).

4. DISCUSSION

4.1 SUBDIVISION OF STUDIED METEORITES AND AFFINITIES WITH OTHER METEORITES

According to petrography and geochemistry the studied ungrouped meteorites can be subdivided in a major group containing four samples (MIL090206, MIL090405, NWA6077, NWA5363) and an individual sample, i.e., NWA11187, which is different for the presence of exsolution lamellae of clinopyroxene in orthopyroxene and for the content of major, minor and trace elements in all the analysed minerals.

Within the main group, a few minor petrographic differences were observed. In MIL090206 and MIL090405, for example, Fe-Ni and orthopyroxene intergrowths commonly occur, while in NWA6077 and NWA5363 they are scarce, and usually smaller than in the previous samples. In addition, in NWA6077 and NWA5363 other minor phases were detected, phosphates for NWA6077 and plagioclase for NWA5363, even though plagioclase was found in the sample MIL090206,5 by Goodrich et al. (2017). Geochemically, NWA6077 and NWA5363 have a slightly higher content of Cr_2O_3 in olivine (**Table 3.1**).

Geochemically, NWA11187 differs significantly from the other meteorites (see Chapter 3). NWA11187 contains clinopyroxene as exsolution lamellae within orthopyroxene, a feature never found in the other meteorites of this study, though they were identified in other categories of meteorites, for example in lunar meteorites (e.g. Cao et el. 2024).

In order to tentatively classify the studied ungrouped meteorites a comparison of the results of this thesis with literature data has been carried out. According to literature studies based on mineralogical, petrographic and geochemical investigations the four meteorites of the main group (MIL090206, MIL090405, NWA6077, NWA5363) share similarities with two meteorites: MIL 090340 and NWA5400, classified as “brachinite-like”. In particular, MIL090340 is similar to MIL 090206 (Goodrich et al., 2017) and NWA 6077 is similar to NWA 5400 (Day et al., 2012).

4.2 ARE MIL090206, MIL090405, NWA6077 AND NWA5363 BRACHINITE-LIKE UNGROUPED?

Brachinites are olivine rich achondrites with up to 15 modal% augite; various abundances of plagioclase (0–10 modal %); and minor to trace abundances of orthopyroxene, chromite, phosphates, metal, and sulfides (e.g. Keil, 2014, and Krot et al., 2013). The olivine rich areas usually have medium to coarse grained granoblastic textures (up to 1.5 mm) and display triple junctions, while plagioclase and orthopyroxene grains show intergranular morphologies (Goodrich et al., 2017). Silicate compositions are homogeneous, with a Fo of 64-68. Brachinite-like meteorites have similar characteristics to those of brachinites, but olivine and orthopyroxene are more magnesian (e.g. 70-80 Fo in olivine) and contain significantly more orthopyroxene than brachinites (Day et al., 2012). In addition, pyroxenes in brachinite-like meteorites are usually poikilitic, an uncommon feature in brachinites (Goodrich et al., 2017).

MIL090340, MIL090206 and MIL090405 have important common petrographic features. Fine-grained intergrowths of orthopyroxene, Fe-Ni phases and Sulphur have been identified in all these three meteorites by Goodrich et al. 2017, Singerling et al. 2013 and this study (see Fig. 2.a in Goodrich et al. 2017 and **Fig. 3.1.3**; **3.1.7.a**, this study). These intergrowths form linings along olivine grain boundaries, from which are usually separated by a narrow strip of Fe-Ni phases which marks the boundary, and are usually 5-50 μm in width (Goodrich et al., 2017).

MIL090340 has also 120° triple junctions between olivine grains (Goodrich et al., 2017), as also reported for MIL090206 and MIL090405 (**Fig. 3.1.2** and **Fig. 3.1.8**, respectively). In addition, in MIL090206 (this study and Goodrich et al. 2017) and in MIL090405 are reported pyroxene poikiloblasts enclosing olivine (**Fig. 3.1.3**, Fig. 4 in Goodrich et al. 2017 and **3.1.9**, respectively).

NWA6077, NWA5363 and NWA5400 (**Fig. 3.1.11.b**, **Fig. 3.1.14** and Fig. 4.e in Gardner-Vandy et al. 2013, respectively) have common petrographic features to MIL090206, MIL090405 and MIL090340. In fact, these three meteorites also have triple junctions and pyroxene poikiloblasts enclosing olivine (**Fig. 3.1.11.a**, **Fig. 3.1.14** and Fig. 4.e in Gardner-Vandy et al. 2013, respectively), but there is a noticeable difference. In fact, FIOFs (Fine-grained Intergrowths of Orthopyroxene and Fe-Ni phases) in this study were also identified for NWA6077 and NWA5363, although they are less evident and frequent compared to the ones in MIL090206 and MIL090405, while they were not identified by both Day et al. (2012), and Gardner-Vandy et al. (2013). Based on these differences, a kinship between NWA5400 and NWA6077/NWA5363 was first proposed by Weisberg et al. (2009), while in Day et al. (2012) only NWA6077 is mentioned.

Geochemically, the major and minor elements data of the meteorites MIL090206, MIL090405, NWA6077, NWA5363, MIL090340 and NWA5400 are very similar (see **Tables S10, S11, S12, S13, S14 and S15**). For example, the Fo content in olivine of the six meteorites previously mentioned ranges between 69.6 and 72.4 mol% (**Table S10** and **Fig. 4.2.1**).

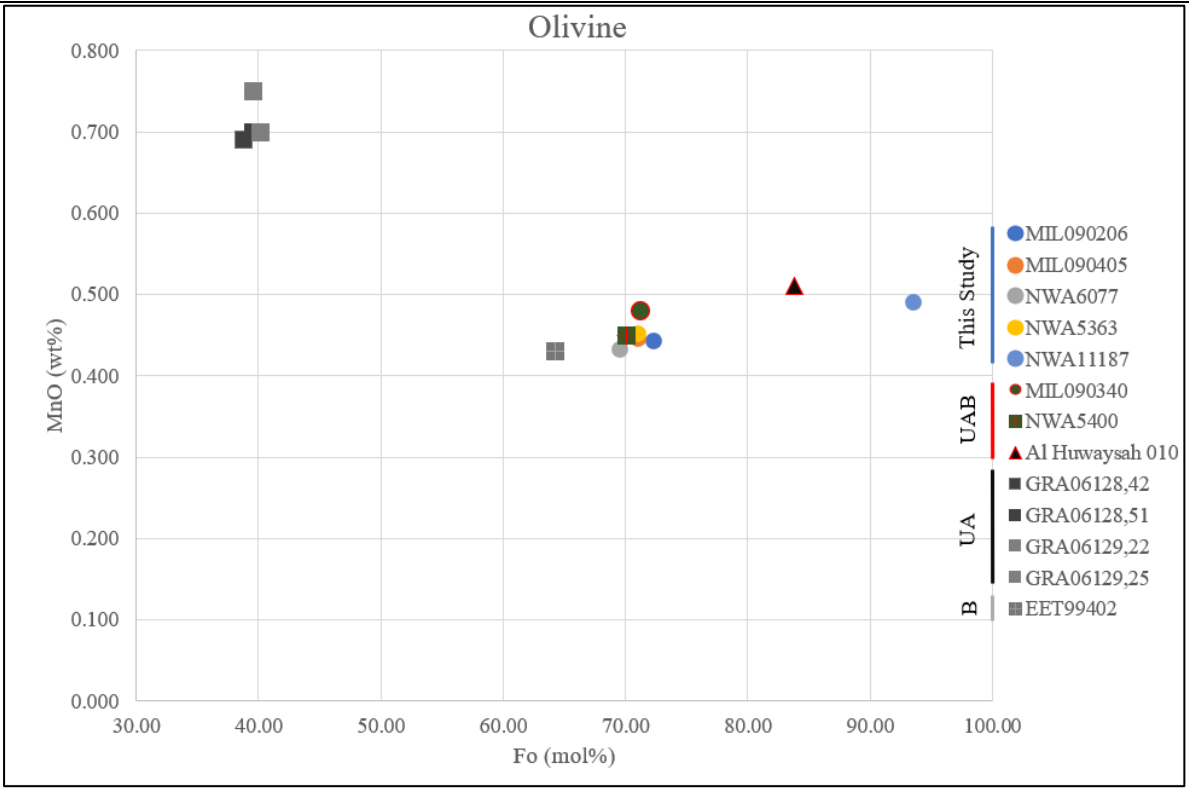

Fig. 4.2.1, Fo vs MnO for olivine diagram for MIL090206, MIL090405, NWA6077, NWA5363, NWA11187, MIL090340, NWA5400, Al Huwaysah 010 (brachinite-like ungrouped achondrite), GRA06128,42 (ungrouped achondrite), GRA06128,51 (ungrouped achondrite), GRA06129,22 (ungrouped achondrite), GRA06129,25 (ungrouped achondrite) and EET99402 (brachinite). The different shapes of the markers indicate different papers. B = brachinite, UA = ungrouped achondrite, UAB = brachinite-like ungrouped achondrite. Data from Goodrich et al. (2017), Carli et al. (2023), Day et al. (2012) and Gardner-Vandy et al. (2013).

Even though the major and minor elements data of MIL090206, MIL090405, NWA6077, NWA5363, MIL090340 and NWA5400 are comparable, there is a noticeable difference in the content of Cr_2O_3 in olivine for NWA 5363 and NWA 6077 (see **Fig. 4.2.2**). MIL090206, MIL090405, MIL090340 plot exactly in the brachinite field, while NWA11187 plots in the ureilite field.

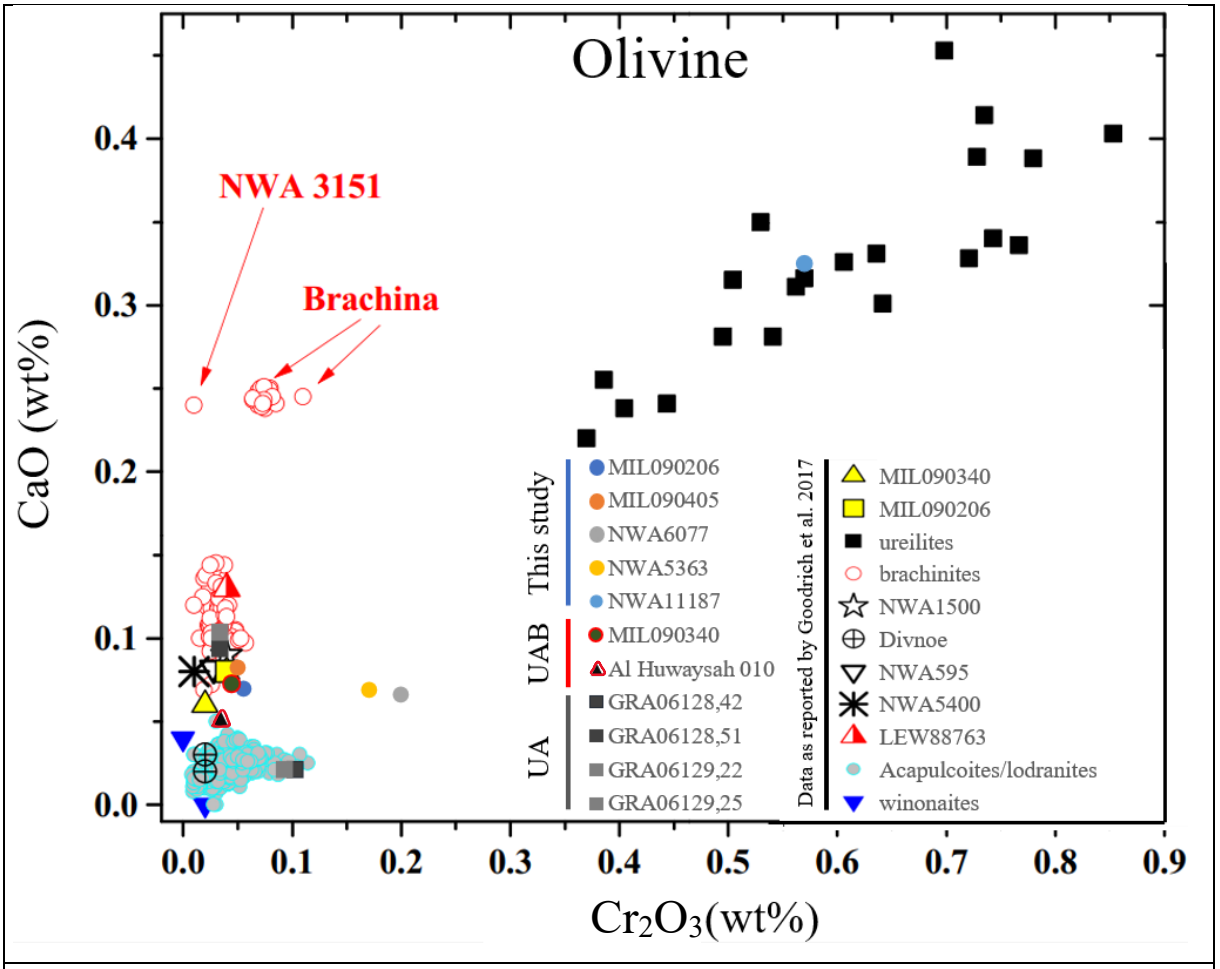

Fig. 4.2.2, Cr_2O_3 vs CaO for olivine diagram for MIL090206, MIL090405, NWA6077, NWA5363, NWA11187, MIL090340, Al Huwaysah 010 (brachinite-like ungrouped achondrite), GRA06128,42 (ungrouped achondrite), GRA06128,51 (ungrouped achondrite), GRA06129,22 (ungrouped achondrite), GRA06129,25 (ungrouped achondrite) and selected meteorites from Goodrich et al (2017). The different shapes of the markers indicate different papers.UA = ungrouped achondrite, UAB= brachinite-like ungrouped achondrite. As can be easily seen, there are two MIL090206 samples in the diagram, the one from this study is an orange circle, while the one from Goodrich et al. (2017) is a yellow triangle. Image modified from Goodrich et al. (2017). Brachinite data from Nehru et al. (1983), Warren and Kallemeyn (1989), Goodrich and Righter (2000), Mittlefehldt et al. (2003), and Goodrich et al. (2011). Data for NWA 1500 (ungrouped achondrite) from Goodrich et al. (2006); NWA 595 (brachinite) from Goodrich et al. (2011); NWA 5400/6077 from Gardner-Vandy et al. (2013); Divnoe from Petaev et al. (1994); LEW 88763 (brachinite) from Gardner-Vandy (2012) and Day et al. (2015). For sources of ureilite, lodranite, and winonaite data, see fig. 5 of Goodrich et al. (2011). Cr_2O_3 value for NWA5400 was not reported in Day et al. (2012).

The trace elements data are also very similar among the meteorites for clinopyroxene, whereas they are different for plagioclase (if present) (**Tables S16 and S17**).

The trace elements compositions of clinopyroxene are particularly comparable in NWA6077 and NWA5363, where also Y-REE elements are similar, whereas in MIL090405 Y-REE are higher than in NWA6077 and NWA5363, while in NWA5400 are lower compared to NWA6077 and NWA5363. The only differences between NWA6077 and NWA5363 in the trace elements content can be found in Co, Ni and Cu. In general, as can be seen in **Fig. 4.2.3**, the Y-REE pattern for MIL090405,

NWA6077, NWA5363 and NWA5400 have the exact same shape, even if MIL090405 has higher concentrations and a more pronounced Eu anomaly. The observed features suggest that clinopyroxene was in equilibrium with melts of the same origin but with a different degree of fractional crystallization. No trace elements data were found for MIL090206 and MIL090340 in the literature.

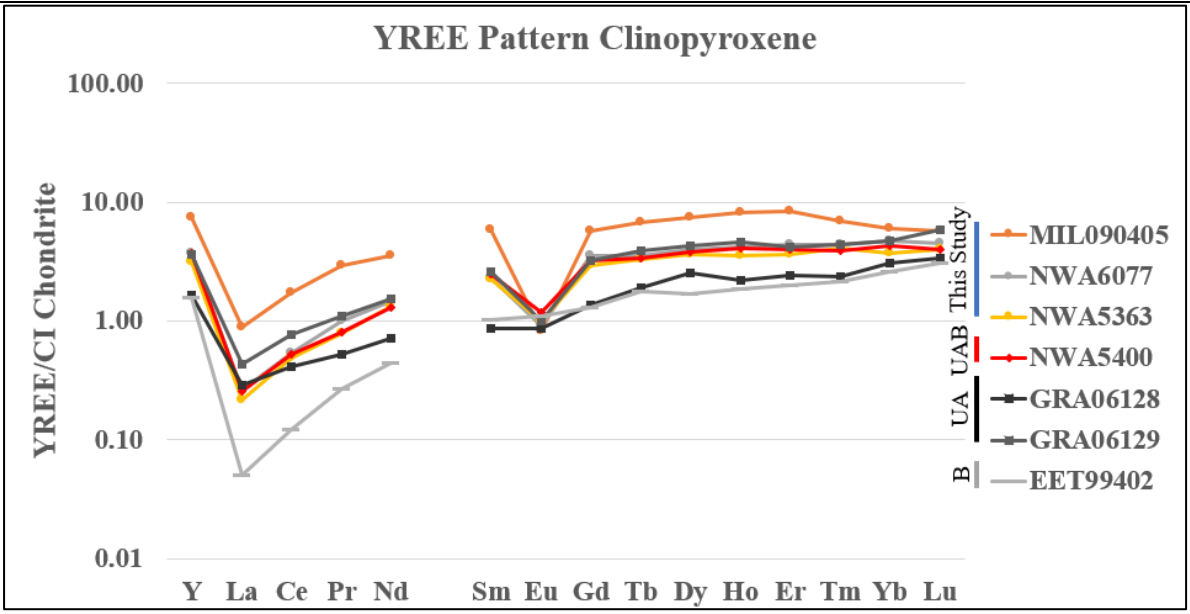

Fig. 4.2.3, Y-REE pattern for clinopyroxene in MIL090405, NWA6077, NWA5363, NWA5400, GRA06128 (ungrouped achondrite), GRA06129 (ungrouped achondrite), EET99402 (brachinite). NWA5400, GRA06128, GRA06129 and EET99402 data from Day et al. (2012). Data normalized to the average CI composition from McDonough and Sun (1995). The different shapes of the markers indicate different papers. UAB = brachinite-like ungrouped achondrite, UA = ungrouped achondrite, B = brachinite.

4.3 IS NWA11187 AN UREILITE?

Ureilites are among the most common achondritic meteorites, originating from a partially differentiated, carbon-rich asteroid (Goodrich et al. 2022). These meteorites are derived from the residual mantle of a reduced, differentiated asteroid, known as the "Ureilite Parent Body" (Downes et al Available at SSRN 4688703). NWA11187 has common features with the ureilite group. As reported in Fig. 10 (b) in Li et al. 2018, where a $\Delta^{17}O$ - $\varepsilon^{54}Cr$ diagram containing data of different meteorite groups is displayed, NWA11187 plots in the ureilite area. Furthermore, as already displayed in **Fig. 4.2.2** of this work, even Cr_2O_3 and CaO content are comparable with values from many different ureilites. Ureilites can contain interstitial carbon phases (graphite and minor diamond) up to 10% (Goodrich et al. 2022), which were not identified for NWA11187 during the analyses performed for this work, even though Gattacceca et al. (2019) reports the presence of bladed graphite as an accessory phase. Additionally, Rosén et al. (2019) report that the higher the content of forsterite in olivine (93.6 mol% in NWA11187), the lesser is the content of graphite. Given these main common features of NWA11187 with ureilites, this chapter aims to tentatively classify NWA11187 as an ureilite.

Ureilites, as described by Goodrich et al. (2022), can be divided into two categories: main group ureilites (~95%) and polymict ureilites (~5%). Main group ureilites (Fo 75-95 mol%) are unbrecciated, coarse-grained ultramafic rocks, with an average grain size of ~0.5–1 mm, consisting primarily of olivine and pyroxene, and containing up to 10% interstitial carbon. Polymict ureilites, on the other hand, are breccias (both fragmental and regolith) that include lithic clasts derived from main group ureilites (Goodrich et al., 2022). Main group ureilites are further classified into low-Ca ureilites (Fo 75-85 mol%) and augite ureilites (Fo 86-95 mol%), with the latter being subdivided into orthopyroxene/pigeonite ureilites and orthopyroxene ureilites (Goodrich et al. 2022). As previously mentioned, NWA11187 has a forsterite content in olivine of 93.6 mol%, placing it within the range of augite ureilites, and it contains both orthopyroxene and pigeonite. Meteorites from the Hughes Cluster and LEW85540 share significant petrographic and geochemical similarities with NWA11187.

The “Hughes Cluster” is a group of ureilites which share common features. This terminology was first used by Goodrich et al. (2001). The name is derived from Hughes 009, which was first discovered in 1994 (Wlotzka 1994), and Hughes 009 derives its name from the asteroid Hughes (Goodrich et al. 2001), which also names meteorites not belonging to the ureilite group (e.g. Hughes 004/005, howardites, Wlotzka 1992). LEW85440 was instead first discovered in 1987 (Mason, AMN 10 (1)). The name is derived from the location where it was found, Lewis Cliff (LEW), Antarctica, in the Upper Ice Field (Score et al. 1990).

For the petrography of the Hughes Cluster (Fo 86-88 mol%), the petrography of Hughes 009 and FRO 90054/93008 will be described, which share common petrographic features (Goodrich et al. 2009). The modal abundances for Hughes 009 and FRO 90054/93008 are very comparable with NWA11187, and are: olivine (23-47 vol%), augite (7-52 vol%) and orthopyroxene (12-56 vol%), as reported by Goodrich et al. (2009). The three Hughes Cluster meteorites previously mentioned have a coarse-grained texture, with grains up to 3 mm (Goodrich et al. 2009). The texture is also highly-equilibrated, with triple junctions at a 120° angle (Goodrich et al. 2009). In the meteorites a preferential alignment of elongated grains (mainly olivine) is clearly noticeable (Goodrich et al. 2009). These meteorites show low to moderate shock effects, and do not contain carbon phases (Goodrich et al. 2009). All of the characteristics previously mentioned for these Hughes Cluster meteorites are in common with NWA11187 (for a detailed petrographic description of NWA11187 see Chapter 3). No carbon phases were identified in Hughes 009 and FRO 90054/93008 (Goodrich et al. 2009). In addition to what previously described, these Hughes Cluster meteorites contain melt inclusions (Goodrich et al. 2009), which were not identified in NWA11187. LEW85440 petrography was instead described by Takeda (1989), where it was described as similar to Y791538 and Y74659, apart from Ca in clinopyroxene. It is mainly composed of olivine, orthopyroxene and clinopyroxene, and have a forsterite content in olivine of 91.3 mol% (Takeda 1989). LEW85440 has a crystal size of up to 1.5 mm, contains C phases and according to Takeda (1989) is moderately shocked, even if Mason (AMN 10 (1), 1987) described LEW85440 as relatively unshocked. NWA11187 has exsolution lamellae of clinopyroxene in orthopyroxene (**Fig. 3.1.18**), thus indicating a particularly slow cooling process at a later crystallization stage (Hibiya et al., 2015), which were not identified in the meteorites previously described.

Geochemically, the major and minor elements (obtained through EPMA) of Hughes 009, FRO 90054/93008 and LEW85440 (and related meteorites) for olivine, orthopyroxene and clinopyroxene (Tables S18, S19 and S20) are very similar with NWA11187, especially LEW85440 and related meteorites. The only noticeable difference is in the content of FeOT, for all the three minerals, where LEW85440 (and related meteorites) and Hughes Cluster meteorites have a higher content with respect to NWA11187 (and Hughes Cluster meteorites have a higher FeOT content than LEW85440 and related meteorites).

The Y-REE patterns for orthopyroxene and clinopyroxene (**Fig. 4.2.5**, **Fig. 4.2.6**) for Hughes Cluster meteorites and LEW85440 are comparable with NWA11187, while the Y-REE pattern for olivine (**Fig. 4.2.4**) is not. In fact, in the Y-REE pattern for olivine, is not possible to see a common trend among the Hughes Cluster meteorites and NWA11187.

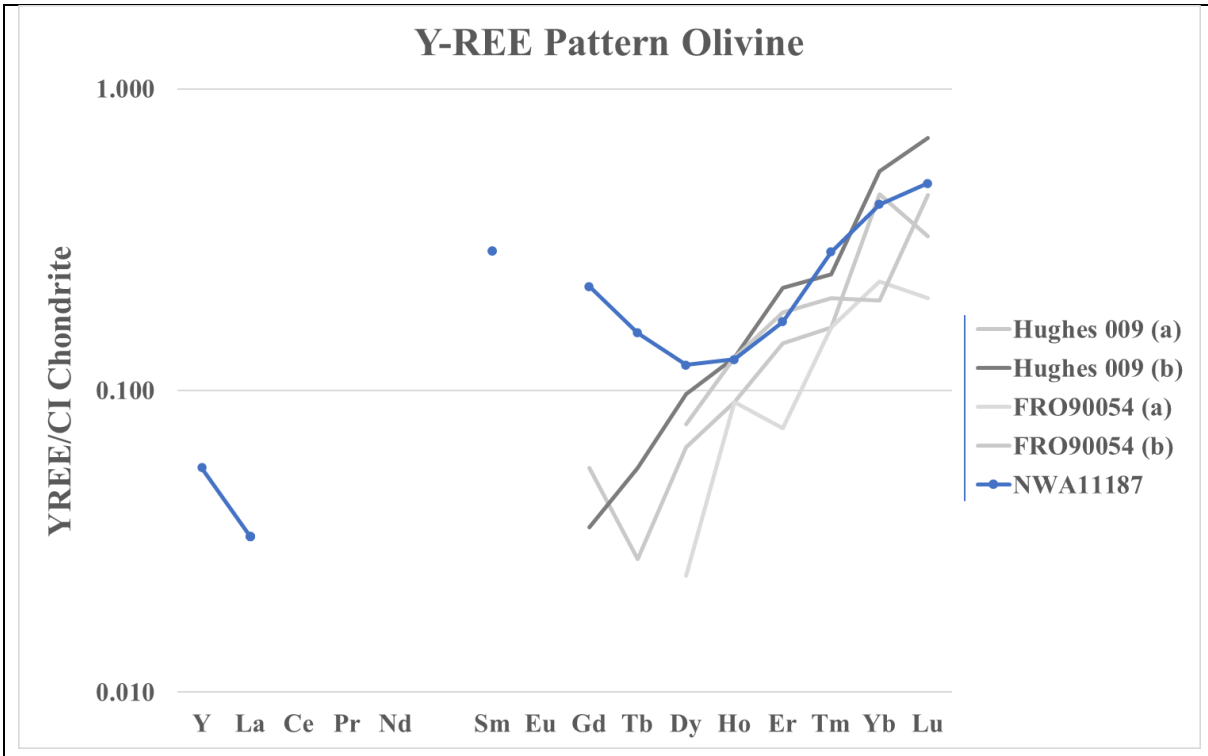

Fig. 4.2.4, Y-REE pattern of olivine for NWA11187, Hughes 009 (a and b; Goodrich et al. 2009) and FRO90054 (a and b; Goodrich et al. 2009). Data normalized to the average CI composition from McDonough and Sun (1995). Blue line in legend = data obtained through LA-ICP-MS.

In the Y-REE pattern for orthopyroxene (**Fig. 4.2.5**), the patterns for both the Hughes Cluster Meteorites and LEW 85440 are generally comparable with NWA11187, even if LEW85440 (b) is the one to show the best fit. Hughes Cluster meteorites contain on average less LREE than NWA11187 and LEW85440.

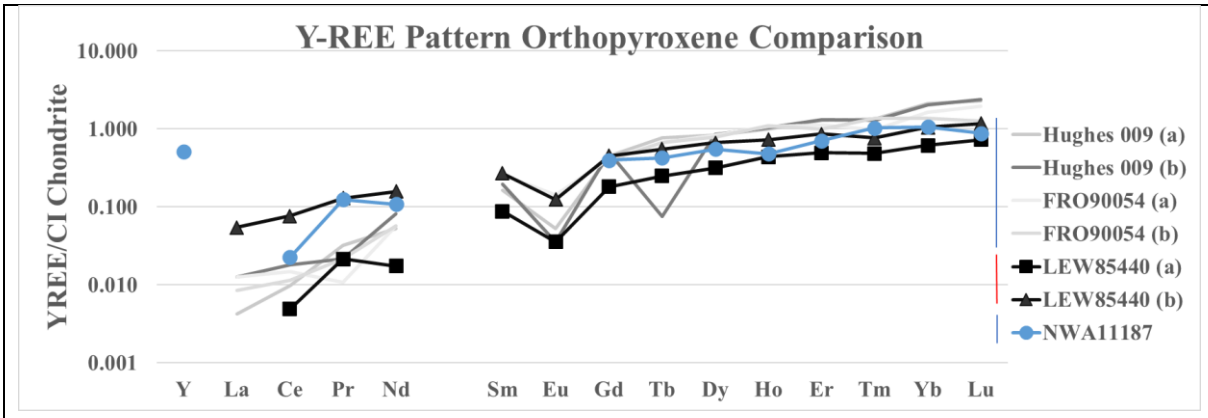

Fig. 4.2.5, Y-REE pattern of orthopyroxene for NWA11187, Hughes 009 (a and b; Goodrich et al. 2009), FRO90054 (a and b; Goodrich et al. 2009) and LEW85440 (a and b; Guan et al. 2000). Data normalized to the average CI composition from McDonough and Sun (1995). Blue line in legend = data obtained through LA-ICP-MS. Red line in legend = data obtained through ion microprobe.

In the Y-REE pattern for clinopyroxene (**Fig. 4.2.6**) only the pattern of LEW85440 (a and b) is comparable with NWA11187. Even if the three patterns are very similar between each other, NWA11187 is slightly enriched in L-REE compared with LEW85440 (a and b). The patterns for Hughes Cluster meteorites, even if they share a common trend with NWA11187 and LEW85440, are more evolved than NWA11187 and LEW85440, being more enriched in all the REE, therefore, NWA11187 and LEW85440 appear to have a common formation history.

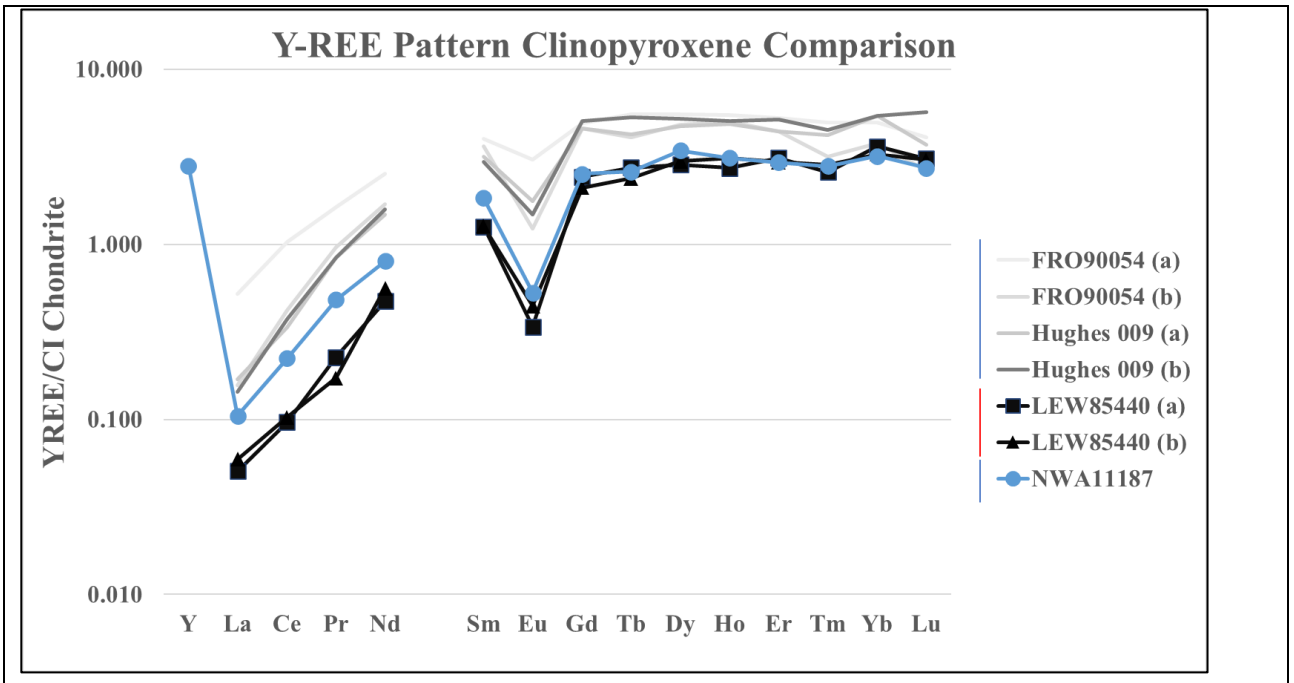

Fig. 4.2.6, Y-REE pattern of clinopyroxene for NWA11187, Hughes 009 (a and b; Goodrich et al. 2009), FRO90054 (a and b; Goodrich et al. 2009) and LEW85440 (a and b; Guan et al. 2000). Data normalized to the average CI composition from McDonough and Sun (1995). Blue line in legend = data obtained through LA-ICP-MS. Red line in legend = data obtained through ion microprobe.

5. CONCLUSIONS

A classification as brachinite-like achondrite is proposed for MIL090206, MIL090405, NWA6077 and NWA5363, based on the petrography, major and minor elements and trace elements. In fact, most of the data are consistent with those of other brachinite-like achondrites (e.g. MIL090340 in Goodrich et al. 2017) therefore suggesting that their parent body probably formed from a common nebular reservoir in the early stages of the Solar System history (Goodrich et al. 2017, Carli et al. 2023). Even though most of the data from the four potential brachinite-like meteorites are coherent, there were some differences between NWAs and MILs in petrography and geochemistry (see Chapter 3). For example, based on the Y-REE pattern for clinopyroxene (**Fig. 4.2.3**), MIL090405 is more evolved than NWA6077 and NWA5363, since it has a higher amount of all the Y-REE. A detailed bulk oxygen isotopes study is recommended for MIL090206, MIL090405, NWA6077 and NWA5363, in order to address incontrovertibly these four meteorites as brachinite-like achondrites, but also to understand if the four meteorites formed from the same parent body (the common nebular reservoir might have generated more than one parent body, according to Goodrich et al. 2017).

Regarding NWA11187, a classification as ureilite is instead proposed, based on major and minor elements data and Y-REE patterns. In particular, major and minor elements data are similar between NWA11187 and both Hughes Cluster (Hughes 009 and FRO90054) meteorites and LEW85440 (and related meteorites), while Y-REE patterns have comparable values only between NWA11187 and LEW85440 (orthopyroxene and clinopyroxene) suggesting that NWA11187 and LEW85440 could have a common formation history, which is different from that of Hughes Cluster meteorites. As a consequence, NWA11187 and LEW85440 would be derived from the same parent body. In order to classify ultimately NWA11187 as an ureilite, a companion work to this thesis is advised.

In particular, bulk oxygen isotopes and a detailed trace elements study (thus implementing the Y-REE data) for both NWA11187 and LEW85440 would be needed and oxygen isotopes analyses will be required for the other four meteorites of this thesis work.

Once the companion studies will be carried out, it would be possible to definitively classify all the studied samples. If it were confirmed that MIL090206, MIL090405, NWA6077 and NWA5363 are brachinite-like achondrites, this work would support what already reported in Goodrich et al. 2017 and Day et al. 2012. Furthermore, if NWA11187 were officially declared as an ureilite, the ureilite clan would gain a unique specimen to its wide collection, since it has some features that are not common in ureilites (e.g. very high Fo in olivine, no carbon phases detected and exsolution lamellae of clinopyroxene in orthopyroxene).

6. SUPPLEMENTARY MATERIAL

Major and Minor Elements

In the following tables all the analyses of major and minor elements for MIL090206, MIL090405, NWA6077, NWA5363 and NWA11187 are reported, organized for minerals.

Table S1 - Olivine

Sample	MIL090206	MIL090206	MIL090206	MIL090206	MIL090206	MIL090206	MIL090206	MIL090206	MIL090206	MIL090206	MIL090206	MIL090206	MIL090206	MIL090206	MIL090206	MIL090206	MIL090206	MIL090206		MIL090206	MIL090206	MIL090206
n° analysis	8	9	10	11	12	13	14	15	16	17	18	19	20	21	22	23	24	25		26	27	28
SiO2	38.14	38.22	38.31	38.02	37.96	37.57	38.13	37.96	37.74	37.58	37.56	37.19	37.21	37.35	37.12	37.33	37.88	37.33		37.38	37.64	37.46
TiO2	0.02	0.02	0.03	0.01	0.02	0.03	0.03	0.01	0.04	0.00	0.03	0.01	0.02	0.01	0.05	0.05	0.04	0.03		0.05	0.01	0.02
Al2O3	0.01	0.00	0.01	0.00	0.00	0.00	0.00	0.00	0.00	0.00	0.00	0.00	0.00	0.01	0.00	0.01	0.00	0.01		0.00	0.00	0.00
Cr2O3	0.04	0.00	0.04	0.01	0.04	0.08	0.04	0.00	0.07	0.03	0.40	0.02	0.05	0.07	0.05	0.06	0.00	0.02		0.03	0.03	0.03
FeOT	22.08	22.64	22.61	22.66	22.44	24.31	22.34	23.44	23.64	25.53	23.86	26.07	25.30	26.04	26.41	25.05	23.33	23.71		25.02	23.50	24.51
MnO	0.40	0.41	0.42	0.41	0.43	0.41	0.40	0.46	0.44	0.47	0.41	0.45	0.44	0.45	0.45	0.44	0.44	0.42		0.47	0.44	0.46
NiO	0.03	0.01	0.04	0.01	0.00	0.03	0.01	0.00	0.00	0.02	0.00	0.01	0.00	0.00	0.02	0.00	0.00	0.04		0.02	0.01	0.00
MgO	38.81	38.09	38.34	37.76	37.98	36.84	38.64	37.35	36.84	35.59	36.72	34.93	35.79	35.32	34.70	35.96	37.46	36.69		36.45	37.24	36.41
CaO	0.05	0.06	0.06	0.05	0.07	0.07	0.04	0.06	0.07	0.10	0.05	0.10	0.10	0.10	0.09	0.10	0.08	0.08		0.09	0.09	0.09
Total	99.58	99.45	99.86	98.94	98.95	99.33	99.63	99.27	98.83	99.34	99.02	98.78	98.90	99.34	98.89	99.01	99.22	98.32		99.51	98.95	98.98
Si	0.996	1.002	1.000	1.002	1.000	0.995	0.996	1.001	1.002	1.001	0.997	1.000	0.995	0.998	0.999	0.996	0.999	0.997		0.991	0.997	0.997
Ti	0.000	0.000	0.001	0.000	0.000	0.001	0.001	0.000	0.001	0.000	0.001	0.000	0.000	0.000	0.001	0.001	0.001	0.001		0.001	0.000	0.000
Al	0.000	0.000	0.000	0.000	0.000	0.000	0.000	0.000	0.000	0.000	0.000	0.000	0.000	0.000	0.000	0.000	0.000	0.000		0.000	0.000	0.000
Cr	0.001	0.000	0.001	0.000	0.001	0.002	0.001	0.000	0.001	0.001	0.008	0.000	0.001	0.001	0.001	0.001	0.000	0.000		0.001	0.001	0.001
Fe2+	0.475	0.496	0.494	0.500	0.494	0.530	0.482	0.517	0.525	0.569	0.530	0.586	0.557	0.579	0.594	0.554	0.515	0.525		0.539	0.514	0.541
Fe3+	0.007	0.000	0.000	0.000	0.000	0.008	0.006	0.000	0.000	0.000	0.000	0.000	0.009	0.003	0.000	0.005	0.000	0.004		0.016	0.006	0.005
Mn	0.009	0.009	0.009	0.009	0.010	0.009	0.009	0.010	0.010	0.011	0.009	0.010	0.010	0.010	0.010	0.010	0.010	0.009		0.010	0.010	0.010
Ni	0.001	0.000	0.001	0.000	0.000	0.001	0.000	0.000	0.000	0.000	0.000	0.000	0.000	0.000	0.000	0.000	0.000	0.001		0.000	0.000	0.000
Mg	1.510	1.488	1.492	1.484	1.491	1.453	1.504	1.468	1.457	1.413	1.452	1.400	1.426	1.406	1.392	1.430	1.473	1.460		1.440	1.470	1.444
Ca	0.001	0.002	0.002	0.001	0.002	0.002	0.001	0.002	0.002	0.003	0.001	0.003	0.003	0.003	0.003	0.003	0.002	0.002		0.003	0.003	0.002
cations	3.000	2.998	2.999	2.997	2.999	3.000	3.000	2.998	2.997	2.998	2.998	3.000	3.000	3.000	3.000	3.000	3.000	3.000		3.000	3.000	3.000
Fo (mol%)	75.5	74.7	74.8	74.5	74.8	72.6	75.2	73.6	73.2	70.9	73.0	70.1	71.3	70.4	69.7	71.5	73.8	73.0		71.8	73.5	72.2
Fa (mol%)	24.1	24.9	24.7	25.1	24.8	26.9	24.4	25.9	26.3	28.5	26.6	29.4	28.3	29.1	29.8	28.0	25.8	26.5		27.7	26.0	27.3
Tp (mol%)	0.4	0.5	0.5	0.5	0.5	0.5	0.4	0.5	0.5	0.5	0.5	0.5	0.5	0.5	0.5	0.5	0.5	0.5		0.5	0.5	0.5
#mg	80.6	80.7	80.7	80.8	80.7	81.2	80.6	80.9	81.0	81.5	81.1	81.7	81.4	81.6	81.8	81.4	80.9	81.1		81.3	81.0	81.2

MIL090206	MIL090206	MIL090206	MIL090206	MIL090206	MIL090206	MIL090206	MIL090206	MIL090206	MIL090206	MIL090206	MIL090206	MIL090206	MIL090206	MIL090206			MIL090405	MIL090405	MIL090405	MIL090405
29	30	31	32	33	34	35	36	37	38	39	40	41	42	Mean	St. Dev.	Rel. St. Dev.	8	9	10	11
37.43	37.04	37.47	37.13	37.52	37.42	37.43	37.90	37.51	37.51	37.57	37.34	37.65	37.33	37.58	0.33	0.88%	37.77	37.72	37.57	37.54
0.01	0.02	0.04	0.03	0.03	0.05	0.04	0.02	0.01	0.02	0.03	0.02	0.04	0.03	0.03	0.01	50.38%	0.02	0.03	0.02	0.03
0.00	0.00	0.01	0.00	0.00	0.00	0.00	0.00	0.01	0.00	0.01	0.00	0.00	0.01	0.00	0.00	141.06%	0.00	0.00	0.00	0.00
0.01	0.08	0.05	0.02	0.01	0.02	0.00	0.06	0.06	0.04	0.06	0.07	0.22	0.04	0.05	0.07	135.50%	0.08	0.13	0.18	0.03
25.39	26.17	24.63	25.87	25.21	25.11	24.63	22.96	25.13	23.97	25.31	26.03	24.52	25.27	24.42	1.26	5.16%	25.48	24.82	25.38	26.08
0.46	0.48	0.41	0.44	0.45	0.47	0.47	0.42	0.49	0.44	0.46	0.48	0.46	0.44	0.44	0.02	5.60%	0.43	0.44	0.45	0.45
0.02	0.00	0.00	0.00	0.00	0.00	0.01	0.00	0.02	0.19	0.00	0.01	0.00	0.01	0.01	0.03	223.46%	0.01	0.00	0.00	0.01
35.77	34.83	36.61	35.72	35.79	36.23	36.41	37.62	35.89	36.58	35.92	35.21	36.75	35.66	36.54	1.08	2.96%	36.09	36.56	36.15	35.86
0.10	0.10	0.09	0.09	0.09	0.09	0.08	0.05	0.10	0.08	0.06	0.10	0.06	0.05	0.08	0.02	24.93%	0.08	0.07	0.09	0.09
99.18	98.72	99.30	99.30	99.09	99.39	99.07	99.03	99.22	98.83	99.42	99.27	99.69	98.82	99.15	0.32	0.32%	99.97	99.77	99.83	100.09
0.998	0.997	0.993	0.990	1.001	0.994	0.995	1.000	0.999	0.998	0.999	0.998	0.994	0.999	0.998	0.003	0.30%	0.999	0.997	0.995	0.994
0.000	0.000	0.001	0.001	0.001	0.001	0.001	0.000	0.000	0.000	0.001	0.000	0.001	0.001	0.001	0.000	50.45%	0.000	0.001	0.000	0.001
0.000	0.000	0.000	0.000	0.000	0.000	0.000	0.000	0.000	0.000	0.000	0.000	0.000	0.000	0.000	0.000	140.92%	0.000	0.000	0.000	0.000
0.000	0.002	0.001	0.000	0.000	0.000	0.000	0.001	0.001	0.001	0.001	0.002	0.005	0.001	0.001	0.002	135.33%	0.002	0.003	0.004	0.001
0.563	0.587	0.536	0.559	0.562	0.548	0.540	0.507	0.560	0.532	0.563	0.582	0.537	0.566	0.539	0.032	5.85%	0.564	0.546	0.556	0.567
0.003	0.003	0.010	0.018	0.000	0.010	0.008	0.000	0.000	0.002	0.000	0.001	0.005	0.000	0.004	0.005	130.64%	0.000	0.003	0.006	0.011
0.010	0.011	0.009	0.010	0.010	0.011	0.011	0.009	0.011	0.010	0.010	0.011	0.010	0.010	0.010	0.001	6.10%	0.010	0.010	0.010	0.010
0.000	0.000	0.000	0.000	0.000	0.000	0.000	0.000	0.000	0.004	0.000	0.000	0.000	0.000	0.000	0.001	223.93%	0.000	0.000	0.000	0.000
1.422	1.397	1.447	1.419	1.422	1.434	1.443	1.479	1.425	1.451	1.423	1.403	1.447	1.422	1.445	0.032	2.20%	1.423	1.440	1.426	1.415
0.003	0.003	0.003	0.003	0.003	0.002	0.002	0.001	0.003	0.002	0.002	0.003	0.002	0.001	0.002	0.001	25.42%	0.002	0.002	0.002	0.003
3.000	3.000	3.000	3.000	2.999	3.000	3.000	2.999	3.000	3.000	3.000	3.000	3.000	3.000	2.999	0.001	0.03%	3.000	3.000	3.000	3.000
71.2	70.0	72.3	70.8	71.3	71.6	72.1	74.2	71.4	72.8	71.3	70.3	72.4	71.2	72.4	1.6	2.22%	71.3	72.1	71.4	70.7
28.3	29.5	27.3	28.7	28.2	27.8	27.4	25.4	28.0	26.7	28.2	29.2	27.1	28.3	27.1	1.6	5.84%	28.2	27.4	28.1	28.8
0.5	0.6	0.5	0.5	0.5	0.5	0.5	0.5	0.6	0.5	0.5	0.5	0.5	0.5	0.5	0.0	6.10%	0.5	0.5	0.5	0.5
81.5	81.7	81.2	81.5	81.4	81.4	81.3	80.8	81.4	81.1	81.4	81.6	81.2	81.5	81.2	0.3	0.0	71.6	72.4	71.7	71.0

MIL090405	MIL090405	MIL090405	MIL090405	MIL090405	MIL090405	MIL090405	MIL090405	MIL090405	MIL090405	MIL090405	MIL090405	MIL090405	MIL090405	MIL090405	MIL090405	MIL090405	MIL090405	MIL090405	MIL090405	MIL090405	MIL090405	MIL090405	MIL090405
12	13	14	15	16	17	18	19	20	21	22	23	24	25	26	27	28	29	30	31	32	33	34	35
37.31	37.47	37.79	37.61	37.92	37.60	37.55	37.42	37.53	37.06	37.50	37.34	37.54	37.29	37.17	37.79	37.47	37.74	37.63	37.61	37.53	37.50	37.34	37.60
0.04	0.02	0.03	0.03	0.02	0.03	0.04	0.02	0.04	0.02	0.02	0.03	0.01	0.03	0.02	0.03	0.01	0.03	0.04	0.04	0.03	0.05	0.02	0.03
0.00	0.00	0.00	0.00	0.00	0.00	0.01	0.00	0.00	0.01	0.00	0.00	0.01	0.00	0.00	0.01	0.00	0.01	0.00	0.00	0.00	0.00	0.01	0.00
0.06	0.06	0.02	0.09	0.03	0.03	0.03	0.02	0.05	0.03	0.01	0.00	0.01	0.01	0.04	0.07	0.03	0.07	0.03	0.05	0.01	0.01	0.03	0.00
25.86	26.60	25.52	25.90	24.57	25.06	24.56	25.42	25.40	27.50	24.72	25.65	26.13	26.54	25.59	24.97	24.91	25.25	24.36	25.03	25.32	25.65	25.70	25.06
0.45	0.49	0.43	0.47	0.46	0.44	0.43	0.46	0.47	0.44	0.43	0.46	0.42	0.45	0.46	0.44	0.44	0.42	0.43	0.44	0.43	0.47	0.42	0.43
0.00	0.02	0.02	0.01	0.00	0.01	0.00	0.01	0.03	0.00	0.00	0.00	0.00	0.00	0.01	0.00	0.00	0.00	0.00	0.01	0.00	0.00	0.00	0.00
35.47	35.25	36.35	35.63	36.81	35.03	35.76	35.83	36.05	34.23	36.24	35.21	35.51	34.76	35.68	36.55	36.12	36.07	36.43	35.70	35.16	35.73	35.27	35.98
0.09	0.10	0.08	0.09	0.07	0.30	0.09	0.08	0.09	0.10	0.10	0.10	0.09	0.11	0.09	0.06	0.08	0.07	0.06	0.07	0.10	0.09	0.09	0.08
99.27	100.00	100.25	99.81	99.87	98.50	98.47	99.24	99.65	99.39	99.01	98.79	99.72	99.18	99.06	99.90	99.05	99.65	98.97	98.96	98.57	99.50	98.87	99.19
0.996	0.996	0.996	0.999	0.999	1.008	1.005	0.997	0.996	0.996	0.998	1.001	0.999	1.000	0.993	0.997	0.998	1.000	1.000	1.003	1.006	0.998	1.001	1.001
0.001	0.000	0.000	0.001	0.000	0.001	0.001	0.000	0.001	0.000	0.000	0.001	0.000	0.001	0.000	0.000	0.000	0.000	0.001	0.001	0.001	0.001	0.000	0.001
0.000	0.000	0.000	0.000	0.000	0.000	0.000	0.000	0.000	0.000	0.000	0.000	0.000	0.000	0.000	0.000	0.000	0.000	0.000	0.000	0.000	0.000	0.000	0.000
0.001	0.001	0.000	0.002	0.001	0.001	0.001	0.000	0.001	0.001	0.000	0.000	0.000	0.000	0.001	0.001	0.001	0.002	0.001	0.001	0.000	0.000	0.001	0.000
0.573	0.586	0.556	0.575	0.541	0.562	0.549	0.562	0.557	0.613	0.548	0.575	0.579	0.595	0.560	0.549	0.552	0.560	0.542	0.559	0.568	0.569	0.576	0.558
0.005	0.006	0.007	0.000	0.000	0.000	0.000	0.005	0.006	0.006	0.002	0.000	0.002	0.000	0.012	0.003	0.003	0.000	0.000	0.000	0.000	0.002	0.000	0.000
0.010	0.011	0.010	0.010	0.010	0.010	0.010	0.010	0.011	0.010	0.010	0.010	0.009	0.010	0.010	0.010	0.010	0.010	0.010	0.010	0.010	0.011	0.009	0.010
0.000	0.000	0.000	0.000	0.000	0.000	0.000	0.000	0.001	0.000	0.000	0.000	0.000	0.000	0.000	0.000	0.000	0.000	0.000	0.000	0.000	0.000	0.000	0.000
1.412	1.397	1.428	1.410	1.446	1.400	1.426	1.423	1.425	1.371	1.438	1.407	1.407	1.389	1.421	1.438	1.434	1.425	1.443	1.420	1.405	1.417	1.409	1.427
0.002	0.003	0.002	0.002	0.002	0.009	0.003	0.002	0.003	0.003	0.003	0.003	0.003	0.003	0.003	0.002	0.002	0.002	0.002	0.002	0.003	0.003	0.003	0.002
3.000	3.000	3.000	3.000	3.000	2.991	2.994	3.000	3.000	3.000	3.000	2.998	3.000	2.999	3.000	3.000	3.000	2.998	2.998	2.995	2.993	3.000	2.999	2.999
70.6	69.9	71.4	70.7	72.4	71.0	71.8	71.2	71.3	68.6	72.0	70.6	70.4	69.7	70.9	71.9	71.8	71.5	72.4	71.4	70.9	70.9	70.7	71.6
28.9	29.6	28.1	28.8	27.1	28.5	27.7	28.3	28.2	30.9	27.5	28.9	29.1	29.8	28.5	27.6	27.8	28.1	27.1	28.1	28.6	28.6	28.9	28.0
0.5	0.5	0.5	0.5	0.5	0.5	0.5	0.5	0.5	0.5	0.5	0.5	0.5	0.5	0.5	0.5	0.5	0.5	0.5	0.5	0.5	0.5	0.5	0.5
71.0	70.3	71.7	71.0	72.8	71.4	72.2	71.5	71.7	68.9	72.3	71.0	70.8	70.0	71.3	72.3	72.1	71.8	72.7	71.8	71.2	71.3	71.0	71.9

MIL090405	MIL090405	MIL090405	MIL090405	MIL090405	MIL090405	MIL090405	MIL090405	MIL090405	MIL090405		MIL090405		NWA6077	NWA6077	NWA6077	NWA6077	NWA6077	NWA6077	NWA6077	NWA6077	NWA6077
36	37	38	39	40	41	42	43	44	45	Mean	St.Dev.	Rel. St. Dev									
37.45	37.52	37.33	37.52	37.74	37.61	37.60	37.50	37.87	37.38	37.54	0.18	0%	36.76	36.58	37.14	37.29	37.04	36.45	36.23	36.30	36.45
0.02	0.03	0.04	0.03	0.02	0.02	0.03	0.03	0.03	0.02	0.03	0.01	35%	0.05	0.04	0.05	0.00	0.04	0.04	0.04	0.03	0.03
0.00	0.01	0.00	0.00	0.00	0.00	0.00	0.00	0.00	0.00	0.00	0.00	124%	0.01	0.00	0.00	0.00	0.01	0.00	0.01	0.01	0.00
0.01	0.03	0.08	0.06	0.02	0.01	0.04	0.08	0.13	0.14	0.05	0.04	90%	0.25	0.18	0.57	0.22	1.09	0.44	0.20	0.45	0.02
25.11	26.52	25.00	26.23	25.10	24.79	25.22	24.44	24.77	26.16	25.43	0.69	3%	25.99	25.17	25.10	25.54	25.46	26.06	25.89	25.22	25.58
0.47	0.47	0.45	0.43	0.43	0.46	0.47	0.42	0.41	0.46	0.44	0.02	4%	0.41	0.46	0.40	0.44	0.42	0.44	0.44	0.43	0.42
0.00	0.00	0.00	0.00	0.00	0.00	0.02	0.00	0.00	0.01	0.00	0.01	146%	0.02	0.03	0.05	0.04	0.04	0.02	0.03	0.02	0.02
35.35	34.92	35.47	35.28	36.18	36.08	35.33	36.27	36.26	35.30	35.73	0.56	2%	36.62	36.40	36.70	36.43	36.75	36.39	36.95	37.03	36.02
0.10	0.10	0.09	0.07	0.09	0.08	0.09	0.06	0.06	0.05	0.09	0.04	42%	0.07	0.07	0.05	0.06	0.05	0.07	0.07	0.06	0.07
98.50	99.59	98.47	99.62	99.60	99.05	98.79	98.79	99.52	99.52	99.31	0.51	0.01	100.17	98.94	100.05	100.03	100.88	99.90	99.85	99.54	98.61
1.005	1.001	1.002	1.000	1.000	1.001	1.006	1.000	1.002	0.997	1.000	0.003	0%	0.969	0.975	0.980	0.985	0.971	0.965	0.957	0.960	0.976
0.000	0.001	0.001	0.001	0.000	0.000	0.001	0.001	0.000	0.000	0.001	0.000	35%	0.001	0.001	0.001	0.000	0.001	0.001	0.001	0.000	0.001
0.000	0.000	0.000	0.000	0.000	0.000	0.000	0.000	0.000	0.000	0.000	0.000	124%	0.000	0.000	0.000	0.000	0.000	0.000	0.000	0.000	0.000
0.000	0.001	0.002	0.001	0.000	0.000	0.001	0.002	0.003	0.003	0.001	0.001	90%	0.005	0.004	0.012	0.005	0.023	0.009	0.004	0.009	0.001
0.563	0.592	0.561	0.584	0.556	0.552	0.564	0.545	0.548	0.582	0.564	0.016	3%	0.520	0.517	0.526	0.539	0.524	0.518	0.491	0.489	0.527
0.000	0.000	0.000	0.000	0.000	0.000	0.000	0.000	0.000	0.002	0.002	0.003	151%	0.053	0.044	0.027	0.026	0.034	0.059	0.081	0.069	0.046
0.011	0.011	0.010	0.010	0.010	0.010	0.011	0.009	0.009	0.010	0.010	0.000	4%	0.009	0.010	0.009	0.010	0.009	0.010	0.010	0.010	0.009
0.000	0.000	0.000	0.000	0.000	0.000	0.000	0.000	0.000	0.000	0.000	0.000	146%	0.000	0.001	0.001	0.001	0.001	0.000	0.001	0.000	0.000
1.413	1.389	1.418	1.401	1.429	1.432	1.409	1.441	1.431	1.404	1.418	0.017	1%	1.439	1.446	1.443	1.434	1.436	1.436	1.454	1.460	1.438
0.003	0.003	0.003	0.002	0.003	0.002	0.002	0.002	0.002	0.001	0.003	0.001	43%	0.002	0.002	0.001	0.002	0.001	0.002	0.002	0.002	0.002
2.995	2.997	2.997	2.999	2.999	2.998	2.993	2.999	2.996	3.000	2.998	0.002	0%	3.000	3.000	3.000	3.000	3.000	3.000	3.000	3.000	3.000
71.1	69.8	71.3	70.2	71.6	71.8	71.0	72.2	72.0	70.3	71.1	0.8	1%	68.8	69.0	69.1	68.9	68.7	69.2	68.9	68.9	69.5
28.3	29.7	28.2	29.3	27.9	27.7	28.4	27.3	27.6	29.2	28.4	0.8	3%	30.7	30.4	30.4	30.6	30.8	30.3	30.5	30.5	30.0
0.5	0.5	0.5	0.5	0.5	0.5	0.5	0.5	0.5	0.5	0.5	0.0	4%	0.5	0.5	0.5	0.5	0.5	0.5	0.6	0.6	0.5
71.5	70.1	71.7	70.6	72.0	72.2	71.4	72.6	72.3	70.6	71.5	0.8	1%	69.2	69.4	69.5	69.2	69.1	69.6	69.3	69.3	69.9

NWA6077	NWA6077	NWA6077	NWA6077	NWA6077	NWA6077	NWA6077	NWA6077	NWA6077	NWA6077	NWA6077	NWA6077	NWA6077	NWA6077	NWA6077	NWA6077	NWA6077	NWA6077	NWA6077	NWA6077	NWA6077	NWA6077	NWA6077
36.76	36.84	35.99	37.17	36.89	36.92	36.94	36.91	37.07	37.13	36.86	36.68	36.78	36.21	36.67	36.55	36.79	36.94	37.06	36.84	36.85	36.35	36.69	36.75
0.04	0.04	0.04	0.02	0.04	0.05	0.03	0.00	0.04	0.02	0.03	0.04	0.04	0.03	0.03	0.03	0.03	0.02	0.04	0.03	0.02	0.02	0.04	0.03
0.01	0.00	0.00	0.01	0.01	0.01	0.00	0.00	0.01	0.01	0.00	0.01	0.01	0.00	0.00	0.00	0.01	0.00	0.00	0.01	0.00	0.01	0.00	0.01
0.90	0.39	0.42	0.42	0.50	0.02	0.01	0.02	0.04	0.01	0.04	0.00	0.00	0.07	0.00	0.05	0.06	0.04	0.03	0.05	0.00	0.04	0.01	0.00
25.39	24.95	26.67	25.50	25.07	26.41	25.50	26.25	26.30	25.81	25.90	26.02	26.58	26.30	26.53	26.71	26.18	26.00	26.26	26.21	26.12	26.80	26.40	26.05
0.42	0.39	0.45	0.41	0.40	0.44	0.44	0.46	0.46	0.41	0.44	0.46	0.44	0.44	0.41	0.45	0.45	0.45	0.44	0.41	0.42	0.41	0.45	0.45
0.01	0.01	0.28	0.03	0.01	0.02	0.03	0.03	0.01	0.00	0.01	0.01	0.01	0.00	0.00	0.03	0.01	0.00	0.02	0.01	0.01	0.01	0.00	0.01
36.00	37.60	35.61	36.92	37.27	36.13	36.52	36.22	36.33	36.48	36.34	36.26	36.12	36.09	36.25	36.22	36.23	36.49	36.12	35.98	36.46	35.07	36.03	36.80
0.06	0.07	0.08	0.08	0.06	0.09	0.08	0.07	0.09	0.07	0.08	0.06	0.10	0.08	0.07	0.08	0.08	0.08	0.06	0.09	0.08	0.08	0.10	0.09
99.57	100.29	99.55	100.55	100.26	100.11	99.54	99.94	100.34	99.94	99.72	99.53	100.06	99.21	99.96	100.12	99.85	100.02	100.02	99.64	99.96	98.78	99.72	100.19
0.978	0.965	0.960	0.975	0.969	0.977	0.979	0.977	0.978	0.981	0.977	0.974	0.973	0.965	0.971	0.967	0.975	0.976	0.981	0.979	0.974	0.978	0.974	0.968
0.001	0.001	0.001	0.000	0.001	0.001	0.001	0.000	0.001	0.000	0.001	0.001	0.001	0.001	0.001	0.001	0.001	0.000	0.001	0.001	0.000	0.000	0.001	0.001
0.000	0.000	0.000	0.000	0.000	0.000	0.000	0.000	0.000	0.000	0.000	0.000	0.000	0.000	0.000	0.000	0.000	0.000	0.000	0.000	0.000	0.000	0.000	0.000
0.019	0.008	0.009	0.009	0.010	0.000	0.000	0.000	0.001	0.000	0.001	0.000	0.000	0.001	0.000	0.001	0.001	0.001	0.001	0.001	0.000	0.001	0.000	0.000
0.540	0.487	0.527	0.520	0.500	0.540	0.525	0.535	0.538	0.534	0.530	0.528	0.537	0.520	0.530	0.527	0.532	0.528	0.545	0.543	0.526	0.561	0.536	0.511
0.024	0.060	0.069	0.040	0.051	0.044	0.040	0.046	0.042	0.037	0.044	0.050	0.051	0.067	0.057	0.064	0.048	0.047	0.036	0.040	0.051	0.042	0.050	0.063
0.010	0.009	0.010	0.009	0.009	0.010	0.010	0.010	0.010	0.009	0.010	0.010	0.010	0.010	0.009	0.010	0.010	0.010	0.010	0.009	0.009	0.009	0.010	0.010
0.000	0.000	0.006	0.001	0.000	0.000	0.001	0.001	0.000	0.000	0.000	0.000	0.000	0.000	0.000	0.001	0.000	0.000	0.000	0.000	0.000	0.000	0.000	0.000
1.427	1.468	1.416	1.444	1.459	1.424	1.442	1.429	1.428	1.436	1.435	1.435	1.425	1.434	1.430	1.428	1.431	1.436	1.425	1.425	1.436	1.406	1.426	1.445
0.002	0.002	0.002	0.002	0.002	0.003	0.002	0.002	0.002	0.002	0.002	0.002	0.003	0.002	0.002	0.002	0.002	0.002	0.002	0.003	0.002	0.002	0.003	0.002
3.000	3.000	3.000	3.000	3.000	3.000	3.000	3.000	3.000	3.000	3.000	3.000	3.000	3.000	3.000	3.000	3.000	3.000	3.000	3.000	3.000	3.000	3.000	3.000
69.0	69.0	68.4	68.6	68.7	69.0	69.1	70.1	69.9	70.9	69.8	70.2	70.8	70.3	71.0	70.5	71.2	70.2	70.9	69.9	69.6	69.8	69.0	69.1
30.5	30.5	31.0	30.9	30.7	30.4	30.4	29.4	29.6	28.7	29.7	29.3	28.7	29.2	28.5	29.0	28.3	29.3	28.6	29.6	29.9	29.7	29.9	30.1
0.5	0.5	0.5	0.5	0.6	0.5	0.6	0.5	0.5	0.4	0.5	0.5	0.5	0.5	0.5	0.5	0.5	0.5	0.5	0.5	0.5	0.5	0.5	9.5
69.3	69.3	68.8	68.9	69.1	69.4	69.4	70.4	70.2	71.2	70.1	70.6	71.1	70.6	71.4	70.9	71.6	70.5	71.3	70.2	69.9	70.1	69.5	69.6

NWA6077 Mean	NWA6077 St.Dev.	NWA6077 Rel. St. Dev 1%	NWA5363	NWA5363	NWA5363	NWA5363	NWA5363	NWA5363	NWA5363	NWA5363	NWA5363	NWA5363	NWA5363	NWA5363	NWA5363	NWA5363	NWA5363	NWA5363	NWA5363
36.75	0.31		36.23	36.43	36.95	36.59	36.87	37.04	37.18	36.81	37.03	36.96	36.82	37.07	36.89	36.43	37.20	36.96	38.10	37.99	38.04
0.03	0.01	37%	0.02	0.02	0.03	0.00	0.03	0.02	0.05	0.02	0.02	0.01	0.02	0.02	0.02	0.02	0.03	0.01	0.04	0.04	0.05
0.00	0.00	75%	0.01	0.00	0.00	0.01	0.00	0.00	0.00	0.00	0.01	0.01	0.00	0.01	0.00	0.00	0.00	0.00	0.00	0.01	0.01
0.20	0.27	138%	0.10	0.04	0.05	0.04	0.04	0.03	0.06	0.04	0.02	0.00	0.04	0.04	0.04	0.03	0.00	0.07	0.06	0.15	0.49
25.94	0.52	2%	27.02	26.76	26.76	27.01	27.37	26.71	26.89	26.98	26.35	27.00	26.88	27.32	27.46	27.18	26.98	26.84	26.60	26.68	26.06
0.43	0.02	5%	0.46	0.47	0.46	0.45	0.44	0.41	0.50	0.49	0.46	0.41	0.44	0.48	0.48	0.50	0.47	0.49	0.45	0.46	0.40
0.02	0.05	199%	0.00	0.03	0.00	0.01	0.02	0.02	0.03	0.00	0.01	0.00	0.01	0.01	0.00	0.00	0.00	0.00	0.00	0.01	0.03
36.39	0.47	1%	34.00	34.07	34.18	34.05	34.30	34.25	34.03	34.16	34.29	34.19	34.10	33.82	34.21	34.07	34.30	34.21	35.56	35.31	36.10
0.07	0.01	17%	0.10	0.09	0.10	0.11	0.09	0.08	0.09	0.10	0.06	0.09	0.09	0.07	0.08	0.09	0.10	0.10	0.06	0.06	0.06
99.84	0.47	0.47%	97.93	97.92	98.53	98.28	99.14	98.54	98.83	98.60	98.24	98.68	98.40	98.81	99.19	98.33	99.10	98.67	100.87	100.70	101.24
0.973	0.007	1%	0.987	0.992	1.000	0.994	0.993	1.001	1.003	0.996	1.003	0.999	0.998	1.002	0.994	0.989	1.001	0.999	1.003	1.002	0.996
0.001	0.000	37%	0.000	0.000	0.001	0.000	0.001	0.000	0.001	0.000	0.000	0.000	0.000	0.000	0.000	0.000	0.001	0.000	0.001	0.001	0.001
0.000	0.000	75%	0.000	0.000	0.000	0.000	0.000	0.000	0.000	0.000	0.000	0.000	0.000	0.000	0.000	0.000	0.000	0.000	0.000	0.000	0.000
0.004	0.006	138%	0.002	0.001	0.001	0.001	0.001	0.001	0.001	0.001	0.001	0.000	0.001	0.001	0.001	0.001	0.000	0.001	0.001	0.003	0.010
0.526	0.016	3%	0.593	0.596	0.606	0.602	0.604	0.604	0.607	0.605	0.597	0.610	0.608	0.618	0.608	0.597	0.607	0.607	0.585	0.589	0.571
0.049	0.013	27%	0.022	0.014	0.000	0.012	0.013	0.000	0.000	0.006	0.000	0.001	0.002	0.000	0.011	0.020	0.000	0.000	0.000	0.000	0.000
0.010	0.000	5%	0.011	0.011	0.010	0.010	0.010	0.009	0.011	0.011	0.010	0.009	0.010	0.011	0.011	0.012	0.011	0.011	0.010	0.010	0.009
0.001	0.001	200%	0.000	0.001	0.000	0.000	0.000	0.000	0.001	0.000	0.000	0.000	0.000	0.000	0.000	0.000	0.000	0.000	0.000	0.000	0.001
1.436	0.013	1%	1.381	1.383	1.378	1.378	1.377	1.380	1.368	1.378	1.384	1.378	1.378	1.363	1.373	1.378	1.376	1.378	1.394	1.388	1.409
0.002	0.000	17%	0.003	0.003	0.003	0.003	0.003	0.002	0.003	0.003	0.002	0.003	0.003	0.002	0.002	0.003	0.003	0.003	0.002	0.002	0.002
3.000	0.000	0%	3.000	3.000	2.999	3.000	3.000	2.998	2.995	3.000	2.997	3.000	3.000	2.997	3.000	3.000	2.998	3.000	2.996	2.995	2.998
69.6	0.8	1%	72.0	71.4	71.7	71.0	71.4	72.0	71.2	71.3	72.6	70.1	71.8	72.3	70.6	71.5	70.7	70.8	71.3	71.1	70.9
29.8	0.8	3%	27.6	28.1	27.9	28.5	28.1	27.5	28.3	28.2	27.0	29.4	27.8	27.3	28.9	28.0	28.8	28.7	28.3	28.4	28.6
0.8	1.6	202%	0.4	0.5	0.5	0.5	0.5	0.5	0.5	0.5	0.4	0.5	0.5	0.4	0.5	0.5	0.5	0.5	0.5	0.5	0.5
70.0	0.8	1%	81.97	81.96	81.91	81.90	81.96	81.98	81.88	81.94	81.94	81.81	81.93	81.93	82.04	82.01	81.98	81.92	81.91	81.69	81.74

NWA5363	NWA5363	NWA5363	NWA5363	NWA5363	NWA5363	NWA5363	NWA5363	NWA5363	NWA5363	NWA5363	NWA5363				NWA11187	NWA11187	NWA11187	NWA11187	NWA11187	NWA11187	NWA11187
												Mean	St.Dev.	Rel. St. Dev							
38.09	38.08	38.28	37.77	38.34	37.88	37.96	37.92	38.01	38.16	38.11	37.55	37.41	0.64	2%	41.61	41.31	41.49	41.29	41.28	41.23	41.35
0.05	0.05	0.05	0.03	0.04	0.02	0.02	0.04	0.04	0.00	0.05	0.02	0.03	0.01	50%	0.03	0.04	0.03	0.03	0.03	0.03	0.04
0.00	0.01	0.01	0.01	0.01	0.00	0.01	0.01	0.01	0.00	0.01	0.01	0.00	0.00	91%	0.03	0.02	0.02	0.01	0.02	0.01	0.03
0.86	0.34	0.45	0.55	0.27	0.25	0.23	0.59	0.32	0.00	0.02	0.03	0.17	0.22	129%	0.64	0.59	0.59	0.61	0.57	0.60	0.55
26.85	26.32	26.06	26.57	25.62	26.50	25.53	26.56	25.74	26.80	27.02	26.83	26.69	0.48	2%	5.50	5.31	5.32	5.39	5.45	5.63	5.40
0.44	0.43	0.42	0.43	0.45	0.44	0.45	0.45	0.44	0.44	0.44	0.46	0.45	0.02	6%	0.45	0.51	0.48	0.50	0.49	0.49	0.48
0.02	0.01	0.00	0.01	0.02	0.01	0.04	0.03	0.00	0.01	0.00	0.00	0.01	0.01	100%	0.00	0.00	0.00	0.00	0.00	0.00	0.00
35.39	35.42	36.02	35.89	35.83	36.21	36.04	35.63	35.83	35.43	35.27	35.34	34.89	0.82	2%	52.53	52.73	52.66	52.86	53.13	53.27	52.88
0.06	0.08	0.07	0.06	0.05	0.05	0.07	0.05	0.06	0.06	0.07	0.08	0.08	0.02	24%	0.31	0.32	0.31	0.33	0.32	0.33	0.32
101.76	100.74	101.36	101.32	100.63	101.36	100.35	101.27	100.44	100.91	100.99	100.31	99.72	1.27	0.01	101.11	100.82	100.90	101.01	101.30	101.59	101.05
							(4) normalizzazione a 4 ossigeni e <3 cationi per f.u.														
0.996	1.003	1.000	0.991	1.007	0.991	1.000	0.995	1.001	1.004	1.003	0.995	0.998	0.005	0%	0.992	0.987	0.990	0.984	0.981	0.977	0.985
0.001	0.001	0.001	0.001	0.001	0.000	0.000	0.001	0.001	0.000	0.001	0.000	0.001	0.000	49%	0.001	0.001	0.001	0.001	0.001	0.001	0.001
0.000	0.000	0.000	0.000	0.000	0.000	0.000	0.000	0.000	0.000	0.000	0.000	0.000	0.000	91%	0.001	0.001	0.001	0.000	0.001	0.000	0.001
0.018	0.007	0.009	0.011	0.006	0.005	0.005	0.012	0.007	0.000	0.000	0.001	0.004	0.004	128%	0.012	0.011	0.011	0.012	0.011	0.011	0.010
0.587	0.580	0.570	0.577	0.563	0.568	0.563	0.583	0.567	0.590	0.595	0.587	0.592	0.016	3%	0.109	0.092	0.100	0.089	0.082	0.078	0.090
0.000	0.000	0.000	0.006	0.000	0.011	0.000	0.000	0.000	0.000	0.000	0.008	0.004	0.007	162%	0.001	0.014	0.006	0.019	0.026	0.033	0.017
0.010	0.010	0.009	0.010	0.010	0.010	0.010	0.010	0.010	0.010	0.010	0.010	0.010	0.001	6%	0.009	0.010	0.010	0.010	0.010	0.010	0.010
0.000	0.000	0.000	0.000	0.000	0.000	0.001	0.001	0.000	0.000	0.000	0.000	0.000	0.000	100%	0.000	0.000	0.000	0.000	0.000	0.000	0.000
1.380	1.390	1.403	1.403	1.402	1.412	1.416	1.394	1.407	1.390	1.384	1.396	1.387	0.013	1%	1.867	1.877	1.873	1.878	1.881	1.881	1.878
0.002	0.002	0.002	0.002	0.002	0.001	0.002	0.001	0.002	0.002	0.002	0.002	0.002	0.001	25%	0.008	0.008	0.008	0.008	0.008	0.008	0.008
2.994	2.993	2.994	3.000	2.990	3.000	2.997	2.998	2.994	2.996	2.995	3.000	2.998	0.003	0%	3.000	3.000	3.000	3.000	3.000	3.000	3.000
70.4	70.6	70.6	70.4	70.8	71.1	70.7	70.7	71.0	69.7	70.5	71.2	68.9	12.6	18%	93.6	93.8	93.8	93.7	93.7	93.6	93.7
29.1	28.9	29.0	29.1	28.7	28.4	28.8	28.9	28.5	29.9	29.0	28.3	27.6	5.1	18%	5.5	5.3	5.3	5.4	5.4	5.5	5.4
0.5	0.5	0.5	0.5	0.5	0.5	0.5	0.5	0.5	0.5	0.5	0.5	0.5	0.3	52%	0.5	0.5	0.5	0.5	0.5	0.5	0.5
81.54	81.75	81.66	81.55	81.65	81.49	81.60	81.45	81.68	81.52	81.74	81.80	81.79	14.46	18%	94.4	94.7	94.6	94.6	94.6	94.4	94.6

NWA11187	NWA11187	NWA11187	NWA11187	NWA11187	NWA11187	NWA11187	NWA11187	NWA11187	NWA11187	NWA11187	NWA11187	NWA11187	NWA11187	NWA11187	NWA11187 Mean 41.40	NWA11187 St.Dev. 0.50	NWA11187 Rel. St. Dev 1%
41.62	41.71	41.38	41.83	40.83	41.39	42.25	41.46	41.92	41.56	40.48	41.81	41.55	39.84	41.66			
0.04	0.05	0.03	0.03	0.05	0.03	0.04	0.05	0.04	0.04	0.03	0.03	0.05	0.03	0.02	0.04	0.01	22%
0.02	0.02	0.02	0.02	0.07	0.03	0.02	0.02	0.03	0.03	0.03	0.03	0.03	0.03	0.02	0.03	0.01	47%
0.55	0.55	0.58	0.58	0.58	0.53	0.48	0.58	0.55	0.53	0.61	0.55	0.59	0.54	0.57	0.57	0.03	6%
5.71	5.25	5.35	5.46	6.03	5.54	3.75	5.43	5.46	5.53	7.04	5.46	5.52	5.36	5.30	5.46	0.53	10%
0.49	0.48	0.45	0.48	0.66	0.47	0.49	0.50	0.47	0.48	0.48	0.48	0.51	0.46	0.47	0.49	0.04	8%
0.01	0.00	0.01	0.00	0.07	0.00	0.02	0.00	0.01	0.00	0.04	0.00	0.00	0.01	0.00	0.01	0.02	197%
53.22	52.65	52.76	52.64	51.55	52.47	54.14	53.05	52.33	52.70	51.31	52.49	52.46	51.30	52.91	52.64	0.64	1%
0.32	0.32	0.31	0.33	0.36	0.32	0.35	0.31	0.32	0.31	0.36	0.32	0.32	0.36	0.32	0.32	0.02	5%
101.98	101.03	100.89	101.38	100.19	100.77	101.53	101.40	101.12	101.16	100.37	101.16	101.02	97.95	101.28	100.95	0.77	0.77%
0.983	0.994	0.987	0.995	0.986	0.990	0.995	0.984	0.999	0.990	0.978	0.996	0.992	0.979	0.990	0.988	0.006	1%
0.001	0.001	0.001	0.001	0.001	0.001	0.001	0.001	0.001	0.001	0.001	0.000	0.001	0.001	0.000	0.001	0.000	22%
0.001	0.001	0.001	0.001	0.002	0.001	0.000	0.001	0.001	0.001	0.001	0.001	0.001	0.001	0.001	0.001	0.000	48%
0.010	0.010	0.011	0.011	0.011	0.010	0.009	0.011	0.010	0.010	0.012	0.010	0.011	0.010	0.011	0.011	0.001	6%
0.092	0.105	0.094	0.109	0.108	0.102	0.074	0.090	0.109	0.102	0.112	0.109	0.108	0.081	0.098	0.097	0.011	12%
0.021	0.000	0.012	0.000	0.014	0.008	0.000	0.018	0.000	0.008	0.031	0.000	0.002	0.029	0.007	0.012	0.011	90%
0.010	0.010	0.009	0.010	0.013	0.010	0.010	0.010	0.010	0.010	0.010	0.010	0.010	0.010	0.009	0.010	0.001	9%
0.000	0.000	0.000	0.000	0.001	0.000	0.000	0.000	0.000	0.000	0.001	0.000	0.000	0.000	0.000	0.000	0.000	198%
1.874	1.871	1.876	1.866	1.855	1.870	1.901	1.877	1.858	1.871	1.847	1.864	1.867	1.879	1.875	1.872	0.011	1%
0.008	0.008	0.008	0.008	0.009	0.008	0.009	0.008	0.008	0.008	0.009	0.008	0.008	0.010	0.008	0.008	0.000	6%
3.000	2.999	3.000	2.999	3.000	3.000	2.999	3.000	2.995	3.000	3.000	2.998	3.000	3.000	3.000	3.000	0.001	0%
93.5	93.9	93.8	93.6	92.8	93.6	95.4	93.7	93.6	93.6	92.0	93.6	93.6	93.6	93.8	93.6	0.6	1%
5.6	5.2	5.3	5.5	6.1	5.5	3.7	5.4	5.5	5.5	7.1	5.5	5.5	5.5	5.3	5.5	0.5	10%
0.5	0.5	0.5	0.5	0.7	0.5	0.5	0.5	0.5	0.5	0.5	0.5	0.5	0.5	0.5	0.5	0.0	9%
94.3	94.7	94.6	94.5	93.8	94.4	96.3	94.6	94.5	94.4	92.9	94.5	94.4	94.5	94.7	94.50	0.56	1%

Table S2 - Orthopyroxene

	MIL09020 9	MIL09020 10	MIL09020 11	MIL09020 12	MIL09020 13	MIL09020 14	MIL09020 15	MIL09020 16	MIL09020 17	MIL09020 18	MIL09020 19	MIL090206 20	MIL090206 23	MIL090206 24	MIL090206 25	MIL090206 26	MIL090206 27	MIL090206 28	MIL090206 29	MIL090206 30	MIL090206 31	MIL090206 32	MIL090206 33	MIL090206 34	MIL090206 35	MIL090206 36	MIL090206 37	MIL090206 38	MIL090206 39	MIL090206 40	MIL090206 41
SiO2	54.72	54.84	54.49	54.59	54.29	54.13	54.65	53.92	54.25	54.26	54.28	54.48	54.32	54.30	54.28	54.29	54.51	54.22	54.50	54.45	54.33	54.43	54.57	54.18	54.17	54.43	54.22	54.42	54.36	53.19	54.22
TiO2	0.14	0.14	0.11	0.13	0.14	0.14	0.13	0.13	0.17	0.13	0.15	0.11	0.16	0.14	0.15	0.15	0.16	0.14	0.13	0.16	0.15	0.14	0.14	0.15	0.14	0.16	0.12	0.15	0.13	0.06	0.03
Al2O3	0.23	0.26	0.25	0.24	0.25	0.24	0.26	0.27	0.26	0.25	0.23	0.23	0.25	0.23	0.26	0.23	0.25	0.22	0.25	0.27	0.26	0.24	0.24	0.26	0.27	0.23	0.25	0.25	0.24	0.03	0.01
Cr2O3	0.21	0.23	0.21	0.17	0.18	0.21	0.21	0.18	0.19	0.20	0.19	0.22	0.19	0.18	0.19	0.18	0.18	0.18	0.19	0.18	0.21	0.18	0.18	0.21	0.21	0.20	0.17	0.20	0.19	0.05	0.05
FeOT	16.90	16.65	16.94	16.57	16.89	16.94	16.43	16.70	16.78	16.71	16.67	16.88	16.88	16.86	17.00	16.94	16.46	16.64	17.00	17.13	17.09	16.95	16.86	16.60	16.83	16.61	16.70	16.81	16.85	14.87	16.27
MnO	0.40	0.37	0.40	0.44	0.42	0.42	0.40	0.42	0.39	0.38	0.37	0.38	0.39	0.41	0.40	0.39	0.42	0.38	0.41	0.37	0.44	0.39	0.40	0.40	0.37	0.38	0.39	0.38	0.40	0.44	0.46
MgO	26.17	25.83	25.90	25.83	26.24	26.17	25.93	26.00	26.11	26.06	25.99	26.28	26.00	26.41	26.05	26.17	26.18	26.04	25.99	25.95	26.07	25.91	26.05	25.97	26.14	26.00	25.94	26.07	26.12	29.90	28.55
CaO	1.12	1.20	1.14	1.15	1.15	1.11	1.17	1.13	1.18	1.12	1.14	1.15	1.15	1.13	1.14	1.17	1.16	1.16	1.15	1.15	1.12	1.11	1.12	1.19	1.18	1.13	1.14	1.15	1.12	0.38	0.37
Na2O	0.03	0.04	0.01	0.00	0.05	0.04	0.02	0.01	0.04	0.03	0.02	0.04	0.05	0.00	0.03	0.02	0.02	0.03	0.03	0.01	0.02	0.04	0.03	0.04	0.00	0.02	0.07	0.04	0.04	0.01	0.00
K2O	0.01	0.01	0.00	0.01	0.00	0.01	0.00	0.00	0.00	0.00	0.00	0.00	0.00	0.01	0.00	0.00	0.01	0.00	0.00	0.00	0.00	0.00	0.00	0.01	0.00	0.01	0.02	0.00	0.00	0.01	0.01
Total	99.93	99.57	99.45	99.13	99.62	99.42	99.18	98.76	99.37	99.14	99.03	99.77	99.39	99.66	99.48	99.55	99.33	99.01	99.63	99.67	99.68	99.40	99.60	99.00	99.30	99.16	99.02	99.46	99.45	98.92	99.98
	(4) normalizzazione a 6 ossigeni e <4 cationi per f.u.																														
Si	1.990	1.998	1.991	1.998	1.979	1.977	1.997	1.983	1.982	1.988	1.990	1.982	1.986	1.977	1.983	1.981	1.990	1.988	1.989	1.987	1.982	1.990	1.990	1.987	1.981	1.992	1.988	1.988	1.985	1.915	1.949
Ti	0.004	0.004	0.003	0.004	0.004	0.004	0.004	0.004	0.005	0.004	0.004	0.003	0.004	0.004	0.004	0.004	0.004	0.004	0.004	0.004	0.004	0.004	0.004	0.004	0.004	0.004	0.003	0.004	0.004	0.002	0.001
Al	0.010	0.011	0.011	0.010	0.011	0.010	0.011	0.012	0.011	0.011	0.010	0.010	0.011	0.010	0.011	0.010	0.011	0.009	0.011	0.011	0.011	0.010	0.010	0.011	0.011	0.010	0.011	0.011	0.010	0.001	0.001
Cr	0.006	0.007	0.006	0.005	0.005	0.006	0.006	0.005	0.006	0.006	0.005	0.006	0.005	0.005	0.005	0.005	0.005	0.005	0.005	0.005	0.006	0.005	0.005	0.006	0.006	0.006	0.005	0.006	0.005	0.001	0.001
Fe2+	0.514	0.507	0.518	0.507	0.493	0.493	0.502	0.502	0.501	0.508	0.511	0.497	0.509	0.490	0.507	0.500	0.503	0.508	0.517	0.521	0.508	0.518	0.514	0.506	0.502	0.508	0.505	0.510	0.505	0.282	0.391
Fe3+	0.000	0.000	0.000	0.000	0.022	0.024	0.000	0.011	0.012	0.004	0.000	0.016	0.007	0.024	0.012	0.017	0.000	0.003	0.002	0.002	0.013	0.000	0.000	0.003	0.013	0.000	0.008	0.003	0.009	0.166	0.099
Mn	0.012	0.011	0.012	0.014	0.013	0.013	0.012	0.013	0.012	0.012	0.011	0.012	0.012	0.013	0.012	0.012	0.013	0.012	0.013	0.011	0.013	0.012	0.012	0.012	0.012	0.012	0.012	0.012	0.012	0.013	0.014
Mg	1.418	1.403	1.411	1.409	1.425	1.425	1.412	1.425	1.422	1.423	1.421	1.426	1.417	1.433	1.418	1.424	1.425	1.424	1.414	1.412	1.417	1.413	1.417	1.420	1.425	1.419	1.418	1.419	1.422	1.605	1.530
Ca	0.043	0.047	0.045	0.045	0.045	0.044	0.046	0.044	0.046	0.044	0.045	0.045	0.045	0.044	0.044	0.046	0.046	0.045	0.045	0.045	0.044	0.043	0.044	0.047	0.046	0.044	0.045	0.045	0.044	0.015	0.014
Na	0.002	0.003	0.001	0.000	0.003	0.003	0.001	0.001	0.003	0.002	0.002	0.003	0.003	0.000	0.002	0.002	0.001	0.002	0.002	0.001	0.001	0.003	0.002	0.003	0.000	0.001	0.005	0.003	0.003	0.000	0.000
K	0.000	0.000	0.000	0.001	0.000	0.000	0.000	0.000	0.000	0.000	0.000	0.000	0.000	0.000	0.000	0.000	0.000	0.000	0.000	0.000	0.000	0.000	0.000	0.000	0.000	0.000	0.001	0.000	0.000	0.000	0.001
cations	4.000	3.991	3.997	3.992	4.000	4.000	3.992	4.000	4.000	4.000	3.999	4.000	4.000	4.000	4.000	4.000	3.998	4.000	4.000	4.000	4.000	3.999	3.999	4.000	4.000	3.996	4.000	4.000	4.000	4.000	4.000
FeT	0.514	0.507	0.518	0.507	0.515	0.517	0.502	0.513	0.513	0.512	0.511	0.514	0.516	0.513	0.519	0.517	0.503	0.510	0.519	0.523	0.521	0.518	0.514	0.509	0.515	0.508	0.512	0.513	0.515	0.448	0.489
mg*(FeT)	0.734	0.734	0.732	0.735	0.735	0.734	0.738	0.735	0.735	0.735	0.735	0.735	0.733	0.736	0.732	0.734	0.739	0.736	0.732	0.730	0.731	0.731	0.734	0.736	0.735	0.736	0.735	0.734	0.734	0.782	0.758
Cr	0.010	0.010	0.010	0.010	0.010	0.010	0.010	0.010	0.010	0.010	0.010	0.010	0.010	0.010	0.010	0.010	0.010	47.010	48.010	49.010	50.010	51.010	52.010	53.010	54.010	55.010	56.010	57.010	58.010	59.010	60.010
FeTM1	0.260	0.255	0.261	0.254	0.262	0.263	0.252	0.261	0.261	0.259	0.259	0.261	0.262	0.261	0.264	0.263	0.254	0.259	0.263	0.265	0.265	0.262	0.260	0.258	0.262	0.256	0.260	0.260	0.261	0.233	0.250
FeTM2	0.254	0.252	0.256	0.253	0.253	0.254	0.250	0.253	0.252	0.252	0.252	0.252	0.254	0.252	0.255	0.254	0.249	0.251	0.256	0.258	0.257	0.256	0.254	0.251	0.253	0.252	0.252	0.253	0.253	0.215	0.239
wollastonite	2.2	2.4	2.2	2.3	2.3	2.2	2.3	2.2	2.3	2.2	2.2	2.2	2.3	2.2	2.2	2.3	2.3	2.3	2.3	2.3	2.2	2.2	2.2	2.4	2.3	2.2	2.2	2.3	2.2	0.7	0.7
enstatite	71.3	71.3	71.1	71.4	71.3	71.3	71.6	71.4	71.4	71.5	71.5	71.4	71.2	71.6	71.1	71.2	71.8	71.5	71.0	70.9	71.0	71.1	71.3	71.4	71.3	71.5	71.4	71.3	71.3	77.1	74.7
ferrosilite	26.5	26.4	26.7	26.4	26.4	26.5	26.1	26.4	26.3	26.3	26.3	26.3	26.5	26.3	26.7	26.5	26.0	26.2	26.7	26.8	26.8	26.7	26.5	26.2	26.3	26.2	26.4	26.4	26.4	22.2	24.6

MIL090206	MIL090206	MIL090206	MIL090206	MIL090405	MIL090405	MIL090405	MIL090405	MIL090405	MIL090405	NWA6077	NWA6077	NWA6077	NWA6077	NWA6077	NWA6077	NWA6077	NWA6077	NWA6077	NWA6077	NWA6077	NWA6077	NWA6077	NWA6077	NWA6077	NWA6077	NWA6077
42				28	29	30					10	12	18	20	22	23	26	27	29	30	31	32	33	34	35	37	38	39
	Mean	St. Dev.	Rel. St. Dev.				Mean	St. Dev.	Rel. St. Dev.	21																	
54.77	54.35	0.29	1%	55.01	54.71	55.34	55.02	0.31	1%	54.13	54.12	54.37	54.01	53.89	54.28	54.12	54.05	53.58	52.77	53.85	53.14	54.55	54.26	54.48	54.12	54.15	54.33	54.34
0.04	0.13	0.03	24%	0.01	0.04	0.04	0.03	0.02	54%	0.12	0.14	0.13	0.12	0.10	0.11	0.09	0.10	0.09	0.11	0.12	0.12	0.11	0.13	0.11	0.10	0.11	0.11	0.10
0.02	0.23	0.07	30%	0.03	0.03	0.03	0.03	0.00	10%	0.27	0.27	0.28	0.27	0.28	0.28	0.25	0.29	0.28	0.28	0.29	0.32	0.26	0.29	0.29	0.26	0.28	0.31	0.28
0.07	0.18	0.04	24%	0.09	0.07	0.06	0.07	0.01	17%	0.21	0.18	0.19	0.18	0.20	0.17	0.19	0.20	0.19	0.18	0.17	0.22	0.18	0.17	0.19	0.21	0.20	0.20	0.22
14.80	16.66	0.52	3%	15.36	15.22	15.10	15.23	0.13	1%	15.78	15.23	15.37	15.60	16.17	15.80	15.41	15.51	15.57	15.68	15.97	15.59	15.66	15.66	15.47	15.32	15.81	15.67	15.80
0.43	0.40	0.02	6%	0.43	0.38	0.40	0.41	0.02	5%	0.26	0.25	0.27	0.27	0.25	0.26	0.25	0.26	0.27	0.26	0.26	0.26	0.25	0.26	0.26	0.25	0.25	0.26	0.26
28.95	26.34	0.94	4%	28.04	27.93	28.46	28.14	0.28	1%	28.03	27.74	27.84	27.82	27.91	27.81	27.64	27.74	27.69	27.40	28.01	27.81	27.71	27.77	27.86	27.82	28.00	27.81	27.68
0.38	1.07	0.23	21%	0.53	0.54	0.45	0.51	0.05	9%	1.11	1.08	1.13	1.07	1.06	1.06	1.08	1.13	1.11	1.05	1.04	1.11	1.09	1.09	1.07	1.09	1.07	1.08	1.10
0.00	0.03	0.02	66%	0.02	0.02	0.00	0.01	0.01	90%	0.03	0.02	0.03	0.01	0.04	0.03	0.01	0.04	0.03	0.03	0.04	0.03	0.01	0.03	0.03	0.04	0.04	0.03	0.06
0.01	0.01	0.01	110%	0.00	0.01	0.00	0.00	0.01	154%	0.01	0.00	0.00	0.01	0.00	0.00	0.01	0.00	0.00	0.01	0.03	0.01	0.00	0.01	0.00	0.01	0.02	0.01	0.00
99.46	99.39	0.29	0%	99.50	98.97	99.88	99.45	0.46	0%	99.94	99.03	99.59	99.35	99.89	99.80	99.06	99.31	98.81	97.77	99.76	98.61	99.83	99.67	99.76	99.21	99.93	99.82	99.84
1.970	1.983	0.015	1%	1.987	1.987	1.988	1.987	0.001	0%	1.948	1.965	1.963	1.956	1.942	1.958	1.966	1.958	1.950	1.942	1.941	1.937	1.967	1.959	1.964	1.961	1.949	1.958	1.960
0.001	0.004	0.001	24%	0.000	0.001	0.001	0.001	0.000	54%	0.003	0.004	0.003	0.003	0.003	0.003	0.003	0.003	0.003	0.003	0.003	0.003	0.003	0.004	0.003	0.003	0.003	0.003	0.003
0.001	0.010	0.003	30%	0.001	0.001	0.001	0.001	0.000	10%	0.011	0.012	0.012	0.012	0.012	0.012	0.011	0.012	0.012	0.012	0.012	0.014	0.011	0.012	0.012	0.011	0.012	0.013	0.012
0.002	0.005	0.001	24%	0.002	0.002	0.002	0.002	0.000	17%	0.006	0.005	0.005	0.005	0.006	0.005	0.005	0.006	0.005	0.005	0.005	0.006	0.005	0.005	0.005	0.006	0.006	0.006	0.006
0.390	0.492	0.048	10%	0.442	0.439	0.435	0.439	0.003	1%	0.392	0.414	0.412	0.406	0.392	0.413	0.420	0.405	0.395	0.387	0.384	0.373	0.429	0.413	0.416	0.405	0.394	0.412	0.415
0.055	0.016	0.033	205%	0.022	0.023	0.018	0.021	0.003	13%	0.083	0.048	0.052	0.066	0.096	0.064	0.048	0.064	0.079	0.096	0.097	0.103	0.044	0.060	0.051	0.059	0.082	0.061	0.061
0.013	0.012	0.001	6%	0.013	0.012	0.012	0.012	0.001	5%	0.008	0.008	0.008	0.008	0.008	0.008	0.008	0.008	0.008	0.008	0.008	0.008	0.008	0.008	0.008	0.008	0.008	0.008	0.008
1.552	1.433	0.044	3%	1.510	1.512	1.524	1.515	0.008	1%	1.503	1.501	1.499	1.502	1.499	1.495	1.497	1.498	1.503	1.503	1.505	1.511	1.490	1.495	1.497	1.503	1.502	1.495	1.488
0.014	0.042	0.009	22%	0.020	0.021	0.017	0.020	0.002	10%	0.043	0.042	0.044	0.042	0.041	0.041	0.042	0.044	0.043	0.042	0.040	0.043	0.042	0.042	0.041	0.042	0.041	0.042	0.042
0.000	0.002	0.001	66%	0.001	0.002	0.000	0.001	0.001	90%	0.002	0.002	0.002	0.000	0.002	0.002	0.001	0.003	0.002	0.002	0.002	0.002	0.001	0.002	0.002	0.003	0.003	0.002	0.004
0.000	0.000	0.000	110%	0.000	0.001	0.000	0.000	0.000	154%	0.000	0.000	0.000	0.000	0.000	0.000	0.000	0.000	0.000	0.000	0.001	0.001	0.000	0.000	0.000	0.000	0.001	0.000	0.000
4.000	3.999	0.003	0%	4.000	4.000	4.000	4.000	0.000	0%	4.000	4.000	4.000	4.000	4.000	4.000	4.000	4.000	4.000	4.000	4.000	4.000	4.000	4.000	4.000	4.000	4.000	4.000	4.000
0.445	0.508	0.017	3%	0.464	0.462	0.454	0.460	0.006	1%	0.475	0.462	0.464	0.472	0.487	0.477	0.468	0.470	0.474	0.483	0.481	0.475	0.472	0.473	0.466	0.464	0.476	0.472	0.477
0.777	0.738	0.012	2%	0.765	0.766	0.771	0.767	0.003	0%		0.764	0.764	0.761	0.755	0.758	0.762	0.761	0.760	0.757	0.758	0.761	0.759	0.760	0.762	0.764	0.759	0.760	0.757
61.010	25.323	27.543	109%	62.010	63.010	64.010	63.010	1.000	2%		65.010	66.010	68.010	69.010	70.010	71.010	72.010	73.010	74.010	75.010	76.010	77.010	78.010	79.010	80.010	82.010	83.010	84.010
0.226	0.258	0.008	3%	0.234	0.233	0.228	0.232	0.003	1%		0.237	0.238	0.243	0.253	0.245	0.240	0.242	0.245	0.250	0.249	0.247	0.242	0.243	0.239	0.239	0.246	0.243	0.245
0.220	0.251	0.009	4%	0.230	0.229	0.225	0.228	0.002	1%		0.225	0.226	0.229	0.235	0.231	0.228	0.228	0.229	0.232	0.232	0.228	0.230	0.230	0.227	0.225	0.230	0.230	0.231
0.7	2.1	0.5	22%	1.0	1.0	0.9	1.0	0.1	10%	2.1	2.1	2.2	2.1	2.0	2.0	2.1	2.2	2.1	2.0	2.0	2.1	2.1	2.1	2.1	2.1	2.0	2.1	2.1
76.6	71.8	1.5	2%	75.2	75.3	75.9	75.5	0.4	1%	74.1	74.6	74.4	74.2	73.7	74.0	74.3	74.2	74.1	73.9	74.0	74.2	74.0	74.1	74.4	74.5	74.1	74.1	73.9
22.6	26.1	1.0	4%	23.8	23.6	23.2	23.5	0.3	1%	23.8	23.4	23.4	23.7	24.3	24.0	23.6	23.7	23.8	24.1	24.1	23.7	23.9	23.8	23.6	23.4	23.9	23.8	24.0

NWA6077	NWA6077	NWA6077	NWA5363	NWA5363	NWA5363	NWA5363	NWA5363	NWA5363	NWA5363	NWA5363	NWA5363	NWA5363	NWA5363	NWA5363	NWA5363
Mean	St. Dev.	Rel. St. Dev.													
54.03	0.45	1%	53.54	55.62	55.63	55.50	55.29	55.59	55.67	55.59	55.43	55.57	55.55	55.51	55.62
0.11	0.01	11%	0.08	0.11	0.12	0.11	0.11	0.14	0.11	0.09	0.11	0.12	0.12	0.14	0.13
0.28	0.02	6%	0.29	0.28	0.27	0.29	0.27	0.29	0.29	0.26	0.28	0.28	0.32	0.35	0.30
0.19	0.02	8%	0.22	0.19	0.18	0.21	0.19	0.20	0.19	0.20	0.21	0.20	0.22	0.19	0.22
15.64	0.23	1%	15.88	15.58	15.78	15.62	15.94	15.84	15.84	15.94	15.61	15.56	15.60	15.45	15.56
0.26	0.01	2%	0.41	0.27	0.27	0.27	0.25	0.27	0.27	0.25	0.27	0.27	0.26	0.27	0.26
27.79	0.15	1%	26.14	27.33	27.26	27.14	27.56	27.11	27.19	27.33	27.29	27.15	27.21	27.23	27.38
1.09	0.03	2%	1.08	1.09	1.11	1.13	1.08	1.06	1.06	1.08	1.08	1.08	1.08	1.07	1.08
0.03	0.01	41%	0.03	0.04	0.03	0.04	0.03	0.03	0.01	0.03	0.01	0.03	0.01	0.02	0.02
0.01	0.01	104%	0.00	0.01	0.00	0.00	0.00	0.01	0.01	0.01	0.00	0.00	0.00	0.01	0.00
99.42	0.57	1%	97.66	100.51	100.64	100.30	100.72	100.54	100.63	100.77	100.29	100.26	100.36	100.23	100.57
1.955	0.009	0%	1.985	1.995	1.994	1.995	1.980	1.995	1.995	1.991	1.993	1.997	1.995	1.995	1.993
0.003	0.000	11%	0.002	0.003	0.003	0.003	0.003	0.004	0.003	0.002	0.003	0.003	0.003	0.004	0.003
0.012	0.001	6%	0.012	0.012	0.011	0.012	0.011	0.012	0.012	0.011	0.012	0.012	0.013	0.015	0.013
0.006	0.000	8%	0.006	0.005	0.005	0.006	0.005	0.006	0.005	0.006	0.006	0.006	0.006	0.005	0.006
0.404	0.014	4%	0.483	0.467	0.473	0.469	0.458	0.475	0.475	0.478	0.469	0.468	0.468	0.464	0.466
0.069	0.019	27%	0.009	0.000	0.000	0.000	0.019	0.000	0.000	0.000	0.000	0.000	0.000	0.000	0.000
0.008	0.000	2%	0.013	0.008	0.008	0.008	0.008	0.008	0.008	0.007	0.008	0.008	0.008	0.008	0.008
1.499	0.005	0%	1.444	1.461	1.456	1.454	1.472	1.450	1.453	1.460	1.462	1.455	1.457	1.459	1.462
0.042	0.001	2%	0.043	0.042	0.043	0.044	0.041	0.041	0.041	0.041	0.041	0.042	0.041	0.041	0.041
0.002	0.001	41%	0.002	0.003	0.002	0.003	0.002	0.002	0.001	0.002	0.001	0.002	0.001	0.001	0.001
0.000	0.000	104%	0.000	0.000	0.000	0.000	0.000	0.000	0.000	0.001	0.000	0.000	0.000	0.000	0.000
4.000	0.000	0%	4.000	3.996	3.996	3.994	4.000	3.994	3.994	3.999	3.996	3.992	3.993	3.992	3.995
0.473	0.007	1%	0.492	0.467	0.473	0.469	0.477	0.475	0.475	0.478	0.469	0.468	0.468	0.464	0.466
0.760	0.003	0%	0.746	0.758	0.755	0.756	0.755	0.753	0.754	0.754	0.757	0.757	0.757	0.759	0.758
74.566	5.772	8%	85.010	86.010	87.010	88.010	89.010	90.010	91.010	92.010	93.010	94.010	95.010	96.010	97.010
0.244	0.004	2%	0.250	0.236	0.239	0.237	0.243	0.239	0.239	0.242	0.237	0.235	0.235	0.233	0.235
0.229	0.003	1%	0.243	0.231	0.234	0.233	0.234	0.236	0.236	0.236	0.233	0.233	0.233	0.231	0.231
2.1	0.1	2%	2.2	2.1	2.2	2.2	2.1	2.1	2.1	2.1	2.1	2.1	2.1	2.1	2.1
74.1	0.2	0%	72.5	73.9	73.6	73.6	73.7	73.4	73.5	73.5	73.8	73.8	73.8	74.0	73.9
23.8	0.3	1%	25.4	24.0	24.3	24.2	24.3	24.5	24.4	24.4	24.1	24.1	24.1	24.0	24.0

NWA5363	NWA5363	NWA5363	NWA11187	NWA11187	NWA11187	NWA11187	NWA11187	NWA11187	NWA11187	NWA11187	NWA11187	NWA11187
			56	58	60	61	64	67	69	72	73	75
Mean	St. Dev.	Rel. St. Dev.										
55.39	0.57	1%	58.25	57.81	58.17	57.10	54.80	56.41	55.14	58.01	57.96	58.07
0.11	0.02	15%	0.16	0.14	0.14	0.15	0.13	0.14	0.13	0.13	0.16	0.15
0.29	0.02	8%	0.53	0.51	0.52	0.49	0.52	0.50	0.52	0.53	0.48	0.51
0.20	0.02	7%	0.86	0.87	0.84	0.86	0.85	0.84	0.87	0.83	0.84	0.85
15.71	0.17	1%	3.26	3.49	3.44	3.36	3.49	3.40	3.31	3.33	3.37	3.52
0.27	0.04	15%	0.48	0.46	0.50	0.50	0.49	0.47	0.48	0.48	0.50	0.47
27.18	0.34	1%	34.59	34.74	34.72	34.27	34.74	34.76	35.08	35.15	34.89	34.76
1.08	0.02	2%	2.69	2.77	2.67	2.66	2.67	2.72	2.64	2.65	2.68	2.68
0.03	0.01	40%	0.03	0.03	0.03	0.03	0.04	0.04	0.02	0.03	0.02	0.04
0.00	0.00	115%	0.01	0.00	0.00	0.01	0.00	0.00	0.01	0.00	0.00	0.00
100.27	0.80	1%	100.84	100.81	101.02	99.42	97.72	99.27	98.19	101.12	100.89	101.05
1.992	0.005	0%	1.982	1.971	1.979	1.974	1.921	1.948	1.922	1.969	1.973	1.976
0.003	0.000	14%	0.004	0.004	0.004	0.004	0.003	0.004	0.003	0.003	0.004	0.004
0.012	0.001	8%	0.021	0.020	0.021	0.020	0.021	0.020	0.021	0.021	0.019	0.020
0.006	0.000	8%	0.023	0.024	0.022	0.024	0.024	0.023	0.024	0.022	0.023	0.023
0.470	0.006	1%	0.093	0.091	0.098	0.094	0.000	0.042	0.000	0.080	0.091	0.100
0.002	0.006	260%	0.000	0.009	0.000	0.003	0.102	0.056	0.096	0.014	0.005	0.000
0.008	0.001	16%	0.014	0.013	0.014	0.015	0.014	0.014	0.014	0.014	0.014	0.014
1.457	0.007	0%	1.755	1.766	1.760	1.766	1.815	1.790	1.823	1.778	1.771	1.763
0.042	0.001	2%	0.098	0.101	0.097	0.098	0.100	0.101	0.099	0.096	0.098	0.098
0.002	0.001	40%	0.002	0.002	0.002	0.002	0.003	0.003	0.002	0.002	0.002	0.002
0.000	0.000	115%	0.000	0.000	0.000	0.000	0.000	0.000	0.000	0.000	0.000	0.000
3.995	0.003	0%	3.993	4.000	3.997	4.000	4.004	4.000	4.005	4.000	4.000	4.000
0.473	0.007	2%	0.093	0.099	0.098	0.097	0.102	0.098	0.096	0.094	0.096	0.100
0.755	0.003	0%	0.950	0.947	0.947	0.948	0.947	0.948	0.950	0.950	0.949	0.946
91.010	3.894	4%	98.010	99.010	100.010	101.010	102.010	104.010	105.010	106.010	107.010	108.01(
0.238	0.004	2%	0.048	0.052	0.050	0.050	0.054	0.052	0.051	0.049	0.050	0.052
0.234	0.003	1%	0.045	0.048	0.047	0.047	0.048	0.047	0.045	0.045	0.046	0.048
2.1	0.0	2%	5.0	5.1	4.9	5.0	4.9	5.0	4.9	4.9	4.9	5.0
73.6	0.4	1%	89.6	89.2	89.4	89.4	89.3	89.4	89.7	89.7	89.5	89.3
24.3	0.4	2%	5.4	5.7	5.7	5.7	5.7	5.6	5.4	5.5	5.6	5.8

NWA11187	NWA11187	NWA11187	NWA11187	NWA11187	NWA11187	NWA11187	NWA11187	NWA11187	NWA11187	NWA11187	NWA11187	NWA11187	NWA11187	NWA11187	NWA11187	NWA11187
77	80	81	82	83	85	86	88	89	92	93	96	98	100			
														Mean	St. Dev.	Rel. St. Dev.
57.96	57.96	57.25	57.60	57.82	57.53	57.65	58.18	58.07	57.90	57.77	56.98	56.99	58.28	57.49	0.91	2%
0.12	0.15	0.11	0.13	0.13	0.13	0.15	0.13	0.15	0.15	0.14	0.16	0.12	0.12	0.14	0.01	10%
0.49	0.49	0.50	0.50	0.51	0.49	0.52	0.53	0.51	0.53	0.54	0.52	0.52	0.51	0.51	0.02	3%
0.87	0.86	0.87	0.88	0.83	0.86	0.86	0.86	0.85	0.83	0.80	0.87	0.85	0.82	0.85	0.02	2%
3.37	3.37	3.57	3.54	3.47	3.48	3.66	3.50	3.63	3.60	3.57	3.54	3.55	3.47	3.47	0.11	3%
0.48	0.47	0.55	0.55	0.46	0.47	0.46	0.47	0.49	0.47	0.48	0.49	0.45	0.46	0.48	0.02	5%
34.83	34.91	33.00	33.00	34.80	34.81	34.99	34.70	34.70	34.90	34.58	35.13	34.96	35.05	34.67	0.55	2%
2.68	2.69	4.79	4.86	2.67	2.71	2.69	2.70	2.66	2.71	2.70	2.69	2.68	2.69	2.86	0.60	21%
0.05	0.05	0.06	0.08	0.06	0.04	0.04	0.04	0.06	0.04	0.03	0.06	0.06	0.05	0.04	0.01	33%
0.00	0.00	0.00	0.00	0.00	0.00	0.01	0.01	0.00	0.00	0.00	0.01	0.00	0.00	0.00	0.00	128%
100.84	100.96	100.70	101.13	100.76	100.50	101.03	101.12	101.13	101.14	100.61	100.44	100.17	101.47	100.51	0.94	1%
1.974	1.972	1.965	1.970	1.971	1.966	1.960	1.978	1.975	1.967	1.974	1.945	1.952	1.973	1.965	0.016	1%
0.003	0.004	0.003	0.003	0.003	0.003	0.004	0.003	0.004	0.004	0.004	0.004	0.003	0.003	0.004	0.000	10%
0.020	0.020	0.020	0.020	0.021	0.020	0.021	0.021	0.021	0.021	0.022	0.021	0.021	0.020	0.021	0.001	3%
0.023	0.023	0.024	0.024	0.022	0.023	0.023	0.023	0.023	0.022	0.022	0.024	0.023	0.022	0.023	0.001	3%
0.090	0.087	0.079	0.087	0.087	0.078	0.073	0.100	0.101	0.086	0.099	0.040	0.051	0.090	0.077	0.029	38%
0.006	0.009	0.024	0.014	0.012	0.022	0.031	0.000	0.002	0.016	0.003	0.061	0.050	0.009	0.023	0.029	130%
0.014	0.014	0.016	0.016	0.013	0.014	0.013	0.014	0.014	0.013	0.014	0.014	0.013	0.013	0.014	0.001	5%
1.769	1.770	1.689	1.683	1.769	1.773	1.774	1.758	1.759	1.768	1.762	1.788	1.785	1.769	1.767	0.030	2%
0.098	0.098	0.176	0.178	0.097	0.099	0.098	0.098	0.097	0.099	0.099	0.098	0.098	0.098	0.105	0.022	21%
0.003	0.003	0.004	0.005	0.004	0.003	0.003	0.003	0.004	0.003	0.002	0.004	0.004	0.003	0.003	0.001	33%
0.000	0.000	0.000	0.000	0.000	0.000	0.000	0.000	0.000	0.000	0.000	0.000	0.000	0.000	0.000	0.000	128%
4.000	4.000	4.000	4.000	4.000	4.000	4.000	3.998	4.000	4.000	4.000	4.000	4.000	4.000	4.000	0.002	0%
0.096	0.096	0.103	0.101	0.099	0.099	0.104	0.100	0.103	0.102	0.102	0.101	0.102	0.098	0.099	0.003	3%
0.949	0.949	0.943	0.943	0.947	0.947	0.945	0.946	0.945	0.945	0.945	0.946	0.946	0.947	0.947	0.002	0%
109.010	110.010	117.010	118.010	119.010	120.010	121.010	122.010	123.010	124.010	125.010	126.010	128.010	129.010	113.385	10.253	9%
0.050	0.050	0.056	0.055	0.051	0.052	0.054	0.051	0.053	0.053	0.053	0.053	0.053	0.051	0.052	0.002	4%
0.046	0.046	0.047	0.046	0.048	0.048	0.050	0.048	0.050	0.049	0.049	0.048	0.048	0.047	0.047	0.001	3%
5.0	5.0	8.9	9.0	4.9	5.0	4.9	5.0	4.9	5.0	5.0	4.9	4.9	4.9	5.3	1.1	21%
89.5	89.5	85.1	85.1	89.4	89.3	89.2	89.3	89.1	89.2	89.1	89.3	89.3	89.4	89.0	1.2	1%
5.5	5.5	6.0	5.9	5.7	5.7	5.9	5.7	5.9	5.8	5.9	5.8	5.7	5.6	5.7	0.2	3%

Table S3 - Clinopyroxene

		MIL090206	MIL090206	MIL090206	MIL090206	MIL090206	MIL090405	MIL090405	MIL090405	MIL090405	MIL090405	MIL090405	MIL09040	MIL09040	MIL09040	MIL09040	MIL09040	MIL09040	MIL09040	MIL09040	MIL09040
				Mean	St. Dev.	Rel. St. Dev.															
	n°	21	22				9	10	11	12	13	14	15	16	17	18	19	20	21	22	23
	SiO2	53.45	53.56	53.51	0.07	0%	53.78	53.52	53.88	53.57	53.44	53.40	53.62	53.37	53.69	53.43	53.31	54.22	53.60	53.37	53.79
	TiO2	0.30	0.31	0.31	0.01	2%	0.33	0.27	0.30	0.31	0.31	0.32	0.31	0.28	0.30	0.28	0.29	0.27	0.32	0.28	0.29
	Al2O3	0.64	0.63	0.63	0.01	1%	0.66	0.69	0.65	0.73	0.68	0.65	0.69	0.61	0.62	0.63	0.60	0.58	0.63	0.62	0.63
	Cr2O3	0.72	0.74	0.73	0.02	2%	0.81	0.78	0.75	0.85	0.85	0.73	0.88	0.76	0.72	0.72	0.73	0.67	0.77	0.74	0.74
	FeOT	6.71	6.51	6.61	0.14	2%	6.47	6.43	6.49	6.67	6.54	6.50	6.72	6.61	6.43	6.32	6.22	6.97	6.64	6.70	6.47
	MnO	0.20	0.22	0.21	0.01	6%	0.19	0.19	0.20	0.21	0.17	0.17	0.22	0.19	0.19	0.21	0.19	0.17	0.20	0.21	0.24
	MgO	15.80	15.80	15.80	0.00	0%	16.03	15.92	15.74	15.74	15.84	15.86	15.91	15.80	15.76	15.97	15.98	15.86	15.92	16.02	15.82
	CaO	21.33	21.09	21.21	0.17	1%	21.15	21.13	21.28	20.67	21.05	21.19	20.87	21.25	21.30	21.21	21.33	21.31	21.22	21.30	21.48
	Na2O	0.50	0.49	0.49	0.01	2%	0.50	0.51	0.48	0.57	0.55	0.47	0.61	0.51	0.48	0.51	0.46	0.48	0.47	0.45	0.52
	K2O	0.00	0.01	0.00	0.00	94%	0.00	0.00	0.00	0.00	0.00	0.00	0.00	0.01	0.01	0.01	0.00	0.00	0.00	0.00	0.01
	Total	99.65	99.35	99.50	0.21	0%	99.92	99.43	99.77	99.33	99.42	99.29	99.82	99.37	99.49	99.28	99.12	100.54	99.77	99.69	99.97
			(4) normalizzazione a 6 ossigeni e <4 cationi per f.u.																		
Si	Si	1.977	1.986	1.981	0.006	0%	1.982	1.981	1.988	1.986	1.979	1.981	1.979	1.978	1.987	1.980	1.979	1.989	1.980	1.972	1.982
Ti	Ti	0.008	0.009	0.009	0.000	2%	0.009	0.008	0.008	0.009	0.009	0.009	0.009	0.008	0.008	0.008	0.008	0.007	0.009	0.008	0.008
Al	Al	0.028	0.028	0.028	0.000	1%	0.029	0.030	0.028	0.032	0.030	0.029	0.030	0.027	0.027	0.028	0.026	0.025	0.027	0.027	0.027
Cr	Cr	0.021	0.022	0.021	0.001	2%	0.024	0.023	0.022	0.025	0.025	0.021	0.026	0.022	0.021	0.021	0.021	0.019	0.022	0.022	0.021
Fe2+	Fe2+	0.191	0.202	0.196	0.008	4%	0.197	0.193	0.200	0.207	0.193	0.197	0.194	0.189	0.199	0.184	0.182	0.214	0.198	0.183	0.192
Fe3+	Fe3+	0.016	0.000	0.008	0.012	141%	0.003	0.006	0.000	0.000	0.009	0.004	0.013	0.016	0.000	0.012	0.011	0.000	0.007	0.024	0.008
Mn	Mn	0.006	0.007	0.007	0.000	6%	0.006	0.006	0.006	0.007	0.005	0.005	0.007	0.006	0.006	0.007	0.006	0.005	0.006	0.007	0.007
Mg	Mg	0.871	0.873	0.872	0.002	0%	0.881	0.878	0.866	0.870	0.875	0.877	0.875	0.873	0.870	0.882	0.884	0.867	0.876	0.882	0.869
Ca	Ca	0.845	0.838	0.842	0.005	1%	0.835	0.838	0.842	0.821	0.835	0.842	0.825	0.844	0.845	0.842	0.848	0.838	0.840	0.843	0.848
Na	Na	0.036	0.035	0.035	0.001	2%	0.036	0.037	0.034	0.041	0.040	0.034	0.043	0.037	0.034	0.036	0.033	0.034	0.034	0.032	0.037
K	K	0.000	0.000	0.000	0.000	94%	0.000	0.000	0.000	0.000	0.000	0.000	0.000	0.000	0.000	0.000	0.000	0.000	0.000	0.000	0.000
	cations	4.000	3.999	3.999	0.001	0%	4.000	4.000	3.995	3.998	4.000	4.000	4.000	4.000	3.998	4.000	4.000	3.999	4.000	4.000	4.000
	wollastonite	43.8	43.6	43.7	0.1	0%	43.5	43.6	44.0	43.1	43.6	43.7	43.1	43.8	44.0	43.7	43.9	43.5	43.6	43.5	44.1
	enstatite	45.1	45.5	45.3	0.3	1%	45.8	45.7	45.2	45.7	45.6	45.5	45.7	45.3	45.3	45.8	45.8	45.1	45.5	45.5	45.2
	ferrosilite	11.1	10.9	11.0	0.1	1%	10.7	10.7	10.8	11.2	10.8	10.7	11.2	10.9	10.7	10.5	10.3	11.4	11.0	11.0	10.7
	mg* x 100	80.8	81.2	81.002	0.331	0%	81.5	81.5	81.2	80.8	81.2	81.3	80.8	81.0	81.4	81.8	82.1	80.2	81.0	81.0	81.3

MIL09040	MIL09040	MIL09040	MIL090405	MIL09040	MIL09040	MIL090405	NWA6077	NWA6077	NWA6077	NWA6077	NWA6077	NWA6077	NWA6077	NWA6077	NWA6077	NWA6077	NWA6077	NWA6077	NWA6077	NWA6077	NWA6077
				Mean	St. Dev.	el. St. Dev.															
24	25	26	27				9	11	15	17	19	24	25	28	40	41	42	43	44	45	46	47	48
53.54	53.61	53.63	53.54	53.59	0.22	0%	53.49	53.41	53.83	53.08	53.49	52.55	52.93	52.72	53.60	53.03	53.51	53.61	53.76	53.77	53.54	53.34	53.38
0.31	0.32	0.30	0.28	0.30	0.02	6%	0.21	0.21	0.21	0.20	0.19	0.22	0.19	0.20	0.19	0.20	0.19	0.24	0.19	0.21	0.21	0.23	0.22
0.71	0.74	0.64	0.61	0.65	0.04	7%	0.64	0.67	0.65	0.61	0.61	0.70	0.57	0.62	0.63	0.67	0.68	0.78	0.75	0.67	0.86	0.64	0.78
0.92	0.90	0.73	0.71	0.78	0.07	9%	0.67	0.75	0.69	0.69	0.68	0.72	0.66	0.67	0.70	0.73	0.70	0.81	0.78	0.72	0.83	0.71	0.78
6.93	6.55	6.50	6.63	6.57	0.18	3%	5.83	5.87	6.55	5.98	6.38	5.91	6.05	6.11	5.81	5.85	5.66	5.87	6.03	6.22	6.23	6.02	5.98
0.22	0.20	0.21	0.22	0.20	0.02	9%	0.13	0.13	0.12	0.14	0.13	0.12	0.12	0.13	0.13	0.11	0.12	0.14	0.14	0.13	0.14	0.13	0.15
15.75	15.74	15.98	15.90	15.87	0.10	1%	16.74	16.62	16.71	16.80	16.84	16.75	16.78	16.59	16.61	16.83	16.85	16.73	16.85	16.56	16.79	16.76	16.59
20.64	20.62	21.18	21.22	21.13	0.25	1%	21.52	21.39	21.55	21.50	21.61	21.39	21.62	21.64	21.59	21.27	21.66	21.11	21.33	21.56	20.91	21.58	21.28
0.53	0.56	0.51	0.46	0.51	0.04	8%	0.45	0.45	0.49	0.46	0.41	0.48	0.41	0.42	0.47	0.49	0.46	0.52	0.46	0.44	0.54	0.43	0.55
0.00	0.00	0.00	0.00	0.00	0.00	123%	0.01	0.00	0.01	0.00	0.00	0.01	0.01	0.00	0.01	0.00	0.00	0.00	0.00	0.01	0.01	0.01	0.00
99.54	99.23	99.67	99.56	99.59	0.33	0%	99.68	99.51	100.80	99.45	100.34	98.84	99.33	99.11	99.72	99.18	99.82	99.82	100.28	100.29	100.06	99.85	99.71
1.983	1.988	1.981	1.981	1.982	0.004	0%	1.967	1.968	1.960	1.955	1.956	1.947	1.953	1.951	1.971	1.957	1.963	1.968	1.965	1.969	1.962	1.959	1.962
0.009	0.009	0.008	0.008	0.008	0.001	6%	0.006	0.006	0.006	0.005	0.005	0.006	0.005	0.006	0.005	0.005	0.005	0.006	0.005	0.006	0.006	0.006	0.006
0.031	0.032	0.028	0.027	0.028	0.002	7%	0.028	0.029	0.028	0.026	0.026	0.031	0.025	0.027	0.027	0.029	0.029	0.034	0.032	0.029	0.037	0.028	0.034
0.027	0.026	0.021	0.021	0.023	0.002	9%	0.019	0.022	0.020	0.020	0.020	0.021	0.019	0.019	0.020	0.021	0.020	0.024	0.023	0.021	0.024	0.021	0.023
0.215	0.203	0.192	0.198	0.196	0.009	5%	0.139	0.148	0.144	0.119	0.134	0.106	0.118	0.120	0.144	0.121	0.126	0.151	0.147	0.157	0.148	0.132	0.138
0.000	0.000	0.008	0.008	0.007	0.007	96%	0.040	0.033	0.055	0.065	0.061	0.077	0.068	0.070	0.035	0.059	0.047	0.030	0.037	0.033	0.043	0.053	0.046
0.007	0.006	0.007	0.007	0.006	0.001	9%	0.004	0.004	0.004	0.004	0.004	0.004	0.004	0.004	0.004	0.003	0.004	0.004	0.004	0.004	0.004	0.004	0.005
0.870	0.870	0.880	0.877	0.875	0.006	1%	0.917	0.913	0.907	0.923	0.918	0.925	0.923	0.915	0.910	0.926	0.921	0.916	0.918	0.904	0.917	0.918	0.909
0.819	0.819	0.838	0.841	0.837	0.009	1%	0.848	0.845	0.841	0.849	0.847	0.849	0.855	0.858	0.850	0.841	0.851	0.830	0.835	0.846	0.821	0.849	0.838
0.038	0.040	0.036	0.033	0.036	0.003	8%	0.032	0.032	0.035	0.033	0.029	0.034	0.029	0.030	0.034	0.035	0.032	0.037	0.033	0.031	0.038	0.031	0.039
0.000	0.000	0.000	0.000	0.000	0.000	123%	0.000	0.000	0.000	0.000	0.000	0.000	0.001	0.000	0.000	0.000	0.000	0.000	0.000	0.000	0.000	0.001	0.000
3.998	3.994	4.000	4.000	3.999	0.002	0%	4.000	4.000	4.000	4.000	4.000	4.000	4.000	4.000	4.000	4.000	4.000	4.000	4.000	4.000	4.000	4.000	4.000
42.9	43.2	43.5	43.6	43.6	0.3	1%	43.5	43.5	43.1	43.3	43.1	43.3	43.4	43.6	43.8	43.1	43.7	43.0	43.0	43.5	42.5	43.4	43.3
45.5	45.8	45.7	45.4	45.5	0.2	1%	47.1	47.0	46.5	47.1	46.7	47.2	46.9	46.5	46.8	47.5	47.2	47.4	47.3	46.5	47.4	46.9	47.0
11.6	11.0	10.8	11.0	10.9	0.3	3%	9.4	9.5	10.4	9.6	10.1	9.5	9.7	9.8	9.4	9.4	9.1	9.6	9.7	10.0	10.1	9.7	9.7
80.2	81.1	81.4	81.0	81.160	0.461	1%	83.7	83.5	82.0	83.4	82.5	83.5	83.2	82.9	83.6	83.7	84.1	83.5	83.3	82.6	82.8	83.2	83.2

NWA6077	NWA6077	NWA6077	NWA6077	NWA6077	NWA6077	NWA6077	NWA6077	NWA6077	NWA5363	NWA5363	NWA5363	NWA5363	NWA5363	NWA5363	NWA5363	NWA5363	NWA5363	NWA5363	NWA5363	NWA5363	NWA5363
						Mean	St. Dev.	Rel. St. Dev.													
				13	36																
49	50	51	52						20	21	22	24	25	26	27	28	29	30	31	32	33
53.66	53.46	53.47	53.37	53.47	53.92	53.41	0.34	1%	53.68	53.73	53.93	52.97	52.18	53.17	53.65	54.55	53.88	54.02	54.43	54.30	54.40
0.18	0.23	0.22	0.20	0.22	0.21	0.21	0.02	8%	0.18	0.22	0.23	0.21	0.22	0.26	0.21	0.20	0.23	0.22	0.23	0.23	0.25
0.68	0.68	0.74	0.66	0.68	0.69	0.68	0.07	10%	0.66	0.72	0.79	0.78	0.77	0.79	0.77	0.67	0.76	0.83	0.73	0.74	0.71
0.71	0.73	0.76	0.73	0.74	0.74	0.73	0.05	6%	0.78	0.81	0.85	0.85	0.81	0.83	0.82	0.76	0.81	0.85	0.76	0.78	0.73
6.02	6.04	5.75	5.96	6.03	5.89	6.00	0.20	3%	6.04	6.36	6.05	6.51	6.29	6.11	6.46	6.18	6.16	6.14	5.65	6.30	5.98
0.13	0.13	0.13	0.12	0.14	0.13	0.13	0.01	7%	0.21	0.20	0.23	0.20	0.24	0.23	0.28	0.21	0.25	0.23	0.21	0.20	0.25
16.82	16.81	16.89	16.83	16.74	16.39	16.73	0.12	1%	15.81	15.82	15.67	15.85	15.81	15.95	15.99	15.77	15.80	15.82	15.69	15.70	15.93
21.58	21.36	21.34	21.61	21.44	21.45	21.45	0.19	1%	21.21	21.20	20.97	20.50	20.61	20.73	20.63	21.51	20.97	20.81	21.19	21.07	21.48
0.48	0.49	0.49	0.48	0.39	0.40	0.46	0.04	9%	0.45	0.47	0.45	0.47	0.45	0.52	0.45	0.43	0.48	0.47	0.48	0.45	0.43
0.01	0.00	0.01	0.00	0.01	0.00	0.00	0.00	96%	0.01	0.00	0.00	0.00	0.00	0.01	0.01	0.00	0.00	0.00	0.00	0.00	0.00
100.25	99.92	99.81	99.96	99.86	99.83	99.80	0.44	0%	99.01	99.55	99.16	98.33	97.38	98.59	99.27	100.28	99.34	99.39	99.37	99.78	100.16
1.961	1.961	1.961	1.956	1.964	1.983	1.962	0.008	0%	1.992	1.987	1.996	1.983	1.971	1.983	1.987	1.998	1.992	1.994	2.005	1.998	1.994
0.005	0.006	0.006	0.006	0.006	0.006	0.006	0.000	8%	0.005	0.006	0.006	0.006	0.006	0.007	0.006	0.006	0.006	0.006	0.006	0.006	0.007
0.029	0.029	0.032	0.028	0.030	0.030	0.029	0.003	10%	0.029	0.032	0.035	0.034	0.034	0.035	0.033	0.029	0.033	0.036	0.032	0.032	0.031
0.020	0.021	0.022	0.021	0.022	0.022	0.021	0.001	6%	0.023	0.024	0.025	0.025	0.024	0.024	0.024	0.022	0.024	0.025	0.022	0.023	0.021
0.133	0.136	0.130	0.121	0.148	0.181	0.137	0.016	12%	0.187	0.197	0.187	0.204	0.178	0.190	0.200	0.189	0.191	0.190	0.174	0.194	0.183
0.052	0.050	0.046	0.061	0.037	0.000	0.048	0.017	35%	0.000	0.000	0.000	0.000	0.021	0.000	0.000	0.000	0.000	0.000	0.000	0.000	0.000
0.004	0.004	0.004	0.004	0.004	0.004	0.004	0.000	7%	0.007	0.006	0.007	0.006	0.008	0.007	0.009	0.006	0.008	0.007	0.006	0.006	0.008
0.917	0.919	0.924	0.919	0.917	0.899	0.916	0.007	1%	0.875	0.872	0.864	0.884	0.890	0.887	0.883	0.861	0.871	0.871	0.862	0.861	0.871
0.845	0.839	0.839	0.849	0.844	0.846	0.844	0.008	1%	0.844	0.840	0.832	0.822	0.834	0.828	0.819	0.844	0.831	0.823	0.836	0.831	0.844
0.034	0.035	0.035	0.034	0.028	0.028	0.033	0.003	9%	0.032	0.033	0.032	0.034	0.033	0.038	0.033	0.031	0.034	0.034	0.034	0.032	0.031
0.000	0.000	0.000	0.000	0.001	0.000	0.000	0.000	96%	0.000	0.000	0.000	0.000	0.000	0.001	0.000	0.000	0.000	0.000	0.000	0.000	0.000
4.000	4.000	4.000	4.000	4.000	3.999	4.000	0.000	0%	3.993	3.996	3.984	3.998	4.000	4.000	3.995	3.986	3.990	3.986	3.978	3.984	3.989
43.3	43.1	43.2	43.4	43.3	43.8	43.3	0.3	1%	44.1	43.9	44.0	42.9	43.2	43.3	42.9	44.4	43.7	43.5	44.5	43.9	44.3
47.0	47.2	47.5	47.0	47.0	46.6	47.0	0.3	1%	45.7	45.5	45.7	46.1	46.1	46.4	46.2	45.3	45.8	46.1	45.9	45.5	45.7
9.6	9.7	9.3	9.5	9.7	9.6	9.7	0.3	3%	10.1	10.6	10.3	11.0	10.7	10.3	10.9	10.3	10.4	10.4	9.6	10.6	10.0
83.3	83.2	84.0	83.4	83.2	83.2	83.250	0.476	1%	82.4	81.6	82.2	81.3	81.8	82.3	81.5	82.0	82.0	82.1	83.2	81.6	82.6

NWA5363	NWA5363	NWA5363	NWA5363	NWA5363	NWA5363	NWA5363	NWA5363	NWA5363				NWA11187	NWA11187	NWA11187	NWA11187	NWA11187	NWA11187	NWA11187	NWA11187	NWA11187	NWA11187
									Mean	St. Dev.	Rel. St. Dev.										
34	35	36	37	38	39							51	52	53	54	55	57	59	62	63	65
54.73	54.47	54.40	54.48	54.54	54.11	54.32	54.32	54.13	54.02	0.61	1%	54.80	55.19	55.35	55.49	55.40	54.86	55.36	54.16	54.83	53.06
0.22	0.20	0.21	0.20	0.22	0.21	0.23	0.22	0.24	0.22	0.02	7%	0.24	0.26	0.24	0.25	0.26	0.25	0.25	0.29	0.27	0.25
0.72	0.74	0.69	0.76	0.85	0.79	0.67	0.64	0.72	0.74	0.06	7%	0.85	0.83	0.85	0.85	0.81	0.84	0.85	0.84	0.88	0.83
0.77	0.81	0.69	0.84	0.87	0.89	0.74	0.71	0.79	0.80	0.05	7%	0.81	0.83	0.80	0.80	0.82	0.80	0.82	0.84	0.86	0.82
6.03	6.15	5.99	6.39	6.27	6.57	5.96	6.12	6.18	6.18	0.21	3%	2.04	1.92	1.91	1.91	2.17	2.03	2.05	2.11	2.10	1.91
0.22	0.25	0.20	0.24	0.22	0.23	0.13	0.13	0.14	0.21	0.04	18%	0.35	0.34	0.36	0.33	0.37	0.36	0.37	0.36	0.36	0.38
15.77	15.86	15.79	15.71	15.63	15.95	16.47	16.40	16.41	15.89	0.24	1%	22.12	22.07	21.88	21.96	21.96	21.78	21.96	21.80	21.94	22.25
21.29	21.03	21.50	20.94	20.85	20.61	21.56	21.55	21.47	21.08	0.34	2%	18.66	18.82	18.74	18.60	18.71	18.88	18.67	18.97	18.78	18.75
0.46	0.50	0.48	0.48	0.47	0.48	0.42	0.42	0.45	0.46	0.03	5%	0.15	0.18	0.19	0.18	0.19	0.19	0.19	0.15	0.18	0.20
0.00	0.00	0.00	0.01	0.00	0.00	0.00	0.00	0.00	0.00	0.00	106%	0.01	0.00	0.00	0.00	0.00	0.00	0.01	0.00	0.01	0.00
100.20	100.03	99.95	100.05	99.92	99.85	100.48	100.53	100.53	99.60	0.78	1%	100.03	100.43	100.33	100.35	100.71	99.98	100.53	99.51	100.20	98.45
2.003	1.998	1.998	2.000	2.002	1.992	1.985	1.986	1.979	1.992	0.009	0%	1.959	1.965	1.973	1.976	1.970	1.964	1.971	1.948	1.958	1.928
0.006	0.006	0.006	0.005	0.006	0.006	0.006	0.006	0.007	0.006	0.000	7%	0.006	0.007	0.006	0.007	0.007	0.007	0.007	0.008	0.007	0.007
0.031	0.032	0.030	0.033	0.037	0.034	0.029	0.028	0.031	0.032	0.003	8%	0.036	0.035	0.036	0.035	0.034	0.035	0.036	0.035	0.037	0.035
0.022	0.024	0.020	0.024	0.025	0.026	0.021	0.021	0.023	0.023	0.002	7%	0.023	0.023	0.023	0.023	0.023	0.023	0.023	0.024	0.024	0.024
0.185	0.189	0.184	0.196	0.192	0.202	0.182	0.187	0.181	0.189	0.008	4%	0.040	0.048	0.057	0.057	0.063	0.047	0.061	0.023	0.043	0.000
0.000	0.000	0.000	0.000	0.000	0.000	0.000	0.000	0.008	0.001	0.005	360%	0.021	0.009	0.000	0.000	0.002	0.014	0.000	0.040	0.020	0.058
0.007	0.008	0.006	0.007	0.007	0.007	0.004	0.004	0.004	0.007	0.001	18%	0.010	0.010	0.011	0.010	0.011	0.011	0.011	0.011	0.011	0.012
0.860	0.867	0.865	0.860	0.855	0.875	0.897	0.894	0.894	0.874	0.013	1%	1.178	1.172	1.163	1.165	1.164	1.162	1.165	1.169	1.168	1.205
0.835	0.827	0.846	0.823	0.820	0.813	0.844	0.844	0.841	0.833	0.010	1%	0.715	0.718	0.716	0.710	0.713	0.724	0.712	0.731	0.719	0.730
0.033	0.036	0.034	0.034	0.033	0.034	0.030	0.029	0.032	0.033	0.002	6%	0.011	0.012	0.013	0.012	0.013	0.013	0.013	0.011	0.012	0.014
0.000	0.000	0.000	0.000	0.000	0.000	0.000	0.000	0.000	0.000	0.000	107%	0.000	0.000	0.000	0.000	0.000	0.000	0.000	0.000	0.000	0.000
3.981	3.986	3.989	3.984	3.978	3.989	3.999	3.999	4.000	3.990	0.007	0%	4.000	4.000	3.998	3.995	4.000	4.000	4.000	4.000	4.000	4.013
44.2	43.7	44.5	43.6	43.8	42.8	43.8	43.7	43.6	43.7	0.5	1%	36.4	36.7	36.8	36.5	36.5	37.0	36.5	37.0	36.7	36.4
45.6	45.9	45.5	45.6	45.6	46.1	46.6	46.3	46.4	45.9	0.3	1%	60.0	59.9	59.7	60.0	59.6	59.4	59.8	59.2	59.6	60.1
10.1	10.4	10.0	10.8	10.6	11.0	9.6	9.9	10.0	10.4	0.4	4%	3.6	3.4	3.5	3.4	3.9	3.7	3.7	3.8	3.8	3.5
82.3	82.1	82.5	81.4	81.6	81.2	83.1	82.7	82.6	82.097	0.554	1%	95.1	95.3	95.3	95.4	94.7	95.0	95.0	94.9	94.9	95.4

NWA11187	NWA11187	NWA11187	NWA11187	NWA11187	NWA11187	NWA11187	NWA11187	NWA11187	NWA11187	NWA11187	NWA11187	NWA11187	NWA11187	NWA11187	NWA11187	NWA11187	NWA11187	NWA11187	NWA11187	NWA11187	NWA11187	NWA11187	NWA11187
																							Mean
66	68	70	71	74	76	78	79	84	87	90	91	94	95	97	99	101	102	103	104	105	106		
52.89	52.97	55.86	55.34	55.21	55.42	55.22	55.50	55.05	54.77	55.14	54.96	55.05	55.61	54.12	54.68	54.98	55.71	55.80	59.11	56.02	55.65		55.11
0.25	0.26	0.26	0.25	0.27	0.25	0.24	0.26	0.28	0.25	0.26	0.25	0.25	0.27	0.23	0.27	0.23	0.27	0.24	0.22	0.25	0.25		0.25
0.82	0.84	0.83	0.83	0.85	0.87	0.80	0.82	0.82	0.84	0.85	0.84	0.86	0.84	0.82	0.87	0.87	0.84	0.83	0.74	0.82	0.83		0.84
0.84	0.84	0.88	0.85	0.85	0.85	0.85	0.81	0.83	0.83	0.84	0.85	0.84	0.81	0.82	0.86	0.80	0.83	0.82	0.82	0.81	0.82		0.83
2.09	2.11	2.21	2.17	2.07	2.07	1.98	2.05	2.34	2.05	2.20	2.83	1.99	1.83	2.19	2.22	1.98	2.03	1.89	1.86	2.16	1.98		2.08
0.34	0.35	0.35	0.36	0.36	0.36	0.37	0.36	0.35	0.38	0.38	0.34	0.34	0.31	0.33	0.36	0.36	0.36	0.37	0.34	0.38	0.36		0.36
22.00	22.01	22.06	22.25	22.24	22.00	22.25	22.03	22.09	22.12	22.23	21.83	21.96	22.05	21.92	22.06	22.41	22.12	22.18	19.45	21.91	22.19		21.97
18.90	18.67	18.81	18.81	18.56	18.50	18.56	18.80	18.93	18.67	18.71	18.67	18.76	18.73	18.77	18.80	18.90	18.75	18.79	17.59	18.72	18.88		18.71
0.17	0.20	0.15	0.18	0.18	0.18	0.14	0.15	0.15	0.18	0.14	0.18	0.17	0.15	0.17	0.16	0.19	0.17	0.20	0.15	0.18	0.17		0.17
0.00	0.00	0.01	0.00	0.01	0.00	0.00	0.00	0.00	0.01	0.00	0.00	0.00	0.00	0.00	0.01	0.00	0.00	0.00	0.00	0.00	0.00		0.00
98.32	98.24	101.42	101.03	100.59	100.48	100.42	100.78	100.84	100.09	100.75	100.76	100.23	100.61	99.36	100.28	100.71	101.08	101.12	100.29	101.26	101.13		100.32
1.926	1.929	1.972	1.959	1.963	1.973	1.967	1.971	1.955	1.956	1.958	1.957	1.966	1.975	1.948	1.951	1.950	1.972	1.973	2.078	1.979	1.969		1.964
0.007	0.007	0.007	0.007	0.007	0.007	0.006	0.007	0.008	0.007	0.007	0.007	0.007	0.007	0.006	0.007	0.006	0.007	0.006	0.006	0.007	0.007		0.007
0.035	0.036	0.034	0.035	0.036	0.037	0.034	0.034	0.034	0.035	0.035	0.035	0.036	0.035	0.035	0.036	0.037	0.035	0.035	0.031	0.034	0.035		0.035
0.024	0.024	0.024	0.024	0.024	0.024	0.024	0.023	0.023	0.023	0.023	0.024	0.024	0.023	0.023	0.024	0.023	0.023	0.023	0.023	0.023	0.023		0.023
0.000	0.000	0.065	0.042	0.048	0.062	0.053	0.061	0.042	0.034	0.045	0.058	0.052	0.054	0.021	0.032	0.016	0.060	0.056	0.055	0.064	0.055		0.044
0.064	0.064	0.000	0.022	0.014	0.000	0.006	0.000	0.028	0.028	0.020	0.026	0.007	0.000	0.045	0.034	0.042	0.000	0.000	0.000	0.000	0.004		0.018
0.011	0.011	0.011	0.011	0.011	0.011	0.011	0.011	0.011	0.011	0.011	0.010	0.010	0.009	0.010	0.011	0.011	0.011	0.011	0.010	0.011	0.011		0.011
1.195	1.195	1.161	1.175	1.179	1.167	1.181	1.167	1.169	1.178	1.177	1.158	1.169	1.167	1.176	1.173	1.185	1.167	1.169	1.019	1.154	1.170		1.168
0.738	0.728	0.711	0.713	0.707	0.705	0.708	0.715	0.720	0.715	0.712	0.712	0.717	0.713	0.724	0.719	0.718	0.711	0.712	0.663	0.709	0.715		0.715
0.012	0.014	0.011	0.013	0.012	0.012	0.010	0.011	0.010	0.012	0.010	0.012	0.012	0.010	0.012	0.011	0.013	0.011	0.013	0.010	0.012	0.012		0.012
0.000	0.000	0.000	0.000	0.000	0.000	0.000	0.000	0.000	0.000	0.000	0.000	0.000	0.000	0.000	0.000	0.000	0.000	0.000	0.000	0.000	0.000		0.000
4.011	4.009	3.997	4.000	4.000	3.997	4.000	3.999	4.000	4.000	4.000	4.000	4.000	3.994	4.000	4.000	4.000	3.998	3.998	3.895	3.992	4.000		3.997
36.8	36.4	36.5	36.3	36.1	36.3	36.1	36.6	36.6	36.4	36.2	36.2	36.7	36.7	36.6	36.5	36.4	36.5	36.5	37.9	36.6	36.6		36.6
59.5	59.8	59.6	59.8	60.2	60.0	60.3	59.7	59.4	59.9	59.9	58.9	59.8	60.1	59.5	59.6	60.1	59.9	60.0	58.4	59.5	59.9		59.7
3.7	3.8	3.9	3.8	3.7	3.7	3.6	3.7	4.1	3.7	3.9	4.8	3.6	3.3	3.8	3.9	3.5	3.6	3.4	3.7	3.9	3.5		3.7
94.9	94.9	94.7	94.8	95.0	95.0	95.2	95.0	94.4	95.1	94.7	93.2	95.2	95.5	94.7	94.6	95.3	95.1	95.4	94.9	94.8	95.2		94.965

St. Dev.	Rel. St. Dev.
1.07	2%
0.01	6%
0.03	3%
0.02	2%
0.18	9%
0.02	4%
0.48	2%
0.23	1%
0.02	10%
0.00	139%
0.80	1%
0.025	1%
0.000	6%
0.001	3%
0.001	2%
0.019	43%
0.020	113%
0.000	4%
0.029	2%
0.012	2%
0.001	10%
0.000	138%
0.019	0%
0.3	1%
0.4	1%
0.3	7%
0.415	0%

Table S4 - Plagioclase

	nwa5363_plg_0	wa5363_plg_0	wa5363_plg_0	wa5363_plg_0	wa5363_plg_0	wa5363_plg_0	wa5363_plg_0	wa5363_plg_0	wa5363_plg_0	wa5363_plg_10	Mean	St. Dev.	Rel. St. Dev.
SiO2	62.84	62.85	62.76	63.78	62.83	63.19	63.14	63.10	63.13	62.99	63.06	0.30	0%
TiO2	0.04	0.04	0.03	0.06	0.05	0.04	0.06	0.03	0.03	0.04	0.04	0.01	28%
Al2O3	23.68	23.77	23.62	23.31	23.82	23.60	23.75	23.70	23.46	23.53	23.62	0.16	1%
FeO	0.11	0.15	0.21	0.19	0.15	0.23	0.17	0.13	0.15	0.10	0.16	0.04	27%
MnO	0.02	0.00	0.00	0.02	0.03	0.01	0.03	0.01	0.00	0.01	0.01	0.01	86%
MgO	0.02	0.02	0.02	0.02	0.04	0.03	0.03	0.02	0.01	0.02	0.02	0.01	37%
CaO	5.15	5.09	5.20	5.33	5.24	5.20	5.34	5.30	5.58	6.34	5.38	0.36	7%
Na2O	7.96	8.15	8.08	7.78	8.13	8.12	8.02	7.97	7.55	6.96	7.87	0.37	5%
K2O	0.28	0.28	0.27	0.38	0.25	0.35	0.26	0.26	0.29	0.26	0.29	0.04	15%
BaO(Mass%)	0.04	0.06	0.04	0.04	0.04	0.03	0.06	0.05	0.04	0.05	0.05	0.01	21%
SrO(Mass%)	0.07	0.04	0.04	0.07	0.04	0.06	0.07	0.05	0.02	0.00	0.05	0.02	48%
Total	100.22	100.44	100.28	100.98	100.61	100.85	100.93	100.62	100.27	100.29	100.547	0.294	0%
	(2) calcolo dei cationi per f.u. assumendo FeT=Fe2+												
Si	2.092	2.092	2.089	2.123	2.091	2.103	2.102	2.100	2.101	2.097	2.099	0.010	0%
Ti	0.001	0.001	0.001	0.002	0.001	0.001	0.002	0.001	0.001	0.001	0.001	0.000	27%
Al	1.232	1.235	1.230	1.204	1.236	1.222	1.229	1.229	1.219	1.223	1.226	0.010	1%
Cr	0.000	0.000	0.000	0.000	0.000	0.000	0.000	0.000	0.000	0.000	0.000	0.000	#DIV/0!
FeT	0.004	0.006	0.008	0.007	0.006	0.008	0.006	0.005	0.005	0.004	0.006	0.002	27%
Mn	0.001	0.000	0.000	0.001	0.001	0.000	0.001	0.000	0.000	0.000	0.001	0.000	86%
Ni	0.000	0.000	0.000	0.000	0.000	0.000	0.000	0.000	0.000	0.000	0.000	0.000	#DIV/0!
Mg	0.001	0.001	0.001	0.001	0.003	0.002	0.002	0.001	0.001	0.001	0.001	0.001	37%
Ca	0.244	0.241	0.246	0.250	0.247	0.245	0.251	0.250	0.264	0.299	0.254	0.017	7%
Na	0.682	0.697	0.692	0.661	0.694	0.692	0.682	0.680	0.646	0.595	0.672	0.031	5%
K	0.016	0.016	0.015	0.021	0.014	0.020	0.015	0.015	0.017	0.014	0.016	0.002	15%
NUMERAZIONE	1	1	1	1	1	1	1	1	1	1	1.000	0.000	0%
An	25.9	25.2	25.8	26.8	25.9	25.6	26.5	26.4	28.5	32.9	26.950	2.279	8%
Ab	72.4	73.1	72.6	70.9	72.6	72.4	72.0	72.0	69.7	65.5	71.320	2.270	3%
Or	1.7	1.6	1.6	2.3	1.5	2.1	1.5	1.6	1.8	1.6	1.730	0.267	15%
K+Na	0.697	0.712	0.707	0.682	0.708	0.712	0.697	0.694	0.662	0.609	0.688	0.032	5%

Table S5 - Phosphates

	NWA6077	NWA6077	NWA6077	NWA6077	NWA6077	NWA6077	NWA6077	NWA6077	NWA6077	NWA6077	NWA6077	NWA6077	NWA6077	NWA6077
Point	3	4	5	6	7	8	9	10	11	12	13	14	15	16
Comment	phop01	phop02	phop03	phop03r	phop06	phop06r	phop06r2	phop07c	phop07r	phop07r2	phop08c	phop08c2	phop08r	phop010c
SiO2	0.10	0.17	0.12	0.18	0.11	0.04	0.36	0.12	0.05	0.78	0.09	0.05	1.70	0.09
F	0.21	0.28	0.51	0.00	0.56	0.00	0.15	0.61	0.00	0.27	0.44	0.00	0.16	0.41
P2O5	35.32	41.02	41.84	45.31	41.21	46.50	39.69	41.18	46.68	29.03	41.77	46.78	30.17	42.03
SrO	0.05	0.12	0.03	0.00	0.00	0.00	0.02	0.04	0.00	0.00	0.00	0.03	0.04	0.00
Cl	4.12	6.63	5.52	0.02	5.81	0.01	0.01	6.22	0.01	0.09	6.18	0.02	0.24	6.02
SO3	0.07	0.08	0.04	0.10	0.03	0.04	0.58	0.14	0.04	5.91	0.07	0.06	1.12	0.22
FeO	0.98	1.31	0.43	1.89	0.39	1.37	19.13	0.40	1.35	52.62	0.18	1.24	46.90	1.21
CaO	40.26	52.19	52.74	45.96	52.45	47.07	32.07	52.76	47.65	0.26	52.42	46.71	2.65	51.93
Na2O	0.29	0.32	0.32	1.10	0.29	1.04	0.65	0.31	1.06	0.00	0.22	1.05	0.06	0.30
MgO	0.02	0.06	0.04	3.68	0.05	3.70	2.57	0.05	3.69	0.85	0.03	3.68	0.49	0.06
TOT	81.41	102.18	101.59	98.24	100.90	99.76	95.22	101.83	100.51	89.80	101.39	99.62	83.53	102.26
	Cl-apat	Cl-apat	Cl-apat	Merrill.	Cl-apat	Merrill.	Fe-phop	Cl-apat	Merrill.	Fe-phop	Cl-apat	Merrill.	Fe-phop	Cl-apat

NWA6077 17	NWA6077 Min	NWA6077 Max	NWA6077 Mean	NWA6077 St.Dev.	NWA6077 Rel. St. Dev.	NWA5363 7	NWA5363 8	NWA5363 9	NWA5363 10	NWA5363 11	NWA5363 12
phop010r						nwa5363_apat	a5363_apat	a5363_apat	a 5363_apat	a5363_apat	a5363_apat_ 06
1.93	0.04	1.93	0.39	0.61	155%	3.02	5.86	0.12	1.13	0.12	0.11
0.22	0.00	0.61	0.25	0.21	83%	0.15	0.26	0.35	0.12	0.54	0.52
28.62	28.62	46.78	39.81	6.23	16%	26.92	25.81	41.59	28.01	42.31	41.67
0.00	0.00	0.12	0.02	0.03	148%	0.01	0.01	0.04	0.03	0.00	0.01
0.01	0.01	6.63	2.73	3.01	110%	0.08	0.08	6.10	0.06	5.90	5.94
0.83	0.03	5.91	0.62	1.50	242%	0.98	0.92	0.10	0.88	0.10	0.06
48.46	0.18	52.62	11.86	19.98	168%						
0.20	0.20	52.76	38.49	20.18	52%	0.92	0.98	52.60	0.56	51.62	52.17
0.11	0.00	1.10	0.48	0.39	83%	0.05	0.05	0.27	0.07	0.26	0.31
0.29	0.02	3.70	1.28	1.63	127%	0.24	0.19	0.03	0.15	0.06	0.05
80.67	80.67	102.26	95.93	7.98	8%	32.37	34.15	101.20	31.01	100.90	100.85
Fe-phop						??	??	Cl-Apat.	??	Cl-Apat.	Cl-Apat.

NWA5363	NWA5363	NWA5363	NWA5363	NWA5363
Min	Max	Mean	St.Dev.	Rel. St. Dev.
0.11	5.86	1.73	2.32	134%
0.12	0.54	0.32	0.18	55%
25.81	42.31	34.38	8.22	24%
0.00	0.04	0.02	0.01	84%
0.06	6.10	3.03	3.24	107%
0.06	0.98	0.51	0.46	91%
0.56	52.60	26.47	28.11	106%
0.05	0.31	0.17	0.12	73%
0.03	0.24	0.12	0.08	71%
31.01	101.20	66.75	37.52	56%

Table S6 - Spinels

	MIL090206	MIL090206	MIL090206	MIL090206	MIL090206	MIL090206	MIL090206	MIL090206	MIL090206	MIL090206	MIL090206	MIL090206	MIL090206
Point	7	8	9	10	11	12	13	14	15	16	Mean	St.Dev.	Rel. St. Dev.
Comment	chr01	chr02_01	chr02_02	chr02_03	chr02_04	chr02_05	chr02_06	chr02_07	chr03	chr04			
SiO_2	0.00	0.00	0.00	0.00	0.00	0.00	0.00	0.00	0.00	0.00	0.00	0.00	#DIV/0!
TiO_2	0.72	2.48	2.52	2.41	2.52	2.35	2.43	2.09	1.72	2.33	2.16	0.56	26%
Al_2O_3	0.10	6.55	6.55	6.47	6.54	6.58	6.66	6.85	5.93	6.50	5.87	2.04	35%
V_2O_3	0.73	0.72	0.70	0.77	0.61	0.65	0.64	0.67	0.51	0.60	0.66	0.07	11%
Cr_2O_3	63.63	52.01	51.98	51.28	52.40	50.75	50.78	50.27	51.67	49.78	52.46	4.01	8%
FeO	27.05	27.47	27.19	26.99	27.23	28.08	28.00	29.09	28.88	29.49	27.95	0.92	3%
MnO	0.33	0.25	0.26	0.23	0.31	0.26	0.29	0.27	0.24	0.33	0.28	0.04	13%
NiO	0.00	0.00	0.00	0.06	0.01	0.04	0.09	0.06	0.00	0.00	0.02	0.03	133%
MgO	2.85	4.73	4.54	4.62	4.58	4.32	4.03	3.56	3.30	3.29	3.98	0.68	17%
CaO	0.03	0.00	0.00	0.01	0.00	0.00	0.00	0.01	0.01	0.01	0.01	0.01	132%
ZnO	0.00	0.09	0.07	0.04	0.00	0.00	0.00	0.01	0.05	0.01	0.03	0.03	130%
CoO	0.02	0.04	0.05	0.09	0.04	0.04	0.05	0.06	0.04	0.06	0.05	0.02	44%
CuO	0.00	0.00	0.13	0.06	0.19	0.14	0.11	0.15	0.00	0.03	0.08	0.07	89%
TOT	95.46	94.34	93.99	93.04	94.42	93.21	93.07	93.07	92.35	92.42	93.54	0.99	1%
Tot cat.	24.05	24.14	24.11	24.14	24.11	24.19	24.15	24.21	24.20	24.20	24.15	0.05	0%
#Fe	0.84	0.77	0.77	0.77	0.77	0.78	0.80	0.82	0.83	0.83	0.80	0.03	4%
#Cr	0.82	0.84	0.84	0.84	0.84	0.84	0.84	0.83	0.85	0.84	0.84	0.01	1%
#Mg	0.16	0.23	0.23	0.23	0.23	0.22	0.20	0.18	0.17	0.17	0.20	0.03	15%
Mg/Fe	0.19	0.31	0.30	0.31	0.30	0.27	0.26	0.22	0.20	0.20	0.25	0.05	19%
Al (atomic)	0.06	3.47	3.47	3.43	3.46	3.48	3.53	3.62	3.14	3.44	3.11	1.08	35%
V (atomic)	0.41	0.40	0.39	0.43	0.34	0.37	0.36	0.37	0.29	0.34	0.37	0.04	11%
Cr (atomic)	43.53	35.59	35.56	35.08	35.85	34.72	34.74	34.39	35.35	34.06	35.89	2.75	8%
x100/(Cr+A	0.94	1.03	1.00	1.12	0.86	0.96	0.94	0.98	0.75	0.90	0.95	0.10	11%
Ti (apfu)	0.17	0.55	0.56	0.54	0.56	0.53	0.55	0.48	0.40	0.54	0.49	0.12	25%
Al (apfu)	0.04	2.28	2.29	2.29	2.28	2.33	2.36	2.44	2.14	2.34	2.08	0.72	35%
V (apfu)	0.18	0.17	0.17	0.19	0.14	0.16	0.15	0.16	0.13	0.15	0.16	0.02	11%
Cr (apfu)	15.36	12.16	12.20	12.16	12.25	12.06	12.08	12.02	12.53	12.03	12.49	1.02	8%
Fe (apfu)	6.91	6.79	6.75	6.77	6.73	7.06	7.05	7.36	7.41	7.54	7.04	0.30	4%
Mn (apfu)	0.09	0.06	0.07	0.06	0.08	0.07	0.07	0.07	0.06	0.08	0.07	0.01	14%
Ni (apfu)	0.00	0.00	0.00	0.03	0.00	0.02	0.04	0.03	0.00	0.00	0.01	0.01	133%
Mg (apfu)	1.30	2.09	2.01	2.07	2.02	1.94	1.81	1.60	1.51	1.50	1.78	0.28	16%
Ca (apfu)	0.01	0.00	0.00	0.00	0.00	0.00	0.00	0.00	0.00	0.00	0.00	0.00	133%

MIL090405 7	MIL090405 8	MIL090405 9	MIL090405 10	MIL090405 11	MIL090405 12	MIL090405 13	MIL090405 14	MIL090405 15	MIL090405 Mean	MIL090405 St.Dev.	MIL090405 Rel. St. Dev.	NWA6077 7	NWA6077 8
chr01	chr02	chr03	chr04c	chr04rim	chr05	chr06	chr07	chr08				chr01c	chr01r
0.00	0.00	0.00	0.00	1.86	0.00	0.00	0.00	0.00	0.21	0.62	300%	0.00	0.00
2.27	0.75	2.28	2.40	2.03	2.26	2.26	0.94	2.29	1.94	0.63	33%	1.49	1.42
6.70	0.25	6.55	6.38	4.30	6.63	6.27	0.43	6.57	4.90	2.69	55%	7.61	7.42
53.35	63.76	53.53	52.92	52.20	53.94	52.42	61.33	52.17	55.07	4.32	8%	0.67	0.64
0.63	0.80	0.61	0.66	0.64	0.61	0.59	0.83	0.65	0.67	0.09	13%	55.78	55.65
29.66	28.39	29.88	30.28	30.33	30.16	29.86	29.31	29.24	29.68	0.62	2%	26.80	27.24
0.31	0.26	0.28	0.32	0.31	0.26	0.29	0.29	0.31	0.29	0.02	8%	0.16	0.20
0.04	0.01	0.10	0.00	0.01	0.00	0.02	0.00	0.00	0.02	0.03	166%	0.04	0.00
3.52	2.85	3.16	3.02	4.83	3.53	3.21	2.37	3.47	3.33	0.67	20%	4.66	4.18
0.00	0.00	0.01	0.02	0.00	0.01	0.00	0.01	0.01	0.01	0.01	92%	0.01	0.02
0.00	0.02	0.00	0.04	0.07	0.00	0.06	0.06	0.00	0.03	0.03	106%	0.36	0.13
0.03	0.00	0.01	0.01	0.09	0.04	0.02	0.02	0.04	0.03	0.03	97%	0.00	0.00
0.00	0.00	0.01	0.07	0.00	0.13	0.08	0.00	0.00	0.03	0.05	153%	0.00	0.00
96.51	97.09	96.42	96.11	96.66	97.58	95.08	95.57	94.74	96.19	0.92	1%	97.56	96.89
24.12	24.11	24.10	24.12	24.20	24.14	24.16	24.16	24.13	24.14	0.03	0%	24.06	24.04
0.83	0.85	0.84	0.85	0.78	0.83	0.84	0.87	0.83	0.83	0.03	3%	0.76	0.79
0.84	0.99	0.85	0.85	0.89	0.85	0.85	0.99	0.84	0.88	0.06	7%	0.83	0.83
0.17	0.15	0.16	0.15	0.22	0.17	0.16	0.13	0.17	0.17	0.03	16%	0.24	0.21
0.21	0.18	0.19	0.18	0.28	0.21	0.19	0.14	0.21	0.20	0.04	19%		
3.54	0.13	3.47	3.38	2.28	3.51	3.32	0.23	3.48	2.59	1.42	55%	4.03	3.93
0.35	0.45	0.34	0.37	0.36	0.34	0.33	0.46	0.36	0.37	0.05	13%	0.38	0.36
36.50	43.62	36.62	36.20	35.71	36.91	35.86	41.96	35.69	37.68	2.96	8%	38.16	38.07
0.88	1.02	0.85	0.94	0.94	0.85	0.85	1.10	0.93	0.93	0.09	9%	0.89	0.85
0.50	0.17	0.50	0.53	0.44	0.49	0.51	0.22	0.51	0.43	0.14	32%	0.32	0.31
2.30	0.09	2.26	2.22	1.47	2.26	2.20	0.15	2.30	1.70	0.93	55%	2.55	2.51
12.31	15.16	12.39	12.32	12.00	12.33	12.34	14.88	12.26	12.89	1.22	9%	0.15	0.15
0.15	0.19	0.14	0.16	0.15	0.14	0.14	0.20	0.16	0.16	0.02	15%	12.55	12.65
7.24	7.14	7.31	7.46	7.38	7.29	7.43	7.52	7.27	7.34	0.12	2%	6.38	6.55
0.08	0.07	0.07	0.08	0.08	0.06	0.07	0.08	0.08	0.07	0.01	8%	0.04	0.05
0.02	0.00	0.04	0.00	0.00	0.00	0.01	0.00	0.00	0.01	0.01	165%	0.01	0.00
1.53	1.28	1.38	1.33	2.09	1.52	1.43	1.09	1.54	1.46	0.28	19%	1.98	1.79
0.00	0.00	0.00	0.01	0.00	0.00	0.00	0.00	0.00	0.00	0.00	91%	0.00	0.01

NWA6077 9	NWA6077 10	NWA6077 11	NWA6077 12	NWA6077 13	NWA6077 14	NWA6077 15	NWA6077 16	NWA6077 17	NWA6077 18	NWA6077 19	NWA6077 20	NWA6077 21	NWA6077 22	NWA6077 23	NWA6077 24
chr02	chr03c	chr03r	chr04c	chr04r	chr05c	chr06c	chr06r	chr07c	chr08	chr09	chr10c	chr10r	chr11c	chr12c	chr13c
0.00	0.00	0.00	0.00	0.00	0.00	0.00	0.00	0.00	0.00	0.00	0.00	0.00	0.00	0.00	0.00
1.44	1.46	1.41	1.45	1.43	1.42	1.43	1.40	1.42	1.41	1.44	1.41	1.43	1.46	1.51	1.43
7.58	7.73	7.56	7.59	7.86	7.64	7.60	7.67	7.65	7.55	7.52	7.66	7.56	7.60	7.52	7.41
0.69	0.70	0.68	0.68	0.71	0.65	0.66	0.70	0.68	0.67	0.68	0.64	0.69	0.71	0.69	0.69
56.18	55.91	55.56	56.70	56.10	55.28	55.29	55.39	56.79	56.38	55.97	55.46	55.65	56.13	55.27	55.42
27.30	27.52	27.92	26.26	26.44	27.31	26.89	27.95	28.25	27.92	27.81	27.78	28.35	27.84	27.44	27.37
0.17	0.18	0.21	0.17	0.18	0.21	0.15	0.21	0.22	0.20	0.17	0.19	0.19	0.19	0.22	0.20
0.00	0.03	0.00	0.00	0.01	0.00	0.02	0.00	0.02	0.00	0.02	0.04	0.05	0.00	0.02	0.02
4.48	4.35	3.97	5.10	4.86	4.34	4.70	4.11	4.09	4.35	4.26	4.64	4.08	4.30	4.33	4.72
0.00	0.00	0.00	0.00	0.05	0.01	0.00	0.00	0.02	0.02	0.01	0.03	0.01	0.01	0.02	0.02
0.13	0.17	0.03	0.10	0.11	0.18	0.14	0.08	0.11	0.06	0.07	0.13	0.08	0.09	0.09	0.05
0.00	0.00	0.00	0.00	0.00	0.00	0.00	0.00	0.00	0.00	0.00	0.00	0.00	0.00	0.00	0.00
0.00	0.00	0.00	0.00	0.00	0.00	0.00	0.00	0.00	0.00	0.00	0.00	0.00	0.00	0.00	0.00
97.97	98.05	97.35	98.05	97.74	97.02	96.88	97.50	99.26	98.56	97.94	97.98	98.08	98.32	97.10	97.32
24.05	24.05	24.05	24.03	24.03	24.06	24.07	24.07	24.05	24.07	24.06	24.12	24.09	24.06	24.06	24.11
0.77	0.78	0.80	0.74	0.75	0.78	0.76	0.79	0.79	0.78	0.79	0.77	0.80	0.78	0.78	0.76
0.83	0.83	0.83	0.83	0.83	0.83	0.83	0.83	0.83	0.83	0.83	0.83	0.83	0.83	0.83	0.83
0.23	0.22	0.20	0.26	0.25	0.22	0.24	0.21	0.21	0.22	0.21	0.23	0.20	0.22	0.22	0.24
4.01	4.09	4.00	4.02	4.16	4.05	4.02	4.06	4.05	4.00	3.98	4.05	4.00	4.02	3.98	3.92
0.38	0.39	0.38	0.38	0.39	0.36	0.37	0.39	0.38	0.37	0.38	0.36	0.38	0.39	0.39	0.38
38.44	38.25	38.01	38.79	38.38	37.82	37.83	37.90	38.86	38.57	38.29	37.94	38.08	38.40	37.81	37.92
0.91	0.92	0.91	0.88	0.93	0.86	0.88	0.93	0.88	0.88	0.89	0.85	0.91	0.93	0.93	0.92
0.31	0.31	0.30	0.31	0.30	0.31	0.31	0.30	0.30	0.30	0.31	0.30	0.31	0.31	0.33	0.31
2.54	2.58	2.55	2.52	2.62	2.58	2.56	2.58	2.53	2.51	2.52	2.56	2.53	2.54	2.54	2.50
0.16	0.16	0.16	0.15	0.16	0.15	0.15	0.16	0.15	0.15	0.15	0.15	0.16	0.16	0.16	0.16
12.60	12.54	12.59	12.65	12.55	12.52	12.51	12.51	12.60	12.58	12.59	12.45	12.52	12.57	12.53	12.52
6.48	6.53	6.69	6.19	6.26	6.54	6.43	6.67	6.63	6.59	6.62	6.60	6.75	6.60	6.58	6.54
0.04	0.04	0.05	0.04	0.04	0.05	0.04	0.05	0.05	0.05	0.04	0.05	0.05	0.05	0.05	0.05
0.00	0.01	0.00	0.00	0.00	0.00	0.01	0.00	0.01	0.00	0.01	0.02	0.02	0.00	0.01	0.01
1.89	1.84	1.70	2.15	2.05	1.85	2.01	1.75	1.71	1.83	1.81	1.97	1.73	1.82	1.85	2.01
0.00	0.00	0.00	0.00	0.02	0.00	0.00	0.00	0.01	0.01	0.00	0.01	0.00	0.00	0.01	0.01

NWA6077	NWA6077	NWA6077	NWA6077	NWA6077	NWA6077	NWA6077	NWA6077	NWA5363	NWA5363	NWA5363	NWA5363	NWA5363	NWA5363
25	26	27	28	29	Mean	St.Dev.	Rel. St. Dev.	20	21	22	23	24	25
chr13r	chr15r	chr16c	chr16r	chr17r				chr_01	chr_02	chr_03	chr_04	chr_05	chr_06
0.00	0.00	0.00	0.00	0.00	0.00	0.00	#DIV/0!	0.00	0.00	0.00	0.00	0.00	0.00
1.37	1.44	1.46	1.43	1.40	1.43	0.03	2%	1.42	1.45	1.48	1.41	1.46	1.43
7.64	7.48	7.65	7.63	7.39	7.59	0.11	1%	7.93	7.91	7.83	7.84	7.83	7.67
0.64	0.69	0.60	0.67	0.66	0.67	0.03	4%	0.65	0.70	0.63	0.65	0.65	0.69
55.99	55.29	57.48	55.31	55.47	55.85	0.59	1%	55.90	56.65	57.03	55.43	56.03	55.57
28.50	28.61	26.64	27.96	28.64	27.60	0.67	2%	28.77	27.06	27.55	27.99	27.25	27.87
0.21	0.22	0.18	0.23	0.20	0.19	0.02	10%	0.21	0.16	0.16	0.18	0.21	0.19
0.02	0.06	0.02	0.00	0.01	0.02	0.02	111%	0.02	0.05	0.00	0.00	0.03	0.01
3.94	3.79	4.68	3.90	4.00	4.34	0.34	8%	3.58	3.99	4.18	3.75	3.93	3.99
0.02	0.01	0.02	0.01	0.01	0.01	0.01	95%	0.01	0.02	0.01	0.03	0.01	0.01
0.06	0.07	0.07	0.10	0.08	0.11	0.04	35%	0.06	0.00	0.20	0.05	0.10	0.18
0.00	0.00	0.00	0.00	0.00	0.00	0.00	#DIV/0!	0.05	0.03	0.04	0.08	0.03	0.06
0.00	0.00	0.00	0.00	0.00	0.00	0.00	#DIV/0!	0.04	0.00	0.00	0.00	0.00	0.10
98.39	97.68	98.79	97.23	97.85	97.80	0.63	1%	98.64	98.01	99.11	97.41	97.51	97.77
24.07	24.09	23.99	24.05	24.11	24.06	0.03	0%	24.04	23.95	24.00	24.03	23.98	24.06
0.80	0.81	0.76	0.80	0.80	0.78	0.02	2%	0.82	0.79	0.79	0.81	0.80	0.80
0.83	0.83	0.83	0.83	0.83	0.83	0.00	0%	0.83	0.83	0.83	0.83	0.83	0.83
0.20	0.19	0.24	0.20	0.20	0.22	0.02	8%	0.18	0.21	0.21	0.19	0.20	0.20
								0.22	0.26	0.27	0.24	0.26	0.25
4.05	3.96	4.05	4.04	3.91	4.02	0.06	1%	4.20	4.19	4.14	4.15	4.14	4.06
0.36	0.39	0.34	0.37	0.37	0.38	0.01	4%	0.36	0.39	0.35	0.36	0.36	0.39
38.30	37.83	39.32	37.84	37.95	38.21	0.40	1%	38.25	38.76	39.02	37.92	38.33	38.02
0.85	0.93	0.77	0.89	0.89	0.89	0.04	4%	0.85	0.91	0.81	0.86	0.85	0.92
0.29	0.31	0.31	0.31	0.30	0.31	0.01	2%	0.30	0.31	0.31	0.30	0.31	0.31
2.56	2.52	2.53	2.58	2.49	2.54	0.03	1%	2.65	2.64	2.59	2.65	2.63	2.58
0.15	0.16	0.13	0.15	0.15	0.15	0.01	4%	0.15	0.16	0.14	0.15	0.15	0.16
12.57	12.52	12.74	12.55	12.54	12.56	0.06	0%	12.52	12.68	12.65	12.54	12.63	12.54
6.77	6.85	6.25	6.71	6.85	6.57	0.18	3%	6.82	6.41	6.46	6.70	6.50	6.65
0.05	0.05	0.04	0.06	0.05	0.05	0.00	11%	0.05	0.04	0.04	0.04	0.05	0.05
0.01	0.03	0.01	0.00	0.00	0.01	0.01	111%	0.01	0.02	0.00	0.00	0.01	0.00
1.67	1.62	1.96	1.67	1.70	1.84	0.14	8%	1.51	1.69	1.75	1.60	1.67	1.70
0.01	0.00	0.01	0.00	0.00	0.00	0.00	94%	0.00	0.01	0.00	0.01	0.00	0.00

NWA5363	NWA5363	NWA5363	NWA5363	NWA5363	NWA5363	NWA5363	NWA5363	NWA5363	NWA5363	NWA5363	NWA5363	NWA5363
26	27	28	29	30	31	32	33	34	35	Mean	St.Dev.	Rel. St. Dev.
chr_07	chr_08	chr_09	chr_10	chr_11	chr12	chr13	chr14	chr15	chr16			
0.00	0.00	0.00	0.00	0.00	0.00	0.00	0.00	0.00	0.00	0.00	0.00	#DIV/0!
1.46	1.46	1.42	1.47	1.49	1.46	1.49	1.46	1.47	1.48	1.46	0.02	2%
7.63	7.77	7.72	7.83	7.75	7.87	7.70	7.84	7.85	7.80	7.80	0.08	1%
0.66	0.58	0.65	0.66	0.62	0.68	0.66	0.67	0.70	0.64	0.66	0.03	5%
55.96	56.18	56.33	56.03	56.37	56.12	55.30	55.87	56.37	55.88	56.06	0.44	1%
27.21	27.97	27.75	27.41	27.25	28.23	27.86	27.53	27.68	27.15	27.66	0.46	2%
0.18	0.17	0.18	0.21	0.15	0.21	0.18	0.20	0.18	0.17	0.18	0.02	11%
0.00	0.01	0.03	0.00	0.03	0.00	0.00	0.01	0.00	0.03	0.01	0.02	115%
4.16	3.71	3.92	3.94	4.31	3.74	4.21	4.16	4.27	4.41	4.02	0.24	6%
0.03	0.01	0.00	0.01	0.03	0.00	0.00	0.00	0.01	0.00	0.01	0.01	98%
0.12	0.10	0.15	0.05	0.24	0.05	0.09	0.11	0.11	0.21	0.11	0.07	58%
0.07	0.04	0.07	0.03	0.03	0.00	0.00	0.00	0.00	0.00	0.03	0.03	85%
0.00	0.06	0.00	0.03	0.02	0.00	0.00	0.00	0.00	0.00	0.02	0.03	184%
97.47	98.04	98.23	97.67	98.29	98.36	97.50	97.85	98.64	97.78	98.02	0.49	1%
24.02	24.00	24.01	23.99	24.02	24.01	24.06	24.02	24.03	24.03	24.02	0.03	0%
0.79	0.81	0.80	0.80	0.78	0.81	0.79	0.79	0.78	0.78	0.79	0.01	1%
0.83	0.83	0.83	0.83	0.83	0.83	0.83	0.83	0.83	0.83	0.83	0.00	0%
0.21	0.19	0.20	0.20	0.22	0.19	0.21	0.21	0.22	0.22	0.21	0.01	6%
0.27	0.24	0.25	0.26	0.28	0.24	0.27	0.27	0.27	0.29	0.26	0.02	7%
										#DIV/0!	#DIV/0!	#DIV/0!
4.04	4.11	4.09	4.14	4.10	4.17	4.08	4.15	4.15	4.13	4.13	0.04	1%
0.37	0.33	0.37	0.37	0.35	0.38	0.37	0.38	0.39	0.36	0.37	0.02	5%
38.29	38.44	38.54	38.34	38.57	38.40	37.84	38.23	38.57	38.23	38.36	0.30	1%
0.87	0.77	0.86	0.87	0.82	0.90	0.88	0.89	0.92	0.85	0.86	0.04	5%
0.31	0.31	0.30	0.31	0.32	0.31	0.32	0.31	0.31	0.32	0.31	0.00	2%
2.57	2.60	2.58	2.63	2.58	2.63	2.59	2.63	2.61	2.61	2.61	0.03	1%
0.15	0.13	0.15	0.15	0.14	0.15	0.15	0.15	0.16	0.15	0.15	0.01	5%
12.63	12.64	12.64	12.62	12.60	12.58	12.49	12.55	12.56	12.55	12.59	0.05	0%
6.49	6.65	6.58	6.53	6.44	6.69	6.65	6.54	6.52	6.45	6.57	0.11	2%
0.04	0.04	0.04	0.05	0.04	0.05	0.04	0.05	0.04	0.04	0.04	0.00	11%
0.00	0.00	0.01	0.00	0.01	0.00	0.00	0.00	0.00	0.01	0.01	0.01	115%
1.77	1.57	1.66	1.67	1.82	1.58	1.79	1.76	1.79	1.87	1.70	0.10	6%
0.01	0.00	0.00	0.00	0.01	0.00	0.00	0.00	0.00	0.00	0.00	0.00	98%

Trace Elements

In the following tables all the diagrams of trace elements for MIL090206, MIL090405, NWA6077, NWA5363 and NWA11187 are reported, organized for minerals.

Table S7, trace elements diagram of olivine for MIL090206, MIL090405, NWA6077, NWA5363 and NWA11187. a) Li diagram for olivine; b) Na diagram for olivine; c) Sc diagram for olivine; d) Ti diagram for olivine ; e) Mn diagram for olivine; f) Cu diagram for olivine; g) Mo diagram for olivine;

a)

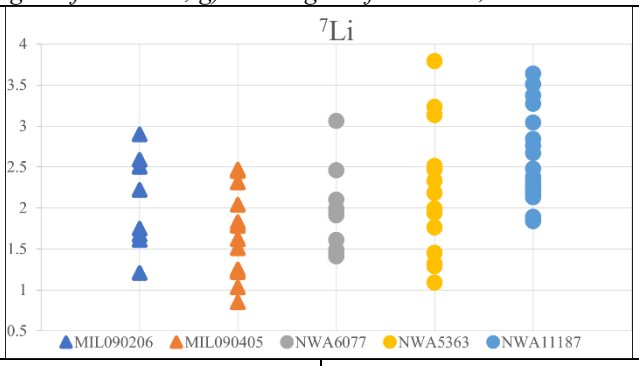

b)

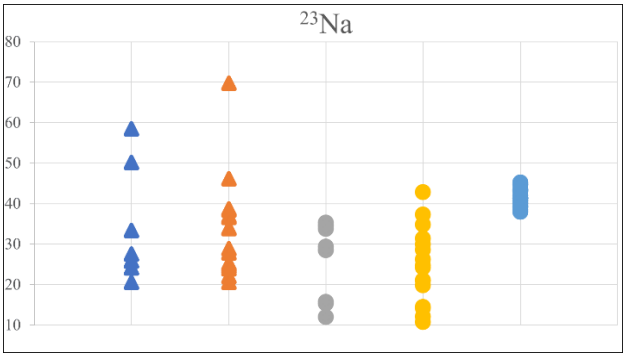

c)

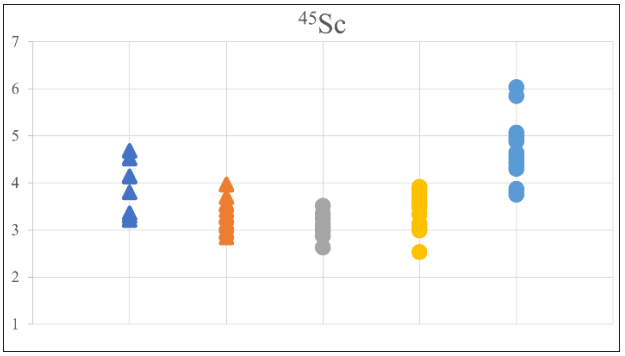

d)

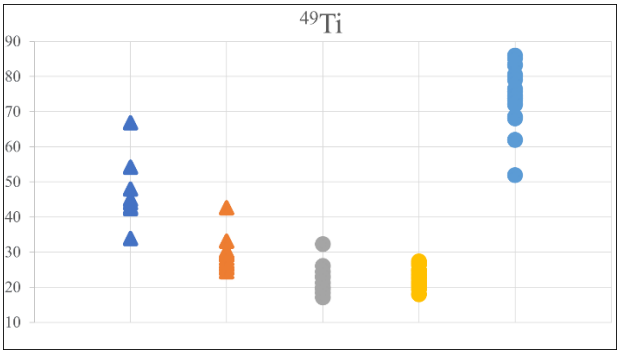

e)

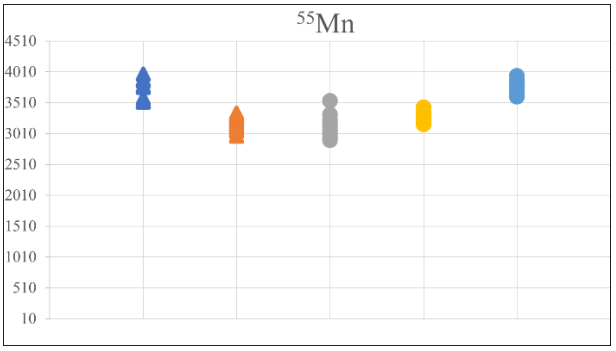

f)

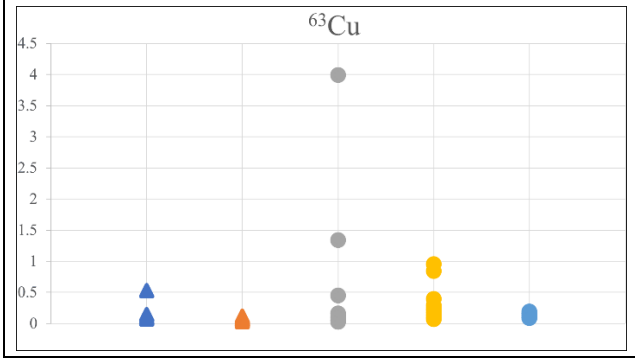

g)

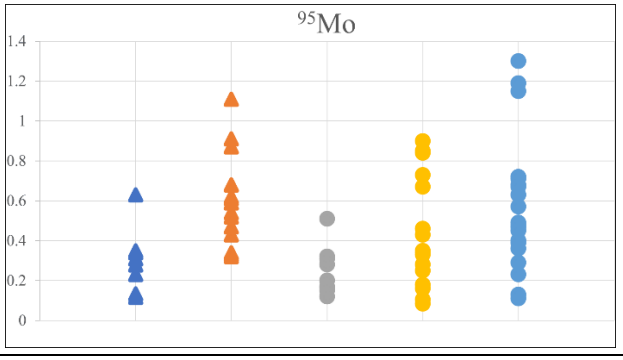

Table S8, trace elements diagram of orthopyroxene for MIL090206, MIL090405, NWA6077, NWA5363 and NWA11187. a) Na diagram for orthopyroxene; b) Ca diagram for orthopyroxene; c) Sc diagram for orthopyroxene; d) Cr diagram for orthopyroxene; e) Mn diagram for orthopyroxene; f) Zn diagram for orthopyroxene; g) Y diagram for orthopyroxene; h) Nb diagram for orthopyroxene.

a)

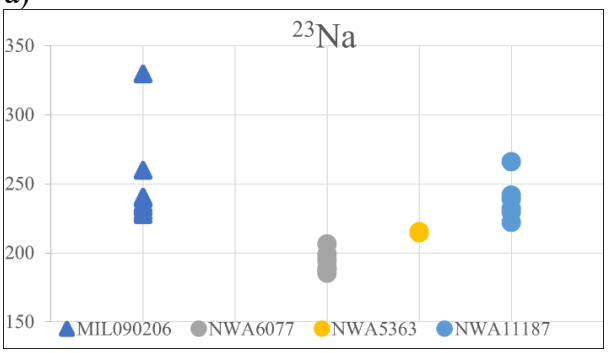

b)

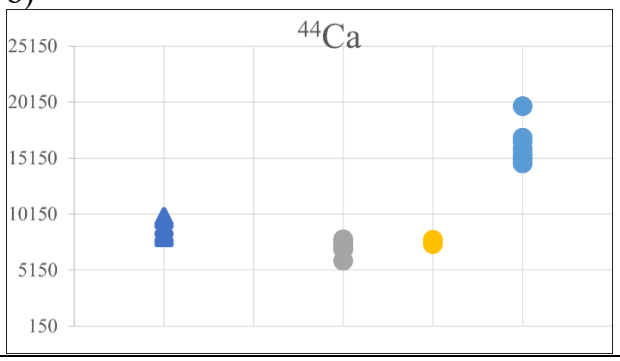

c)

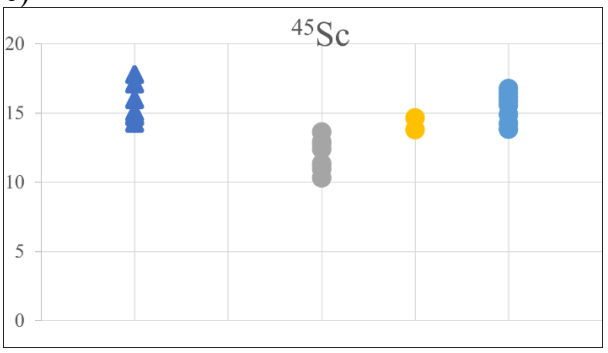

d)

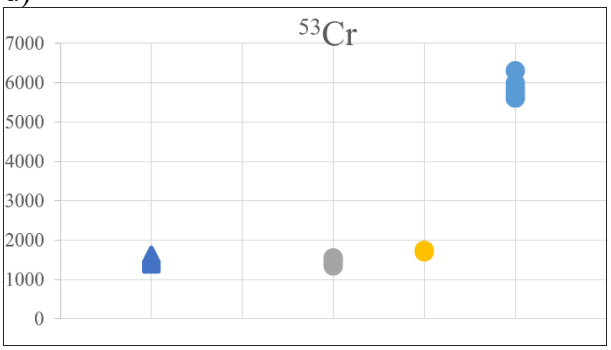

e)

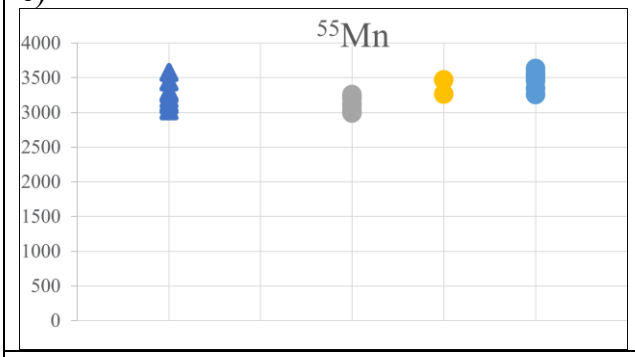

f)

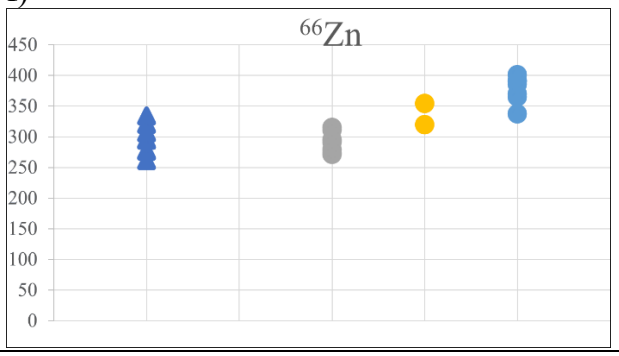

g)

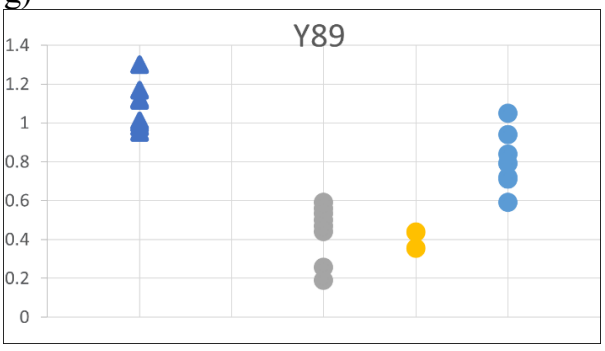

h)

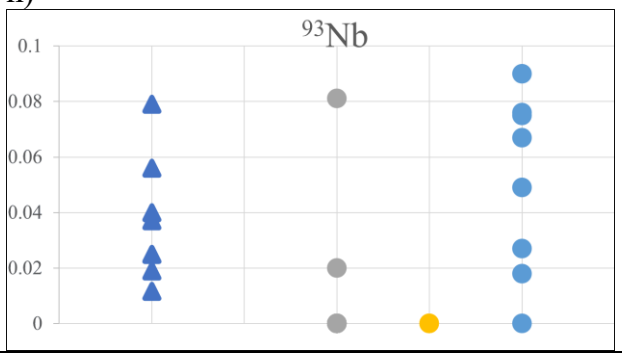

Table S9, trace elements diagram of clinopyroxene for MIL090206, MIL090405, NWA6077, NWA5363 and NWA11187. a) Na diagram for clinopyroxene; b) Al diagram for clinopyroxene; c) Ti diagram for clinopyroxene; d) Mn diagram for clinopyroxene; e) Cu diagram for clinopyroxene; f) Sr diagram for clinopyroxene; g) Y diagram for clinopyroxene; h) Nb diagram for clinopyroxene; i) Mo diagram for clinopyroxene; j) La diagram for clinopyroxene; k) Ce diagram for clinopyroxene; l) Pr diagram for clinopyroxene; m) Sm diagram for clinopyroxene; n) Eu diagram for clinopyroxene; o) Gd diagram for clinopyroxene; p) Tb diagram for clinopyroxene; q) Dy diagram for clinopyroxene; r) Ho diagram for clinopyroxene; s) Er diagram for clinopyroxene; t) Tm diagram for clinopyroxene; u) Yb diagram for clinopyroxene; v) Lu diagram for clinopyroxene; w) Hf diagram for clinopyroxene.

a)

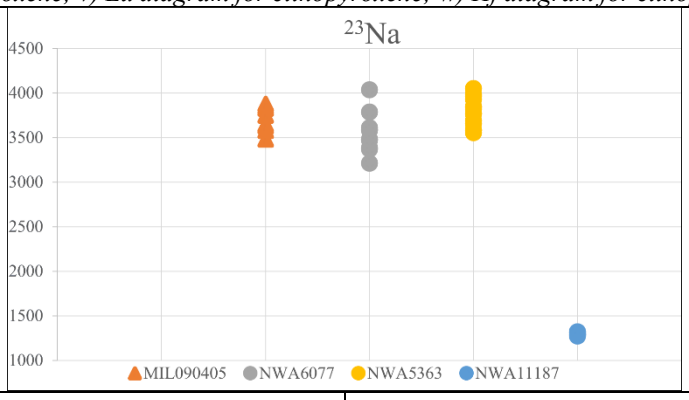

b)

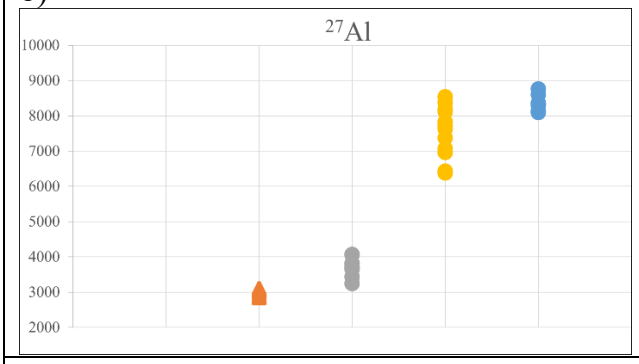

c)

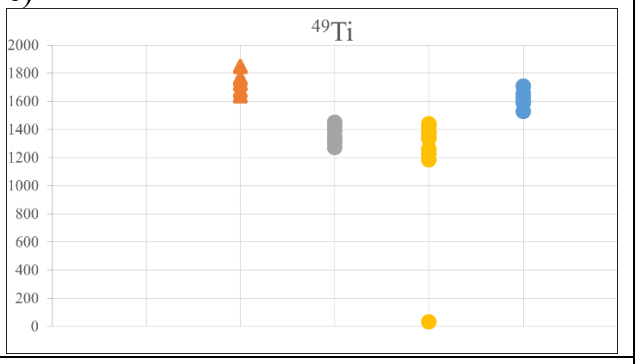

d)

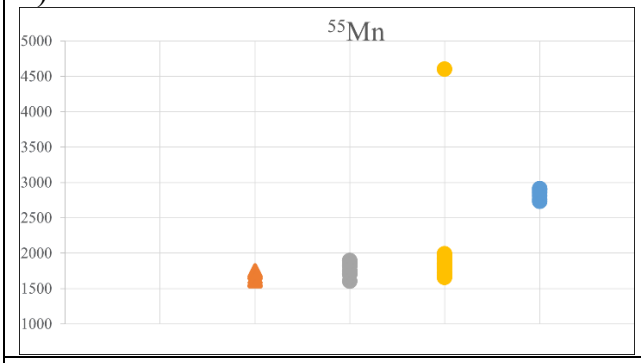

e)

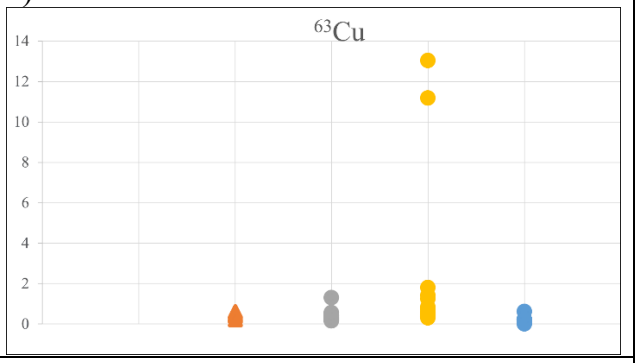

f)

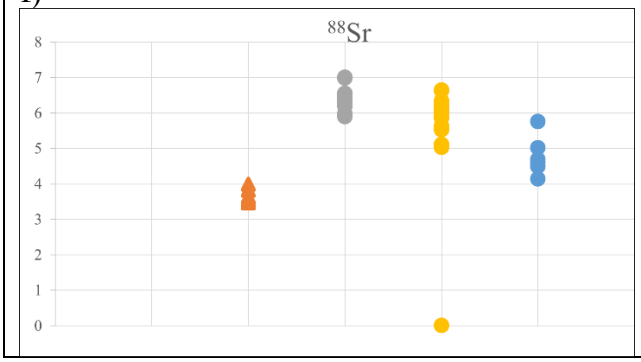

g)

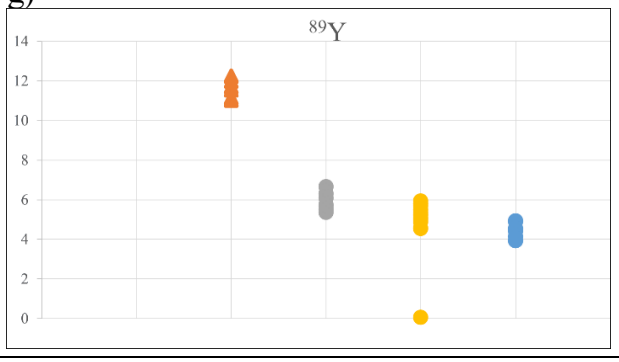

h)

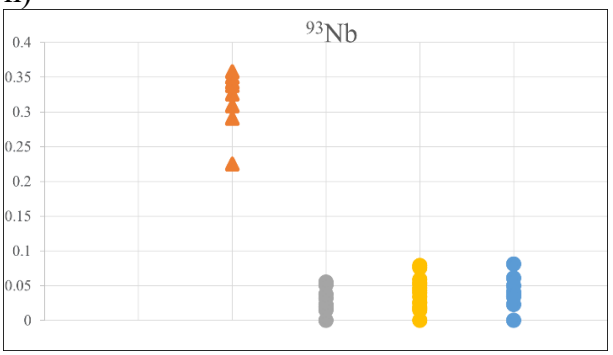
93Nb
0.4
0.35
0.3
0.25
0.2
0.15
0.1
0.05
0

i)

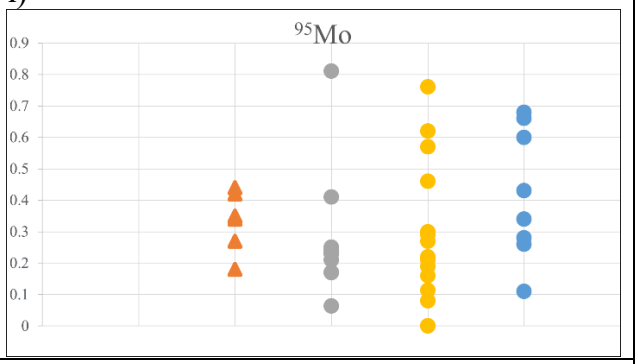
95Mo
0.9
0.8
0.7
0.6
0.5
0.4
0.3
0.2
0.1
0

j)

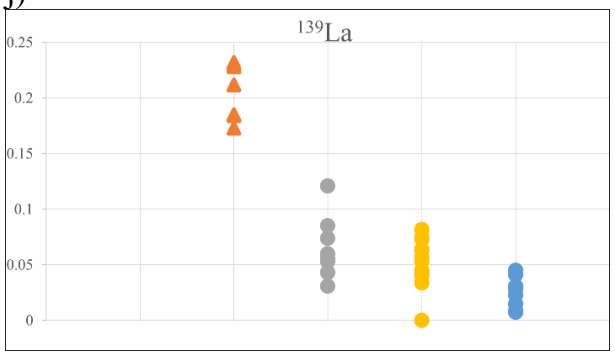
139La
0.25
0.2
0.15
0.1
0.05
0

k)

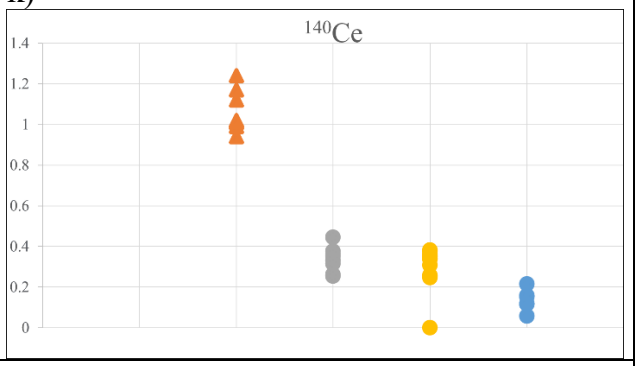
140Ce
1.4
1.2
1
0.8
0.6
0.4
0.2
0

l)

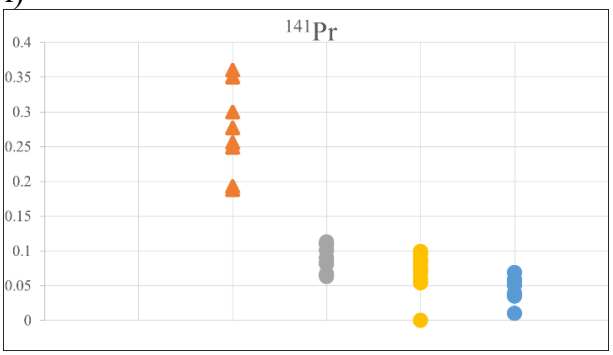
141Pr
0.4
0.35
0.3
0.25
0.2
0.15
0.1
0.05
0

m)

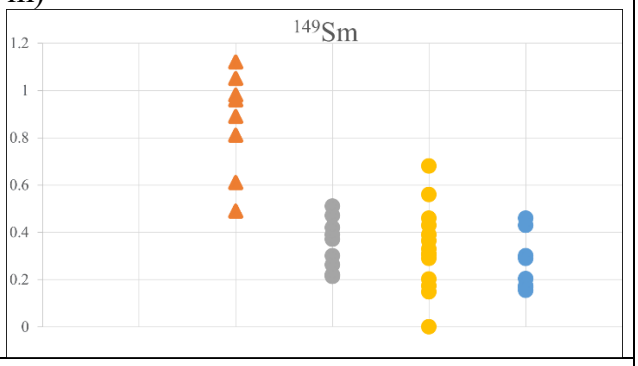
149Sm
1.2
1
0.8
0.6
0.4
0.2
0

n)

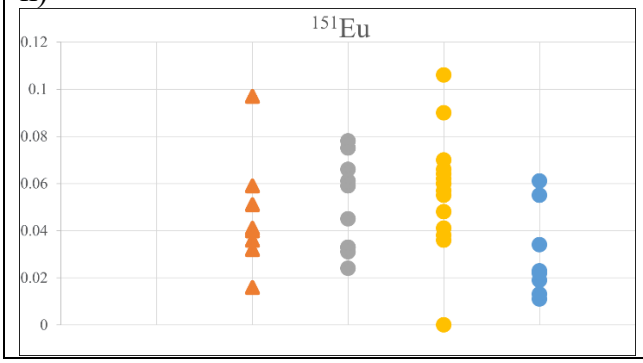
151Eu
0.12
0.1
0.08
0.06
0.04
0.02
0

o)

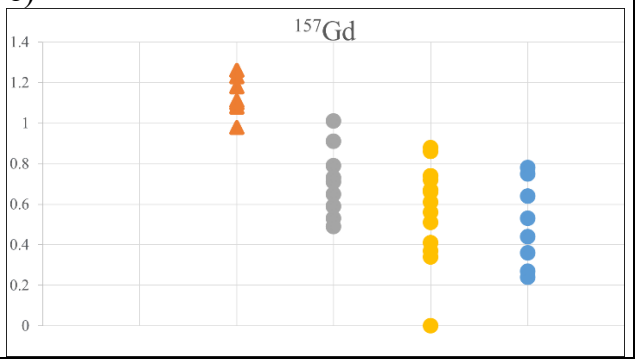
157Gd
1.4
1.2
1
0.8
0.6
0.4
0.2
0

p)

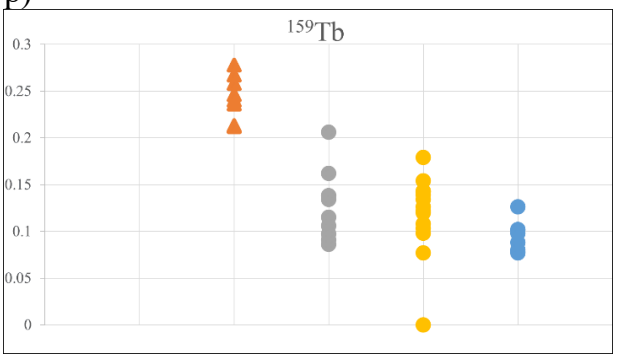
159Tb
0.3
0.25
0.2
0.15
0.1
0.05
0

q)

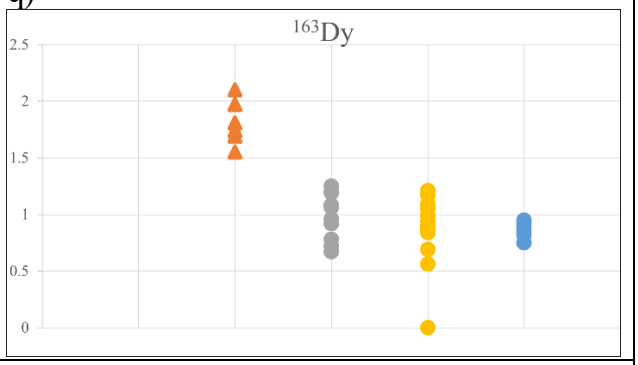
163Dy
2.5
2
1.5
1
0.5
0

r)

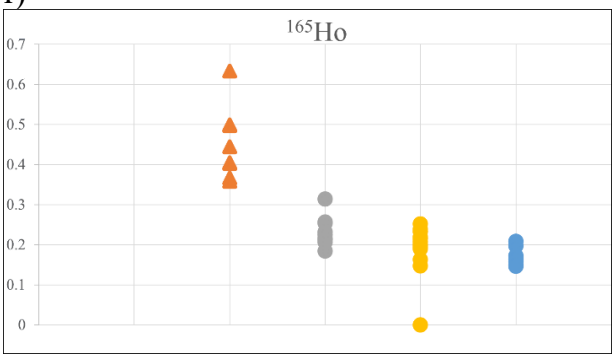
165Ho
0.7
0.6
0.5
0.4
0.3
0.2
0.1
0

s)

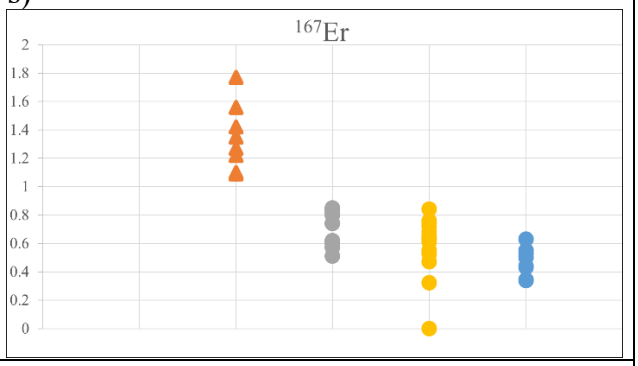
167Er
2
1.8
1.6
1.4
1.2
1
0.8
0.6
0.4
0.2
0

t)

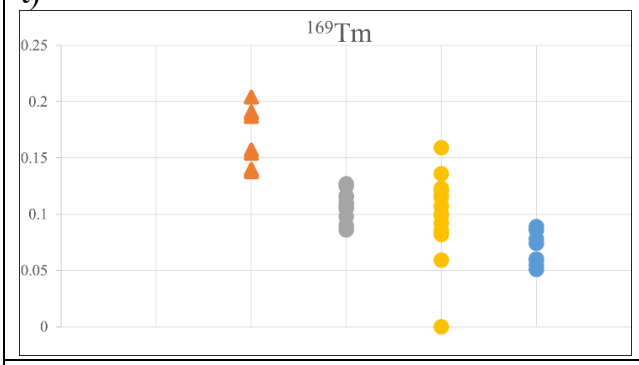
169Tm
0.25
0.2
0.15
0.1
0.05
0

u)

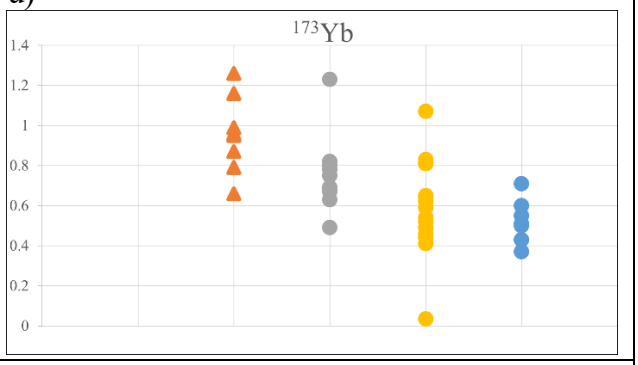
173Yb
1.4
1.2
1
0.8
0.6
0.4
0.2
0

v)

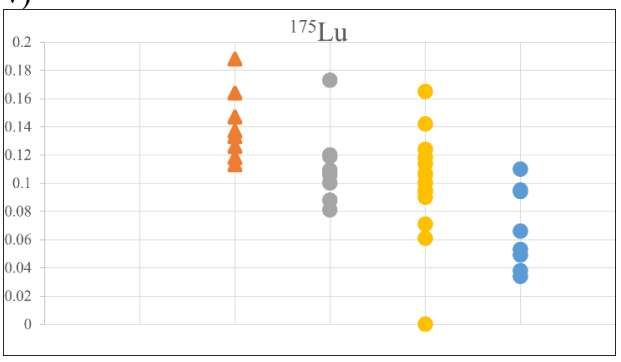
175Lu
0.2
0.18
0.16
0.14
0.12
0.1
0.08
0.06
0.04
0.02
0

w)

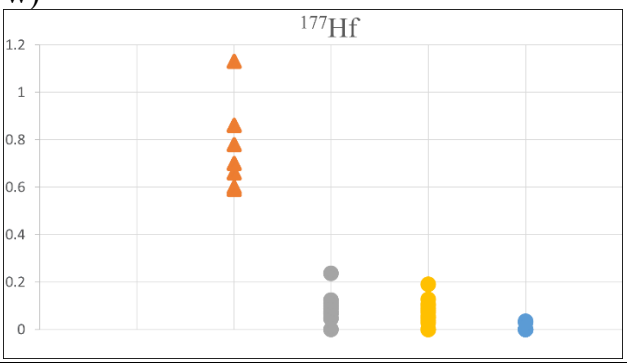
177Hf
1.2
1
0.8
0.6
0.4
0.2
0

Discussion

In the following tables all of the geochemical data used for the discussion are reported. Data from Carli et al. (2023; Al Huwaysah 010), Day et al. (2012; NWA5400, GRA06128, GRA06129), Gardner-Vandy et al. (2013; EET99402), Goodrich et al. (2017; MIL090340), Li et al. (2011; GRV021663), Li et al. (2018; NWA8118), Zeng et al. (2019; NWA725, NWA6448, GRV028890, NWA4024, SAH02029).

Table S10, average olivine composition (EPMA) expressed as wt.% of oxides. The number of point analyses and classification is reported close to the sample name. Fo, Fa and Tp content are also reported. Bdl= below detection limit. un = number of point analyses were not reported by the author.

Olivine (wt%)												
	MIL090206	**MIL090405**	**NWA5363**	**NWA6077**	Al Huwaysah 010	GRA06128,42	GRA06128,51	GRA06129,22	GRA06129,25	EET99402	**NWA5400**	**MIL090340 (grain cores)**
Clan	**Ungrouped**	**Ungrouped**	**Ungrouped**	**Ungrouped**	Ungrouped	Ungrouped	Ungrouped	Ungrouped	Ungrouped	Brachinite	**Ungrouped**	**Ungrouped**
N.	**35**	**38**	**31**	**33**	18	35	32	36	50	un	**un**	**61**
SiO_2	**37.58**	**37.54**	**37.41**	**36.75**	40.32	32.80	33.00	33.60	33.90	36.40	**37.10**	**37.10**
TiO_2	**0.026**	**0.026**	**0.029**	**0.032**	0.020	0.03	0.030	0.030	0.03	bdl	**bdl**	**bdl**
Al_2O_3	**0.002**	**0.002**	**0.004**	**0.005**	0.010	bdl	bdl	bdl	bdl	bdl	**bdl**	**bdl**
Cr_2O_3	**0.053**	**0.047**	**0.17**	**0.20**	0.030	0.03	0.030	0.030	0.030	bdl	**bdl**	**0.040**
FeOT	**24.42**	**25.43**	**26.69**	**25.94**	15.56	48.8	48.10	47.90	48.80	31.50	**26.70**	**26.20**
MnO	**0.44**	**0.45**	**0.45**	**0.43**	0.510	0.69	0.70	0.70	0.75	0.43	**0.450**	**0.48**
NiO	**0.014**	**0.005**	**0.011**	**0.024**	0.010	bdl	bdl	bdl	0.060	bdl	**bdl**	**bdl**
MgO	**36.54**	**35.74**	**34.89**	**36.39**	45.13	17.3	17.70	18.10	18.00	31.50	**35.00**	**36.60**
CaO	**0.077**	**0.089**	**0.076**	**0.074**	0.060	0.1	0.10	0.11	0.09	0.11	**0.080**	**0.08**
Na_2O	**bdl**	**bdl**	**bdl**	**bdl**	bdl	bdl	bdl	bdl	bdl	bdl	**bdl**	**bdl**
K_2O	**bdl**	**bdl**	**bdl**	**bdl**	bdl	bdl	bdl	bdl	bdl	bdl	**bdl**	**bdl**
Total	**99.16**	**99.32**	**99.72**	**99.84**	101.65	99.70	99.60	100.40	101.50	100.00	**99.30**	**100.50**
Fo (mol%)	**72.4**	**71.1**	**71.1**	**69.6**	83.9	38.8	39.6	40.2	39.6	64.2	**70.1**	**71.3**
Fa (mol%)	**27.1**	**28.4**	**28.4**	**29.9**	16.2	61.2	60.4	59.8	60.4	35.8	**29.9**	**28.7**
Tp (mol%)	**0.5**	**0.5**	**0.5**	**0.5**								

Table S11, average orthopyroxene composition (EPMA) expressed as wt.% of oxides. The number of point analyses and classification is reported close to the sample name. Wo, En and Fs content are also reported. Bdl= below detection limit. un = number of point analyses were not reported by the author.

Orthopyroxene (wt%)											
	MIL090206	**MIL090405**	**NWA5363**	**NWA6077**	Al Huwaysah 010	GRA06128,42	GRA06128,51	GRA06129,22	GRA06129,25	NWA5400	**MIL090340 (grain boundary)**
Clan	**Ungrouped**	**Ungrouped**	**Ungrouped**	**Ungrouped**	Ungrouped	Ungrouped	Ungrouped	Ungrouped	Ungrouped	Ungrouped	**Ungrouped**
N.	**32**	**3**	**11**	**19**	13	29	15	15	15	un	**1**
SiO_2	**54.35**	**55.02**	**55.39**	**54.03**	57.55	51	51	52.10	52.00	54.4	**54.10**
TiO_2	**0.13**	**0.03**	**0.11**	**0.11**	0.02	0.17	0.17	0.16	0.18	0.09	**0.04**
Al_2O_3	**0.23**	**0.03**	**0.29**	**0.28**	0.01	0.17	0.19	0.19	0.18	0.29	**0.04**
Cr_2O_3	**0.18**	**0.07**	**0.20**	**0.19**	0.08	0.08	0.09	0.10	0.10	0.21	**0.11**
FeOT	**16.66**	**15.23**	**15.71**	**15.64**	9.97	28.4	27.9	27.70	27.80	15.99	**15.60**
MnO	**0.40**	**0.41**	**0.27**	**0.26**	0.53	0.6	0.6	0.59	0.63	0.42	**0.42**
MgO	**26.34**	**28.14**	**27.18**	**27.79**	32.99	17.9	18.2	18.40	18.10	26.80	**30.40**
CaO	**1.07**	**0.51**	**1.08**	**1.09**	0.39	1.08	1.12	1.11	1.32	1.09	**0.52**
Na_2O	**0.03**	**0.01**	**0.03**	**0.03**	0.01	0.02	0.01	0.01	0.01	bdl	**bdl**
K_2O	**0.01**	**0.00**	**0.00**	**0.01**	0.00	bdl	bdl	bdl	bdl	bdl	**bdl**
Total	**99.39**	**99.45**	**100.27**	**99.42**	101.58	99.40	99.20	100.30	100.30	99.40	**101.30**
wollastonite	**2.1**	**1.0**	**2.1**	**2.1**	0.7	2.2	2.3	2.3	2.7	2.2	**0.9**
enstatite	**71.8**	**75.5**	**73.6**	**74.1**	84.3	51.7	52.5	52.9	52.2	73.3	**76.5**
ferrosilite	**26.1**	**23.5**	**24.3**	**23.8**	15.0	46.1	45.1	44.8	45.1	24.5	**22.6**

Table S12, average clinopyroxene composition (EPMA) expressed as wt.% of oxides. The number of point analyses and classification is reported close to the sample name. Wo, En and Fs content are also reported. Bdl= below detection limit. un = number of point analyses were not reported by the author. na= not analyzed.

Clinopyroxene (wt%)												
	MIL090206	**MIL090405**	**NWA5363**	**NWA6077**	Al Huwaysah 010	GRA06128,42	GRA06128,51	GRA06129,22	GRA06129,25	EET99402	**NWA5400**	**MIL090340 (primary Augite)**
clan	**Ungrouped**	**Ungrouped**	**Ungrouped**	**Ungrouped**	Ungrouped	Ungrouped	Ungrouped	Ungrouped	Ungrouped	Brachinite	**Ungrouped**	**Ungrouped**
N.	**2**	**19**	**22**	**23**	18	44	39	36	49	un	**un**	**2**
SiO_2	**53.51**	**53.59**	**54.02**	**53.41**	54.58	51.6	51.70	52.30	52.30	53.00	**53.40**	**53.20**
TiO_2	**0.31**	**0.30**	**0.22**	**0.21**	0.13	0.38	0.38	0.42	0.47	0.13	**0.19**	**na**
Al_2O_3	**0.63**	**0.65**	**0.74**	**0.68**	0.72	0.42	0.43	0.45	0.49	1.02	**0.72**	**0.71**
Cr_2O_3	**0.73**	**0.78**	**0.80**	**0.73**	0.68	0.41	0.42	0.44	0.46	0.69	**0.76**	**0.75**
FeOT	**6.61**	**6.57**	**6.18**	**6.00**	7.08	12.5	12.10	12.20	12.60	6.37	**6.08**	**6.60**
MnO	**0.21**	**0.20**	**0.21**	**0.13**	0.20	0.31	0.31	0.32	0.34	0.16	**0.22**	**0.23**
MgO	**15.80**	**15.87**	**15.89**	**16.73**	16.06	12.9	13.10	13.10	12.80	15.30	**16.10**	**16.40**
CaO	**21.21**	**21.13**	**21.08**	**21.45**	20.99	20.3	20.40	20.10	20.20	22.30	**21.30**	**20.80**
Na_2O	**0.49**	**0.51**	**0.46**	**0.46**	0.35	0.33	0.33	0.34	0.37	0.40	**0.49**	**0.45**
K2O	**0.00**	**0.00**	**0.00**	**0.00**	0.0	bdl	bdl	bdl	bdl	bdl	**bdl**	**bdl**
Total	**99.50**	**99.59**	**99.60**	**99.80**	100.9	99.1	99.20	99.70	100.10	99.50	**99.20**	**98.30**
wollastonite	**43.7**	**43.6**	**43.7**	**43.3**	42.8	42.3	42.4	42.1	42.1	45.9	**44.0**	**42.6**
enstatite	**45.3**	**45.5**	**45.9**	**47.0**	45.6	37.3	39.0	38.0	37.3	43.8	**46.2**	**46.6**
ferrosilite	**11.0**	**10.9**	**10.4**	**9.7**	11.6	20.4	19.6	19.9	20.6	10.2	**9.8**	**10.9**

Table S13, average plagioclase composition (EPMA) expressed as wt.% of oxides. The number of point analyses and classification is reported close to the sample name. An, Ab and Or content is also reported. Bdl= below detection limit. ? = number of point analyses were not reported by the author. na= not analyzed.

Plagioclase (wt%)					
	NWA5363	**Al Huwaysah 010**	**NWA5400**	EET99402	MIL090206
Clan	**Ungrouped**	**Ungrouped**	**Ungrouped**	Brachinite	Ungrouped
N.	**10**	**8**	**36**	11	158
SiO_2	**63.06**	**61.07**	**62.2**	57.8	64.1
TiO_2	**0.04**	**0.03**	**bdl**	bdl	na
Al_2O_3	**23.62**	**24.16**	**23.4**	27	22.7
FeOT	**0.16**	**0.09**	**0.25**	0.17	0.33
MnO	**0.01**	**bdl**	**bdl**	bdl	0.03
MgO	**0.02**	**0.03**	**bdl**	bdl	0.03
CaO	**5.38**	**6.08**	**5.84**	8.24	3.66
Na_2O	**7.87**	**7.79**	**7.65**	7.13	na
K_2O	**0.29**	**0.10**	**0.24**	0.05	0.57
Total	**100.55**	**99.3**	**99.6**	100.4	100.6
An	**27.0**	**30.6**	**29.2**	38.9	17.5
Ab	**71.3**	**69.5**	**69.3**	60.8	79.2
Or	**1.7**	**0**	**1.4**	0.3	3.3

Table S14, average phosphates composition (EPMA) expressed as wt.% of oxides. The number of point analyses and classification is reported close to the sample name. na= not analyzed.

Phosphates (wt%)						
	NWA6077	NWA5363	**MIL090340**	GRA06128, 42 (Cl-apatite)	GRA06128,51 (Cl-apatite)	GRA06129,22 (Cl-apatite)
Clan	**Ungrouped**	Ungrouped	**Ungrouped**	Ungrouped	Ungrouped	Ungrouped
N.	**15**	6	**4**	41	27	34
SiO_2	**0.39**	1.73	**0.18**	na	na	na
F	**0.25**	0.32	**0.25**	1.23	0.98	0.85
P_2O_5	**39.81**	34.38	**41.3**	41	40.7	41.5
SrO	**0.02**	0.02	**na**	na	na	na
Cl	**2.73**	3.03	**5.5**	4.69	4.88	4.67
SO_3	**0.62**	0.51	**na**	na	na	na
FeO	**11.86**		**1.05**	0.19	0.26	0.22
CaO	**38.49**	26.47	**52.4**	53.5	53.5	54.2
Na_2O	**0.48**	0.17	**0.45**	0.01	0.4	0.41
MgO	**1.28**	0.12	**0.00**	0.04	0.04	0.03
TOT	**95.93**	66.75	**101.3**	99.1	99.2	100.6

Table S15, average spinel composition (EPMA) expressed as wt.% of oxides. The number of point analyses and classification is reported close to the sample name. Bdl= below detection limit. na= not analyzed.

Spinels (wt%)										
	MIL090206	MIL090405	**NWA5363**	**NWA6077**	**Al Huwaysah 010**	**MIL090340 1 (chromite grain core)**	**MIL090340 2 (chromite grain core)**	**MIL090340 3 (chromite grain core)**	**EET99402**	NWA5400
Clan	Ungrouped	Ungrouped	**Ungrouped**	**Ungrouped**	**Ungrouped**	**Ungrouped**	**Ungrouped**	**Ungrouped**	**brachinite**	Ungrouped
N.	10	9	**16**	**23**	**8**	**9**	**36**	**18**	**14**	9
SiO_2	0.00	0.21	**0.00**	**0.00**	**bdl**	**0.04**	**0.03**	**0.04**	**0.06**	bdl
TiO_2	2.16	1.94	**1.46**	**1.43**	**1.07**	**2.44**	**2.41**	**2.42**	**1**	1.43
Al_2O_3	5.87	4.90	**7.80**	**7.59**	**9.76**	**7.20**	**7.20**	**7.10**	**13.6**	8.03
V_2O_3	0.66	55.07	**0.66**	**0.67**	**0.73**	**0.74**	**0.74**	**0.73**	**0.71**	0.71
Cr_2O_3	52.46	0.67	**56.06**	**55.85**	**56.79**	**57.70**	**57.60**	**58.50**	**51.2**	57.4
FeO	27.95	29.68	**27.66**	**27.60**	**22.65**	**27.60**	**27.30**	**27.10**	**28.6**	27.5
MnO	0.28	0.29	**0.18**	**0.19**	**0.46**	**0.50**	**0.47**	**0.49**	**0.36**	0.45
NiO	0.02	0.02	**0.01**	**0.02**	**bdl**	**na**	**na**	**na**	**na**	na
MgO	3.98	3.33	**4.02**	**4.34**	**7.43**	**4.54**	**4.71**	**4.79**	**4.12**	4.47
CaO	0.01	0.01	**0.01**	**0.01**	**0.02**	**na**	**na**	**na**	**na**	na
ZnO	0.03	0.03	**0.11**	**0.11**	**0.04**	**na**	**na**	**na**	**na**	na
CoO	0.05	0.03	**0.03**	**0.00**	**bdl**	**na**	**na**	**na**	**na**	na
CuO	0.08	0.03	**0.02**	**0.00**	**bdl**	**na**	**na**	**na**	**na**	na
TOT	93.54	96.19	**98.02**	**97.80**	**98.97**	**100.70**	**100.50**	**101.30**	**100.4**	100.4

Table S16, Clinopyroxene average Trace Elements data in ppm. The number of point analyses and classification is reported close to the sample name. bdl= below detection limit. Na= not analyzed. un = data not reported by the author.

Clinopyroxene (ppm)							
	MIL090405	**NWA6077**	**NWA5363**	GRA06128	GRA06129	EET99402	**NWA5400**
Clan	Ungrouped	**Ungrouped**	**Ungrouped**	Ungrouped	Ungrouped	Brachinite	**Ungrouped**
N.	8	**10**	**15**	un	un	un	**un**
^{23}Na	3703.43	**3550.58**	**3536.93**	na	na	na	**na**
^{27}Al	2973.97	**3712.83**	**7118.68**	na	na	na	**na**
^{45}Sc	88.32	**81.56**	**79.95**	144.00	205.00	94.00	**86.00**
^{49}Ti	1738.01	**1370.56**	**1256.32**	bdl	3137.00	1249.00	**1897.00**
^{51}V	395.56	**382.21**	**366.05**	847.00	798.00	375.00	**398.00**
^{53}Cr	5943.04	**6379.17**	**6026.47**	3321.00	3372.00	4415.00	**5859.00**
^{55}Mn	1667.42	**1780.72**	**2024.28**	1352.00	2541.00	bdl	**bdl**
^{59}Co	11.31	**12.34**	**22.51**	bdl	bdl	bdl	**bdl**
^{60}Ni	16.81	**62.64**	**152.88**	bdl	bdl	bdl	**bdl**
^{63}Cu	0.44	**0.43**	**2.25**	bdl	bdl	bdl	**bdl**
^{66}Zn	64.39	**84.86**	**84.44**	bdl	bdl	bdl	**bdl**
^{88}Sr	3.64	**6.43**	**5.54**	2.79	2.93	<30.00	**<25.00**
^{89}Y	11.61	**5.80**	**4.91**	2.61	5.72	2.48	**5.80**
^{90}Zr	35.10	**2.28**	**1.55**	128.50	114.40	<0.26	**2.09**
^{93}Nb	0.32	**0.03**	**0.04**	0.05	<0.07	0.02	**0.02**
^{95}Mo	0.34	**0.28**	**0.28**	na	na	na	**na**
^{139}La	0.21	**0.06**	**0.05**	0.07	0.10	0.01	**0.06**
^{140}Ce	1.06	**0.33**	**0.30**	0.25	0.47	0.07	**0.32**
^{141}Pr	0.27	**0.09**	**0.07**	0.05	0.10	0.03	**0.08**
^{146}Nd	1.62	**0.68**	**0.61**	0.33	0.70	0.20	**0.60**
^{149}Sm	0.86	**0.34**	**0.33**	0.13	0.39	0.15	**0.37**
^{151}Eu	0.05	**0.05**	**0.06**	0.05	0.06	0.06	**0.07**
^{157}Gd	1.15	**0.70**	**0.58**	0.27	0.64	0.26	**0.63**
^{159}Tb	0.24	**0.13**	**0.12**	0.07	0.14	0.06	**0.12**
^{163}Dy	1.82	**0.98**	**0.88**	0.53	1.05	0.42	**0.94**
^{165}Ho	0.45	**0.23**	**0.19**	0.12	0.25	0.10	**0.23**
^{167}Er	1.35	**0.71**	**0.58**	0.38	0.67	0.32	**0.64**
^{169}Tm	0.17	**0.11**	**0.10**	0.06	0.11	0.05	**0.10**
^{173}Yb	0.96	**0.76**	**0.59**	0.49	0.75	0.42	**0.70**
^{175}Lu	0.14	**0.11**	**0.10**	0.08	0.14	0.08	**0.10**
^{177}Hf	0.77	**0.09**	**0.07**	5.42	4.04	0.00	**0.08**

Table S17, Plagioclase average Trace Elements data in ppm. The number of point analyses and classification is reported close to the sample name. bdl= below detection limit. Na= not analyzed. un = data not reported by the author.

Plagioclase (ppm)				
	NWA5363	GRA06129	EET99402	NWA5400
Clan	ungrouped	ungrouped	brachinite	ungrouped
N.	6	un	un	un
^{25}Mg	653.97	na	na	na
^{45}Sc	0.84	0.70	1.60	1.50
^{49}Ti	132.08	470.00	114.00	bdl
^{51}V	0.55	0.60	5.30	bdl
^{53}Cr	19.12	<3.51	385.00	bdl
^{55}Mn	75.99	6.30	2.90	bdl
^{57}Fe	11525.23	na	na	na
^{59}Co	100.21	6.30	2.90	bdl
^{60}Ni	1382.86	bdl	bdl	bdl
^{63}Cu	14.41	bdl	bdl	bdl
^{88}Sr	148.62	69.00	178.00	228.00
^{138}Ba	19.07	0.04	0.047	0.03
^{139}La	0.03	0.036	<0.15	0.594
^{140}Ce	0.06	0.071	0.03	1.83
^{151}Eu	0.67	0.026	0.678	0.92

*Table S18, average olivine composition (EPMA) expressed as wt.% of oxides. The number of point analyses and classification is reported close to the sample name. Fo, Fa and Tp content are also reported. Bdl= below detection limit. Un = data not reported by author. * data from Takeda (1989).*

Olivine (wt%)		
wt.%	**NWA11187**	**LEW85440***
Clan	**ungrouped**	**Ureilite**
Classification	This Study	LEW Related
N.	**22**	**un**
SiO_2	**41.40**	**40.1**
TiO_2	**0.04**	**0.02**
Al_2O_3	**0.03**	**0.06**
Cr_2O_3	**0.57**	**0.5**
FeOT	**5.46**	**8.6**
MnO	**0.49**	**0.47**
NiO	**0.01**	**0.01**
MgO	**52.64**	**50.6**
CaO	**0.32**	**0.33**
Na_2O	**bdl**	**0.01**
K_2O	**bdl**	**na**
Total	**99.16**	**100.7**
Fo (mol%)	**93.60**	**91.3**
Fa (mol%)	**5.45**	**8.7**
Tp (mol%)	**0.49**	//

*Table S19, average orthopyroxene composition (EPMA) expressed as wt.% of oxides. The number of point analyses and classification is reported close to the sample name. Wo, En and Fs content are also reported. Bdl= below detection limit. un = data not reported by author. * = data from Takeda (1989). ^ = data from Goodrich et al. (2009).*

Orthopyroxene (wt%)					
wt.%	**NWA11187**	Hughe 009^	FRO90054^	**LEW85440***	Y791538*
Clan	**ungrouped**	Ureilite	Ureilite	**Ureilite**	Ureilite
Classification	**This Study**	Hughes cluster	Hughes Cluster	**LEW Related**	LEW Related
N.	**24**	113	41	**un**	un
SiO_2	**57.49**	55.9	55.8	**56.22**	56.92
TiO_2	**0.14**	0.13	0.11	**0.14**	0.13
Al_2O_3	**0.51**	1.01	1.21	**0.86**	0.82
Cr_2O_3	**0.85**	1.04	1.06	**0.8**	0.9
FeOT	**3.47**	7.3	7.48	**5.31**	4.81
MnO	**0.48**	0.54	0.55	**0.46**	0.44
MgO	**34.67**	31.1	30.7	**33.26**	33.49
CaO	**2.86**	2.51	2.47	**2.6**	2.57
Na_2O	**0.04**	0.05	0.04	**0.05**	0.04
K_2O	**0.00**	na	na	**na**	na
Total	**100.51**	99.6	99.4	**99.7**	100.12
wollastonite	**5.3**	4.9	4.8	**4.9**	4.9
enstatite	**89.0**	83.4	83	**87.3**	88.1
ferrosilite	**5.7**	11.8	12.2	**7.8**	7.1

*Table S20, average clinopyroxene composition (EPMA) expressed as wt.% of oxides. The number of point analyses and classification is reported close to the sample name. Wo, En and Fs content are also reported. Bdl= below detection limit. un = data not reported by author. * = data from Takeda (1989). ^ = data from Goodrich et al. (2009).*

Clinopyroxene (wt%)				
Wt%	**NWA11187**	Hughes009^	FRO90054^	**LEW85440^**
Clan	**ungrouped**	Ureilite	Ureilite	**Ureilite**
Classification	**This Study**	Hughes Cluster	Hughes Cluster	**LEW Related**
N.	**32**	98	31	**un**
SiO_2	**55.11**	53.7	53.4	**53.96**
TiO_2	**0.25**	0.27	0.23	**0.24**
Al_2O_3	**0.84**	1.61	1.93	**1.33**
Cr_2O_3	**0.83**	1.29	1.33	**0.9**
FeOT	**2.08**	4.3	4.34	**3.18**
MnO	**0.36**	0.41	0.42	**0.37**
MgO	**21.97**	19.7	19.3	**21.83**
CaO	**18.71**	18.1	18.5	**18.07**
Na_2O	**0.17**	0.27	0.24	**0.2**
K_2O	**0.00**	na	na	**na**
Total	**100.32**	99.7	99.7	**100.08**
wollastonite	**36.56**	36.8	37.7	**35.5**
enstatite	**59.72**	55.7	54.7	**59.6**
ferrosilite	**3.72**	7.5	7.6	**4.9**

7. FIGURE INDEX

Introduction

Petrography

to-euhedral clinopyroxene, circled in green. The white circles are the LA-ICP-MS spots; c) chromite grain and Fe-Ni; d) intensely fractured area (13);

Fig. 3.1.8, a BSE image of a clinopyroxene. Some triple junctions between one clinopyroxene crystal and two olivine crystals (yellow rectangle). The blue circled areas are the data points for LA-ICP-MS (14);

Fig. 3.1.9, composite EDS map with Ca, Mg and Si on the Red, Green and Blue channels, respectively. In the image, are shown four different minerals: orthopyroxene (light-blue), olivine (green), clinopyroxene (pink-to-red) and Fe-Ni phases (black with scattered red). In the weathered olivines it is possible to see the fine-grained assemblages of Fe-Ni phases and orthopyroxene. A small rounded olivine is poikilitically enclosed in a clinopyroxene (red circle) (15);

Fig. 3.1.10, a BSE image of NWA6077 meteorite. The red dots are the data points of the LA-ICP-MS (the ones marked with a red number were taken first, while the others were taken during a second session of analysis). Yellow rectangles represent areas of the meteorite that will be further analyzed in the next images. The network of fractures is highlighted by the white and grey light color related to Fe-Ni phases and oxides (16);

Fig. 3.1.11, BSE images of: a) orthopyroxene poikiloblasts enclosing some rounded olivines (red circles). The white circled areas are the data points for LA-ICP-MS; b) apatite crystal (purple circle) (17);

Fig. 3.1.12, composite EDS map with Ca, Mg and Si on the Red, Green and Blue channels, respectively. In the image, are shown four different minerals: orthopyroxene (light-blue), olivine (green), clinopyroxene (pink-to-red) and Fe-Ni phases (black with scattered red). The white circled areas are the data points for LA-ICP-MS. In the weathered olivines it is possible to see the fine-grained assemblages of Fe-Ni phases and orthopyroxene (17);

Fig. 3.1.13. a BSE image of NWA5363 meteorite. The red dots are the data points of LA-ICP-MS analysis (the ones marked with a "#" were taken first, while the others were taken during a second session of analysis). Yellow rectangles represent an area of the meteorite that will be further analyzed in the next images (18);

Fig. 3.1.14, composite EDS map with Ca, Mg and Si on the Red, Green and Blue channels, respectively. In the image, are shown four different minerals: orthopyroxene (light-blue), olivine (green), clinopyroxene (pink-to-red) and Fe-Ni phases (black with scattered red). In the weathered olivines it is possible to see the fine-grained assemblages of Fe-Ni phases and orthopyroxene. A small rounded olivine is poikilitically enclosed in a clinopyroxene (red circle). In the yellow rectangle it is

possible to see a triple junction between three olivine grains. The white circled areas are the data points for LA-ICP-MS (19);

Fig. 3.1.15, a BSE image of olivine rounded crystals (red circles) poikilitically enclosed in plagioclase crystals (orange circles). Fine-grained assemblages of orthopyroxene and Fe-Ni phases are less frequent in this meteorite (20);

Fig. 3.1.16, a BSE image of NWA11187 meteorite. The red dots are the data points of the LA-ICP-MS analysis. Yellow rectangles represent areas of the meteorite that will be showed in the next images (21);

Fig. 3.1.17, a BSE image. Triple junction between olivine crystals, highlighted by Fe-Ni phases (yellow rectangle) (22);

Fig. 3.1.18, a BSE image. Exsolution lamellae of clinopyroxene in orthopyroxene (light blue circled areas). Olivine rounded crystals enclosed in orthopyroxene (red circles). The datapoints of the LA-ICP-MS analysis (white circles) (23);

Fig. 3.1.19, composite EDS map with Ca, Mg and Si on the Red, Green and Blue channels, respectively. In the image, are shown four different minerals: orthopyroxene (light-blue), olivine (green), clinopyroxene (pink-to-red) and Fe-Ni phases (black with scattered red). In the yellow rectangles it is possible to see many triple junctions between both olivine and orthopyroxene grains. In addition, it is possible to see the exsolution lamellae of clinopyroxene in orthopyroxene. The white circled areas are the data points for LA-ICP-MS (24).

Major and Minor Elements

Fig. 3.2.1.1, Fo content in mol% for all the studied meteorites showing the internal and intra-sample variability (26);

Fig. 3.2.1.2, En vs Fs vs Wo (orthopyroxene) for all the studied meteorites. All the orthopyroxene grains in NWA11187 are pigeonitic, while orthopyroxene grains from the other four meteorites are enstatitic. The number of point analyses is indicated next to the meteorite name (28);

Fig. 3.2.1.3, En vs Fs vs Wo (clinopyroxene) for all the studied meteorites. All the clinopyroxene grains analyzed are augitic. The number of point analyses is indicated next to the meteorite name (30);

Fig. 3.2.1.4, Or vs Ab vs An for NWA5363. Of the ten plagioclase grains analyzed in NWA5363, eight are oligoclase and one is andesine, while one shows an intermediate composition between oligoclase and andesine. The number of point analyses is indicated next to the meteorite name (32).

Trace Elements

Fig. 3.2.2.1, Trace Elements content for olivine in the meteorites MIL090206, MIL090405, NWA6077, NWA5363 and NWA11187. All values are in ppm. a) ^{44}Ca values; b) ^{53}Cr values (log scale); c) ^{60}Ni values (log scale); d) ^{59}Co values (log scale); e) ^{51}V values; f) ^{66}Zn values (log scale); g) ^{27}Al values (log scale). Modal analyses for the same meteorites are reported in h) (37);

Fig. 3.2.2.2 Y-REE pattern for olivine (logarithmic scale), normalized to average CI carbonaceous chondrite composition (McDonough and Sun, 1995) (39);

Fig. 3.2.2.3, Trace Elements content for orthopyroxene in the meteorites MIL090206, NWA6077, NWA5363 and NWA11187. All values are in ppm. a) ^{27}Al values; b) ^{49}Ti values (log scale); c) ^{51}V values; d) ^{60}Ni values (log scale); e) ^{59}Co values; f) ^{90}Zr values; g) ^{95}Mo values; h) ^{88}Sr values (log scale) Modal analyses for the same meteorites are reported in i) (41);

Fig. 3.2.2.4 Y-REE pattern for orthopyroxene (logarithmic scale), normalized to average CI carbonaceous chondrite composition (McDonough and Sun, 1995) (43);

Fig. 3.2.2.5, Trace Elements content for olivine in the meteorites MIL090206, MIL090405, NWA6077, NWA5363 and NWA11187. All values are in ppm. a) ^{53}Cr values; b) ^{51}V values; c) ^{66}Zn values; d) ^{45}Sc values; e) ^{90}Zr values (log scale); f) ^{60}Ni values (log scale); g) ^{59}Co values (log scale); h) ^{146}Nd. Modal analyses for the same meteorites are reported in i) (46);

Fig. 3.2.2.6 Y-REE pattern for clinopyroxene (logarithmic scale), normalized to average CI carbonaceous chondrite composition (McDonough and Sun, 1995) (50);

Fig. 3.2.2.7 Y-REE pattern plagioclase (logarithmic scale), normalized to average CI carbonaceous chondrite composition (McDonough and Sun, 1995) (52).

Discussions

Fig. 4.2.1, Cr_2O_3 vs CaO for olivine diagram for MIL090206, MIL090405, NWA6077, NWA5363, NWA11187, MIL090340, Al Huwaysah 010, GRA06128,42, GRA06128,51, GRA06129,22, GRA06129,25 and EET99402. The different shapes of the markers indicate different papers. Data from Goodrich et al. (2017), Carli et al. (2023), Day et al. (2012) and Gardner-Vandy et al. (2013) (55);

Fig. 4.2.2, Cr_2O_3 vs CaO for olivine diagram for MIL090206, MIL090405, NWA6077, NWA5363, NWA11187, MIL090340, Al Huwaysah 010, GRA06128,42, GRA06128,51, GRA06129,22, GRA06129,25 and selected meteorites from Goodrich et al (2017). The different shapes of the markers indicate different papers. As can be easily seen, there are two MIL090206 samples in the

diagram, the one from this study is an orange circle, while the one from Goodrich et al. (2017) is a yellow triangle Image modified from Goodrich et al. (2017). Brachinite data from Nehru et al. (1983), Warren and Kallemeyn (1989), Goodrich and Righter (2000), Mittlefehldt et al. (2003), and Goodrich et al. (2011). Data for NWA 1500 from Goodrich et al. (2006); NWA 595 from Goodrich et al. (2011); NWA 5400/6077 from Gardner-Vandy et al. (2013); NWA 7299 and NWA 7499 from Meteoritical Bulletin Database; Zag(b) from Delaney et al. (2000); Divnoe from Petaev et al. (1994); Tafassasset from Gardner-Vandy et al. (2012); LEW 88763 from Gardner-Vandy (2012) and Day et al. (2015). For sources of ureilite, lodranite, and winonaite data, see fig. 5 of Goodrich et al. (2011). Cr_2O_3 value for NWA5400 was not reported in Day et al. (2012) (56);

Fig. 4.2.3, Y-REE pattern for clinopyroxene in MIL090405, NWA6077, NWA5363, NWA5400, GRA06128, GRA06129, EET99402. NWA5400, GRA06128, GRA06129 and EET99402 data from Day et al. (2012). Data normalized to the average CI composition from McDonough and Sun (1995). The different shapes of the markers indicate different papers (57);

Fig. 4.2.4, Y-REE pattern of olivine for NWA11187, Hughes 009 (a and b; Goodrich et al. 2009) and FRO90054 (a and b; Goodrich et al. 2009). Data normalized to the average CI composition from McDonough and Sun (1995). Blue line in legend = data obtained through LA-ICP-MS (60);

Fig. 4.2.5, Y-REE pattern of orthopyroxene for NWA11187, Hughes 009 (a and b; Goodrich et al. 2009), FRO90054 (a and b; Goodrich et al. 2009) and LEW85440 (a and b; Guan et al. 2000). Data normalized to the average CI composition from McDonough and Sun (1995). Blue line in legend = data obtained through LA-ICP-MS. Red line in legend = data obtained through ion microprobe (60);

Fig. 4.2.6, Y-REE pattern of clinopyroxene for NWA11187, Hughes 009 (a and b; Goodrich et al. 2009), FRO90054 (a and b; Goodrich et al. 2009) and LEW85440 (a and b; Guan et al. 2000). Data normalized to the average CI composition from McDonough and Sun (1995). Blue line in legend = data obtained through LA-ICP-MS. Red line in legend = data obtained through ion microprobe (61).

8. TABLE INDEX

Petrography

Major and Minor Elements

deviations (SD) and relative standard deviations (RSD) are reported for each average. The full dataset is available as supplementary Table S6 (33).

Trace Elements

Table 3.7, the olivine trace element content, subdivided and sorted based on their average abundance in the meteorites (36);

Table 3.8, the orthopyroxene trace element content, subdivided and sorted based on their average abundance in the meteorites (40);

Table 3.9, the clinopyroxene trace element content, subdivided and sorted based on their average abundance in the meteorites (45);

Table 3.10, the orthopyroxene trace element content, subdivided and sorted based on their average abundance in the meteorites (51).

9. REFERENCES

Benedix, G. K., McCoy, T. J., Keil, K., Bogard, D. D., & Garrison, D. H. (1998). A petrologic and isotopic study of winonaites: Evidence for early partial melting, brecciation, and metamorphism. Geochimica et Cosmochimica Acta, 62(14), 2535-2553;

Cao, H., Chen, J., Yin, C., Fu, X., Ling, Z., & Che, X. (2024). The lithologic diversity of the Moon recorded in lunar meteorites Northwest Africa 7611 and 10480. *Meteoritics & Planetary Science*;

Carli, C., Barbaro, A., Murri, M., Domeneghetti, M. C., Langone, A., Bruschini, E., ... & Pratesi, G. (2023). Al Huwaysah 010: The most reduced brachinite, so far. *Meteoritics & Planetary Science*, *58*(6), 855-874;

Cloutis, E. A., Reddy, V., & Blewett, D. T. (2018). The ungrouped achondrite Northwest Africa (NWA) 7325: Spectral reflectance properties and implications for parent body identification. *Icarus*, *311*, 384-393;

Cuppone, T., Casalini, M., Carli, C., & Pratesi, G. (2022). OIBODIEs: advancement on mineralogical and geochemical analysis on ungrouped achondrites. In *Geosciences for a sustainable future, Torino 19-21 Settembre 2022* (pp. 780-780). Società Geologica Italiana;

Day, J. M., Corder, C. A., Rumble III, D., Assayag, N., Cartigny, P., & Taylor, L. A. (2015). Differentiation processes in FeO-rich asteroids revealed by the achondrite Lewis Cliff 88763. *Meteoritics & Planetary Science*, *50*(10), 1750-1766;

Day, J. M., Walker, R. J., Ash, R. D., Liu, Y., Rumble III, D., Irving, A. J., ... & Taylor, L. A. (2012). Origin of felsic achondrites Graves Nunataks 06128 and 06129, and ultramafic brachinites and brachinite-like achondrites by partial melting of volatile-rich primitive parent bodies. *Geochimica et Cosmochimica Acta*, *81*, 94-128;

Downes, H., Mittlefehldt, D. W., Herrin, J. S., & Lee, C. T. A. Extra-Terrestrial Mantle Samples: Rare Earth Element Variations in Ureilite Meteorites. *Available at SSRN 4688703*;

Gardner-Vandy, K. G. (2012). *Partial melting on iron (II) oxide-rich asteroids: Insights to the first stage of planetary differentiation* (Doctoral dissertation, The University of Arizona);

Gardner-Vandy, K. G., Lauretta, D. S., Greenwood, R. C., McCoy, T. J., Killgore, M., & Franchi, I. A. (2012). The Tafassasset primitive achondrite: Insights into initial stages of planetary differentiation. *Geochimica et Cosmochimica Acta*, *85*, 142-159;

Gardner-Vandy, K. G., Lauretta, D. S., & McCoy, T. J. (2013). A petrologic, thermodynamic and experimental study of brachinites: Partial melt residues of an R chondrite-like precursor. *Geochimica et Cosmochimica Acta*, *122*, 36-57;

Garvie, L. A. (2012). The Meteoritical Bulletin, No. 99, April 2012. *Meteoritics & Planetary Science*, *47*(11), E1-E52;

Gattacceca, J., Bouvier, A., Grossman, J., Metzler, K., & Uehara, M. (2019). The meteoritical bulletin, No. 106. *Meteoritics & Planetary Science*, *54*(2), 469-471;

Goodrich, C. A., Collinet, M., Treiman, A., Prissel, T. C., Patzek, M., Ebert, S., ... & Decker, S. (2022). The first main group ureilite with primary plagioclase: A missing link in the differentiation of the ureilite parent body. *Meteoritics & Planetary Science*, *57*(8), 1589-1616;

Goodrich, C. A., Fioretti, A. M., Tribaudino, M., & Molin, G. (2001). Primary trapped melt inclusions in olivine in the olivine-augite-orthopyroxene ureilite Hughes 009. *Geochimica et Cosmochimica Acta*, *65*(4), 621-652;

Goodrich, C. A., Fioretti, A. M., & Van Orman, J. (2009). Petrogenesis of augite-bearing ureilites Hughes 009 and FRO 90054/93008 inferred from melt inclusions in olivine, augite and orthopyroxene. *Geochimica et Cosmochimica Acta*, *73*(10), 3055-3076;

Goodrich C. A., Kita N. T., Spicuzza M. J., Valley J. W., Zipfel J., Mikouchi T., and Miyamoto M. (2011). The Northwest Africa 1500 meteorite: Not a ureilite, maybe a brachinite. Meteoritics & Planetary Science 45: 1906–1928;

Goodrich, C. A., Kita, N. T., Sutton, S. R., Wirick, S., & Gross, J. (2017). The Miller Range 090340 and 090206 meteorites: Identification of new brachinite-like achondrites with implications for the diversity and petrogenesis of the brachinite clan. *Meteoritics & Planetary Science*, *52*(5), 949-978;

Goodrich, C. A., Kita, N. T., Warren, P. H., & Rubin, A. E. (2012). MIL 090340 and MIL 090206: Two more brachinite-like achondrites mis-identified as ureilites. Meteoritics and Planetary Science Supplement, 75, 5272;

Goodrich, C. A., & Righter, K. (2000). Petrology of unique achondrite Queen Alexandra Range 93148: A piece of the pallasite (howardite-eucrite-diogenite?) parent body? *Meteoritics & Planetary Science*, *35*(3), 521-535;

Goodrich, C. A., Wlotzka, F., Ross, D. K., & Bartoschewitz, R. (2006). Northwest Africa 1500: Plagioclase-bearing monomict ureilite or ungrouped achondrite? *Meteoritics & Planetary Science*, *41*(6), 925-952;

Guan, Y., & Crozaz, G. (2000). Light rare earth element enrichments in ureilites: a detailed ion microprobe study. *Meteoritics & Planetary Science*, *35*(1), 131-144;

HIBIYA, Y., OZAWA, K., IIZUKA, T., & YAMAGUCHI, A (2015). A mineralogical and chemical study of primitive achondrite NWA 6704;

Keil K. 2014. Brachinite meteorites: Partial melt residues from an FeO-rich asteroid. Chemie der Erde 74:311–329;

Krot A. H., Keil K., Scott E. R. D., Goodrich C. A., and Weisberg M. K. 2013. Classification of meteorites and their genetic relationships. In Meteorites, comets and planets, edited by Davis A. M. Treatise on Geochemistry, Vol. 1, Revised edition. Amsterdam: Elsevier. pp. 1–63;

Lauretta, D. S., & McSween, H. Y. (Eds.). (2006). *Meteorites and the early solar system II*. University of Arizona Press;

Li, S., Yin, Q. Z., Bao, H., Sanborn, M. E., Irving, A., Ziegler, K., ... & Wang, S. (2018). Evidence for a multilayered internal structure of the chondritic acapulcoite-lodranite parent asteroid. *Geochimica et Cosmochimica Acta*, *242*, 82-101;

Jacquet, E. (2022). Meteorite petrology versus genetics: Toward a unified binominal classification;

Mason 1987, *AMN (Antarctic Meteorite Newsletter) 10 (1)*;

McDonough, W. F., & Sun, S. S. (1995). The composition of the Earth. *Chemical geology*, *120*(3-4), 223-253;

McSween, H. Y. (1999). Meteorites and their parent planets. Cambridge University Press;

Mittlefehldt, D. W., Bogard, D. D., Berkley, J. L., & Garrison, D. H. (2003). Brachinites: Igneous rocks from a differentiated asteroid. *Meteoritics & Planetary Science*, *38*(11), 1601-1625;

Mittlefehldt, D. W., Greenwood, R. C., Berger, E. L., Le, L., Peng, Z. X., & Ross, D. K. (2022). Eucrite-type achondrites: Petrology and oxygen isotope compositions. *Meteoritics & Planetary Science*, *57*(2), 484-526;

Nehru, C. E., Prinz, M., Delaney, J. S., Dreibus, G., Palme, H., Spettel, B., & Wänke, H. (1983). Brachina: A new type of meteorite, not a chassignite. *Journal of Geophysical Research: Solid Earth*, *88*(S01), B237-B244;

Pearce, N. J., Perkins, W. T., Westgate, J. A., Gorton, M. P., Jackson, S. E., Neal, C. R., & Chenery, S. P. (1997). A compilation of new and published major and trace element data for NIST SRM 610 and NIST SRM 612 glass reference materials. *Geostandards newsletter*, *21*(1), 115-144;

Petaev M. I., Barsukova L. D., Lipschutz M. E., Wang M.-S., Ariskin A. A., Clayton R. N., and Mayeda T. K. 1994. The Divnoe meteorite: Petrology, chemistry, oxygen isotopes and origin. Meteoritics & Planetary Science 29:182–199;

Rai, N., Hilary Downes, and C. Smith. "Ureilite meteorites provide a new model of early planetesimal formation and destruction." *Geochemical Perspectives Letters* 14 (2020): 20-25;

Rosén, Å. V., Pape, J., Hofmann, B. A., Gnos, E., & Guillong, M. (2019). Quenched primary melt in Ramlat as Sahmah 517–Snapshot of ureilite anatexis in the early solar system. *Geochimica et Cosmochimica Acta*, *246*, 1-20;

Ruzicka, A., Grossman, J. N., & Garvie, L. (2014). The Meteoritical Bulletin, No. 100, 2014 June;

Ruzicka, A., Grossman, J., Bouvier, A., Herd, C. D., & Agee, C. B. (2015). The meteoritical bulletin, no. 101;

Score, R., & Lindstrom, M. M. (1990). *Guide to the US collection of antarctic meteorites 1976-1988 (everything you wanted to know about the meteorite collection). Antarctic Meteorite Newsletter, Volume 13, Number 1* (No. NAS 1.15: 101939);

Singerling, S. A., McCoy, T. J., & Gardner-Vandy, K. G. (2013, March). Possible evidence for sulfidization reactions in the Miller Range brachinites (?). In *44th Lunar and Planetary Science Conference. Abstract* (Vol. 1669);

Takeda, H. (1989). Mineralogy of coexisting pyroxenes in magnesian ureilites and their formation conditions. *Earth and Planetary Science Letters*, *93*(2), 181-194;

Warren, P. H. (2012). Parent body depth–pressure–temperature relationships and the style of the ureilite anatexis. Meteoritics & Planetary Science, 47(2), 209-227;

Warren, P. H., & Kallemeyn, G. W. (1989). Allan Hills 84025-The second brachinite, far more differentiated than brachina, and an ultramafic achondritic clast from L chondrite Yamato 75097. In *IN: Lunar and Planetary Science Conference, 19th, Houston, TX, Mar. 14-18, 1988, Proceedings (A89-36486 15-91). Cambridge/Houston, TX, Cambridge University Press/Lunar and Planetary Institute, 1989, p. 475-486.* (Vol. 19, pp. 475-486);

Warren, P. H., & Rubin, A. E. (2012, March). The Miller Range 090340 dunite: Not a uniquely ferroan ureilite, not even a ureilite. In *43rd Annual Lunar and Planetary Science Conference* (No. 1659, p. 2528);

Weisberg, M. K., McCoy, T. J., & Krot, A. N. (2006). Systematics and evaluation of meteorite classification. *Meteorites and the early solar system II*, *19*, 19-52;

Wlotzka, F. (1992). Meteoritical Bulletin, No. 73. *Meteoritics, vol. 27, page 477-483 (1992).*, *27*;

Wlotzka, F. (1994). The Meteoritical Bulletin, No. 77, 1994 November. *Meteoritics*, *29*(6), 891-897;

Satterwhite, C. E., McBridge, K. M., Harrington, R. S., & Righter, K. (2011, March). Processing of Antarctic Meteorites at NASA/Johnson Space Center. In the 42nd *Lunar and Planetary Science Conference* (No. JSC-CN-22821);

Yang, J., Zhang, C., Miyahara, M., Tang, X., Gu, L., & Lin, Y. (2019). Evidence for early impact on a hot differentiated planetesimal from Al-rich micro-inclusions in ungrouped achondrite Northwest Africa 7325. *Geochimica et Cosmochimica Acta*, *258*, 310-335.

10. ACKNOWLEDGEMENTS

Vorrei ringraziare chi mi ha aiutato durante questo percorso, ovvero i professori Antonio Langone, Mara Murri e Maria Chiara Domeneghetti.